Politehnica University Timișoara
Faculty of Chemical Engineering, Biotechnologies and Environmental Protection
Department of Applied Chemistry and Engineering of Organic and Natural Compounds

HABILITATION THESIS

Doctoral Field: Chemical Engineering

Sustainable and green directed biocatalytic pathways as innovative strategies in chemical processes

Candidate
Assoc. Prof. Dr. Eng. Anamaria TODEA

Timișoara
2025

Contents

Abstract

The habilitation thesis entitled “Sustainable and green directed biocatalytic pathways as innovative strategies in chemical processes” outlines Dr. Anamaria Todea's scientific and professional achievements since completing her PhD, highlighting her contributions to sustainable biocatalysis and green chemistry through international collaborations and multidisciplinary research.

A significant part of the research involved enzyme immobilization using physical (adsorption), chemical (covalent binding and sol–gel entrapment) or combined techniques to significantly improve their thermal and operational stability. These immobilised biocatalysts were then integrated into batch and continuous flow systems (packed-bed reactors) to enable the scalable, reproducible and environmentally friendly synthesis of enantiopure secondary alcohols, aroma esters and sugar esters in solventless or non-conventional reaction media.

A second direction of the thesis is focused on the enzymatic synthesis of bio-based oligoesters, which are intermediates for biodegradable materials, functional ingredients and speciality chemicals. The studies utilised renewable building blocks, including sugar derivatives, fatty acids derived from vegetable oils and natural alcohols such as glycerol, as substrates in enzyme-catalysed esterification and polycondensation reactions. The utilization of biocatalysts, particularly lipases, enabled milder reaction conditions, high selectivity and reduced the environmental impact.

The resulting polyesters' biodegradability was systematically investigated in different liquid media, and structure–degradability relationships were established. Notably, the hydrophobicity and crystallinity of the polymers were found to affect their degradation kinetics, offering valuable insights into the design of eco-friendly materials. This research also introduced the concept of safe-and-sustainable-by-design, incorporating ecotoxicological evaluation and rational oligoesters and monomer selection based on environmental and functional criteria.

The thesis reflects a robust scientific portfolio, supported by eight international academic collaborations and several research projects accomplished within European and national frameworks. It includes over 50 peer-reviewed publications, numerous invited presentations, and active participation in the education and mentoring of students at bachelor, MSc, and PhD levels. These achievements demonstrate technical expertise in biocatalysis and polymer science, as well as leadership and vision in implementing sustainable solutions in chemical and biochemical engineering.

Integrating experimental enzymology, green chemistry strategies and materials engineering, this thesis demonstrates the potential of the biocatalytic technologies to reduce the utilization of hazardous chemicals and the high energy demand characteristic for the traditional synthesis methods. The results have direct applications in the fields of biodegradable packaging, green cosmetics, food additives and functional bio-based polymers, establishing biocatalysis as a transformative tool in the modern chemical industry.

Rezumat

Teza de abilitare intitulată „Sustainable and green directed biocatalytic pathways as innovative strategies in chemical processes” prezintă realizările științifice și profesionale ale doamnei Dr. Anamaria Todea de la finalizarea doctoratului, evidențiind contribuțiile sale la biocataliza durabilă și chimia verde prin colaborări internaționale și cercetare multidisciplinară.

O parte semnificativă a cercetării a implicat imobilizarea enzimelor utilizând tehnici fizice (adsorbție), chimice (legare covalentă și entrapare sol-gel) sau combinate pentru a îmbunătăți semnificativ stabilitatea termică și operațională a acestora. Acești biocatalizatori imobilizați au fost apoi integrați în sisteme discontinue și în flux continuu (reactoare cu pat ambalat) pentru a permite sinteza scalabilă, reproductibilă și ecologică a alcoolilor secundari enantiopuri, a esterilor aromatici și a esterilor de zahăr în medii de reacție fără solvent sau neconvenționale.

O a doua direcție a tezei este axată pe sinteza enzimatică a oligoesterilor biologici, care sunt intermediari pentru materiale biodegradabile, ingrediente funcționale și produse chimice speciale. Studiile au utilizat elemente de bază regenerabile, inclusiv derivați de zahăr, acizi grași derivați din uleiuri vegetale și alcooli naturali precum glicerolul, ca substraturi în reacțiile de esterificare și policondensare catalizate enzimatic.

Utilizarea biocatalizatorilor, în special a lipazelor, a permis condiții de reacție mai blânde, selectivitate ridicată și reducerea impactului asupra mediului.

Biodegradabilitatea poliesterilor rezultați a fost investigată sistematic în diferite medii lichide și au fost stabilite relații structură-degradabilitate. În special, s-a constatat că hidrofobicitatea și cristalinitatea polimerilor afectează cinetica de degradare a acestora, oferind perspective valoroase în proiectarea materialelor ecologice. Această cercetare a introdus, de asemenea, conceptul de proiectare sigură și durabilă, încorporând evaluarea ecotoxicologică și selecția rațională a oligoesterelor și monomerilor pe baza criteriilor de mediu și funcționale.

Teza reflectă un portofoliu științific solid, susținut de opt colaborări academice internaționale și mai multe proiecte de cercetare realizate în cadre europene și naționale. Acesta include peste 50 de publicații revizuite de colegi, numeroase prezentări invitate și participarea activă la educația și îndrumarea studenților la nivel de licență, masterat și doctorat. Aceste realizări demonstrează expertiza tehnică în biocataliză și știința polimerilor, precum și conducerea și viziunea în implementarea soluțiilor durabile în ingineria chimică și biochimică.

Integrând enzimologia experimentală, strategiile de chimie ecologică și ingineria materialelor, această teză demonstrează potențialul tehnologiilor biocatalitice de a reduce utilizarea substanțelor chimice periculoase și cererea mare de energie caracteristică metodelor tradiționale de sinteză. Rezultatele au aplicații directe în domeniul ambalajelor biodegradabile, al produselor cosmetice ecologice, al aditivilor alimentari și al polimerilor biologici funcționali, stabilind biocataliza ca un instrument de transformare în industria chimică modernă.

I. Professional and Academic Achievements

I.1. Professional Achievements

I.1.1. Introduction

The habilitation thesis, 'Sustainable and green-directed biocatalytic pathways as innovative strategies in chemical processes', summarises the scientific research activities of Dr Anamaria Todea, conducted after she obtained her PhD in 2015. Her PhD thesis was defended on 27 March 2015 and confirmed by MECTS Order no. 3869/19 May 2015, in the field of Chemical Engineering.

Dr. Anamaria Todea has gained her professional experience primarily through extensive research activities conducted within eight academic and research institutions in five countries: Romania, Austria, the Netherlands, Hungary and Italy. These international experiences have significantly contributed to consolidating her expertise in biocatalysis, molecular biology, protein engineering, macromolecular chemistry, bioanalytical chemistry, and green chemistry. Each stage of her research career has offered her the opportunity to acquire advanced scientific knowledge, strengthen her technical and transferable skills, and address topics of high relevance at European and global levels. She has taken on a wide range of responsibilities, including planning and executing laboratory experiments, using advanced analytical instrumentation, organizing and participating in international conferences, publishing scientific papers, coordinating or contributing to competitive research projects, and supervising students at undergraduate, master and doctoral levels.

In 2009, she graduated with a degree in Biochemical Engineering from the Faculty of Chemistry and Chemical Engineering at Babeș-Bolyai University in Cluj-Napoca. Supervised by Professor Radu Silaghi-Dumitrescu, her thesis focused on the synthesis and characterisation of glutaraldehyde-crosslinked haemoglobin, and she was awarded a final grade of 9.60. This work involved optimising crosslinking parameters, evaluating oxidative stress, and providing direct evidence, for the first time, of a stable haemoglobin–ascorbate complex using NMR spectroscopy. Between 2009 and 2011, she pursued a MSc degree in Applied Food Chemistry at University Politehnica of Timişoara. During this time, she joined the Biocatalysis Group and contributed to a PN III-IDEI project, which focused on the valorisation of hydroxy alkanoic acids through biocatalytic processes. This involved lipase-catalysed synthesis and characterisation of copolymers between 3-hydroxybutyric acid and sugar-derived monomers, and grafting of unsaturated acid derivatives onto chitosan oligosaccharides.

For her MSc thesis, she completed an eight-months research internship at Graz University of Technology, supervised by Prof. Bernd Nidetzky. During this internship, she investigated the role of specific amino acids in the catalytic site of the enzyme sucrose phosphorylase, employing site-directed mutagenesis and enzyme kinetics. She was awarded the maximum grade (10/10) for her dissertation.

In 2011, she was enrolled on a doctoral programme at University Politehnica of Timişoara, focusing on the enzymatic synthesis and characterisation of new polyester-

based biomaterials. During her PhD, she completed two internships at Wageningen University's Food and Biobased Research Institute (in 2012–13 and 2014), one of them including a cooperation with the Delft University of Technology's Microbiology Laboratory.

Her doctoral research included as main topics (i) the enzymatic synthesis of hydroxy acids from unsaturated carboxylic acids using purified hydratases; (ii) the stabilisation and immobilisation of *Elizabethkingia meningoseptica* oleate hydratase; and (iii) the biotransformation of hydroxy fatty acids into estolides using free and immobilized lipases. Notably, she demonstrated lipase-catalysed transformations of 10-hydroxystearic acid for the first time. She also developed new oligomeric compounds through the enzymatic ring-opening polymerisation of ε-caprolactone with hydroxy acids and carbohydrate-derived co-monomers. These compounds were fully structurally characterised using MALDI-TOF MS, 2D NMR, and thermal analysis. The development of an innovative one-pot, cascade, enzymatic process using lipase and oleate hydratase enabled the direct synthesis of estolides from triolein, demonstrating the potential for the upcycling of vegetable oil-based feedstocks.

From December 2013 to February 2016, Dr. Todea held a research assistant position in the Department of Organic Chemistry at the Institute of Chemistry of the Romanian Academy in Timişoara, under the coordination of Dr. Simona Muntean. Her research work involved the adsorption of direct dyes onto various organic and inorganic materials, the kinetics of the sorption process and the enzymatic degradation of azo compounds using horseradish peroxidase immobilized via sol-gel entrapment and epoxy-based covalent binding.

From February 2016 to February 2018, she was enrolled as Assistant Professor at the Faculty of Industrial Chemistry and Environmental Engineering of the University Politehnica of Timişoara, where she continued her research within the Biocatalysis Group led by Prof. Francisc Peter. During this period, she focused on the separation of racemic alcohol mixtures in continuous flow systems using immobilized lipases, the enzymatic and chemical synthesis of fatty acid copolymers with ε-caprolactone and the covalent immobilisation and stabilisation of hydrolase enzymes on epoxy-activated and magnetic supports. From February 2018 to 2024, she was employed as lecturer at the same institution, continuing and expanding her research in the field of biocatalysis to include lactose valorisation through enzymatic cascade systems and enzyme immobilisation in collaboration with international partners, including the Hungarian Academy of Sciences. Between 2010 and 2020, she undertook several research visits to the group of Prof. Sándor Kéki at the University of Debrecen to develop her expertise in MALDI-TOF MS spectrometry.

In March 2020, Dr Todea joined the research group of Prof Lucia Gardossi at the Department of Chemical and Pharmaceutical Sciences of the University of Trieste, as a postdoctoral researcher within a PRIME project (POR-FESR Piemonte). In this position, she developed solvent-free biocatalytic processes for synthesising functionalised polyesters in cooperation with the industrial partners Roelmi Spa and Novamont Spa, as well as with the University of Bari. Since June 2021, she has been granted as principal investigator of the RenEcoPol project, in the frame of a Marie

Skłodowska-Curie Individual Fellowship, one of Europe's most competitive and prestigious research and innovation fellowships financed by the European Union. This research used advanced computational and experimental methods to design eco-friendly, renewable and biodegradable polyesters. As part of the project, she has established collaborations with Esteco Spa (Trieste), the Italian Institute of Technology (Genoa) and the Department of Life Sciences at the University of Trieste.

Since February 2024, Dr. Todea has held the position of Associate Professor at the Faculty of Chemical Engineering, Biotechnologies and Environmental Protection of Politehnica University of Timişoara. In this role, she has consolidated her academic and scientific profile by expanding her teaching responsibilities, supervising doctoral research, and fostering new international collaborations.

From 2025 onwards, she is the leader of the Biocatalysis and Green Chemistry Group at the Faculty of Chemical Engineering, Biotechnologies and Environmental Protection at Politehnica University of Timişoara, further strengthening her role in coordinating multidisciplinary research and mentoring activities.

I.1.2. Dissemination of Research Results

Dr. Todea's scientific work has resulted in one international and one national patent, as well as 53 publications in Web of Science (WoS)-indexed journals - 19 of which are ranked Q1 and 21 of which are Q2 - and seven publications in journals indexed in other international databases (BDI). Of the WoS-indexed articles, 41.54% were authored by Dr. Todea as the first or corresponding author, and 54% of these were published in Q1 journals. Dr. Todea has delivered over 40 presentations at international scientific events, including 11 oral communications and invited seminars, and has contributed to more than 16 national events. Additionally, she has participated in numerous specialized seminars and advanced training programs.

I.1.2.1. Articles Published in Journals

1. G. Lombardo, C. M. Warne, G. Damonte, **A. Todea**, L. Nagy, G. M. Guebitz, F. Allais, S.Fadlallah, A. Pellis, Sustainable synthesis of terpolyesters based on a levoglucosenone-derived cyclic acetal diol*, ACS Sustainable Chem. Eng*. 2025, 13, 10, 4068–4077, doi: 10.1021/acssuschemeng.4c10010.

2. A. R. Buzatu, **A. Todea**, R. Pop, D. M. Dreavă, C. Paul, I. Bîtcan, M. Motoc, F. Peter, C. G. Boeriu, Designed Reactive Natural Deep Eutectic Solvents for Lipase-Catalyzed Esterification. *Molecules*. 2025 Feb 7;30(4):778. doi: 10.3390/molecules30040778.

3. N. Schulte, G. Damonte, V. M. Rocca, **A.Todea** , O. Monticelli, A. Pellis, Bis-pyrrolidone structures as versatile building blocks for the synthesis of bio-based polyesters and for the preparation of additives, *Green Chemistry*, 2025, 27, 1984-1996, doi: 10.1039/D4GC04951A

4. D.I. Dăescu, I. M. Păușescu, I.C. Benea, F. Peter, **A. Todea**, F. Zappaterra, A.A. Alexa, A.R. Buzatu, Natural and Synthetic Flavylium Derivatives: Isolation/Synthesis, Characterization and Application. *Molecules* **2025**, *30*, 90, doi.org/10.3390/molecules30010090.

5. I. C. Benea, D. Dăescu, **A. Todea**, L. Nagy, S. Keki, I. Păușescu, A. Pellis, F. Peter, Efficient biotransformation of biobased raw materials into novel polyesters/polyesteramides; comparative investigation of enzymatic synthesis of block and random copolymers and terpolymers*, International Journal of Biological Macromolecules*, **2024**, 12, 1, 137046, doi.org/10.1016/j.ijbiomac.2024.137046.

6. A. Tămaș, I. Bîtcan, S. Nițu, C. Paul, I.C Benea, G. Rusu, E. Perot, F. Peter, **A. Todea**, Novel Aromatic Estolide Esters from Biobased Resources by a Green Synthetic Approach. *Appl. Sci*. 2024, 14, 7832, doi.org/10.3390/app14177832.

7. D.I. Dăescu, D.M. Dreavă, **A. Todea**, A, F. Peter, I. Păușescu, Intelligent Biopolymer-Based Films: Promising New Solutions for Food Packaging Applications. *Polymers*, 2024, 16, 2256, DOI: 10.3390/polym16162256.

8. A. R. Buzatu, **A. Todea**, F. Peter, C. G. Boeriu, The Role of Reactive Natural Deep Eutectic Solvents in Sustainable Biocatalysis, *ChemCatChem*, 2024, 16, 13, e202301597, doi.org/10.1002/cctc.202301597.

9. **A. Todea**, I. Bîtcan, M. Giannetto, I. Rădoi, R. Bruschi, M. Renzi, S. Anselmi, F. Provenza, T. Bentivoglio, F. Asaro, F.; et al. Enzymatic Synthesis and Structural Modeling of Bio-Based Oligoesters as an Approach for the Fast Screening of Marine Biodegradation and Ecotoxicity. *Int. J. Mol. Sci.* 2024, 25, 5433, doi.org/10.3390/ijms25105433.

10. I. Bîtcan, A. Pellis, A. Petrovici, D.-M. Dreavă, I. Păușescu, F. Peter, L. Nagy, S. Kéki, L. Gardossi, **A. Todea***, One-pot green synthesis and characterization of novel furan-based oligoesters, *Sustainable Chemistry and Pharmacy 2023*, 35, 101229, doi.org/10.1016/j.scp.2023.101229.

11. A. R. Buzatu, M. A. Soler, S. Fortuna, O. Ozkilinc, D. M. Dreavă, I. Bîtcan, V. Badea, P. Giannozzi, F. Fogolari, L. Gardossi, F. Peter, **A. Todea***, C.G. Boeriu, Reactive natural deep eutectic solvents increase selectivity and efficiency of lipase catalyzed esterification of carbohydrate polyols, *Catalysis Today*, *2023,* 114373, https://doi.org/10.1016/j.cattod.2023.114373.

12. I. C. Benea, I. Kántor, **A. Todea**, A. Pellis, I. Bîtcan, L. Nagy, S. Kéki, D. Maria Dreavă, F. Péter, T. Feczkó, Biocatalytic synthesis of new polyesteramides from ε-caprolactam and hydroxy acids: Structural characterization, biodegradability, and suitability as drug nanocarriers, Reactive and Functional Polymers, *2023*, 191, 105702, https://doi.org/10.1016/j.reactfunctpolym.2023.105702.

13. F. Zappaterra, M. Renzi, M. Piccardo, M. Spennato, F. Asaro, M. Di Serio, R. Vitiello, R. Turco, **A. Todea*,** L. Gardossi, Understanding Marine Biodegradation of

Bio-Based Oligoesters and Plasticizers, Polymers *2023*, 15(6), 1536, https://doi.org/10.3390/polym15061536.

15. I. Bîtcan, A. Petrovici, A. Pellis, S. Klébert, Z. Károly, L. Bereczki, F. Péter, F., A. **Todea*** Enzymatic route for selective glycerol oxidation using covalently immobilized laccases, Enzyme and Microbial Technology, *2023*, 163, https://doi.org/10.1016/j.enzmictec.2022.110168.

16. C. Koch, D.-M. Dreavă, **A. Todea**, F. Péter, M. Medeleanu, I. Păușescu, C. Samoilă, I. O. Sîrbu, Synthesis, Characterization, and Antiproliferative Properties of New Bio-Inspired Xanthylium Derivatives, Molecules *2023*, 28 (3), 1102, https://doi.org/10.3390/molecules28031102.

17. I.-I. Rădoi, D. E. Bedolla, L. Vaccari, **A. Todea**, F. Zappaterra, A. Volkov, L. Gardossi, FTIR microscopy for direct observation of conformational changes on immobilized ω-transaminase: effect of water activity and organic solvent on biocatalyst performance, Catalysis Science & Technology, *2023*, 13, 4955-4967, IF:6.17., DOI: 10.1039/d2cy01949c, **COVER PAPER**

18. I. Păușescu, **A. Todea**, D.-M. Dreavă, T. Boboescu, B. Pațcan, L. Pațcan, D. Albulescu, V. Badea, F. Peter, R. Tőtős, D. Ursu, L. Szolga, M. Medeleanu, Experimental and Computational Studies on Bio-Inspired Flavylium Salts as Sensitizers for Dye-Sensitized Solar Cells, Materials, *2022*, 15 (19), 6985, https://doi.org/10.3390/ma15196985 .

19. **A. Todea**, S. Fortuna, C. Ebert, F. Asaro, S. Tomada, M. Cespugli, F. Hollan, L. Gardossi, Rational guidelines for the two-step scalability of enzymatic polycondensation: experimental and computational optimization of the enzymatic synthesis of poly (glycerolazelate), *ChemSusChem*, 2022, 2, 23, https://doi.org/10.1002/cssc.202102657

20. V. Ferrario, **A. Todea**, L. Wolansky, N. Piovesan, A. Guarneri, D. Ribitsch, G. M Guebitz, L. Gardossi, A. Pellis, Effect of Binding Modules Fused to Cutinase on the Enzymatic Synthesis of Polyesters, *Catalyst*, 2022, 12, 3, 303, https://doi.org/10.3390/catal12030303

21. I. Kántor, D. Dreavă, **A. Todea**, F. Péter, Z. May, E. Biró, G. Babos, T. Feczkó, Co-entrapment of sorafenib and cisplatin drugs and iRGD tumour homing peptide by poly [ε-caprolactone-co-(12-hydroxystearate)] copolymer, *Biomedicines,* 2021,10 (1), 43, https://doi.org/10.3390/biomedicines10010043

22. **A. Todea**, C. Deganutti, M. Spennato, F. Asaro, G. Zingone, T. Milizia, L. Gardossi, Azelaic Acid: A Bio-Based Building Block for Biodegradable, *Polymers*, 2021, 1, 13, 23, 4091, IF: 4.967, https://doi.org/10.3390/polym13234091.

23. S. Fortuna, M. Cespugli, **A. Todea**, A. Pellis, L. Gardossi Criteria for Engineering Cutinases: Bioinformatics Analysis of Catalophores, *Catalysts*, 2021, 11, 7, 748, https://doi.org/10.3390/catal11070784.

24. **A. Todea**, I. C. Benea, I. Bîtcan, F. Péter, et al., One-pot biocatalytic conversion of lactose to gluconic acid and galacto-oligosaccharides using immobilized β-galactosidase and glucose oxidase, *Catalysis Today*, 2021, 366, 202-211, https://doi.org/10.1016/j.cattod.2020.06.090.

25. I. Kántor, D. Aparaschivei, **A. Todea**, E. Biró, G. Babos, D. Szerényi, B. Kakasi, F. Péter, E. Şişu, T. Feczkó, Biocatalytic synthesis of poly [ε-caprolactone-co-(12-hydroxystearate)] copolymer for sorafenib nanoformulation useful in drug delivery, *Catalysis Today*, 2021, 366, 195-201, https://doi.org/10.1016/j.cattod.2020.05.005.

26. A.R. Buzatu, A.t E Frissen, L. AM van den Broek, **A. Todea***, M. Motoc, C. G. Boeriu, Chemoenzymatic synthesis of new aromatic esters of mono-and oligosaccharides, *Processes*, 2020, 8, 12, 1638, https://doi.org/10.3390/pr8121638.

27. **A .Todea**, DM Dreavă, IC Benea, I Bîtcan, F Peter, CG Boeriu, Achievements and Trends in Biocatalytic Synthesis of Specialty Polymers from Biomass-Derived Monomers Using Lipases, *Processes* 2020, 9 (4), 646, https://doi.org/10.3390/pr9040646.

28. DM Dreavă, IC Benea, I Bîtcan, **A Todea***, E Șișu, M Puiu, F Peter, Biocatalytic approach for novel functional oligoesters of ε-caprolactone and malic acid, *Processes*, 2020, 9 (2), 232, https://doi.org/10.3390/pr9020232.

29. **A. Todea**, D. Aparaschivei, I. Bîtcan, I.V.Ledeți, G. Bandur, F. Péter, L. Nagy, S. Kéki, E. Biró, Thermal behavior of oligo[(ε-caprolactone)-co-δ-gluconolactone] enzymatically synthesized in reaction conditions optimized by experimental design, *Journal of Thermal Analysis and Calorimetry*, 2020, 1-10, https://doi.org/10.1007/s10973-020-09557-3.

30. P. Borza, I. C. Benea, I. Bitcan, **A. Todea***, S. G. Muntean, F. Peter Enzymatic degradation of azo dyes using peroxidase immobilized onto commercial carriers with epoxy groups, *Studia Universitatis Babes-Bolyai, Chemia*, 2020, 65, 1, DOI:10.24193/subbchem.2020.1.22.

31. I. Păușescu, **A.Todea**, V. Badea, F. Peter, M. Medeleanu, I. Ledeți, G. Vlase, T. Vlase, Optical and thermal properties of intelligent pH indicator films based on chitosan/PVA and a new xanthylium dye, *Journal of Thermal Analysis and Calorimetry*, 2020, 141, 999-1008, https://doi.org/10.1007/s10973-019-08911-4.

32. **A. Todea**, I. Bîtcan, D. Aparaschivei, et al., Biodegradable oligoesters of ε-caprolactone and 5-hydroxymethyl-2-furancarboxylic acid synthesized by immobilized lipases, *Polymers,* 2019, 11(9), 1402, https://doi.org/10.3390/polym11091402.

33. C. Vasilescu, **A. Todea***, A. Nan, M. Circu, R. Turcu, I.-C. Benea, F. Peter, Enzymatic synthesis of short-chain flavor esters from natural sources using tailored magnetic biocatalysts, *Food chemistry*, 2019, 298, 1-8, https://doi.org/10.1016/j.foodchem.2019.05.179 .

34. D Aparaschivei, **A. Todea**, A E Frissen, V Badea, G Rusu, E Sisu, M Puiu, C G Boeriu, F Peter, Enzymatic synthesis and characterization of novel terpolymers from renewable sources, *Pure and Applied Chemistry*, 2019, 91 (3), 397-408, https://doi.org/10.1515/pac-2018-1015.

35. **A. Todea**, D. Aparaschivei, V. Badea, C.G. Boeriu, F. Peter, Biocatalytic Route for the Synthesis of Oligoesters of Hydroxy-Fatty acids and ε-Caprolactone, *Biotechnology Journal*, 13, 6, 2018, **COVER PAPER**, https://doi.org/10.1002/biot.201700629.

36. **A. Todea**, P. Borza, A. Cimporescu, C. Paul, F. Peter, Continuous kinetic resolution of aliphatic and aromatic secondary alcohols by sol-gel entrapped lipases in packed bed bioreactors, *Catalysis* Today, 2018, 306, 223-232, https://doi.org/10.1016/j.cattod.2017.02.042.

37. SG Muntean, MA Nistor, E Muntean, **A. Todea**, R Ianoş, C Păcurariu, Removal of colored organic pollutants from wastewaters by magnetite/carbon nanocomposites: single and binary systems, *Journal of Chemistry,* 2018, 6249821, https://doi.org/10.1155/2018/6249821.

38. SG Muntean, **A. Todea**, S Bakardjieva, C Bologa, Removal of non-benzidine direct red dye from aqueous solution by using natural sorbents: Beech and Silver Fir, *Desalination and Water Treatment*, 2017, 66, 235-250, doi:10.5004/dwt.2016.0154.

39. A. Cimporescu, **A. Todea**, V. Badea, C. Paul, F. Péter, Efficient kinetic resolution of 1,5-dihydroxy-1,2,3,4-tetrahydronaphthalene catalyzed by immobilized *Burkholderia cepacia* lipase in batch and continuous-flow system, *Process Biochemistry*, 2016, 51, 2076-2083, https://doi.org/10.1016/j.procbio.2016.09.023.

40. D. Aparaschivei, **A. Todea**, I. Păuşescu, V. Badea, M. Medeleanu, E. Şişu, M. Puiu, A. Chiriţă-Emandi F. Peter, Synthesis, characterization and enzymatic degradation of copolymers of ε-caprolactone and hydroxy-fatty acids, *Pure and Applied Chemistry*, 2016, 88, 1191-1201, https://doi.org/10.1515/pac-2016-0920.

41. E Biró, D Budugan, **A. Todea**, F Péter, S Klébert, T Feczkó, Recyclable solid-phase biocatalyst with improved stability by sol–gel entrapment of β-d-galactosidase, *Journal of Molecular Catalysis B: Enzymatic*, 2016, 123, 81-90, https://doi.org/10.1016/j.molcatb.2015.11.006.

42. **A. Todea**, L.G. Otten, A.E. Frissen, I. Arends, F. Peter, C. Boeriu, Selectivity of lipases for estolides synthesis, A. Todea, L.G. Otten, A.E. Frissen, I. Arends, F. Peter, Carmen Boeriu, *Pure and Applied Chemistry*, 87(1) pp. 51-58, 2015, https://doi.org/10.1515/pac-2014-0716.

43. **A. Todea**, A. Hiseni, L.G. Otten, I. W.C.E. Arends, F. Peter, C. G. Boeriu, Increase of stability of oleate hydratase by appropriate immobilization technique and conditions, *Journal of Molecular Catalysis B: Enzymatic*, 119, 2015, 40-47, https://doi.org/10.1016/j.molcatb.2015.05.012.

44. I. Ledeti, G. Vlase, T. Vlase, L.M. Suta, **A. Todea**, A. Fulias, Selection of solid-state excipients for simvastatin dosage forms through thermal and nonthermal techniques, *Journal of Thermal Analysis and Calorimetry*, 2015, 121(3), 1093-1102, https://doi.org/10.1007/s10973-015-4832-5.

45. I Ledeti, G Vlase, T Vlase, I Ciucanu, T Olariu, **A. Todea**, A Fulias, LM Suta, Instrumental analysis of potential lovastatin excipient interactions in preformulation studies, *Revista de Chimie*, 2015, 66 (6), 879-882.

46. **A. Todea**, E. Biro, V. Badea, C. Paul, A. Cimporescu, L. Nagy, S. Keki, G. Bandur, C. Boeriu, F. Peter, Optimization of enzymatic ring-opening copolymerizations involving δ-gluconolactone as monomer by experimental design, *Pure and Applied Chemistry*, 2014, 86(11) 1781-1792, https://doi.org/10.1515/pac-2014-0717.

47. S. Muntean, **A. Todea**, M.E. Rădulescu-Grad, Decontamination of colored wastewater using synthetic sorbents, *Pure and Applied Chemistry*, 2014, 86(11) 1771-1780, https://doi.org/10.1515/pac-2014-0805.

48. **A. Todea**, V. Badea, L. Nagy, S. Keki, C. G. Boeriu, F. Peter, Biocatalytic synthesis of δ-gluconolactone and ε-caprolactone copolymers, *Acta Biochimica Polonica*, 2014, 61(2), 205-210, https://doi.org/10.18388/abp.2014_1887 .

49. I Ledeti, CS Bosca, C Cosma, V Badea, **A. Todea**, VN Bercean, Study on obtaining 3-oxolup-20 (29)-en-28-oic acid (betulonic acid) from (3β)-lup-20 (29)-en-3, 28-diol (betulin), *Revista de Chimie* 2014, 65 (11), 1289-1293, (2014):0.806.

50. P. Wildberger, **A. Todea**, B. Nidetzky, Probing enzyme-substrate interactions at the catalytic subsite of *Leuconostoc mesenteroides* sucrose phosphorylase with site-directed mutagenesis: the roles of Asp49 and Arg395, *Biocatalysis and Biotransformation Journal*, 2012, 30(3), pp. 327-337, https://doi.org/10.3109/10242422.2012.674720.

51. S. Kakasi-Zsurka, **A. Todea**, A. But, C. Paul, C. G. Boeriu, C. Davidescu, L. Nagy, A. Kuki, S. Keki, F. Péter, Biocatalytic synthesis of new copolymers from 3-hydroxybutyric acid and a carbohydrate lactone, *Journal of Molecular Catalysis B: Enzymatic*, 2011, 71, 22-28, https://doi.org/10.1016/j.molcatb.2011.03.004.

52. S. Kakasi-Zsurka, **A. Todea**, A. But, C. Paul, C. Boeriu, L. Nagy, F. Péter, Novel enzymatic synthesis of 3-hydroxybutyric acid oligomers with inserted lactobionic acid moieties, *Revista de Chimie*, 2011, 62(10), 958-963.

53. Patent, C. G. Boeriu, A Todea, I.W.C.E Arends, L.G. Otten, Production of fatty acid estolides, US11414684B2, 2022.

54. Brevet, L.V. Ordodi, G.A. Dumitrel, A.M Pană, A. Todea Anamaria, et. Al, Dispozitiv pentru reducerea încărcăturii microbiologice a aerului expirat de pacienții ventilați mecanic, A_00280_2020.

I.1.3. Research Projects

Dr. Anamaria Todea has actively contributed to several nationally and internationally funded research projects, both as project leader and as a team member. Her work has covered areas such as biocatalysis, green chemistry, magnetic nanocomposites, and enzyme design. These projects, funded through prestigious programs including Horizon 2020, UEFISCDI, and regional European development funds, reflect her interdisciplinary expertise and strong engagement in collaborative research.

1. Since 01/09/2022 – *ITC Conference Manager and Management Committee Member* in COST Action CA21162 - Computationally Assisted Design of Enzymes (COZYME), funded by the European Cooperation in Science and Technology (COST). https://www.cost.eu/actions/CA21162/.

2. 01/06/2021 – 31/05/2023 – *Principal Investigator* of the Marie Skłodowska–Curie Individual Fellowship under grant agreement 101029444, H2020-MSCA-IF-2020, entitled *"Sustainable route for circularity of renewable polyesters"*, funded by the European Union's Horizon 2020 program. Project funding: €171,473.28.

3. 09/03/2020 – 30/05/2021 – *Researcher* in the project PRIME – Innovative Processes and Products in Green Chemistry, funded by the Piedmont Region, Italy (POR-FESR funds). Total duration: 36 months. Local unit contribution: €90,000.

4. 30/01/2017 – 29/06/2018 – *Researcher* in the project "Recyclable multilayer magnetic biocatalyst for synthesis of natural esters", PN-III-P2.2.1-PED-2016-0168, funded by the Romanian Executive Agency for Higher Education, Research, Development and Innovation Funding (UEFISCDI). Project funding: 600,000 RON (~€120,000).

5. 01/10/2015 – 15/11/2017 – *Researcher* in the project "Selective decontamination of colored wastewaters by magnetic nanocomposites", PNII-RU-TE-2014-4-1319, funded by UEFISCDI, Romania. Project funding: 600,000 RON (~€120,000).

6. 01/07/2014 – 30/09/2017 – *Researcher* in the project "Biocatalyst-click chemistry downstreaming tandem based innovative kit for optically pure fine chemicals synthesis", PN-II-PT-PCCA-2013-4-0734, contract 206/2014, funded by UEFISCDI, Romania. Project funding: 1,437,500 RON (~€287,500).

I.2. Academic Achievements

I.2.1. Teaching Activity

Her teaching experience has been developed in parallel with her research activity. Since October 2015 (as associated academic staff) and from February 2016 (as Assistant Professor), she coordinated the practical courses of the academic disciplines Organic Chemistry I and II, Food Chemistry, Principles of Food

Preservation, Veterinary Control and Food Safety, Chemistry of Natural Compounds, Fragrances and Odorants, Fine Organic Synthesis and Sensory Analysis at the Faculty of Industrial Chemistry and Environmental Engineering at the Politehnica University of Timişoara.

Since October 2016, Dr. Todea has developed and delivered the lectures of the “Sensory Analysis” course for fourth-year Food Engineering undergraduate students. She also supervised the practical course at this discipline, contributing to the curriculum and introducing new laboratory activities.

Between 2018 and 2020, I held the position of Lecturer at the the Faculty of Industrial Chemistry and Environmental Engineering at the Politehnica University of Timişoara. During this period, she was responsible for several teaching activities in the field of chemical and food engineering. Specifically, in the academic year 2018–2019, she coordinated and delivered the following master's level practical courses in Chemical Engineering: Advanced organic synthesis, Chromatography methods, and Natural and synthetic cosmetic products. Furthermore, between 2016 and 2019 she continue continued to be the Sensory analysis discipline holder from the bachelor's programme in Food Engineering. She was also involved in the bachelor's course Environmental Biotechnology, part of the Environmental Engineering curriculum.

In 2017, she authored the laboratory manual *Sensory Analysis of Food Products – Practical Work* and co-authored another book, *Phytosanitary and Veterinary Food Control – Theoretical and Practical Concepts*.

Between 2016 and 2020, she also served as internship coordinator and academic tutor for the graduate students of the faculty.

Since 2024 to date, she is Associate Professor at Faculty of Chemical Engineering, Biotechnologies and Environmental Protection, Politehnica University of Timișoara, Romania. The teaching activity include the main courses in the field of Chemical Engineering and Food Engineering, including Biotechnology (bachelor, 3rd year), Applied Biotechnology and Enzymatic Biotransformation’s, and Bioactive Ingredients in Pharmaceutical, Cosmetic, and Food Products (master level, Chemical Engineering Field). She also continue to teach Sensory Analysis within the bachelor programme in Food Product Engineering.

From 2014 to the present day, she has supervised 30 bachelor's theses and 11 MSc dissertations, as well as partially guiding the research activities of four doctoral students at University Politehnica of Timişoara.

Between 2020 and 2022, she also coordinated the research of three MSc students at the University of Trieste. In February 2022, she delivered a doctoral course entitled 'Enzyme Immobilisation: Rational Basis for Designing Efficient Biocatalysts” at the University of Pisa in Italy.

Between 2020 and 2023, she supervised a doctoral student as part of the PRIN 2017 national project, CARDIGAN, which focused on sustainable routes to bioplasticisers and biolubricants. This project was carried out in collaboration with the University of Naples Federico II and the CNR IPCB in Pozzuoli. She also participated in the European INTERfaces (ITN-Marie Curie) project, supervising a PhD student

engaged in advanced characterisation of enzyme immobilisation materials via infrared microscopy.

I.2.2. Professional Training

In line with her commitment to continuous professional development, Dr Anamaria Todea has completed several specialised postdoctoral training programmes in leadership, molecular modelling, biocatalysis and research management. These courses have strengthened her interdisciplinary expertise, supporting her academic and research career in biotechnology and green chemistry.

September 12, 2022: “COST Academy Leadership Workshop”, organized by the European Commission, COST Association, Avenue du Boulevard - Bolwerklaan 21, 1210 Brussels, Belgium.

June 10 – July 28, 2021: “Molecular Modelling Principles & Applications of Molecular Modelling to Biocatalysis”, taught by Dr. Sara Fortuna at the University of Trieste, Department of Chemical and Pharmaceutical Sciences.

September 13–17, 2021: “ICTP-SISSA-CECAM Workshop on Molecular Dynamics and its Applications to Biological Systems (SMR 3627)”, SISSA, Trieste, Italy. Online.

June 30 - October 18, 2021: “Management Course”, British Academy of Business Communication, certificate serial no. BS 20385/2021. Online.

I.3. Awards

Dr. Anamaria Todea has received several awards and distinctions in recognition of her scientific achievements, excellence in research, and active involvement in education and training. These honors reflect her contribution to the fields of biotechnology and biocatalysis, as well as her impact as a researcher and mentor in the academic community.

- December 2019 - *Excellence in Research Award for Young Researchers* in the field of “Biotechnology and Biocatalysis”, awarded by Politehnica University of Timișoara, Romania.
- May 2019 - *Professor Bologna Award*, offered by the National Alliance of Student Organizations in Romania (ANOSR), during the award ceremony in Iași, Romania.
- September 2015 - *Award for Excellence* for outstanding achievements within the project “Increasing the attractiveness and performance of doctoral and postdoctoral training in engineering sciences - ATRACTING POSDRU/159/1.5/S/137070”.
- June 2022 - *Best Poster Award* at the 6th International Conference Implementation of Microreactor Technology in Biotechnology - IMTB 2022, held in Portorož, Slovenia (5–8 June 2022), for the poster entitled "Designing new immobilized biocatalysts for the efficient synthesis of renewable and biodegradable poly(glycerolazelate)", authored by A. Todea, S. Fortuna, F. Asaro, S. Tomada, M. Cespugli, F. Hollan, L. Gardossi.

II. Scientific achievements

The results presented in this thesis were obtained within the Biocatalysis and Green Chemistry Group at Politehnica University of Timișoara, Romania and the Laboratory of Applied and Computational Biocatalysis, University of Trieste, Italy. These achievements are the outcome of collaborative research efforts carried out together with colleagues and group members who are co-authors of the respective scientific publications. Their valuable contributions, both experimental and theoretical, played a key role in the development and successful completion of the studies included in this work.

II.1. Introduction

In the dynamic and rapidly evolving field of chemical engineering, the incorporation of biocatalytic processes has emerged as a promising means of meeting the growing demand for environmentally friendly and sustainable synthesis methods. Enzymes are highly selective and efficient catalysts that have proven their versatility in various industrial applications, including food processing and pharmaceutical production. [1], [2].

In this regard, various sectors, including energy production and material synthesis, are being encouraged to transition from fossil fuel-based industries to the use of renewable resources [3]. One way of achieving greater sustainability is to develop new materials derived from biomass or bio-based resources. The goal is to replace the use of fossil fuels in various technologies with natural resources derived from biological materials. These renewable resources can be used to synthesise a wide range of platform chemicals that have significant potential as key building blocks in the production of innovative materials. A notable category of these materials is bio-based polymers, which exhibit desirable properties such as biodegradability and biocompatibility [4], [5].

II.2. Biocatalysis in chemical engineering: principles and advantages

Biocatalysis refers to the use of biological catalysts, such as enzymes or whole cells, to carry out chemical reactions. In chemical engineering, it has emerged as a powerful approach for designing more efficient and environmentally friendly processes. Unlike traditional inorganic catalysts, enzymes are produced from renewable resources, are biodegradable and are often non-toxic. As industries seek sustainable alternatives, biocatalytic processes are becoming increasingly popular as a way to improve efficiency and reduce environmental impact. This trend is central to white biotechnology, the branch of biotechnology devoted to industrial processes, where biocatalysis is key to developing sustainable chemical manufacturing [6], [7].

Enzymes as catalysts: versatile biocatalytic tools for environmentally friendly and efficient chemical processes

Enzymes are highly efficient and selective catalysts that accelerate reactions by lowering activation energies via specialised active sites. They can have enormous turnover frequencies - a single enzyme molecule may convert thousands of substrate molecules per second - far outperforming typical chemical catalysts. Enzymes are also remarkably specific, with most catalysing either a single reaction or a narrow family of similar reactions. This selectivity can be chemo-, regio-, or stereoselective, meaning that enzymes can distinguish between different functional groups, positions on a molecule, or stereochemical configurations with great precision [8]. The specificity of biocatalysts ensures that the desired product is obtained with minimal side reactions, thus simplifying downstream processing and purification. In industrial practice, this translates to higher yields and purer products.

Enzymes can catalyse a wide variety of reactions relevant to chemical manufacturing. They are classified into six major categories according to the type of reaction they facilitate.

- Oxidoreductases (catalyse oxidation–reduction reactions)
- Transferases (catalyse group transfer)
- Hydrolases (catalyse bond hydrolysis by adding water)
- Lyases (catalyse bond cleavage by means other than hydrolysis or oxidation, often forming a new double bond or ring)
- Isomerases (catalyse intramolecular rearrangements)
- Ligases (catalyse the joining of two molecules with the input of energy, e.g. ATP) [9]

In industrial biocatalysis, hydrolases and oxidoreductases have historically dominated, accounting for ~65% and 25% of industrial enzyme applications, respectively [10].

Such processes include the hydrolysis of amides or esters using hydrolases such as lipases and proteases, and stereoselective reductions or oxidations using dehydrogenases or oxidases, which often involve cofactor recycling.

Modern biocatalysis also exploits whole-cell systems to facilitate multi-step transformations, including those requiring enzyme cofactors (e.g. NADH/NADPH), which the cells themselves can regenerate in situ. The versatility of enzyme catalysis means that many traditional organic reactions have biocatalytic analogues, thereby expanding the chemist’s toolkit for synthesis.

A defining feature of biocatalysis is that enzymatic reactions usually take place under mild conditions, such as near-ambient temperatures, atmospheric pressure, and a pH close to neutral. These conditions are far gentler than those often required for conventional catalysis, which may necessitate high temperatures or pressures, as well as strong acids, bases or metal reagents. Mild operating conditions not only save energy, but also enable the transformation of heat-sensitive or complex molecules that would decompose under harsher conditions. For example, many pharmaceutical

compounds with multiple functional groups can be synthesised or modified by enzymes without the need for protecting groups, since enzymes can selectively target specific sites [11].

Integrating biocatalysis into chemical processes usually necessitates specialised reactor designs and handling strategies for the catalysts. Although enzymes in solution can be used in batch or continuous stirred-tank reactors, they are often immobilized on solid supports to improve stability and enable reuse. This enables them to be retained in fixed-bed or flow reactors, facilitating continuous operation and the separation of products from the catalyst. Since the mid-1990s, large-scale production of antibiotic intermediates under mild, aqueous conditions has been achieved using immobilized enzymes such as penicillin acylase. This allows the enzymes to be retained in fixed-bed or flow reactors, enabling continuous operation and facilitating the separation of products from the catalyst. Since the mid-1990s, large-scale production of antibiotic intermediates under mild, aqueous conditions has been achieved using immobilized enzymes such as penicillin acylase [12].

Another aspect of process integration is cofactor management. Many enzymatic reactions, particularly oxidoreductases, require cofactors such as NAD(P)H [13].

Chemical engineers address this issue by coupling reactions for cofactor regeneration using a second enzyme or electrochemical methods. This enables the recycling of costly cofactors instead of their stoichiometric consumption. Advances in protein engineering, particularly directed evolution, have further enhanced enzyme properties such as stability in organic solvents and a broader range of substrates, facilitating the integration of biocatalysts into various processes. Directed evolution, recognised with the 2018 Nobel Prize (awarded to Frances Arnold), enables enzymes to be tailored to meet industrial requirements. For instance, tolerance to higher temperatures or non-natural substrates can be increased. Together, these innovations in enzyme engineering and process design have expanded the range of chemical reactions and process settings that biocatalysis can effectively cover [14], [15] .

The push for sustainable industrial processes has established biocatalysis as a vital component of green chemistry initiatives. Notably, Roger Sheldon observed that "biocatalysis conforms to ten of the twelve principles of green chemistry"[16]. This strong alignment stems from the intrinsic qualities of biocatalysts: enzymes are derived from renewable raw materials, such as microorganisms or plants; using them often eliminates the need for toxic reagents and heavy-metal catalysts; and their exquisite selectivity means fewer by-products are generated, resulting in less waste. Switching from a traditional chemical route to a biocatalytic one often eliminates the need for 'end-of-pipe' pollution control or extensive waste remediation, since the process generates less hazardous waste by its very nature. Biocatalysis therefore plays a pivotal role in white biotechnology, the application of biotechnology to develop sustainable industrial processes. White biotechnology essentially involves using biotechnology to reduce environmental impact and improve resource efficiency. Biocatalysis is often described as the 'pivot of white biotechnology', acting as a key

enabling technology that allows the chemical industry to meet green chemistry and engineering goals [6].

In practice, the sustainability benefits of biocatalysis can be quantified using green chemistry metrics. For example, enzymatic processes generally have a much lower E-factor (waste mass per product mass) and atom economy [17]. The pharmaceutical industry, which has historically produced large amounts of waste per unit of product, has adopted biocatalysis to reduce waste and increase selectivity. One example is the production of the antidiabetic drug sitagliptin: Merck & Co. replaced a rhodium-catalysed step with transaminase, an enzyme developed through directed evolution. This eliminated the need for a metal catalyst, reducing waste while improving yield and safety. This biocatalytic process won a Presidential Green Chemistry Challenge award in recognition of its significant environmental and safety advantages. These examples show how recent advances in biocatalysis can contribute directly to sustainability by replacing hazardous chemicals and processes with more efficient, lower-step pathways that maximise yield and minimise resource consumption [17].

Biocatalysis has evolved from a specialised technique into a widely adopted method across various industries. A significant milestone in the production of bulk chemicals was the development of biocatalytic methods for producing acrylamide. Acrylamide was traditionally produced by copper-catalysed hydration of acrylonitrile, but can now be produced using nitrile hydratase enzymes in water at moderate temperatures. By the mid-1980s, this enzymatic process had become the first commercially viable biotransformation of a commodity chemical, with an annual production capacity of 30,000 tonnes. Such enzyme-based processes have since been scaled up dramatically - for instance, a single plant using *Rhodococcus*-derived nitrile hydratase now produces over 200,000 tonnes of acrylamide per year - and have almost entirely replaced the older copper-catalyst process. The advantages driving this shift include higher selectivity and yields, a cleaner product with virtually no by-products, and lower energy requirements (as there is no need for high heat). Similarly, biocatalysis is employed in the bulk synthesis of nicotinamide (vitamin B3) from 3-cyanopyridine using the same class of enzyme. This enables the mild conversion of a nitrile to an amide to occur without the harsh acidic conditions required by a chemical process. These successes demonstrate how white biotechnology can transform large-scale chemical production, achieving economic viability alongside environmental benefits.

Biocatalysis has had a profound impact on the fine chemicals and pharmaceuticals industries. Enzymatic processes are now standard practice for synthesising chiral building blocks, active pharmaceutical ingredients (APIs), and intermediates. One notable example is the production of 6-aminopenicillanic acid (6-APA), the core component of semi-synthetic penicillin antibiotics, through the enzymatic breakdown of penicillin. Chemical hydrolysis of penicillin G to produce 6-APA requires hot acidic conditions, generating considerable waste and degrading the product. In contrast, using penicillin G acylase (an enzyme) enables this reaction to occur in water at a mild pH, producing high-purity 6-APA with minimal waste. Since

around 1995, immobilized penicillin acylase has been used industrially to produce approximately 10,000 tonnes of 6-APA each year, demonstrating the scalability of biocatalysis. This enzymatic route is not only cleaner, but also highly selective: the enzyme specifically cleaves the penicillin side-chain without attacking other sensitive ring structures [18]. This avoids the need for multiple protection/deprotection steps. Building on this, the same biocatalyst is used to produce cephalosporin intermediates (7-ADCA) and, subsequently, to assemble final antibiotic molecules via the enzymatic coupling of acyl side chains. The result is a more streamlined antibiotic production process that adheres to green chemistry principles [19].

The pharmaceutical industry has widely adopted biocatalysis to synthesise APIs, especially for introducing stereocentres and performing late-stage functionalisation with high precision. Enzymes such as ketoreductases, transaminases and esterases are commonly used to produce enantiopure alcohols, amines and acids, the selective production of which would be difficult using traditional chemical methods [20]. A notable example is the cholesterol-lowering drug Atorvastatin, for which an early synthetic step involving the production of a chiral alcohol was improved by using an enzyme. Enzymatic resolutions (using lipases or acylases) and deracemisations have also been exploited in the production of agrochemicals and fine fragrances, where there is a preference for greener methods due to regulatory and quality demands. Beyond the pharmaceutical industry, the food and beverage industries have long leveraged biocatalysis, for example using amylase and glucoamylase enzymes to break down starch in sweetener production and proteases in cheese production [9]. Consumer products such as detergents also rely on enzyme additives, including proteases, lipases and amylases, to deliver cleaning performance under mild washing conditions. While these applications are more biotech than chemical synthesis per se, they demonstrate how biocatalysis can enable processes that would otherwise be impractical or uneconomical. As new enzymes and process technologies become available, the range of industries that benefit from biocatalysis continues to grow, from biofuels (e.g. enzymatic hydrolysis of cellulose for ethanol production) to polymers (e.g. enzyme-catalysed polyester synthesis and recycling) [21].

The advantages of biocatalysis in sustainable chemical engineering.

Biocatalysis offers several distinct advantages over conventional chemical catalysis. This is why it plays a central role in advancing sustainable chemical engineering [19].

High selectivity: Enzymes offer unparalleled selectivity, frequently carrying out transformations with chemo-, regio- and enantioselectivity that far surpasses that of traditional catalysts. This means that reactions predominantly yield the desired product with minimal side products, reducing the need for extensive purification and minimising waste. In industries such as pharmaceuticals, where product purity is paramount, this selectivity is a decisive advantage. High specificity also enables one-step conversions where chemical routes might require multiple steps (e.g. to protect certain groups while

modifying others) [22]. Consequently, biocatalytic processes can simplify synthesis pathways. For example, they can produce a single desired stereoisomer directly, rather than having to separate it from a racemic mixture. This improves overall process efficiency and economy [10].

Mild reaction conditions: Biocatalysts operate under relatively mild conditions (typically 20-70°C, atmospheric pressure, and neutral pH), dramatically reducing energy requirements and eliminating the need for extreme processing conditions. Lower temperatures and benign solvents (often water) result in lower utility costs and a smaller carbon footprint for the process. Furthermore, being able to perform reactions under such conditions enables sensitive functional groups and complex molecules, which could not withstand harsher chemistry, to be handled. This was demonstrated in the penicillin acylase example, where the enzyme facilitated the cleavage of penicillin in water rather than hot acid. Mild conditions also improve operational safety, as the absence of high pressures, temperatures or dangerous reagents reduces the risk of accidents and corrosion, and minimises maintenance issues with equipment [8], [22].

Environmental benefits: Perhaps most significantly of all, biocatalysis greatly reduces the environmental impact of chemical manufacturing. Enzymatic processes tend to generate fewer hazardous by-products and often use renewable feedstocks or biodegradable materials. Unlike many metal catalysts, which can leave residues or require special disposal, enzymes are biodegradable proteins and therefore do not pose this risk. By reducing reliance on organic solvents and toxic chemicals, biocatalysis aligns chemical production with the principles of green chemistry. For example, an enzyme-catalysed process can be carried out in water, whereas a traditional process may require chlorinated solvents, thus avoiding the introduction of toxic organics into the waste stream. According to a recent industry analysis, companies view biocatalysis as a convergence of environmental responsibility and operational excellence, enabling them to comply with strict environmental regulations while maintaining competitive efficiency. Furthermore, many biocatalytic processes use renewable raw materials, such as sugars or plant oils processed by microbes, instead of petrochemicals. This contributes to a circular bioeconomy. The result is a process that reduces emissions and waste and often improves the public perception and regulatory compliance profile of a chemical product [23], [24].

Economic and process efficiency: When implemented correctly, biocatalysis can offer significant economic benefits. Higher reaction yields and selectivities mean that more product is produced from the same inputs, resulting in less waste that needs to be treated. This improves process atom economy directly and reduces the cost of goods. Avoiding extreme conditions can also lower capital and operating costs (for example, reactors do not need to withstand very high pressure, and energy costs are lower). Furthermore, enzymes can combine multiple chemical steps into one, shortening production routes and saving time and resources. A concrete example of this is the enzymatic route to sitagliptin, which eliminates the need for costly chiral resolution steps and precious metal catalysts, resulting in a simpler, cheaper process with a higher overall yield. Biocatalytic processes also tend to scale linearly and can

be run in standard bioreactors. For certain transformations, this is more cost-effective than using specialised chemical reactors. Although enzymes themselves have an associated production cost, advances in fermentation technology have made enzyme supply inexpensive on a large scale. Moreover, immobilisation and enzyme recycling can spread the cost of the catalyst over large volumes of product. According to an industry survey, companies that adopt biocatalysis often achieve cost savings through reduced energy usage and minimal waste disposal expenses, as well as fewer process steps. All of these factors strengthen economic viability [10], [24], [25].

Combining with traditional catalysis: It is worth noting that biocatalysis does not always occur in isolation. Hybrid processes that combine enzymatic and classical chemical steps can utilise the strengths of both approaches. For instance, chemical catalysts may be employed for high-temperature steps or inorganic transformations, while enzymes are utilised for steps necessitating high selectivity or occurring late in the synthesis process, such as setting stereochemistry. These chemoenzymatic processes are becoming increasingly common. Integration can be either sequential or concurrent ('one-pot'). For instance, an initial chemical oxidation could be followed by an enzymatic reduction within the same vessel, thereby simplifying operations. Such combinations broaden the scope of feasible manufacturing routes and can improve efficiency and yield beyond what either approach could achieve alone. Process intensification techniques, such as using flow reactors for enzymes or ultrasound to enhance mass transfer in enzyme reactions, are also being explored to improve the performance of biocatalysis.

Biocatalysis has become a fundamental component of modern chemical engineering, driving progress in sustainable manufacturing. As mentioned earlier, it lies at the heart of white biotechnology, enabling industrial processes that are cleaner, safer, and often more economical than traditional methods. Using enzyme catalysis, chemical engineers can carry out transformations under mild, environmentally friendly conditions with a high level of selectivity, minimising waste and the need for further processing. Case studies from various industries, ranging from the production of bulk chemicals such as acrylamide to the manufacture of complex pharmaceuticals, demonstrate the clear advantages of biocatalysis in terms of yield, purity, environmental impact, and cost savings. Furthermore, ongoing innovations in enzyme engineering, process integration techniques, and the discovery of new biocatalysts continue to expand the scope and efficiency of biocatalytic processes. In an era where sustainability is as important as profitability, biocatalysis offers a convergence of the two, acting as a catalyst for sustainability in the chemical industry and transforming the way we design and run chemical processes. The principles and advantages discussed here emphasise why biocatalysis is set to play an increasingly important role in the future of chemical engineering and industrial chemistry. It will help us advance towards more sustainable and innovative production processes for the chemicals and materials that society needs [19].

The efficiency, selectivity and applicability of biocatalytic processes at both laboratory and industrial scales are influenced by a variety of factors. The most important factors include the nature and stability of the biocatalyst, the characteristics

of the substrate, the choice of solvent or reaction medium, operational parameters such as temperature and pH, and the mode of biocatalyst application (e.g. free or immobilized form, batch or continuous operation). Achieving a careful balance of these parameters is essential for optimising the overall performance and sustainability of biocatalytic systems.

The following sub-chapters present the author's contributions to various stages of biocatalytic process development in detail. These contributions include studies on enzyme selection and stabilisation, optimisation of reaction conditions, integration of green solvents and design of robust biocatalysts for specific synthetic applications.

II.3. Enzyme immobilization and optimization for industrial relevance

Enzyme immobilisation, whereby enzymes are attached to solid supports or entrapped in matrices, is a cornerstone of sustainable biocatalytic processes. By preparing enzymes in a reusable form, immobilisation enables their recovery and reuse, thereby aligning with green chemistry principles by reducing waste and lowering costs. As a recent study succinctly noted [26].

Compared to free enzymes in solution, immobilized enzymes often exhibit enhanced stability (e.g. thermal, pH or solvent stability), improved operational stability (e.g. maintaining activity over longer periods or for multiple uses) and easier catalyst separation [27]. These features contribute directly to greener processes: for example, a robust immobilized enzyme can function at higher temperatures or in organic media, potentially increasing reaction rates or enabling solvent-free conditions. It can also be reused for many cycles, decreasing the need for fresh enzyme production. Additionally, immobilisation can reduce product contamination by residual enzymes (important for food and pharmaceutical applications) and allow enzymes to be integrated into continuous flow reactors for process intensification [28].

There are several major classes of immobilisation technique (see Figure 1). Reversible methods include physical adsorption on carriers via hydrophobic or ionic interactions, and affinity binding (e.g. His-tagged enzymes on metal-coated supports). These methods are simple, but enzyme leaching may occur [28].

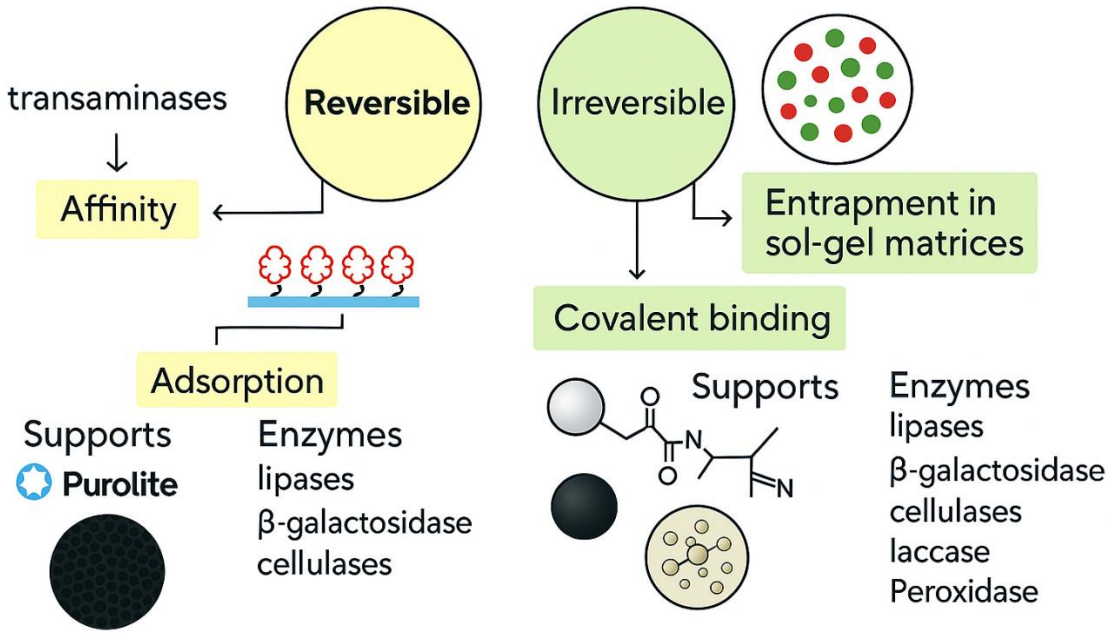

Figure 1 Enzyme immobilization techniques used by the author's research, including reversible (affinity, adsorption) and irreversible (covalent binding, sol-gel entrapment) methods.

Irreversible covalent binding attaches enzymes via covalent bonds to functionalised supports, such as epoxy-activated resins or glutaraldehyde-activated matrices [29]. This method provides strong retention and often improves stability, albeit at the expense of activity if not optimised. Entrapment or encapsulation involves enclosing the enzymes within a gel, polymer or inorganic matrix (e.g. sol-gel or alginate) [30]. This can protect the enzymes and allow diffusion of substrates and products; however, diffusion limitations can occur. Cross-linked enzyme aggregates (CLEAs) form insoluble enzyme networks without an external carrier, achieving high catalyst density. Each method involves trade-offs in terms of enzyme loading, activity retention, mass transfer and mechanical properties. An effective immobilisation strategy must be 'tailored' to the enzyme and process in question, as will be seen in the case studies below, where different approaches (or combinations thereof) were chosen to meet specific green process goals [31], [32].

II.3.1. Enantioselective biotransformation of secondary alcohols in continuous flow using immobilized biocatalysts

Lipases are widely used in kinetic resolutions to obtain chiral compounds. In a 2018 study [33], we were focused on the continuous-flow kinetic resolution of secondary alcohols using *Candida antarctica* lipase B (CALB), which was immobilized using sol-gel entrapment. The aim was to achieve high enantioselectivity and productivity in a sustainable, continuous process that avoids the large solvent volumes and waste associated with batch processes.

A three-component silane sol-gel recipe for encapsulating CALB was developed using a mixture of precursors (e.g. vinyltrimethoxysilane, phenyltrimethoxysilane, and tetramethoxysilane). This produced a porous silica network that stabilised the enzyme while allowing diffusion of the substrate and product. This encapsulation process protected the enzyme in the organic solvent (n-hexane) used for resolution, preventing it from leaching into the continuous packed-bed reactor.

Two model substrates (rac-1 and rac-2), an aliphatic and aromatic secondary alcohol, were selected to accomplish the comprehensive optimization of the factors affecting the continuous kinetic resolution process. The results were compared to literature data and used for the long-term study in operational conditions. In the case of the third studied substrate (rac-3, also holding a secondary alcohol group), an important intermediate for possible pharmaceutical applications, the investigations included the optimization of the immobilization protocol in batch process, subsequently upgraded for utilization in the packed-bed continuous reactor. The overall reaction scheme is presented in Figure 2.

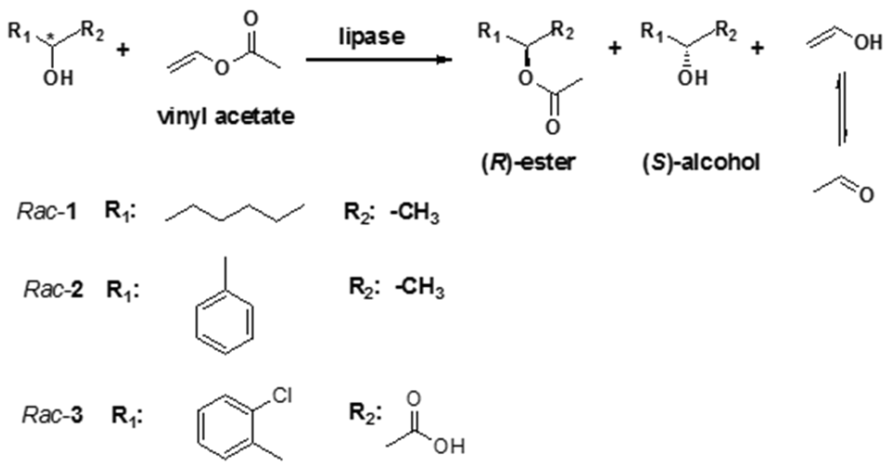

Figure 2 Enzymatic kinetic resolution of rac-2-octanol (rac-1), rac-1-phenylethanol (rac-2) and rac-2-chloromandelic acid (rac-3), catalyzed by lipases.

To elucidate and understand the interactions and the effects of the investigated experimental variables (substrate concentration, flow rate, and temperature) on the responses variables, all data from both experimental designs were combined and common response surface plots were generated. The results depicted in Figure 3, concerning the productivity as a function of substrate concentration and flow rate, indicate continuously increasing tendency of the stability and performances of the biocatalyst at substrate concentrations higher than 1.25 M. Unlike in the case of productivity, the dependence of E as a function of the same parameters allowed to assess the optimal values of substrate concentration and flow rate, leading to the highest enantioselectivity (Figure 3).

Based on the highest values of E and e.e. obtained by the response surface methodology (RSM), the optimal reaction parameters were stated as 0.5 M substrate

concentration of rac-1, 1.5:1 vinyl acetate:substrate molar ratio, reaction temperature of 50°C, and 0.8 mL/min flow rate.

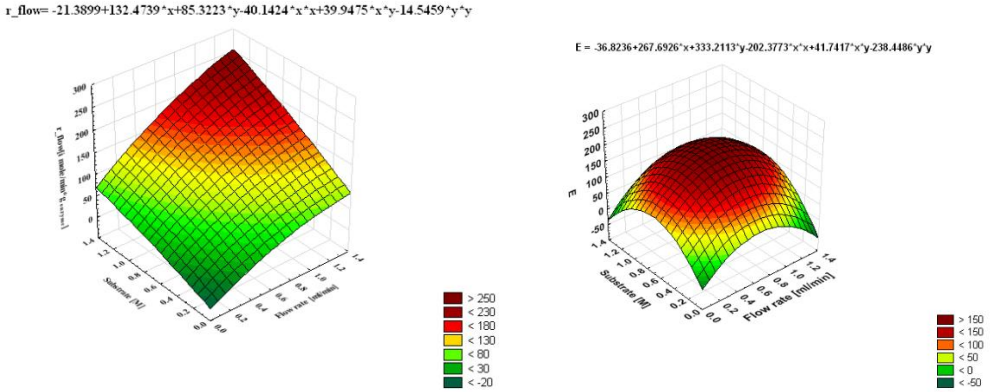

Figure 3 The combined effect of substrate concentration and flow rate on the enantiomeric ratio E, for the experimental design of kinetic resolution of rac-1.

In the next step, the continuous long-term acylation of rac-1 was performed in the aforementioned optimal conditions. The results presented in Figure 4 show that, during 144 h of continuous operation of the packed-bed column, constant values of productivity of about 145 μmoles min^{-1} g^{-1} and enantiomeric ratios higher than 280 were achieved, demonstrating an excellent operational stability of the immobilized biocatalyst.

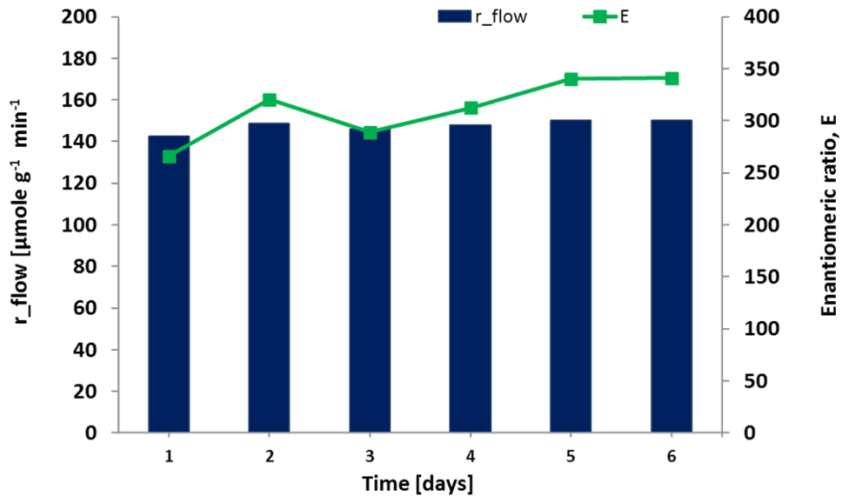

Figure 4 Diagram of productivity (r_{flow}) and enantioselectivity (E) vs. time in the long-term continuous-flow kinetic resolution of rac-1 in the packed bed reactor.

Similarly, for 1-phenylethanol, optimal conditions (40 °C, 0.2 M substrate and a flow rate of 0.45 mL/min) yielded a productivity of ~40 μmol min^{-1} g^{-1} with E > 200. These values were substantially higher than those reported with other immobilisation or reactor approaches, confirming the efficiency of the tailored sol–gel catalyst. Importantly, both enantioselectivity and activity remained stable, demonstrating that the enzyme did not deactivate or lose stereoselectivity with extended use.

The study demonstrated the robustness of the system through continuous operation. CALB immobilized using the sol–gel approach retained full activity for at

least 144 hours. This stability shows that immobilisation can prevent enzyme denaturation in non-aqueous media and under flow conditions. The rigid sol–gel cage likely prevents enzyme unfolding and protects against shear forces, while the tuned hydrophobic/hydrophilic balance in the matrix maintains the enzyme's active conformation.

The enzymatic kinetic resolution of rac-2-chloromandelic (rac-3) was optimized by a detailed evaluation of the effect of the immobilization protocol used. Prior to the transesterification reaction, the solubility of 2-chloromandelic acid was checked in 9 organic solvents since such data were not available for this substrate. Vinyl acetate was selected as acyl donor, based on the previous good results obtained by our group on another aromatic substrate [34]. In the next step, solvents that demonstrated solvation capacity for 2-chloromadelic acid, tetrahydrofuran, toluene, methyl-tertbutylether and diisopropylether, were tested as reaction media for the transesterification reaction with vinyl acetate catalyzed by native CalA lipase, but significant biocatalytic activity of the lipase was observed only in diisopropylether. The reaction was also performed without adding an additional solvent (with excess vinyl acetate), without detecting any reaction product. Based on these results, diisopropylether was used as reaction medium in the transesterification experiments, in both batch and continuous system.

To investigate the effect of the immobilization conditions on the performance of *Cal*A lipase in organic medium, the enzyme was immobilized by sol-gel entrapment using different silane precursors and two immobilization methods. Although this study was not comprehensive, several binary and ternary mixtures of different silane precursors with short chain alkyl (methyl), long chain alkyl (octyl), unsaturated (vinyl) and aromatic (phenyl) non-hydrolysable groups in the composition of the substituted trimethoxysilane precursor were prepared, allowing the selection of the best immobilization protocol.

The results of kinetic resolution of *rac*-**3** in the batch reaction system are presented in Table 1. Obviously, the conversion and enantiomeric ratio were strongly influenced by the immobilization protocol.

The best immobilisation results were obtained using Method A with a ternary silane mixture (PhTMOS:VTMOS:TMOS at a ratio of 1.6:0.4:1), achieving 48% conversion and 86% enantiomeric excess. This increased to 90% when Celite 545 adsorption was combined with the method. Despite the lower enzyme loading, the combined method demonstrated excellent selectivity (E > 200), making it the most effective method. In contrast, method B (prepolymer solution with HCl) yielded similar or higher conversions, but resulted in significant enantioselectivity loss, likely due to changes in matrix morphology. Temperature studies (20–55°C) confirmed that 40°C was the optimal temperature for Method A, yielding the highest conversion and enantiomeric excess. Based on these findings, the CalA biocatalyst immobilized via Method A with Celite 545 was selected for further continuous-flow experiments.

Effect of the immobilization parameters and reaction temperature on the catalytic efficiency and enantioselectivity of sol-gel immobilized *Cal*A lipase. The

transesterification reaction of *rac*-**3** with vinyl acetate (1:3 molar ratio) was carried out in diisopropylether, for 24h, in a batch system.

Table 1 Effect of the immobilization parameters and reaction temperature on the catalytic efficiency and enantioselectivity of sol-gel immobilized CalA lipase. The transesterification reaction of rac-3 with vinyl acetate (1:3 molar ratio) was carried out in diisopropylether, for 24 h, in a batch system.

Method	Silane precursors	Molar ratio	Conversion [%]			ee_s [%]		
			20°C	40°C	55°C	20°C	40°C	55°C
A	VTMOS:TMOS	1:1	19	14	35	13	6	22
A	OcTMOS:TMOS	1:1	19	44	27	38	60	27
A	PhTMOS:TMOS	1:1	21	43	33	32	67	50
A	PhTMOS:MeTMOS: TMOS	1.6:0.4:1	24	47	30	48	82	17
A	PhTMOS:VTMOS: TMOS	1.6:0.4:1	19	48	31	32	86	44
A	PhTMOS:VTMOS: TMOS + Celite 545	1.6:0.4:1	22	48	43	31	90	86
B	OcTMOS:TMOS	1:1	31	32	39	1	3	7
B	VTMOS:TMOS	1:1	40	43	43	7	1	3
B	PhTMOS:MeTMOS: TMOS	1.6:0.4:1	45	48	49	0	0	0
B	PhTMOS:VTMOS: TMOS	1.6:0.4:1	44	47	50	0	2	0
B	PhTMOS:VTMOS: TMOS + Celite 545	1.6:0.4:1	n.d.	22	50	n.d.	0	0

n.d. - not determined

The exquisite selective properties of the immobilized *Cal*A lipase provided an efficient kinetic resolution of *rac*-**3** through transesterification reaction in a discontinuous process. Maintaining the optimized conditions (40°C and diisopropylether as reaction medium), the enzymatic kinetic resolution of this substrate was carried out in continuous-flow mode. The solution of substrate (5mM or 10 mM) and vinyl acetate (3:1 molar ratio related to *rac*-**3**) was fed continuously at a constant flow rate (0.3 mL/min or 0.5 mL/min) into the column (95 x 3 mm).

Analysis of the column outflow (at different time intervals, up to 2.5 h runtime) was performed by chiral HPLC, to assess whether the formation of the products was achieved in steady-state conditions. The productivity of the continuous-flow system was expressed as specific reaction rate (r_{flow}), the amount of product (μmole) synthesized in 1 h reaction time by 1 g immobilized biocatalyst.

The conversion did not exceed 30%, meaning that the residence time was not high enough in the reactor, related to the amount of the immobilized enzyme (Table 2) As anticipated, the conversions were higher at higher substrate concentration, but unexpectedly they also increased at higher flow rate. The explanation could be the necessity of a minimal flow rate needed to realize uniform flow throughout the packed-bed column and allow the enzyme to perform appropriately. Increasing the flow rate was beneficial for the productivity, which was stabilized at a steady state value around 100 μmole $h^{-1}g^{-1}$.

At the same time, higher flow rate and substrate concentration resulted in decrease of the enantiomeric excess of the unreacted substrate. However, the enantiomeric ratio values were above 200 for all continuous experiments, due to the acylation of practically only the (*R*)-2-chloromandelic acid. The results of these preliminary experiments can be considered promising, as the kinetic resolution was accomplished with acceptable conversion, excellent enantioselectivity and good productivity. The forthcoming studies will use a larger column with higher lipase loading, to achieve increased conversion in the steady-state conditions, for long-term exploitation.

*Table 2 Influence of substrate concentration and flow rate on the kinetic resolution of rac-**3** in continuous-flow mode. The investigations were carried out at 40 °C and two substrate concentrations, 5 mM and 10 mM, in diisopropylether*

Flow [mL min^{-1}]	Runtime [h]	Conversion [%]		ee_s [%]		ee_p		Productivity [µmole h^{-1} g^{-1}]	
		5 mM	10 mM	5 mM	10 mM	5 mM	10 mM	5 mM	10 mM
0.3	1.0	24	24	27	26	>99%	>99%	80	94
	1.5	22	22	39	25			31	95
	2.0	19	20	25	29			55	89
	2.5	21	19	39	20			26	67
0.5	1.0	17	25	26	19	>99%	>99%	63	78
	1.5	16	24	13	17			104	94
	2.0	18	27	12	22			122	103
	2.5	15	28	13	26			95	110

From a green chemistry perspective, this continuous biocatalytic process is more efficient in terms of waste and energy. Substrates are converted in a flow process using minimal solvent, and the high selectivity eliminates the need for extensive product separation.

For example, the undesired enantiomer can be recycled or racemised in a full DKR scheme. The stability of the immobilized enzyme means the catalyst turnover numbers are high, as the enzyme performs many reaction cycles per unit of catalyst, making the process resource efficient. Furthermore, operating at relatively high substrate concentrations (0.5 M) and producing chiral products with >99% ee in a single step is a significant improvement on more dilute, stepwise resolutions.

II.3.2. Biocatalytic production of natural flavour esters using tailored magnetic enzymes

Another innovative strategy involves combining multiple immobilisation techniques to harness synergistic benefits. In 2019 we developed a core-shell magnetic biocatalyst for solvent-free ester synthesis with the specific aim of achieving the green synthesis of natural flavour esters (short-chain esters used as food flavour additives). This design incorporated covalent binding and sol-gel encapsulation within a single particle [35].

First, single-core magnetite nanoparticles were coated with an organic polymer shell made of poly(benzofurane-co-arylacetic acid), which provides functional carboxyl groups. *Candida antarctica* lipase B (CALB) was then covalently attached to this polymer layer via carbodiimide coupling to the carboxyl groups. This yielded a 'primary' immobilised enzyme on the particle surface. Subsequently, these enzyme-coated magnetic particles were encapsulated in a thin silica sol–gel layer. This layer effectively embeds the enzyme and its support, creating a robust core–shell structure comprising: The core was made of Fe_3O_4 for magnetic handling, the middle layer is organic for enzyme attachment and the outer layer is glassy for additional stabilisation. The combination of covalent and sol–gel immobilization was intentional, ensuring additional operational stability through multi-point linkages. Covalent attachment firmly anchors the enzyme (preventing leaching and increasing thermal stability via rigidification), while the sol–gel layer provides a protective microenvironment and may introduce further gentle covalent bonds (e.g. via silanes with glycidoxy groups that can bond with the enzyme). This multi-layer immobilization essentially locks the enzyme in a favourable conformation. The covalent binding or sol-gel entrapment alone worked, but the combination yielded superior operational stability, demonstrating an innovative strategy for addressing enzyme deactivation pathways (Table 3).

Table 3 Multilayer magnetic biocatalyst obtained by the entrapment of the covalently attached Candida antarctica B lipase in different sol-gel matrices. Esterification of hexanoic acid with 1-pentanol (1:1 molar ratio), 24 h, 70℃ has been used as test reaction

Magnetic nanoparticles with covalently bound lipases	Silane precursors (molar ratio)	Catalytic efficiency (μmole $h^{-1}mg^{-1}$)	Ester yield (%)
COV-COOH	3-GOPrTMOS:TMOS (1:1)	2.26	46
COV-COOH	1,3-*bis*(GOPr)TMeDSO:TMOS (1:1)	2.25	44
COV-COOH	PhTMOS:VTMOS:TMOS (1,6:0,4:1)	1.73	35
COV-NH_2	3-GOPrTMOS:TMOS (1:1)	1.14	23
COV-NH_2	1,3-bis(GOPr)TMeDSO:TMOS (1:1)	1.09	22
COV-NH_2	PhTMOS:VTMOS:TMOS (1,6:0,4:1)	1.08	22

The immobilised CALB was used in the solvent-free synthesis of flavour esters, specifically the esterification of various natural carboxylic acids with isoamyl alcohol to produce isoamyl acetate and isoamyl butyrate, which have banana and fruity aromas respectively. In a solvent-free system (with neat substrates), the biocatalyst demonstrated high catalytic efficiency, converting the substrates into the desired esters with a high yield.

The best-performing multilayer magnetic biocatalysts were used in consecutive esterification cycles for the synthesis reaction of the flavour esters isoamyl propanoate, hexanoate, octanoate and decanoate. The biocatalyst was recovered from the reaction mixture after each esterification reaction through magnetic separation, washed multiple times with acetone and reused in another reaction cycle. Six reaction cycles were performed in solvent free systems. The relative activity values

are presented in Figure 5 for COV-COOH-SG2, the lipase covalently immobilized on magnetic nanoparticles coated with poly(benzofuran)-co-arylacetic acid and embedded in a sol-gel layer from 1,3-bis(glycidoxypropyl)tetramethyl disiloxane and tetramethoxysilane (1:1). The results indicate that after six reactions cycles more than 65% of the initial activity was recovered in all cases. The highest operational stability was determined for the isoamyl propionate synthesis and the lowest one for the isoamyl hexanoate, but the differences are not substantial (about 15-20%). These results will be improved by optimization of the immobilization process using experimental design and running the process in a continuous system.

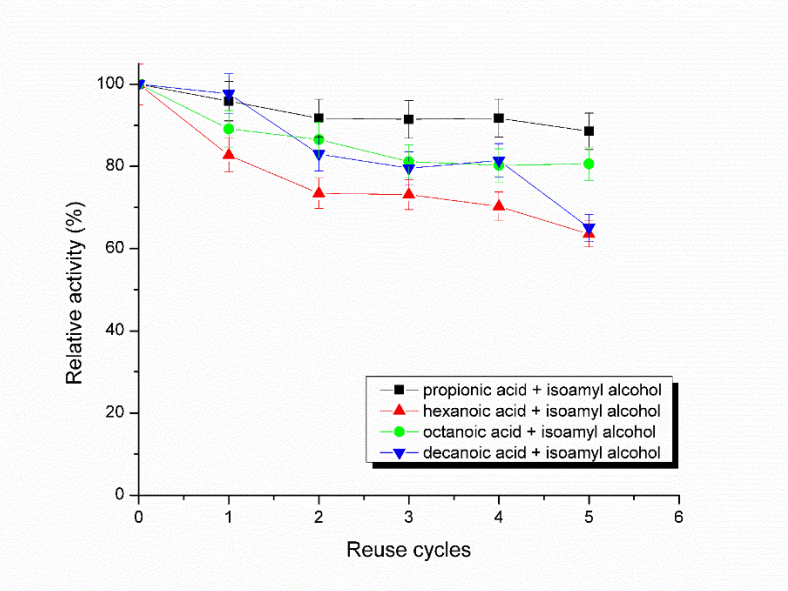

Figure 5 Multiple use of the multilayer magnetic biocatalysts in esterification reactions of four natural carboxylic acids and natural isoamyl alcohol, catalyzed by Candida antactica B lipase covalently immobilized on magnetic nanoparticles coated with poly(benzofuran-co-arylacetic acid) and embedded in a sol-gel layer from (3-glycidoxypropyl)trimethoxysilane and tetramethoxysilane (1:1)

The magnetic core enabled the biocatalyst to be easily separated from the viscous reaction mixtures by applying a magnetic field, thereby ensuring that no enzymes remained in the final product. The researchers also conducted a detailed characterisation using TEM, SEM-EDX (Figure 6) and VSM magnetometry to confirm the structure. It was observed the core-shell architecture and verified that the enzyme had been successfully confined. The new biocatalyst retained over 90% of its initial activity after multiple uses in ester synthesis. It also exhibited enhanced thermal stability, remaining active even at the high temperatures often used to drive esterification. In short, this case study illustrates how the combination of covalent immobilization and encapsulation on a magnetic carrier can result in an efficient, recyclable and easily separable enzyme system for solvent-free green synthesis.

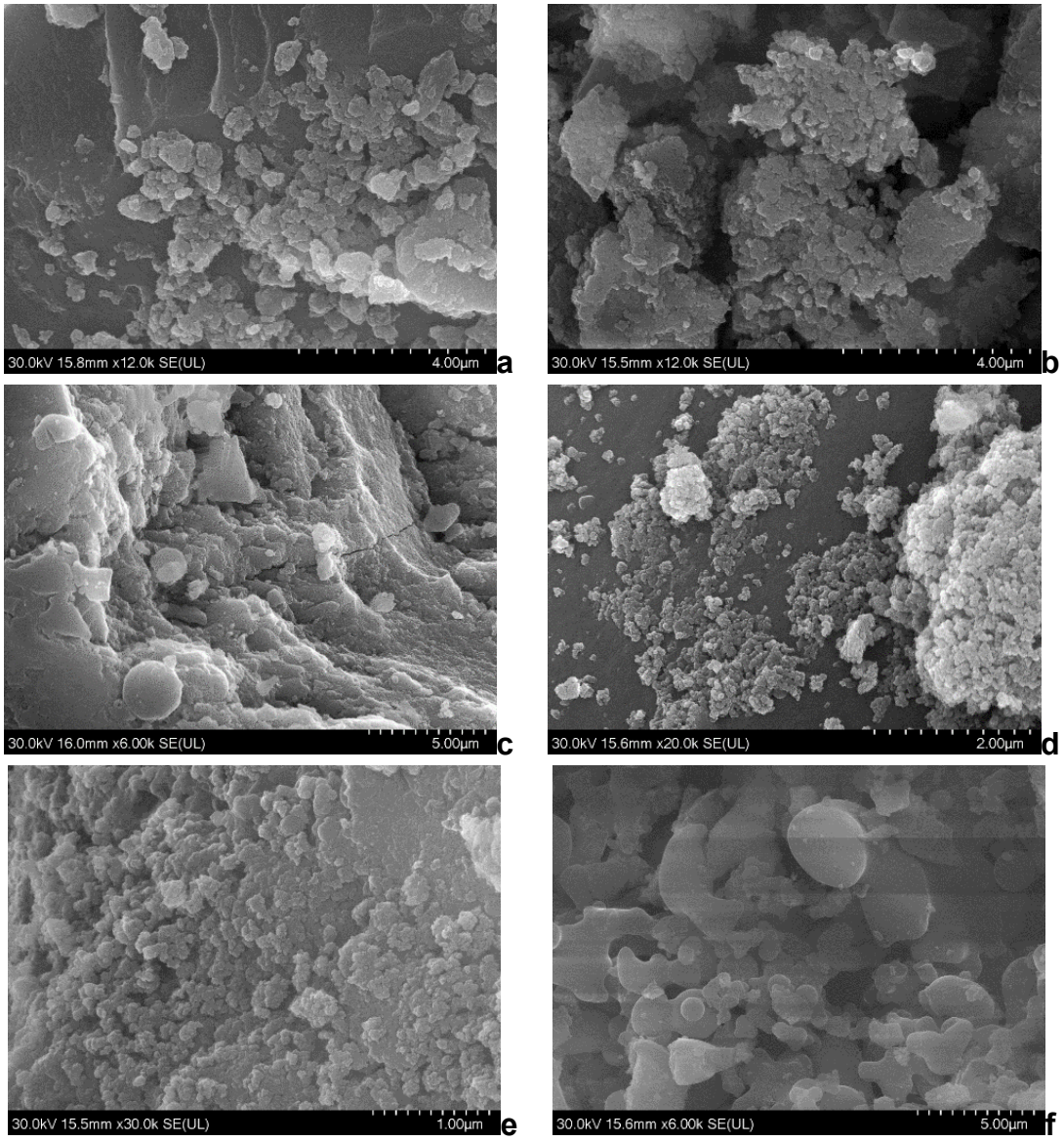

Figure 6 SEM images of the Multilayer magnetic sol-gel immobilized biocatalyst magnetic sol-gel biocatalysts: a) COV-COOH-SG1; b) COV-COOH-SG2; c) COV-COOH-SG3; d) COV-NH_2-SG1; e) COV-NH_2-SG2; f) COV-NH_2-SG3

The success of the magnetic CALB biocatalyst in flavour ester synthesis directly addresses industrial needs: flavour esters are traditionally produced using chemical catalysis (acid catalysts at high temperatures), which can result in by-products and require extensive purification. However, by using an immobilised enzyme for durability, the reaction can be performed at moderate temperatures with high selectivity. Furthermore, the biocatalyst can simply be pulled out with a magnet and reused, dramatically reducing waste and energy. This case also highlights the trend of using hybrid immobilization techniques to overcome the limitations of single methods.

II.2.4. Immobilization of β-galactosidase and glucose oxidase for one-pot biocatalytic conversion of lactose to gluconic acid and galacto-oligosaccharides

Immobilization is equally important in multi-enzyme cascade processes, in which multiple biocatalysts act sequentially within a single reaction vessel [8].

One example is the conversion of lactose to galacto-oligosaccharides (GOS) and gluconic acid in one pot, which requires two enzymes to work together: β-galactosidase (β-GAL) from *Kluyveromyces lactis* and glucose oxidase from *Aspergillus oryzae* (GOX) Figure 7. In 2021 [36] we designed an integrated process to convert lactose (e.g. from whey) into the prebiotic GOS (a valuable food ingredient), while simultaneously converting glucose into gluconic acid (a useful organic acid). This process takes place in a single reactor. Careful enzyme immobilization was required for both catalysts to ensure compatibility and efficiency.

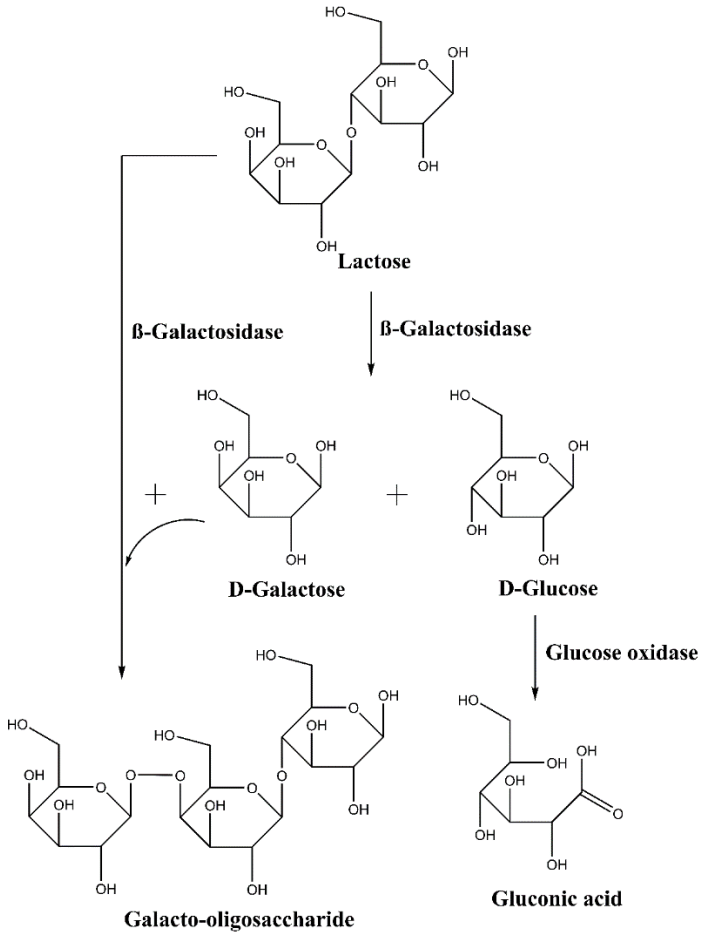

Figure 7 Lactose conversion scheme into gluconic acid and galacto-oligosaccharides using a combination of β-galactosidase and glucose oxidase in a one-pot system

Four solid supports were selected: two magnetic supports containing different amounts of Co, Ni and Zn and two methacrylate resins bearing amino and oxirane functional groups. Even though several supports were used for β-GAL immobilization, there are few reports related to covalent immobilization onto magnetic particles. Compared to the well-known Fe_3O_4 magnetic particles, these Ni-Zn or Ni-Zn-Co based magnetic particles spinel ferrites (MFe_2O_4) with different metallic cations (M: Zn, Mn, Co, Cr, Ni) have attracted interest due to their magnetic properties like superparamagnetism, spin glass behaviour, with a range of applications in different

fields such as magnetic recording, high frequency electronic cores, biomedical applications [37].

The magnetic particles were obtained by the co-precipitation method and the size distribution of the particles was measured by laser particle size analyser, showing that for both samples the particles average diameter was less than 10 μm.

To be suitable for immobilization, the magnetic particles were functionalized with amino surface groups, using 3-aminopropyl trymethoxysilane. Glutaraldehyde was used as linker for all amino activated supports. The immobilization experiments were carried out for all three selected enzymes, and the resulted activities are presented in Table 4.

Table 4 Influence of the support nature and functionalization on the activity of the immobilized enzymes

Entry	Support	Immobilized enzyme activity [μmol $h^{-1}g^{-1}$]		
		β-GAL from *A. oryzae*	β-GAL from *K. lactis*	GOX from *A. niger*
1	$(Ni_{0,4}Co_{0,2}Zn_{0,4}Fe_2O_4)-3NH_2$TMOS	146.6	37.07	41.92
2	$(Ni_{0,5}Zn_{0,5}Fe_2O_4)$ -3NH_2TMOS	321.8	30.15	30.35
3	NH_2-functionalized beads	222.7	42.16	62.04
4	Epoxy-functionalized beads	136.5	28.99	92.60

The magnetic nanocarrier $Ni_{0.5}Zn_{0.5}Fe_2O_4$ yielded the highest β-GAL activity of all the tested carriers, indicating favourable surface chemistry for the enzyme. Using magnetic particles facilitated the easy removal or recycling of the enzyme again, which is crucial because, in a milk-derived substrate mixture, one wants to avoid introducing contaminants (the immobilised enzyme remains confined).

GOX was immobilised on a porous, controlled carrier with epoxy functional groups (a commercially available epoxy-activated resin). This method provided a strong covalent attachment for the robust enzyme GOX.

Immobilised β-galactosidase (β-GAL) and glucose oxidase (GOX) were used together in a batch with lactose as the substrate. The β-GAL enzyme performed transgalactosylation on the lactose, producing GOS (oligosaccharides) and glucose. The GOX enzyme then consumed the glucose, producing gluconic acid. GOX pulls the equilibrium of β-GAL forward by removing glucose, favouring the formation of more oligosaccharides (and also preventing glucose from accumulating, since glucose is known to inhibit GOS synthesis by β-GAL). This resulted in a significant increase in GOS yield compared to using β-GAL alone. For instance, at a high lactose concentration (approximately 24% solution), the one-pot system with immobilised enzymes produced a GOS yield of around 70%, whereas the GOS yield with free enzymes (β-GAL and GOX in solution) was approximately 45–50% under similar conditions (and even lower without GOX). This significant improvement highlights the power of coupling enzymes in cascade and the necessity of immobilization to achieve this efficiently. The gluconic acid was produced in near-quantitative yield relative to the glucose removed, adding value and eliminating a waste by-product.

Both pH and temperature studies were carried out with the immobilized enzymes which demonstrated the highest activities in the previous studies, β-GAL

covalently attached to $Ni_{0,5}Zn_{0,5}Fe_2O_4$ magnetic particles, surface-coated with NH_2-TMOS, at 10% protein loading (MG2-βGAL), and GOX covalently attached to butyl-epoxy polymethacrylate beads, at 10% protein loading (EPX-GOX), respectively.

Usually, native enzymes present activity in a narrow pH range, but this inconvenience could be solved by immobilization. In this study, the pH profiles of native and immobilized β-GAL and GOX were assayed in the pH unit ranges of 4 to 8, and 4 to 9, respectively.

The results indicate the improvement of the pH profiles for both biocatalysts subsequent to immobilization (Figure 8 a and b). The immobilized β-GAL maintained its highest activity up to 5.5, and at pH 6.5 the activity was 55% of the maximal value. The covalent binding had a positive effect for GOX, too. In a broad pH range (from 5.5 to 9) the activity of the immobilized EPX-GOX was at least 80% of the maximal value. Similar effect of pH on enzyme activity was reported when β-GAL from *Aspergillus oryzae* was immobilized onto chitosan magnetic particles. The GOX immobilization was not intensively studied and there are only a few reports related to the full characterization of the immobilized biocatalyst.

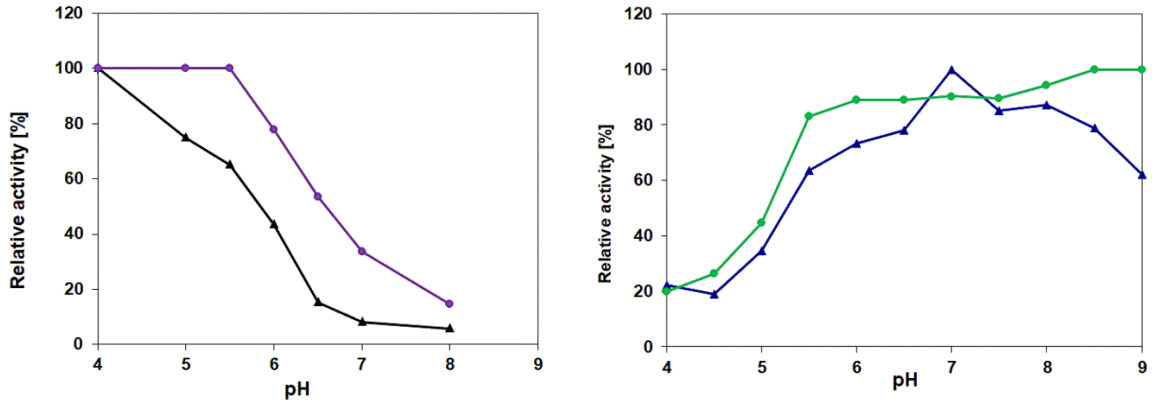

Figure 8 (a) pH profiles of native (black) and covalently immobilized (purple) β-GAL from Aspergillus oryzae; (b) pH profiles of native (blue) and covalently immobilized (green) GOX from Aspergillus niger.

The effect of the temperature on the activity of the native and covalently immobilized β-GAL and GOX was investigated at temperatures in the 30-60°C range, by incubation for 2 h. The activities were expressed as percentage of the highest value. The results (Figure 9 a and b) indicate a significant increase of the thermal stability for both covalently attached biocatalysts (MG2-βGAL and EPX-GOX), particularly at temperatures higher than 40°C. At 50°C, the native GOX lost 80% of the initial activity, while the immobilized GOX still preserved about 75% of this value. In the case of β-GAL, the relative activity percentages at the same temperature were 60% for the native and 95% for the immobilized enzyme, respectively.

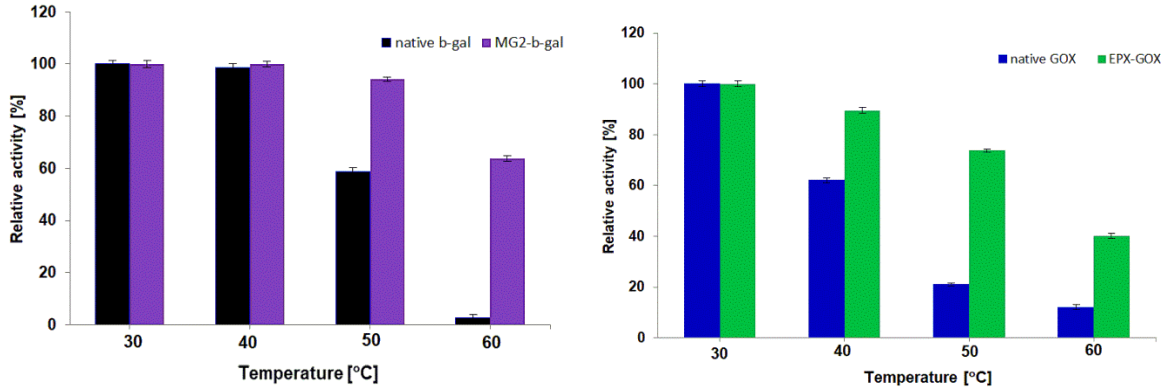

Figure 9 Thermal stabilities of (a) native (black) and covalently immobilized (purple) β-GAL from Aspergillus oryzae (b) native (blue) and covalently immobilized (green) GOX from Aspergillus niger.

The best-performing immobilized biocatalysts were used in consecutive reaction cycles, at the optimal pH values for the ONPG and lactose hydrolysis (MG2-βGAL) and glucose oxidation (EPX-GOX), respectively. The biocatalysts were recovered from the reaction mixture after each batch reaction cycle through magnetic/filtration separation, were washed 4 times with phosphate buffer, and reused in another reaction. Ten reaction cycles were performed using MG2-βGAL as biocatalyst and ONPG as substrate. The results indicate excellent stability of the biocatalyst, as about 85% of the activity was recovered after 10 reaction cycles. The increase of the operational stability of MG2-βGAL in multiple uses was also demonstrated for the lactose substrate (Figure 10). After 5 reaction cycles, more than 90% of the initial activity was recovered.

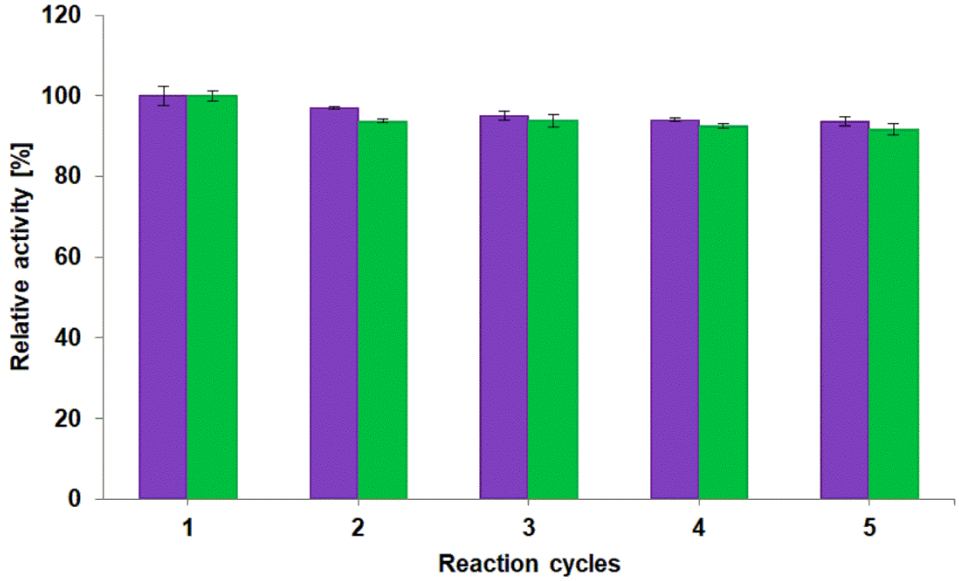

Figure 10 Stability of β-galactosidase immobilized on magnetic particles MG2- βGAL (violet) and glucose oxidase immobilized on epoxy-functionalized methacrylate resin EPX-GOX (green), in repeated batches of conversion of lactose and glucose, respectively.

This lactose bioconversion process is an example of green innovation: an otherwise waste product (whey lactose) can be converted into the prebiotic GOS and gluconic acid in one reactor, without the use of chemicals, by employing immobilised enzymes. This process eliminates the need for separate enzymatic or chemical steps to produce gluconic acid. Since the enzymes are immobilised, they can easily be

separated from the food-grade products (which is important for regulatory reasons) and reused. The success of the process was dependent on the strategy used for immobilization (magnetic for β-GAL and epoxy for GOX), which enabled the precise coordination of the two enzymes and the labile intermediate (H_2O_2) in terms of both space and function.

The time-course studies of the one-pot reactions were performed at six different substrate concentrations (from 40 to 165 mM), using native and immobilized biocatalysts. The reaction parameters were set at the optimal values resulted from the experimental design. Using the immobilized biocatalysts (MG2-βGAL and EPX-GOX) higher reaction time was needed for lactose conversion, and high conversions were reached only after 20 h of reaction (Table 5). Compared to the native multienzyme system, the formation of GOS was affected, but higher gluconic acid yields were achieved. At lower initial substrate concentrations, up to 80 mM, higher than 90% lactose conversions were obtained and the gluconic acid yields exceeded 80%, gluconic acid and galactose being the main products identified at the end of the reaction. The presence of GOS was observed only in the experiments with higher initial substrate concentration. The chain elongation was favoured at increased reaction time, the presence of 4-unit GOS being observed after 48 h. Based on the outcome of the time course study, the efficiency of the immobilized biocatalyst was demonstrated, and the process can be considered able for upgrading at continuous level.

Table 5 Lactose conversion, gluconic acid and GOS yields in the one-pot system using immobilized β-galactosidase MG2-β-GAL and glucose oxidase EPX-GOX

Initial lactose concentration 40 mM				
Time [h]	Lactose conversion [%]	Gluconic acid yield [%]	GOS yield [%]	$DP_{max.}$
3	11.92	19.01	n.d.	n.d.
6	37.15	36.04	n.d.	n.d.
20	44.48	54.26	n.d.	n.d.
24	47.53	64.71	n.d.	n.d.
48	99.28	70.48	n.d.	n.d.
72	99.77	79.57	n.d.	n.d.
Initial lactose concentration 60 mM				
Time [h]	Lactose conversion [%]	Gluconic acid yield [%]	GOS yield [%]	DP max
3	15.01	19.22	n.d.	n.d.
6	41.08	47.75	n.d.	n.d.
20	63.64	56.34	n.d.	n.d.
24	72.27	79.28	n.d.	n.d.
48	99.88	85.22	n.d.	n.d.
72	99.98	88.40	n.d.	n.d.
Initial lactose concentration 80 mM				
Time [h]	Lactose conversion [%]	Gluconic acid yield [%]	GOS yield [%]	DP max
3	4.24	5.88	n.d.	n.d.
6	12.13	21.43	n.d.	n.d.

20	40.86	49.21	n.d.	n.d.
24	43.49	57.91	n.d.	n.d.
48	53.89	55.06	n.d.	n.d.
72	65.01	69.29	n.d.	n.d.
Initial lactose concentration 120 mM				
Time [h]	Lactose conversion [%]	Gluconic acid yield [%]	GOS yield [%]	DP max
3	3.82	1.26	2.56	3
6	9.01	7.82	1.19	3
20	32.68	18.31	7.25	3
24	33.04	25.80	8.67	3
48	83.46	46.06	15.20	3
72	83.53	68.33	27.40	3
Initial lactose concentration 140 mM				
Time [h]	Lactose conversion [%]	Gluconic acid yield [%]	GOS yield [%]	DP max
3	3.72	2.81	4.95	3
6	15.36	6.66	7.01	3
20	23.82	12.15	14.69	3
24	32.22	30.48	20.22	3
48	86.88	47.11	23.41	4
72	86.71	59.93	22.39	4
Initial lactose concentration 165 mM				
Time [h]	Lactose conversion [%]	Gluconic acid yield [%]	GOS yield [%]	DP max
3	5.76	4.05	1.72	3
6	7.62	13.59	12.85	3
20	20.80	14.92	15.88	3
24	33.19	17.34	22.56	3
48	87.72	25.69	27.80	4
72	91.51	37.46	34.06	4

These results demonstrate the viability of the one-pot concept, using immobilized biocatalysts, for the studied system. Among the possible immobilization methods, covalent binding is more suitable, because the reaction media is aqueous and leaching of the enzyme from the support is avoided. Since the stability of the investigated enzymes is different, two different immobilization supports were tested, allowing the selection of the best solution for every case. If the activity of one enzyme is affected, this enzyme can be replaced, meanwhile the other can be further used, allowing the development of a cost-effective biocatalytic process.

II.3.3. Covalent immobilization of laccases for waste valorisation: glycerol oxidation

The biodiesel industry produces glycerol as a waste by-product, so finding environmentally friendly ways to upgrade it is highly desirable. In a 2023 study, we addressed this issue by using covalently immobilised laccase enzymes to selectively oxidise glycerol. Laccases (multi-copper oxidases) usually oxidise phenolic compounds, but with the right mediators, they can also oxidise aliphatic polyols such as glycerol to create valuable products such as glyceric acid and dihydroxyacetone [38]. Prior to the experimental work, computational analysis of all four commercially available laccases from *Trametes versicolor (TvL), Aspergillus* sp.(*AspL*), *Rhus vernicifera* and *Agaricus bisporus* was carried out, to assess the possibilities of covalent bonds forming with the support without involving the active site region, as well as allowing supplementary attachment of the enzyme by hydrophobic interactions. First, the number and the position of lysine residues potentially involved in the covalent binding was evaluated [38]. The analysis indicates that the laccase from *T. versicolor* (Figure 11A) has 8 superficial Lys residues, *Aspergillus sp*. (Figure 11B) and *A. bisporus* (Figure 11C) have 12, and the laccase from *R. vernicifera* (Figure 11D). In this latter case, at least six residues are located in the proximity of the active site, a feature that can affect the immobilization, since the formation of the covalent bond can occlude the active site [36].

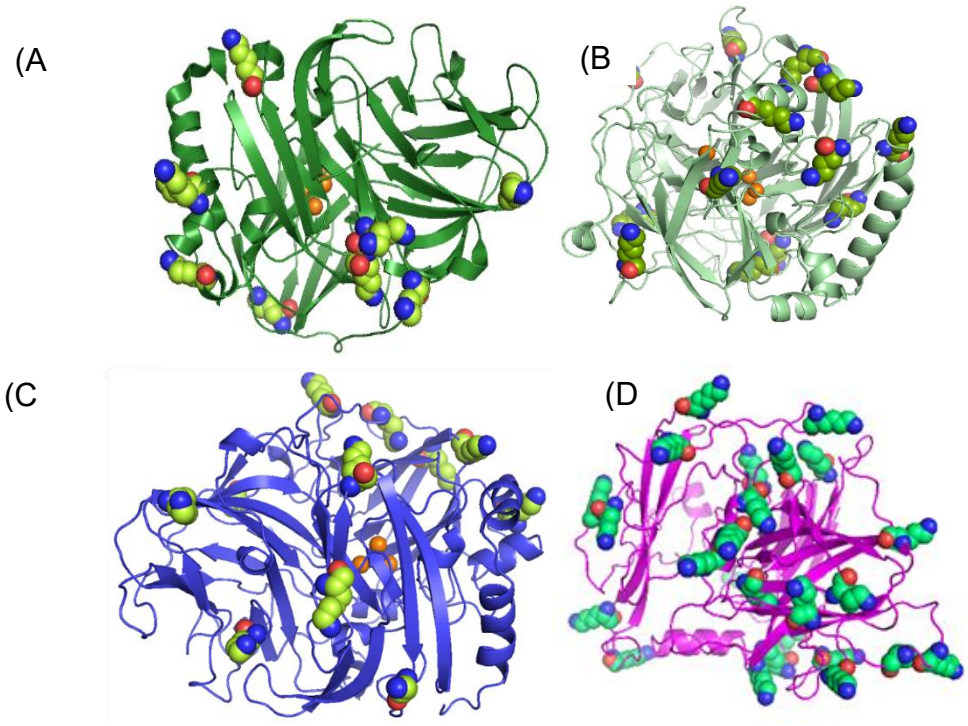

Figure 11 Structures of laccases from T. versicolor (PDB 1GYC) (A) Aspergillus sp. (PDB code 6F5K) (B), and homology models of A. bisporus (C) and R. vernicifera (D) represented in new cartoon mode. The Lys residues are highlighted in green (sphere mode) whereas Cu ions are orange.

The screening study was performed at the optimum pH value, experimentally determined for each laccase: pH 5 for *T. versicolor*, pH 3 for *Aspergillus sp*., pH 7.0 for *R. vernicifera* and pH 8.0 for *A. bisporus*.

The obtained results, expressed as glycerol conversions for all 4 selected laccases after 96 hours reaction time were included in Table 6, indicating that the laccase from *T. versicolor* was the most effective one, as the conversion of glycerol after 96 hours reached 70%. In the presence of the laccase from *Aspergillus* sp. the conversion value was only about 10%, while in the case of laccases from *R. vernicifera* and *A. bisporus* it did not exceed 5%. Based on these results, the laccases from *T. versicolor* and *Aspergillus sp*. were considered for the subsequent optimization experiments.

Table 6 Glycerol conversions obtained in the oxidation catalyzed using free laccases from various sources, using 30 mM TEMPO at 25 °C, 1000 rpm and 96h

Laccase source	Glycerol conversion [%]
T. versicolor	70.1 ± 4.6
Aspergillus sp.	10.2 ± 2.8
R. vernicifera	4.9 ± 1.6
A. bisporus	4.8 ± 1.4

Nine different supports (Figure 12) were investigated for the covalent bonding immobilization of both selected laccases. Three were methacrylic resins, two of them functionalized with epoxy groups and one with amino groups, and six were magnetic supports, mixed ferrites functionalized with amino groups by reaction with NH_2-TMOS or NH_2-TEOS. As magnetic supports Ni-Zn ferrites and Ni-Co-Zn ferrites were considered, for the first time as carriers for the covalent immobilization of laccases. Although the specific optical and magnetic properties which made these materials suitable for a wide range of applications are probably less important for biocatalysis, we presumed that the physical interactions with the enzyme at the surface of the microparticles could influence the conformation and catalytic properties of the enzyme. The catalytic efficencies of the resulted immobilized enzymes were evaluated by using 2,6-dimethylphenol (2,6-DMP) as substrate.

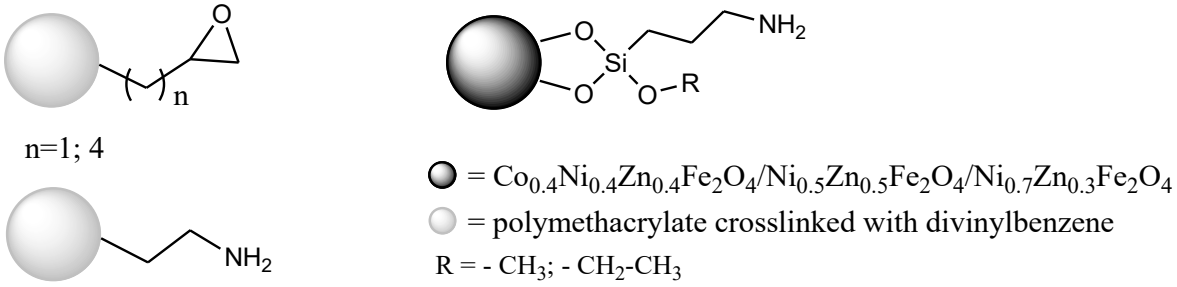

Figure 12 Schematic representation of the carriers used in the immobilization study of laccases

Eighteen different covalent immobilization preparations of fungal laccases were evaluated. These included laccases immobilised on various carriers (e.g. agarose, silica and synthetic resins), which were functionalised with groups such as aldehyde (glutaraldehyde-activated), epoxy or carboxyl to form covalent bonds with the enzyme. Screening allowed the identification of supports that produced high immobilization yields and retained activity. A key observation was that supports creating multipoint

attachment could greatly enhance thermal and operational stability; however, too much binding could reduce activity, so achieving an optimal balance was essential.

The results obtained using the methacrylic resin supports are presented in Figure 13, showing that the highest enzymatic activity values were obtained for the *TvL* preparations. The preparation obtained using the support functionalized with epoxy-butyl groups proved the highest catalytic efficiency (760.99 U/g), followed by the support functionalized with amino groups (581.32 U/g). Contrary, for the laccase from *AspL*., the highest activity value was obtained for the preparation immobilized on methacrylic resin functionalized with amino groups (156.33 U/g). It can also be seen that the activity of both enzymes was lower for covalent binding on supports with epoxymethyl groups (327.61U/g and 28.80 U/g for *TvL* and *AspL*. respectively), indicating a dependency of the recovered enzyme's activity on the length of the spacer chain [39].

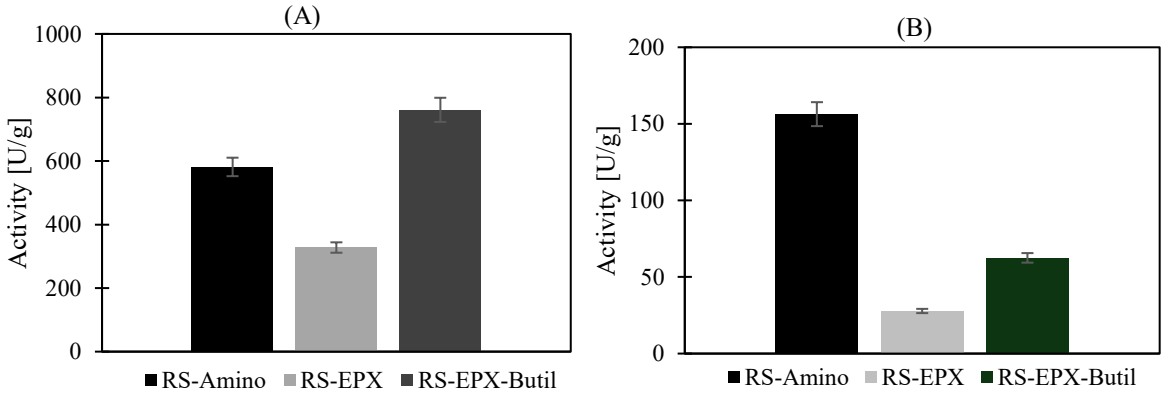

Figure 13 Activity of Trametes versicolor (A) and Aspergillus sp. (B) laccases covalently immobilized on Lifetech™ methacrylic resins functionalized with amino (RS-Amino), epoxy (RS-EPX) and butyl-epoxy (RS-EPX-Butil) groups, respectively.

Prior to the immobilization, the supports were functionalized with amino groups by using two silane precursors. The results presented in Figure 14 show higher activity values for all preparations obtained using the laccase from *T. versicolor* and 3-NH_2-PrTMOS as functionalization silane. Among the 3 types of magnetic particles tested, the highest activity value was obtained for the MG-Zn_2 particles.

In the case of preparations obtained using laccase from *AspL*, the activity values were slightly higher when 3-NH_2-PrTEOS was used as silane precursor, and for the MG-Zn2 support the activity value was 250 U/g, the highest obtained for this type of support.

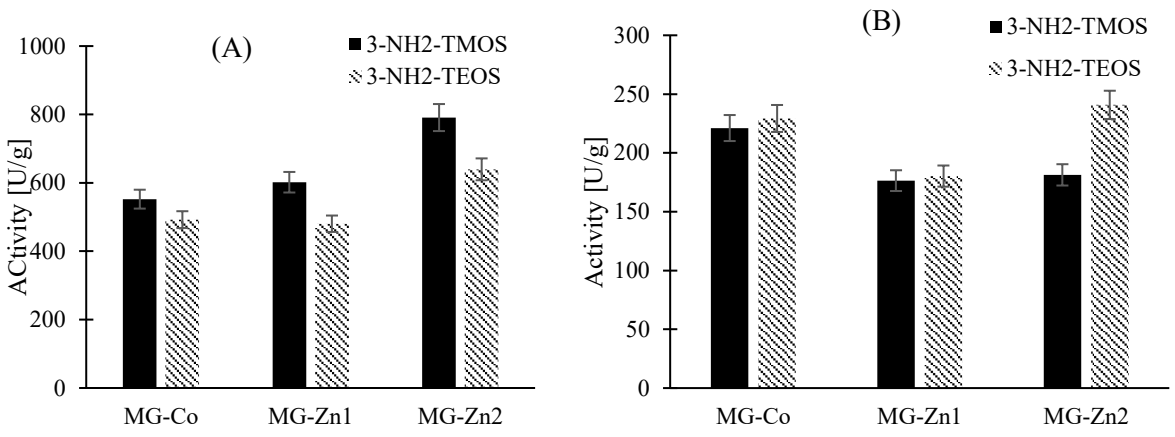

Figure 14 Activity of TvL (A) and AspL. (B) laccases immobilized on magnetic supports functionalized with amino groups.

pH and temperature profiles of the native and immobilized laccases

The results are presented in Figure 15 for the *TvL.* The results indicate that TvL immobilized on epoxymethacrylate support had optimal activity value at pH 4.0, while for the same enzyme immobilized on magnetic support functionalized with 3-aminopropyltrimethoxysilane groups the optimal pH was 6.5.

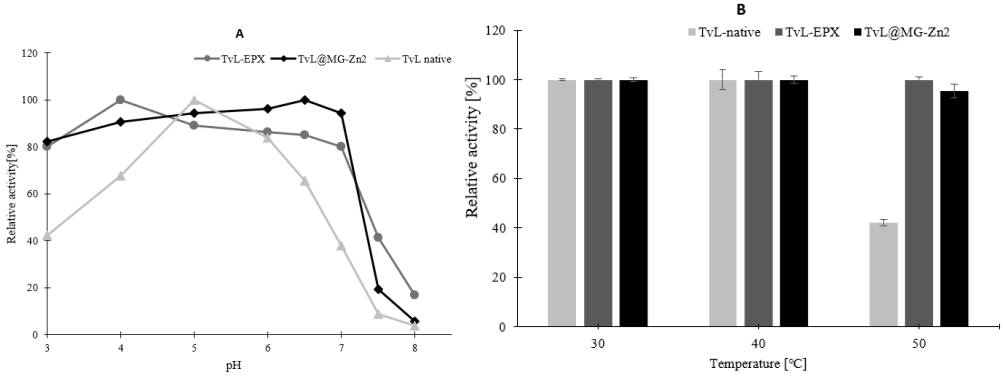

Figure 15 pH profile (A) and influence of the temperature on the activity (B) of Trametes versicolor laccase, native (TvL-native) or immobilized on epoxymethacrylate support (TvL-EPX), and on magnetic support functionalized with 3-NH_2-PrTMOS (TvL@MG-Zn_2).

The effect of temperature was evaluated onto the activity of native and immobilized TvL by covalent binding on methacrylate support functionalized with epoxy-butyl groups and on magnetic support functionalized with 3-aminopropyltrimethoxysilane, in the temperature range from 30°C to 50°C (Figure 15B). For the native laccase the activity decreased significantly at temperatures higher than 40°C. Compared to the native enzyme, both immobilized enzyme preparations demonstrated higher activity at 50°C.

The operational stability of all 18 immobilized laccase preparations was studied in consecutive batch reaction cycles of the 2,6-dimethylphenol model substrate. The results are presented in Figure 16A for the *ApsL* preparations and in Figure 16B for the *TvL* preparations. Overall, the stability in consecutive reaction cycles of the immobilized laccases was dependent on the immobilization support.

For the *AspL* immobilized onto magnetic supports, the activity decreased dramatically (>90%) after the first reaction cycle, especially when 3-NH_2-PrTEOS was used for support functionalization. These results suggest that even though the activity after immobilization was higher compared to the samples functionalized by 3-NH_2-PrTMOS, the stability in consecutive reaction cycles was lower. Among the biocatalysts obtained by immobilization onto methacrylic resins, the preparate obtained by using the support functionalized with epoxybutyl groups (Figure 16B) was the most stable, preserving more than 60% of the initial activity after 6 reaction cycles.

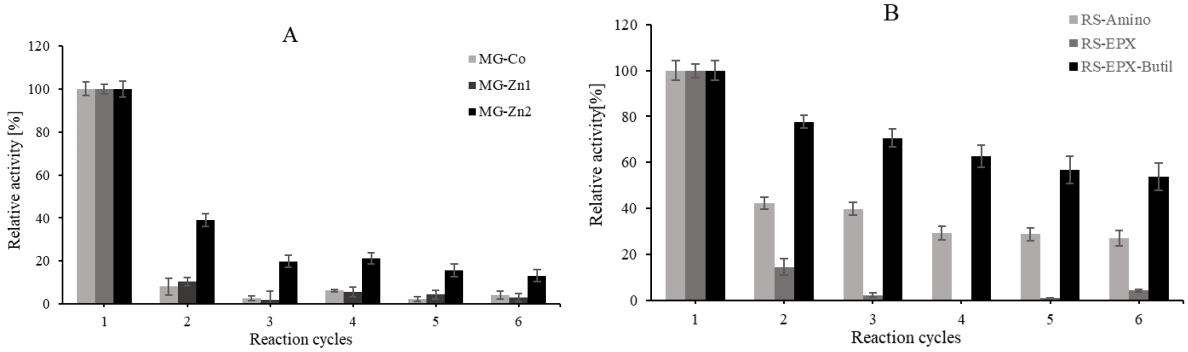

Figure 16 Operational stability of ApsL immobilized (A) on magnetic microparticles functionalized with 3-NH_2-PrTMOS and (B) covalently immobilized on Lifetech™ methacrylic resins functionalized with amino (RS-Amino), epoxy (RS-EPX) and butyl-epoxy (RS-EPX-Butil) groups, respectively. The activity in the first cycle was considered as reference.

For the *TvL* immobilized on magnetic supports, the best results were obtained when 3-aminopropyltrimethoxysilane silane was used for functionalization (Figure 17), when the activity drop after the first reaction cycle was lower, for all types of magnetic supports. Particularly, the recovery of over 47% of the initial activity after five reaction cycles in case of the MG-Zn_2 biocatalyst can be appreciated as good operational stability.

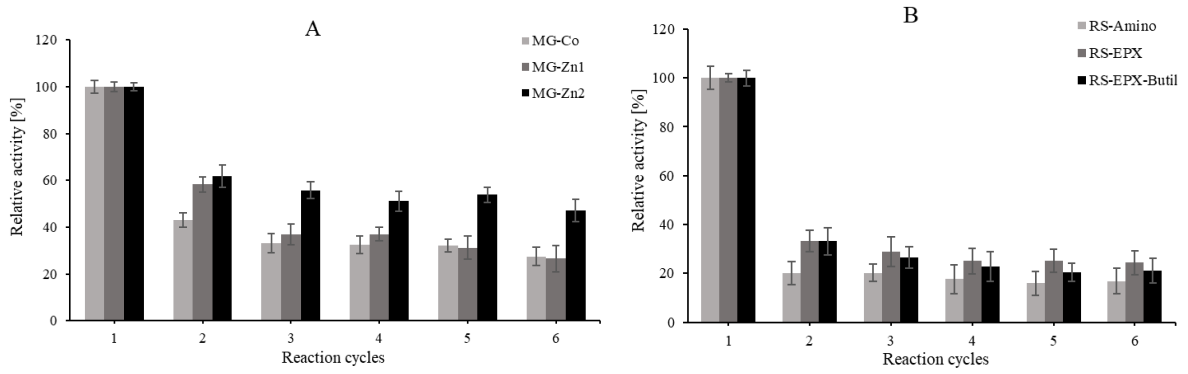

Figure 17 Operational stability of TvL preparations immobilized on (A) on magnetic microparticles functionalized with 3-NH_2-PrTMOS; (B) covalently immobilized on Lifetech™ methacrylic resins functionalized with amino (RS-Amino), epoxy (RS-EPX) and butyl-epoxy (RS-EPX-Butil) groups, respectively. The activity in the first cycle was considered as reference.

Characterization of the immobilized laccases

Surface chemical compositions of the best performing biocatalyst, TvL@MG-Zn_2, were investigated following immobilization and reduction with $NaBH_4$, and after 5 reutilizations, respectively, by X-ray photoelectron spectroscopy (XPS). The initial

immobilization support before functionalization, MG-Zn_2, a nominal $Ni_{0.7}Zn_{0.3}Fe_2O_4$ magnetic ferrite sample, was used as reference. XPS spectra of the magnetic particle and of the enzyme immobilized on magnetic particles are shown in Figure 18.

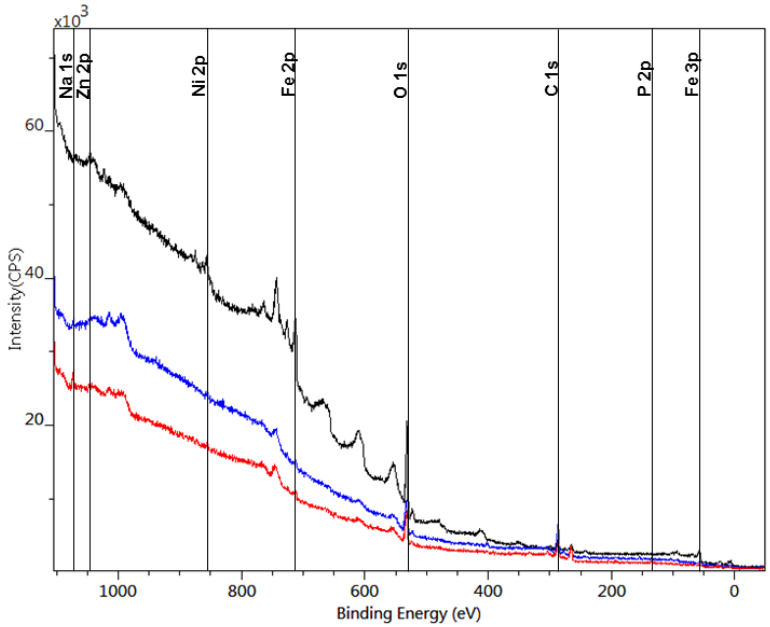

Figure 18 Overlay of the XPS wide spectra of MG-Zn2 (black), TvL@MG-Zn2 (blue) and TvL@MG-Zn2-RT (red) samples.

After the immobilization of laccase enzyme on the magnetic particle surface, iron was still detectable by XPS in a decreased quantity. On the original MG-Zn_2 surface, iron was present in 17 atomic % which in the case of the enzyme coated samples decreased to 3 atomic %. After enzyme immobilization, nickel and zinc could not be detected on the particle surfaces. Silicon from the activator NH_2-TMOS or NH_2-TEOS could neither be detected on the surfaces of TvL@MG-Zn2 and TvL@MG-Zn2-RT by means of XPS.

In the case of MG-Zn_2 sample, surface oxygen was found in oxide (BE 529.7 eV) and hydroxide (BE 531.204 eV) forms (Figure 19). The presence of hydroxyl groups is advantageous since they activate the surface and promote the adhesion of the coating. In TvL@MG-Zn_2 sample, the chemical shift of oxygen refers to the original oxide form and furthermore, carbonyl (BE ≈ 530.4 eV) and hydroxyl groups (BE ≈ 532.0 eV) of the immobilized enzyme moiety. In TvL@MG-Zn_2-RT sample, after several use of the enzyme coated MPs in catalytic reactions, carboxylate compounds appeared in the sample with an increased chemical shift of the O 1s line (BE ≈ 533.0

eV).

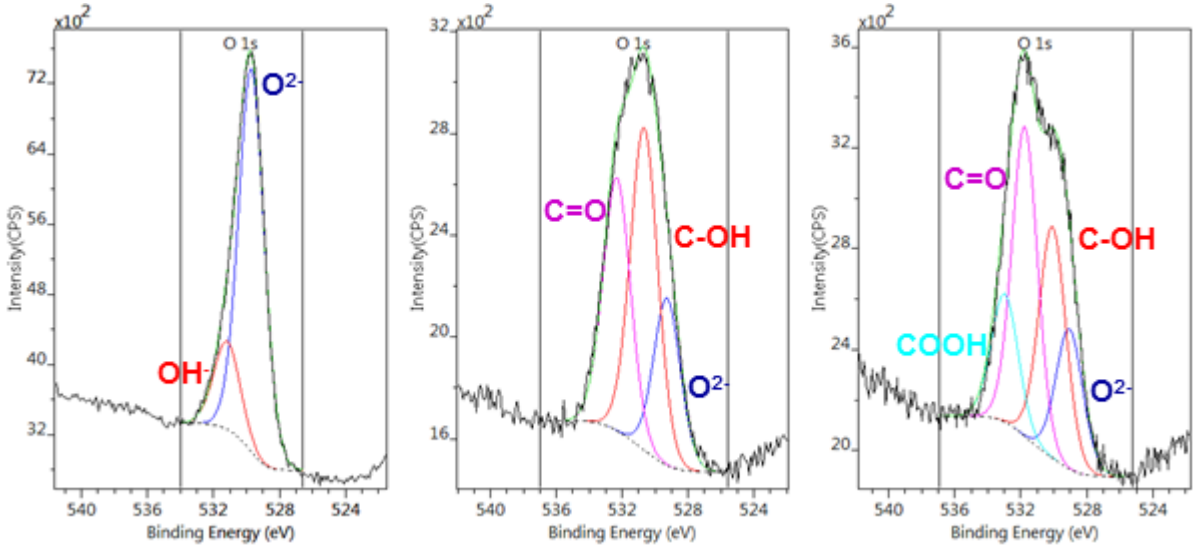

Figure 19 Oxygen 1s spectra of MG-Zn2 (A), TvL@MG-Zn2 (B) and TvL@MG-Zn2-RT (C) samples.

The SEM images of the MG-Zn support magnetic particles before (Figure 20A) and after immobilization of *Tv*L (Figure 20B) and also after the utilization of the TvL@MG-Zn2-RT in 5 reaction cycles indicates a similar morphology of the particles. Not any changes were expected though, since the nanometer thick laccase layer assessed from XPS calculations does not affect the microstructure of the particles. However, an important issue is that long-term use of the biocatalyst, in repeated batch cycles (Figure 20C), did not affect the surface morphology, hence the physical stability is high and represents the fundament of the good operational stability.

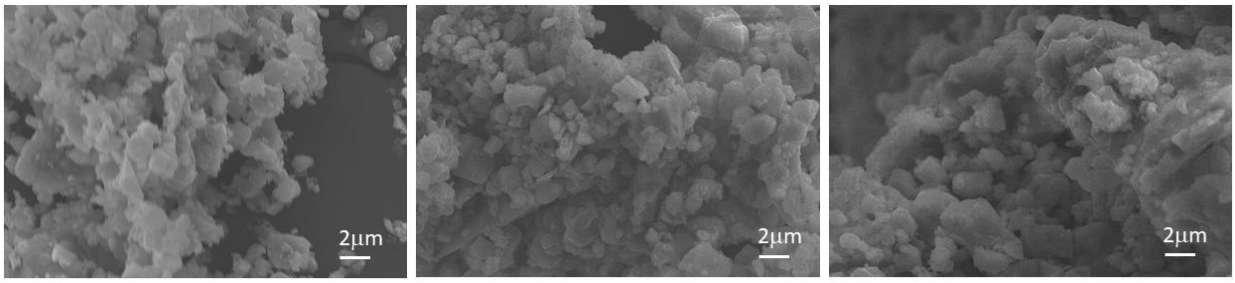

Figure 20 SEM images of MG-Zn support before immobilization (A), after TvL immobilization onto MG-Zn_2 magnetic particles using 3NH_2-TMOS and $NaBH_4$ (TvL@MG-Zn_2) (B), and after 5 reutilizations of TvL@MG-Zn_2-RT, (C) at 10000x magnitude.

The immobilised laccases were tested for their ability to oxidise glycerol in the presence of a mediator that shuttles electrons. The aim was to achieve a high conversion of glycerol to glyceric acid, a valuable chemical used in cosmetics and pharmaceuticals. Free laccase in solution produced a low conversion rate and was not reusable, but the most effective immobilised laccase system achieved a glycerol conversion rate of around 75%. There was a shift in selectivity towards glyceric acid, with a yield of around 20% of glyceric acid under these conditions, and the remainder being mostly dihydroxyacetone and tartronic acid. Although a 20% yield may seem modest, it represents a significant increase in glyceric acid selectivity compared to

unoptimised conditions (some initial trials yielded <5–10% glyceric acid). Immobilization was key to achieving this improved selectivity: by confining the laccase to a support, the local concentrations of the mediator and substrate near the enzyme can differ from those in the bulk solution, potentially favouring certain reaction pathways.

The results (Figure 21) show the increase in conversion in the first 72 hours. Compared to the native enzyme, there is a decrease of the biocatalyst efficiency, which may be due to the limited substrate access to the catalytic site of the enzyme because of the covalent binding, or due to a possible long-term temperature instability of the preparations.

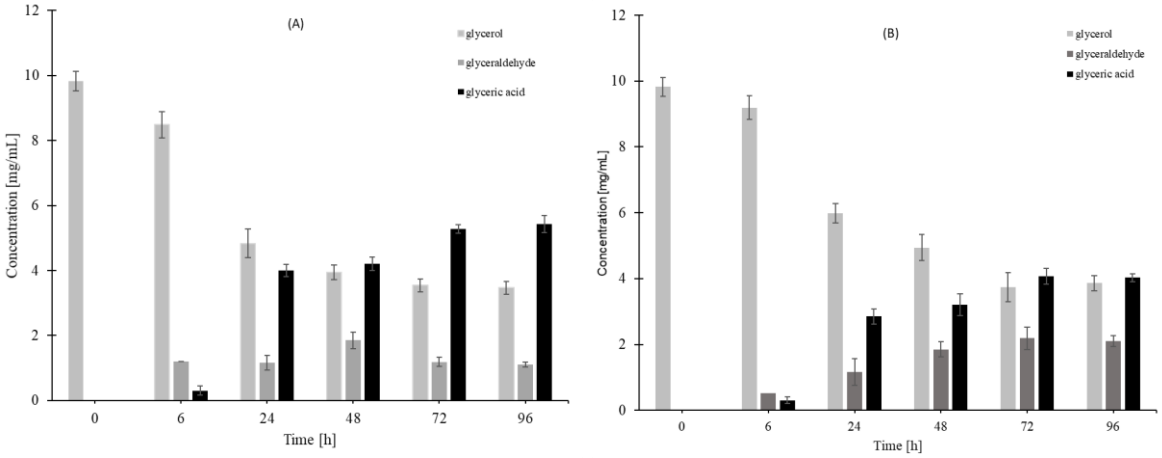

Figure 21 Concentration values of glycerol, glyceraldehyde and glyceric acid over time in the presence of immobilized T. versicolor laccase on (A) Ni-Zn ferrite magnetic support (TvL@MG-Zn2) and (B) on methacrylic resin functionalized with epoxy butyl groups (RS-EPX-Butil), at 50°C, using 20 mg mL^{-1} immobilized enzyme.

The selectivity of the enzyme towards glyceric acid as main oxidation product does not change following the immobilization process compared to the native laccase, but the immobilized biocatalyst owns all the well-known advantages, particularly reusability.

The results demonstrated that by appropriate selection of the immobilization supports and parameters the glyceric acid yield can be increased up to 50% and the biocatalyst preserves its activity and selectivity over several batch reaction cycles.

Glyceric acid is a dihydroxy acid with very promising applications, e.g. as bioplastic monomer [40]. Although it can be obtained by microbial fermentation too [41], the biocatalytic oxidation could represent a better alternative owing to the higher yields that can be achieved and the advantage of avoiding the possible drawbacks of a fermentation process.

Even though the enzymatic oxidation process is not enantioselective, most of these applications, like for surfactants or bioplastic monomers, do not require the utilization of a single monomer, and can be accomplished with D,L-glyceric acid, as well.

The performances of the selected biocatalyst were evaluated in multiple reaction cycles, also for glycerol oxidation. Each reaction cycle was performed for 72 h and the results are presented in Figure 22 as percentage compared to the initial

value. After 5 reaction cycles about 46% of the initial activity was recovered. The decrease in activity can be attributed to the long term incubation of the biocatalyst during each reaction cycle.

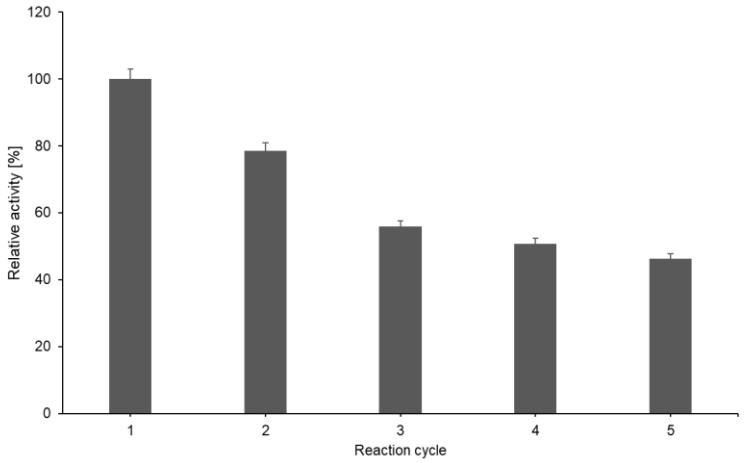

Figure 22 Operational stability of Trametes versicolor laccase immobilized on Ni-Zn ferrite magnetic support functionalized with 3-NH_2-PrTMOS (TvL@MG-Zn_2) and reduced with $NaBH_4$, on glycerol substrate

II.3.4. Immobilization of transaminases in non-aqueous media

Another important example is the immobilization of ω-transaminase for use in organic solvent systems. Although transaminases are promising biocatalysts for chiral amine synthesis, they typically require an aqueous environment. In our work [42] we adopted a pioneering approach, directly observing the enzyme's conformation upon immobilization to inform the design of a transaminase immobilised on EziG resin (a porous glass with metal-affinity properties, marketed by EnginZyme), which can be used in organic solvents and low-water conditions.

These studies were conducted as part of Iulia Radoi's doctoral research project, entitled 'Advanced Morphological and Spectroscopic Characterisation of Immobilised Enzymes and Surface Analysis'. The project received funding from the European Union's Horizon 2020 Research and Innovation Programme, under Grant Agreement No. 860414.

Transaminases (TAs), also known as aminotransferases (EC 2.6.1), are enzymes that catalyze the transamination reaction between an amino acid and an α-keto acid, by using the coenzyme pyridoxal-5'-phosphate (PLP) [43]. PLP, the active form of vitamin B6, forms a Schiff base with the ε-amino residue of lysine in the active site. The amino group is transferred from an amino donor to PLP, yielding the pyridoxamine-5-phosphate (PMP), while the amino donor is released as the corresponding ketone. The amino acceptor compound reacts with PMP to form the corresponding amine and thereby automatically regenerates the PLP. The position of the amino group in the substrates accepted by the transaminases determines their classification as α-TAs and ω-TAs. α-TA allows the formation of only α-amino acids, while ω-TA can perform transfer of an amino group from a substrate that have several carbon atoms between the carboxyl and the amino groups. ω-TAs are of higher

interest since they can aminate a wider range of substrates, such as keto acids, aldehydes, ketones, ketones and amines..

The aim of the study was to perform a detailed characterization of immobilized ω-TAs within the carrier exploiting, in addition to confocal microscopy, the advantage brought by Fourier Transform infrared (FTIR) microscopy and imaging.

By comparing three EziG carriers (hydrophilic, hydrophobic and intermediate), it was demonstrated that the properties of the support influenced the amount of water retained by the immobilised enzyme and thus its conformation. They identified an optimal support that balanced the retention of essential water (to maintain enzyme flexibility) with the exposure of hydrophobic regions (to stabilise the structure in an organic solvent).

The immobilised ω-transaminase on the optimised support was used for amine synthesis in an organic solvent with a controlled water activity. It exhibited significantly higher activity than the free enzyme under the same conditions and retained high stereoselectivity. Furthermore, it remained stable during prolonged use in this low-water environment, whereas the free enzyme would rapidly become inactive. In essence, immobilization enabled the enzyme to function within an almost anhydrous, continuous-flow system for amine production (as referenced in related works). This expands the scope of biocatalysis to include biosolvents or solvent-intensive reactions that would typically exclude enzymes.

Figure 23B indicates the presence of several hydrophobic regions on the surface of the ω-transaminase, which are expected to interact differently with the carriers depending on their hydrophobic or hydrophilic nature. To be underlined that the enzyme was expressed in *E.coli* and, conversely, does not bear glycans that might shield such hydrophobic regions on the surface in aqueous media.

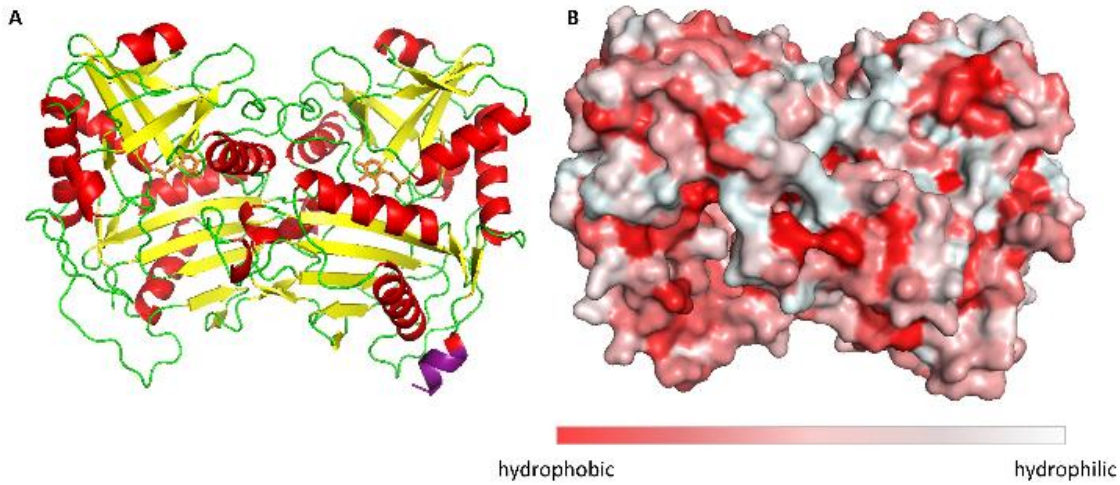

Figure 23 A: Visualization of the secondary structure of N-terminal His-tagged (R)-selective ω-transaminase from Arthrobacter sp. (His6-ATA-117). In purple the histidine tag and in orange the PLP cofactor. B: Surface hydrophobicity: in red the hydrophobic areas and in light-grey the hydrophilic areas. The figures were prepared with the PyMOL program.

Table 7 Weight variation (% w·w-1) after drying of the enzyme-free carriers (dried at 100°C) and the immobilized enzymes (dried at 25°C) pretreated with different solutions and organic solvents

Entry	Pretreatment	EziG[1]-Opal *hydrophilic* (pd: 500 ± 50 Å)		EziG[2]-Coral *hydrophobic* (pd: 300 ± 50 Å)		EziG[3]-Amber *semi-hydrophobic* (pd: 300 ± 50 Å)	
		Water adsorbed by the carrier	Weight variation after drying (+His_6-ATA-117)	Water adsorbed by the carrier	Weight variation after drying (+His_6-ATA-117)	Water adsorbed by the carrier	Weight variation after drying (+His_6-ATA-117)
1	buffer	3.4±1.1	-4.1±0.6	3.3±0.2	-0.2±0.0	3.3±0.1	-1.2±0.2
2	buffer + PLP	2.7±0.2	-2.4±0.4	3.0±0.3	+1.1±0.1	2.7±0.2	+0.3±0.1
3	buffer + sucrose	3.6±0.1	+15.3±2.1	4.4±0.1	+22.1±0.2	4.1±0.0	+19.6±0.8
4	buffer + sucrose + PLP	3.4±0.1	+17.1±1.1	4.2±0.1	+22.8±1.2	3.8±0.2	+21.3±1.2
5	iPrOH followed by toluene	1.6±0.3*	-2.0±1.4*	2.3±0.3*	-1.4±0.0*	2.0±0.6*	-3.9±1.4*

FTIR imaging, being a non-confocal microscopy, does not allow to distinguish between surface and core penetration of the enzyme. So, to have a second confirmation on the distribution of the enzyme on the surface of the carriers, but also to get information about its infiltration along the carrier depth, we used confocal laser scanning microscopy (CLSM) imaging. To this aim, we chemically labelled the His_6-ATA-117 with FITC and then immobilized it to perform the studies (the immobilized enzyme was treated according to entry 1 of Table 7). We found that His_6-ATA-117 was mainly located in the outer regions, with all three carriers following a similar distribution pattern to what it was observed with FTIR imaging. The distribution and accumulation of the enzyme differs from one bead to another, as well as from one carrier type (EziG[1]-Opal, EziG[2]-Coral or EziG[3]-Amber) to another, because they do not have a regular shape or size. In all three carriers the enzyme infiltrated towards the core of the carriers: EziG[1]-Opal 45.8±0.1 μm, EziG[2]-Coral 43.7±0.1 μm and EziG[3]-Amber 38.7± 0.1 μm respectively. The radial cross-section fluorescence profile of these EziG carriers is presented in Figure 24.

Cutting-edge analytical techniques are used to create immobilised enzymes that operate under unconventional conditions (in pure organic solvents), which could replace hazardous chemical processes used to produce chiral amines. This evolution in immobilization science marks a shift from a trial-and-error approach to a more rational, data-driven design process, aiming to create an optimal microenvironment that maximises enzyme performance and stability.

The integration of different experimental studies provided information necessary to develop rational protocols for preserving the activity of a ω-transaminase immobilized on EziGTM carriers when applied in hydrophobic organic solvent (toluene). Infrared microspectroscopy and imaging, coupled with confocal microscopy, not only allowed the direct observation of the distribution of the immobilized transaminase on the carriers but also disclosed a specific conformational change in a β-sheet domain of the immobilized transaminase as a consequence of the exposure to toluene. Unexpectedly, the conformational change resulted in activity increase for the enzyme immobilized on the most hydrophilic EziGTM carrier. When such

formulation was applied in toluene at different a_w values the best reaction conditions were characterized with a_w values close to water saturation, which ensured the shift of the thermodynamic equilibrium between the amine donor and its imine in favour of the first species. Overall, careful preservation of the hydration of the biocatalyst during the whole post-immobilization procedures appears crucial for the enzymatic activity and simple preparation protocols are reported herein.

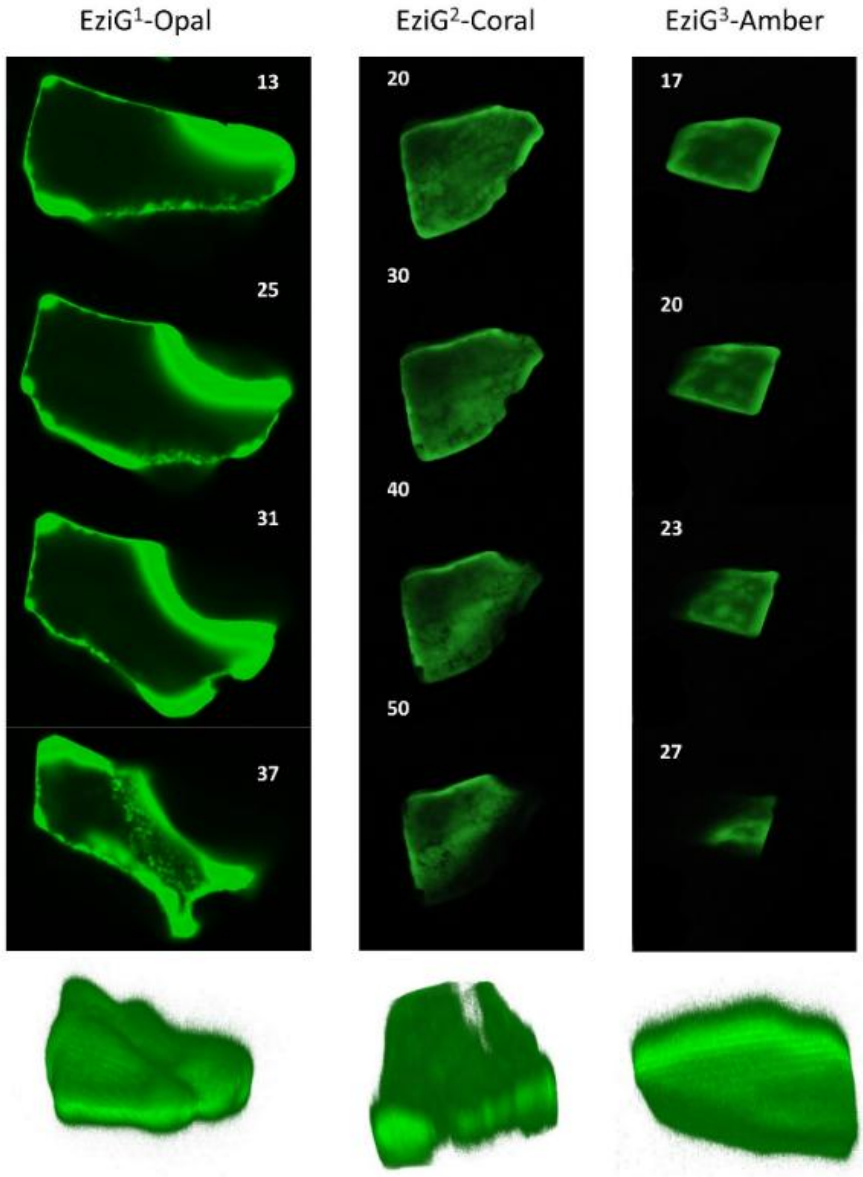

Figure 24 2D images (40x) of different layers of EziG1, EziG2 and EziG3 carriers obtained by acquiring 3D image stacks with scanning confocal microscopy showing the FITC labelled His6-ATA-117 distribution (samples were pretreated with NaP buffer before drying - pretreatment 1). Row below: 3D reconstruction of the shown carriers.

The behaviour of the EziG1-Opal-His6-ATA-117 when exposed to toluene provides new hints for future investigations of the conformational behaviour of transaminases in non-aqueous media by means of spectroscopic analysis and molecular dynamics simulations. As a matter of fact, the structural analysis of the enzyme highlighted various hydrophobic regions on its surface. Conformational rearrangements cannot be excluded when the protein is exposed to more hydrophobic environments, therefore the differences in solvation of the enzyme surface and the chemical nature of the carrier might play an active role in such phenomena.

There is no single 'best' immobilization method for all enzymes; the method must be tailored to the specific enzyme. Enzymes differ in structure and sensitivity and supports differ in their chemistry and physical properties. Sol-gel entrapment is ideal for lipases in organic media, while covalent binding plus sol-gel provides a robust environment specifically suited to CALB in solvent-free reactions. Designing the immobilization protocol based on the enzyme's requirements and the process conditions is crucial -a principle that advanced characterisation techniques are making increasingly easy to achieve.

Two keyways in which immobilization contributes to sustainability are reusability and operational stability. A notable outcome of the case studies was the ability to reuse immobilised enzymes for numerous cycles or extended continuous runs with minimal loss of activity.

A summary of the immobilization methods is presented in Table 8. For instance, there were 6+ cycles for magnetic CALB, over 10 cycles for sol–gel lipase and laccase systems, and multi-day continuous operations for CALB and BCL lipases. Reusability means less enzyme consumption and less frequent reactor downtime, providing economic benefits that reduce the environmental footprint of enzyme production and disposal. Furthermore, immobilization enables the development of enzyme 'reactors' that are analogous to heterogeneous chemical catalysts, which is transformative for scaling up biocatalysis.

Certain immobilization strategies offer additional benefits, such as facilitating separation and co-immobilization for cascades, thereby extending the applicability of enzymes. Magnetic supports, for instance, greatly simplify catalyst handling and are widely adopted in industry for this reason. Affinity immobilization (e.g. a His-tag on metal affinity carriers, as in EziG) combines enzyme purification and immobilization into one process. Co-immobilising multiple enzymes on the same support can improve intermediate channelling and balance enzyme ratios in multistep reactions. While not explicitly detailed above aside from GOX, this is an area that is growing in popularity in cascades. Immobilization on flow-friendly carriers (e.g. packed bed particles, monoliths, and membranes) enables continuous processing. Therefore, immobilization is an enabling technology for integrating biocatalysis into various process configurations and intensification strategies.

Table 8 Comparative summary of immobilization strategies, supports and performance outcomes for various enzymes. Key improvements in stability, reusability and catalytic efficiency are noted for each enzyme

Enzyme (Process)	Immobilization Method & Support	Performance outcomes	Reference
CALB lipase (Kinetic resolution in continuous flow)	**Sol–gel entrapment** (ternary silane matrix) in packed-bed reactor	~100% activity retained over 144 h continuous use; high productivity (145 $\mu mol \cdot min^{-1} \cdot g^{-1}$) and **E > 280** maintained; **Robust in organic solvent** (n-hexane); reusable for long runs with no enzyme leaching.	[33]
CALB lipase (Solvent-free ester synthesis)	**Covalent + sol–gel** on **magnetic core-shell** (polymer shell + silica coat)	High initial activity; **multi-point stabilization** gave excellent operational stability; >90% activity after 6 reuse cycles; easy magnetic recovery; solvent-free **isoamyl ester yields ~90–100%**	[35]
β-Gal & GOX (One-pot lactose conversion)	β-GAL: Covalent on **Ni–Zn ferrite** magnetic particles; GOX (with catalase): Covalent on epoxy resin (co-immobilized CAT)	Free enzymes: GOS yield ~45% (24% lactose); **Immobilized cascade: GOS yield ~72%** (with glucose converted to gluconic acid); enzymes **stable over multiple batches**; easy separation from product (food-grade). GOX co-immobilization prevented H_2O_2 inactivation.	[36]
Laccase (Glycerol oxidation)	**Covalent binding** on activated supports (screened optimal)	Best prep: ~75% glycerol conversion, **20% glyceric acid yield** (vs <<10% free); maintained activity over >10 cycles; tolerant to substrate and mediator; **no enzyme leaching**, product stream enzyme-free.	[38]
ω-Transaminase (Chiral amine synthesis)	**Affinity binding** on EziG resin (immobilized via His-tag; varied hydrophobicity)	Immobilization enabled operation in **low-water toluene**; enzyme adopted beneficial β-sheet-rich conformation in solventhigher activity in organic phase vs free; retained >95% activity after 24 h in 100% toluene (with controlled water).	[42]

Ultimately, advancements in enzyme immobilization technology are broadening the scope of biocatalysis in the chemical industry. This technology allows enzymes to be used in ways that were previously impractical, for example continuously and on a large scale in unconventional media.

Research continues to address remaining challenges, such as improving the yield of immobilised enzyme activity, developing more sustainable and cost-effective carriers, and creating self-regenerating or collaborative enzyme systems (e.g. multi-enzyme modules). Given these trends, it is reasonable to expect that immobilised biocatalytic pathways will increasingly become the norm in green chemical manufacturing, from bulk chemicals to high-value pharmaceuticals. This will embody the principles of sustainability and innovation in chemical processes. The case studies presented here demonstrate current successes and the potential for future developments at this exciting intersection of biotechnology and green engineering.

II.4. Deep eutectic solvents as reaction media in biocatalysis.

Over the past decade, deep eutectic solvents (DESs) have emerged as an environmentally friendly and sustainable new generation of media for extraction and catalytic transformations, particularly in biorefineries and a variety of chemical and biotechnological applications [44]. Enzymatic reactions in particular have benefited significantly from the unique physicochemical properties of DESs, which improve substrate solubility, enhance enzyme stability and increase operational performance. Recent investigations have highlighted the potential of natural deep eutectic solvents (NADESs), which are typically composed of hydrogen bond acceptors, such as choline chloride or betaine, and a variety of naturally derived hydrogen bond donors, including carbohydrates, polyols, and carboxylic acids, as multifunctional systems [45]. These NADESs can serve as extraction solvents, reaction media, substrate sources and catalytic agents simultaneously. Introducing such reactive NADESs (R-NADESs) into catalytic processes is a promising strategy for developing more sustainable biocatalytic and chemo-catalytic methodologies. This facilitates streamlined downstream processing and reduces waste generation, accelerating their implementation in industry [46].

One of the initial challenges in the pursuit of greener chemical processes was replacing volatile organic solvents with less toxic, more sustainable alternatives. Solutions adopted at the industrial level include supercritical carbon dioxide (sCO_2) and ionic liquids (ILs), while deep eutectic solvents (DESs) have been extensively investigated for potential applications in various fields such as materials science, biomass valorisation, organic synthesis and biocatalysis. DESs are a more environmentally friendly alternative to conventional organic solvents and ILs, the latter of which are limited in their biodegradability and can be ecotoxic.

First and second-generation DESs, which are usually made up of quaternary ammonium salts and metal halides[47], have been shown to be effective as extraction media and reaction solvents [48]. Second-generation DESs are generally formed through hydrogen bonding interactions between a hydrogen bond acceptor (HBA), such as choline chloride, choline acetate, or ethylammonium chloride, and a hydrogen bond donor (HBD), which may include polyols, carbohydrates, carboxylic acids, amines, or amides.

Natural deep eutectic solvents (NADESs) are a class of DESs that can be produced by simply mixing inexpensive and naturally occurring primary metabolites or bio-renewable compounds. These solvents have physicochemical properties similar to ILs, but are derived from biodegradable, non-toxic and abundant natural sources, thereby minimising environmental impact. Furthermore, as DES formation is a purely physical process, they are associated with a low environmental factor (E-factor). Their tunable properties, including polarity, acidity, viscosity and melting point, can be optimised for specific applications. Consequently, NADESs are attractive not only as solvents for extracting a wide range of substances (e.g. phenolic compounds, metals,

proteins, polysaccharides and lignocellulosic fractions) [46],[47] but also as versatile media for chemical and biological transformations [51].

Although enzymes typically exhibit optimal activity in aqueous environments, numerous studies have demonstrated their significant catalytic performance in non-aqueous systems, including organic solvents, ionic liquids and deep eutectic solvents (DESs). Using DESs - particularly natural deep eutectic solvents (NADES) with tunable physicochemical properties - as reaction media for biocatalytic processes has distinct advantages, especially for reactions involving polar, highly hydrophilic substrates, such as carbohydrates and polyols. These are poorly soluble and difficult to convert enzymatically in conventional organic solvents [52].

Emerging evidence suggests that NADESs can actively participate in the catalytic process, either by serving as a substrate source or by exhibiting catalytic activity themselves, rather than merely acting as passive solvents. These multifunctional NADESs constitute a new category of bio-based solvents known as reactive natural deep eutectic solvents (R-NADESs). These systems combine the advantages of green chemistry with functional versatility. Several comprehensive reviews are available for a detailed examination of their roles in biocatalytic transformations and pharmaceutical synthesis [46], [53], [54].

Although numerous studies have investigated the use of natural deep eutectic solvents (NADES) and their influence on lipase activity and thermal stability when used as reaction media, data on the performance of reactive NADESs (R-NADES)-where the solvent acts as both a solvent and a substrate-remains limited. Specifically, little is known about how the intrinsic properties of R-NADESs affect the esterification activity of lipases under such multifunctional conditions.

Most of the existing literature focuses on the hydrolytic activity of lipases, often using *p*-nitrophenyl (PNP) ester hydrolysis as a model reaction. In these studies, R-NADESs act as co-solvents in aqueous systems [55] or in aqueous–organic mixtures, such as dimethyl sulfoxide (DMSO) or tert-butanol [56]. However, it is well established that lipase-catalysed esterification and hydrolysis are mechanistically distinct processes and their activities can differ significantly. These differences arise from various factors, including the composition and physicochemical properties of the reaction medium, and the nature, structure and solvent–enzyme interactions of the substrates involved [57].

This distinction is particularly relevant in R-NADES systems, where the substrate is integrated within an extensive hydrogen-bonding network that encompasses the enzyme, which could influence its conformation and activity. Furthermore, the risk of secondary side reactions must be considered. For instance, esterification reactions involving fatty acids conducted in NADESs comprising choline chloride (as the hydrogen bond acceptor) and sugars and water (as hydrogen bond donors) may result in the formation of choline chloride fatty esters if free, unbound choline chloride is present in the system and not fully engaged in the NADES hydrogen-bonding matrix [46].

In this context, the effect of designed hydrophilic R-NADES mixtures on the esterification activity and thermal stability of free and immobilized lipases for the

synthesis of polyol- and carbohydrate-based biosurfactants was investigated. The application of reactive NADES mixtures as the reaction medium and substrate source for lipase-catalysed carbohydrate ester synthesis is of high importance to prevent a low substrate concentration caused by the limited solubility of carbohydrates in organic solvents and solvent-induced enzyme inactivation. We prepared and characterized 16 binary and ternary R-NADES mixtures with ChCl as the HBA and carbohydrate polyols; mono-, di-, and oligosaccharides; urea (U); and N-methyl urea (MU) as the HBDs, in different combinations and molar ratios. Lipase enzymes were selected for application in an R-NADES based on their experimentally determined reference esterification activity for (a) the solventless synthesis of n-propanol laurate and (b) the synthesis of glucose-6-monolaurate, in DMSO/t-butanol 90/10 (vol%).

The selected enzymes were immobilized by entrapment in a silica sol–gel matrix. All the native enzymes, the immobilized enzymes prepared, and the commercial CalB immobilized on acrylic resins (N435) were utilized as biocatalysts for the synthesis of the lauryl esters of the polyols and carbohydrates in the designed R-NADESs and the operational stability, esterification activity, and LA conversion were determined and evaluated in relation to the properties and composition of the used reactive NADES mixtures.

Preparation and characterization of R-NADESs [58]

R-NADESs were prepared by direct mixing of the HBA component with the HBD components listed in Figure 25, in different molar ratios, as given in Table 9. Choline chloride, with an HBA count of 2, and urea and N-methyl urea, both with HBA count of 1, all can serve as HBA, while U and MU, with a HBD count of 2, can also function as HBD components.

Two sets of R-NADESs were prepared:

(i) one set of binary mixtures containing only a carbohydrate or a polyol as HBD with either ChCl (entries 1,4, 13-16, in Table 9) or U and MU as HBD (entries 6 and 7 in Table 9), and

(ii) another set of ternary mixtures, with additional water (entries 2, 3 and 5, Table 9) and urea (entries 8-12 in Table 9) next to ChCl and the carbohydrate HBDs.

The addition of water to the ChCl-carbohydrate ternary mixtures, (i.e. 5.5 wt.% to R-NADES 2, 3.8 wt.% to R-NADES 3 and 9 wt.% to R-NADES 5) was essential for the formation of the deep eutectic solvents. All pre-pared R-NADES mixtures are clear, transparent liquids between 40 - 80°C, the optimum temperature range for lipase catalytic activity. The molecular and thermal properties of all prepared R-NADES mixtures were determined using computational and experimental methods, respectively.

Thermal and physical properties of R-NADES mixtures

The composition of the mixtures, the molar ratio, the thermal properties, i.e., onset temperature of decomposition (T_{onset}), water loss, melting temperature (T_m),

glass tran-sition (T_g), viscosity (η) and the aspect of the samples at T > 25 °C are listed in Table 9. All binary and ternary ChCl-based R-NADES mixtures with polyols and carbohydrates HBDs (entries 1-5 and 13-16, Table 9) are highly thermostable, with Tonset ranging from 190 °C to 278 °C. They show minor weight loss up to 200 °C, which is mainly water. Only a small part of the crystallization water and the additional water in the ternary choline chloride-carbohydrate R-NADES mixtures (entries 1-5, Table 9) is released at temperatures below 200 °C, which suggests that most of the water is tightly bound to the other components in the extended hydrogen bond network. The major mass loss of about 80% was recorded between 200 – 300 °C. R-NADES mixtures containing urea and MU (entries 6 - 12, Table 9) start decomposing at temperatures between 140 °C and 173 °C, caused by the thermal decomposition of urea and N-methyl urea, with high mass loss of 20- 45 % at temperature up to 200 °C. The low amounts of water in these mixtures are released at temperature below 120 °C. Mixtures containing di- and oligosaccharides have increased thermal stability, irrespective of the other components and molar ratio.

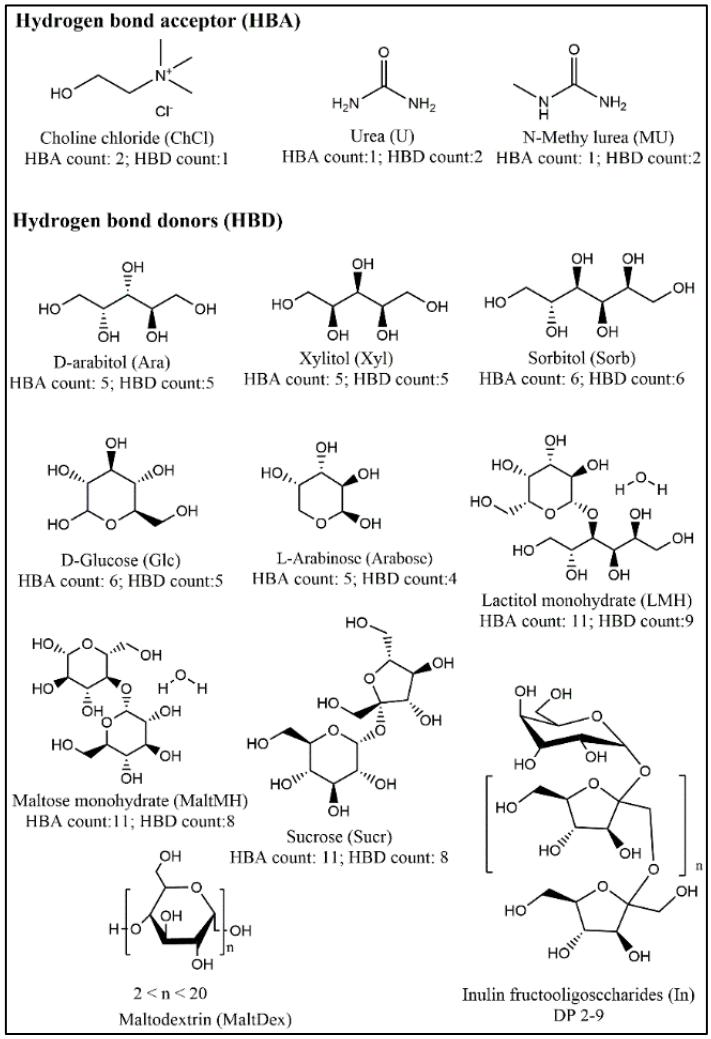

Figure 25 Structure of hydrogen bond donors (HBD) and hydrogen bond acceptors (HBA) used in this study for the preparation of reactive natural deep eutectic solvents (R-NADES)

Table 9 Reactive NADES: composition and properties.

R-NADES		TGA		DSC		Viscosity (η) at 70°C	HBA/HBD
Nr.	Composition	Water loss (w%)	T_{onset} (°C)	T_m (°C)	T_g (°C)	(cP)	(mol/mol)
1	ChCl:Glc (2:1)	3.5	196	76.8	-52.3	1354	2
2	ChCl:Glc:H_2O (1:1:1)	5.5	190	*n.o.	-44.5	767.5	0.5
3	ChCl:Glc:H_2O (2:1:1)	6.08	195	8.7, 73.7	- 22	382	1
4	ChCl:Arabose (2:1)	1.46	195	79.3	-20	1183	2
5	ChCl:MMH:H_2O (4:1:4)	5.46	212	60.5	*n.o.	370	0.8
6	U:Glc (2:1)	0.86	142	89.4	-0.3	845	2
7	MU:Glc (2:1)	0.72	141	62.4	-0.4	1730	2
8	ChCl:Glc:U (1:1:1)	0.58	150	*n.o.	-27.5	1370	0.5
9	ChCl:Glc:U (1:1:2)	0.40	145	*n.o.	-28.5	495	0.33
10	ChCl:MMH:U (1:0.5:2)	1.28	153	*n.o.	-51.5	627.5	0.4
11	ChCl:In:U (1:0.5:2)	1.73	153	*n.o.	-51.5	350	0.4
12	ChCl:MaltDex:U (1:0.5:2)	1.80	150	*n.o.	-51.5	487.5	0.4
13	ChCl:D-Ara (1:1)	1.46	276.6	50.2	-62.1	300	1
14	ChCl:Xyl (1:1)	1.61	277.5	29.4	-58.6	235	1
15	ChCl:D-Sorb (1:1)	1.56	278	44.2	-55.7	655	1
16	ChCl:LMH (2:1)	1.14	245	61, 77.8, 145	*n.o.	2300	2

Differential Scanning Calorimetry (DSC) was used to monitor the thermal behavior of various binary and ternary mixtures. Mixtures containing urea or N-methyl urea (entries 6–12 in Table 9) and the equimolar ChCl:Glc:H_2O (1:1:1) system (entry 5) remained clear upon cooling. These mixtures exhibited low glass transition temperatures ranging from –0.3 to –51.5 °C and no thermal events were observed above 0 °C. Conversely, ChCl:Xyl, ChCl:Ara, and ChCl:Sorb (entries 13–16) exhibited broad endothermic peaks at 29.4 °C, 50.2 °C, and 44.2 °C, respectively. Systems with excess ChCl—ChCl:Glc (2:1), ChCl:Glc:H_2O (2:1:1), and ChCl:LMH (2:1)-displayed peaks around 74–78 °C, likely due to unbound ChCl. The lactitol-based mixture (entry 16) exhibited a melting peak at 145 °C, which was attributed to free lactitol. Most urea-based ternary NADES had clean thermograms; however, MU:Glc (2:1) (entry 7) showed a thermal event at 89.8 °C, possibly due to degradation indicated by discoloration.Rheological measurements allowed determination of the viscosity of all R-NADES.

Results show the structure of the constituents of the R-NADES mixture, the molar ratio in which they are included, the water content and the temperature, all have a strong effect on the fluid properties, and on viscosity (Figure 26).

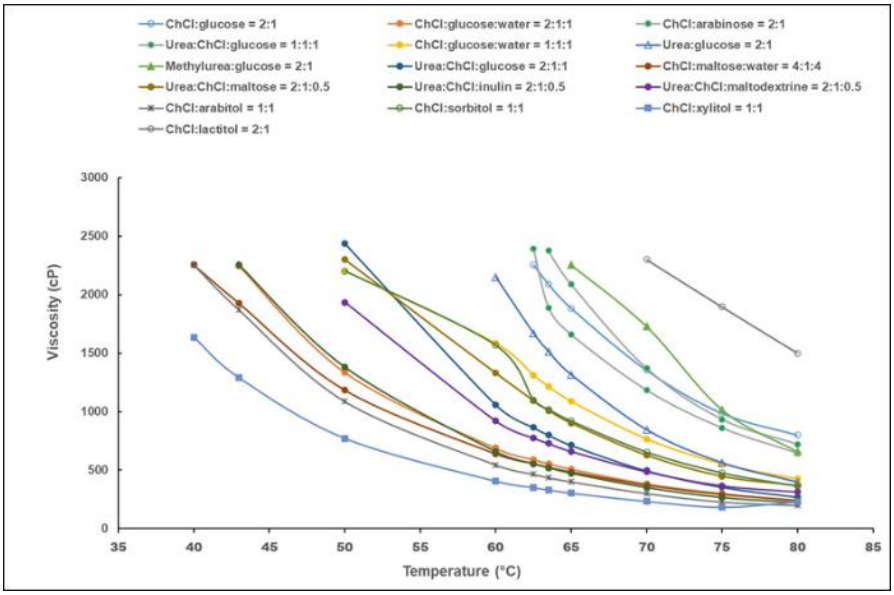

Figure 26 Viscosity (cP) of R-NADES mixtures as a function of temperature.

The water addition to R-NADES mixtures increases viscosity by extending the hydrogen bond network and reducing molecular mobility due to enhanced electrostatic and van der Waals interactions. This is evident from the threefold decrease in viscosity when water is added to the nearly dry ChCl:Glc (2:1) system to form ChCl:Glc:H_2O (2:1:1). Among the studied systems, polyol-based R-NADESs (entries 13–15) have the lowest viscosity. In contrast, carbohydrate- and urea-based mixtures have higher viscosity due to denser hydrogen bonding. The binary mixture with lactitol is highly viscous, even at elevated temperatures, likely due to excess unbound components. A general trend is observed: viscosity increases in the order ChCl:polyol < ChCl:monosaccharide < ChCl:disaccharide. Water addition consistently lowers viscosity. Without water, eutectic mixtures cannot form with disaccharides such as maltose. Importantly, R-NADESs prepared with water structurally embedded during synthesis differ from systems in which NADES is simply dissolved in an aqueous medium. Principal component analysis (PCA) was applied to explore the correlation between viscosity and molecular structure using water content, the HBA/HBD ratio, and the calculated number of hydrogen bonds. Polydisperse mixtures, such as maltodextrin and inulin (entries 11 and 12), were excluded from the analysis. The results are shown in Figure 28.

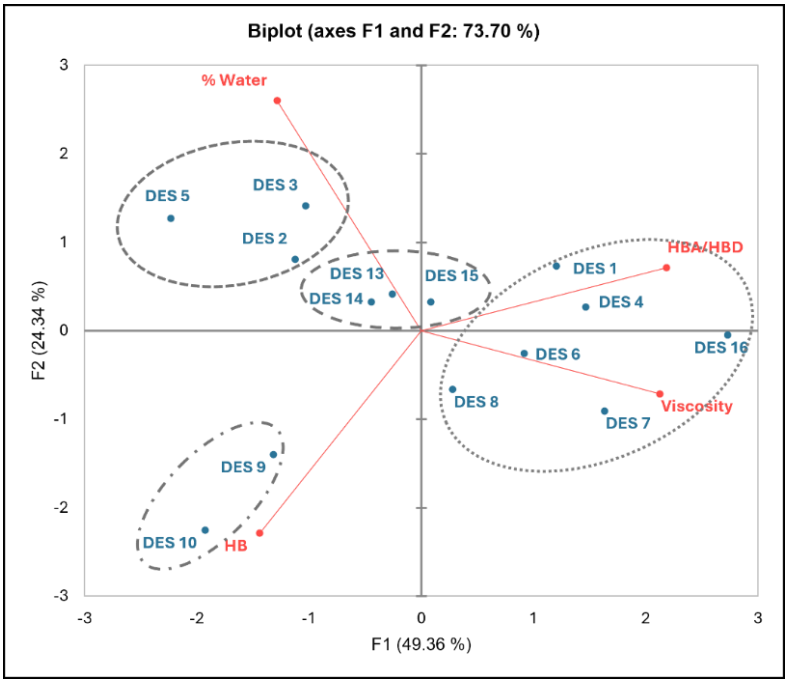

Figure 27 Relationship between the computed molecular properties of R-NADES and their viscosity, as determined by PCA

The results clearly show the strong contribution of molecular properties of the mixtures on their experimentally measured viscosity. We identified four groups of R-NADES that share similar properties. Group 1 is composed of mixtures with high viscosity, i.3. DES 1, DES 4, DES 6 - 8 and DES 16, all binary ChCl based mixtures, with a molar excess HBA/HBD of 2 and with low water content. Group 2, containing ternary R-NADES carbohydrates and added water, i.e. DES 2, DES 3 and DES 5, is characterized by low viscosity and an HBA/HBD ratio lower than 1. Group 3 (DES 13, DES 14 and DES 15) and Group 4 (DES 9 and DES 10), although with different composition, are both characterized by low viscosity, despite the very low water content of these mixtures. The low viscosity of R-NADES mixtures of group 3, which are binary mixtures of ChCl HBA with the xylitol, arabitol and sorbitol, can be associated to equimolar ratio HBA/HBD and the low number of hydrogen bonds. The ternary ChCl:U:Carbohydrate DES 9 and DES 10 in Group 4, are compact mixtures with high HB number and low molar HBA/HBD ratio.

Computational characterization of R-NADES

Computational studies addressed the optimization of HBA and HBD constituents of R-NADES, and the determination of important parameters, like the total energies of both NADES and their components, the energies of the frontier molecular orbitals HOMO and LUMO, polarizabilities, dipole moment and of the steric parameters like Connolly accessible Area, Connolly Solvent-Excluded Volume, ovality and visualization of the hydrogen bonds established among the NADES.

The energies of the HOMO and LUMO molecular orbitals play an important role in the stability and reactivity of the compounds. Lower HOMO-LUMO gaps indicate the tendency for such compound to be less stable and therefore more reactive. Chemical

reactivity descriptors also provide an understanding of the biological activity of molecules. Chemical hardness expresses the tendency to inhibit charge transfer. A molecule is considered highly polarizable when it is found to have a low chemical hardness and a large negative value of the chemical potential. Higher values of the chemical potential (μ) suggest the feasibility of a system to exchange electrons with the environment. When the value of the electrophilicity index is relatively high, it shows that the studied molecule has a high binding capacity with biomolecules and can act as an electrophile.

The energies of the frontier HOMO and LUMO orbitals of the investigated NADES, together with the calculated global descriptors of the reactivity, are given in Table 2. According to the calculated HOMO-LUMO gaps, the most stable (and less reactive) NADES are proven to be NADES 6 and NADES 7, the ones that do not contain choline chloride. Another important feature of these two NADES is the highest values of both the HOMO orbital energies and chemical potential.

The results obtained for NADES 8 and 9 suggest that the presence of a supplementary urea in the DES composition does not have a significant influence on the global descriptors of the mixtures.

The results obtained for NADES 13 and 14, which consist of choline chloride and polyols with five carbon atoms, show similar values for the HOMO energies and chemical potential and a slight increase in the LUMO energy for the NADES 14 (xylitol).

The major differences have been obtained for NADES 1 and 4, the ones that contain choline chloride and a monosaccharide (2:1 ratio). According to the results, they are the least stable mixtures, characterized by very similar values of the frontier molecular orbitals, leading thus to the lowest chemical potential and the highest electrophilic character that suggests an increased reactivity.

Table 10 HOMO and LUMO energies and the computed values of the chemical potential, global hardness and electrophilicity (BLYP/TZP)

Nr.	R-NADES Composition	E HOMO (H)	E LUMO (H)	HL gap (eV)	μ (eV)	η (eV)	ω (eV)
1	ChCl:Glc (2:1)	-0.0825	-0.0798	0.073	-2.207	0.037	65.822
2	ChCl:Glc:H_2O (1:1:1)	-0.1109	-0.0858	0.682	-2.675	0.341	10.492
3	ChCl:Glc:H_2O (2:1:1)	-0.1064	-0.0911	0.416	-2.686	0.208	17.343
4	ChCl:Arabose (2:1)	-0.0954	-0.0946	0.021	-2.585	0.011	303.73
5	ChCl:MMH:H_2O (4:1:4)	-0.0855	-0.0852	0.008	-2.321	0.004	673.68
6	U:Glc (2:1)	-0.2141	-0.0320	4.953	-3.346	2.476	2.261
7	MU:Glc (2:1)	-0.1938	-0.0275	4.523	-3.010	2.262	2.003
8	ChCl:Glc:U (1:1:1)	-0.1003	-0.0774	0.622	-2.417	0.311	9.390
9	ChCl:Glc:U (1:1:2)	-0.1121	-0.0834	0.781	-2.658	0.390	9.058
10	ChCl:MMH:U (1:0.5:2)	-0.1314	-0.0857	1.243	-2.952	0.622	7.005
13	ChCl:D-Ara (1:1)	-0.1311	-0.0804	1.379	-2.876	0.689	6.002
14	ChCl:Xyl (1:1)	-0.1352	-0.0730	1.692	-2.831	0.846	4.737
15	ChCl:D-Sorb (1:1)	-0.1168	-0.0888	0.762	-2.796	0.381	10.259
16	ChCl:LMH (2:1)	-0.1128	-0.0817	0.846	-2.645	0.423	8.270

It has been observed that HOMO orbitals are localized at the chlorine atom of the choline chloride (except NADES 6 and 7, that don't contain choline); they are mainly localized on the urea and methyl-urea structures of DES 6 and DES 7. As regards the LUMO orbital distribution, they appear to be localized on the choline skeleton and, for ES7 and DES8, on the sugar moieties. Figure 28 Distribution of HOMO and LUMO orbitals for NADES 2, ChCL:Glc:H2O (1:1:1) and NADES 6, U:Glc (2:1).below shows the graphical distribution of HOMO and LUMO orbital for NADES 6 (U:Glc 2:1) and NADES 2 (ChCl:Glc:H2O 1:1:1).

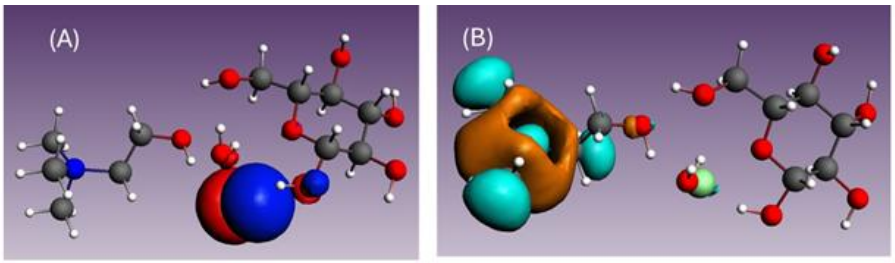

Distribution of HOMO orbital (A) and LUMO orbital (B) for DES 2, ChCl:Glc:H_2O (1:1:1)

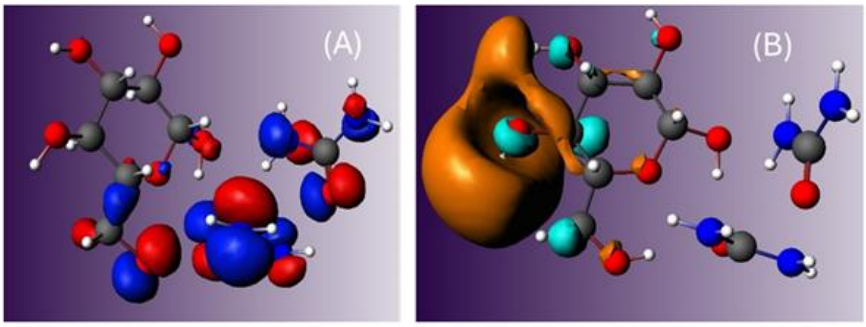

Distribution of (A) HOMO orbital and LUMO orbital (B) for DES 6, U:Glc (2:1)

Figure 28 Distribution of HOMO and LUMO orbitals for NADES 2, ChCL:Glc:H2O (1:1:1) and NADES 6, U:Glc (2:1).

The reactivity of the NADES is strongly influenced by the number of intermolecular forces among their components. The total number of hydrogen bonds for each optimized structure of NADES is given in Table 3. The optimized structures of NADES 2 (ChCl:Glc:H_2O 1:1:1) and NADES 9 (ChCl:Glc:U 1:1:2) and the hydrogen bonds formed are illustrated in Figure 29. The presentation of the hydrogen bond network demonstrates without any doubt that all constituents of R-NADES mixtures have multiple functions, acting both as HBD and as HBA, depending on the composition of the mixtures and the stereochemistry of the molecules. We can conclude that the number of hydrogen bonds increases with the number of components (NADES 10) and with the number of urea and methyl-urea structures, that can easily establish intermolecular forces (NADES 6, 7 and 9).

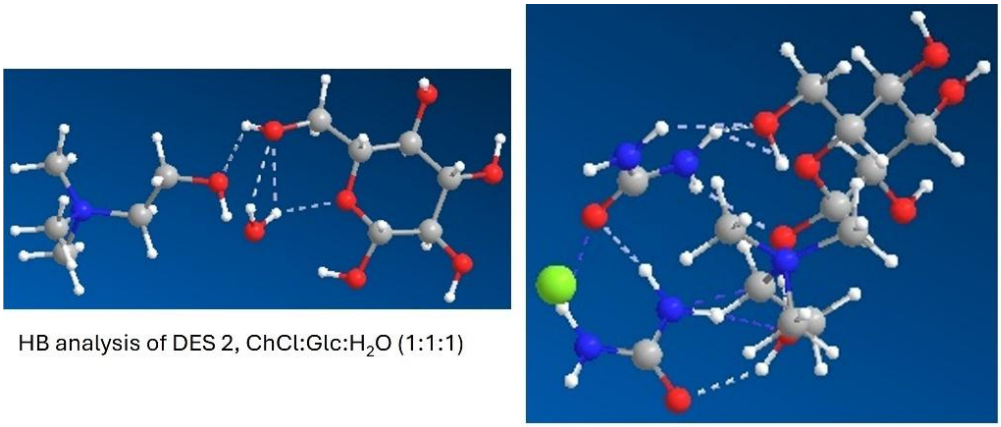

Figure 29 Hydrogen bond network and optimized structures of NADES 2 (ChCl:Glc:H_2O 1:1:1) and NADES 9 (ChCl:Glc:U 1:1:2).

Also, the steric parameters of the NADES: Connolly Accessible Area (CAA) and Connolly Solvent-Excluded Volume (CSEV), have been computed for all the investigated compounds. Results are given in Table 11. The influence of the HB number is reflected in the CAA and CSEV values of NADES 6 and NADES 7. It can be observed that, among the DES that contain three components, they have the smallest accessible area and solvent-excluded volume. Presumably, they are more compact due to the larger number of HB.

Table 11 Computed properties of R-NADES

R-NADES		**H-bonds**	**Steric parameters**		**Polarizability (a.u.)**	**Dipole moment (D)**	**Total energy (H)**
Nr.	**Composition**		**CAA (Å2)**	**CSEV (Å3)**			
1	ChCl:Glc (2:1)	3	703.831	489.463	627.690	28.903	-2265.246
2	ChCl:Glc:H_2O (1:1:1)	4	578.348	316.263	192.431	27.248	-1552.228
3	ChCl:Glc:H_2O (2:1:1)	3	689.734	488.310	389.509	33.830	-2341.678
4	ChCl:Arabose (2:1)	2	663.381	452.222	420.004	36.802	-2151.374
5	ChCl:MMH:H_2O (4:1:4)	9	1160.43	1100.00	*	34.357	-4759.864
6	U:Glc (2:1)	5	484.641	246.967	168.796	3.204	-1137.831
7	MU:Glc (2:1)	7	532.677	288.432	181.260	2.254	-1216.409
8	ChCl:Glc:U (1:1:1)	3	640.500	358.293	256.863	21.018	-1701.511
9	ChCl:Glc:U (1:1:2)	9	600.765	419.292	269.003	22.417	-1926.811
10	ChCl:MMH:U (1:0.5:2)	16	957.111	869.306	*	31.588	-3776.682
13	ChCl:D-Ara (1:1)	1	521.383	288.194	195.500	18.497	-1362.801
14	ChCl:Xyl (1:1)	2	465.509	180.247	164.222	19.817	-1362.909
15	ChCl:D-Sorb (1:1)	1	455.295	214.224	185.314	23.195	-1477.426
16	ChCl:LMH (2:1)	1	657.739	458.275	288.993	22.689	-2088.206

Parameters like polarization, dipole moment and total energy have been computed for the investigated NADES. The results are depicted in Table 11. Largest values of polarizability and dipole moment have been obtained for the NADES that have a higher molar content of ChCl. Instead, lower values have been obtained, as expected, for binary urea-based NADES 6 and 7, but also for NADES 13, 14 and 15, that contain equimolar amounts of ChCl and 5- or 6-carbon atom polyols.

Evidence for the performant use of the R-NADES as solvent and substrate source for lipase catalyzed esterification reactions

A novel strategy was developed for the enzymatic synthesis of fatty acid esters of carbohydrates and carbohydrate polyols using reactive nonaqueous dimethyl sulfoxide (NADES) as a multifunctional medium. Three key aspects had to be addressed: (i) identifying enzymes with high esterification activity, (ii) assessing the effect of NADES composition on the activity and stability of enzymes in both free and immobilized forms, and (iii) evaluating the synthetic potential of the selected enzymes for ester formation in reactive NADES systems.

Thirteen commercial lipases from various microbial sources were screened. Their performance was tested in (i) solvent-free synthesis of propyl laurate and (ii) conventional esterification systems. All the enzymes demonstrated good activity in the solvent-free system (Figure 31A); however, only *Candida antarctica* B (CalB), *Candida antarctica* A (CalA), *Pseudomonas stutzeri*, and *Aspergillus oryzae* were effective in catalyzing glucose esterification (Figure 31B). Reaction progress was monitored by tracking lauric acid consumption, and glucose ester formation was confirmed using TLC, HPLC, and MALDI-TOF-MS analyses.

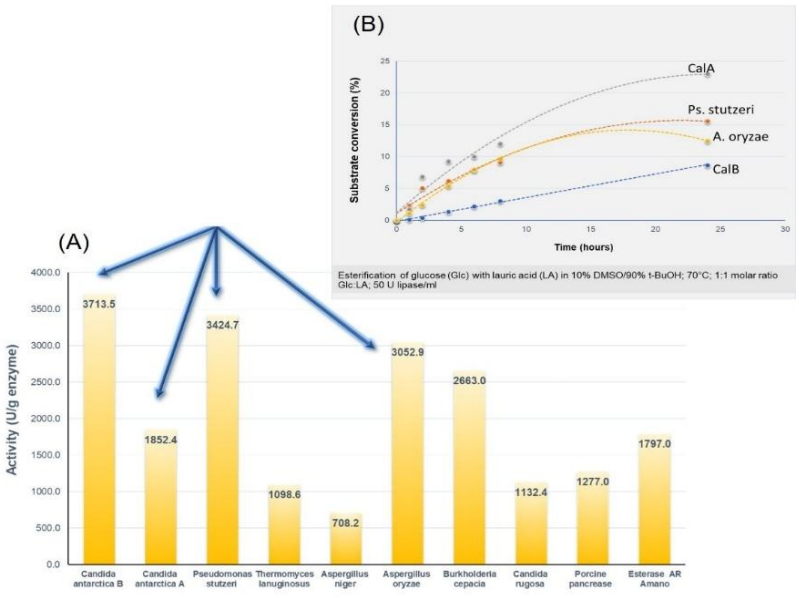

Figure 30 (A) Catalytic activity of native lipases in solvent free esterification of lauric acid (LA) with propanol; 55ºC; 1:1 molar ratio; 20 mg lipase/mL. (B) Synthesis of glucose laurate in 10% DMSO/ 90% ^{t}BuOH, 70 ℃, 1:1 molar ratio Glc/lauric acid, 50 units of enzyme

The fours selected enzymes showed significant esterification activity in all 16 binary and ternary reactive NADES prepared (Figure 31). Enzyme showed good esterification activity in the tested NADES mixtures, although lower than their reference esterification in a solventless esterification reaction. R-NADES mixtures have higher viscosity than the mixture of propanol with lauric acid used in the reference reaction, which can decrease the diffusion and the collision of the molecules, thus reducing the reaction rate. We observed that the esterification activity was also influenced by the composition of the mixtures and the type of enzyme. CalB and *Ps. stutzeri* showed relatively high activity in all ternary NADES mixtures. CalB, *Ps. stutzeri* and CalA enzymes showed the highest catalytic activity in the ternary equimolar ternary U:ChCl:Glc NADES.

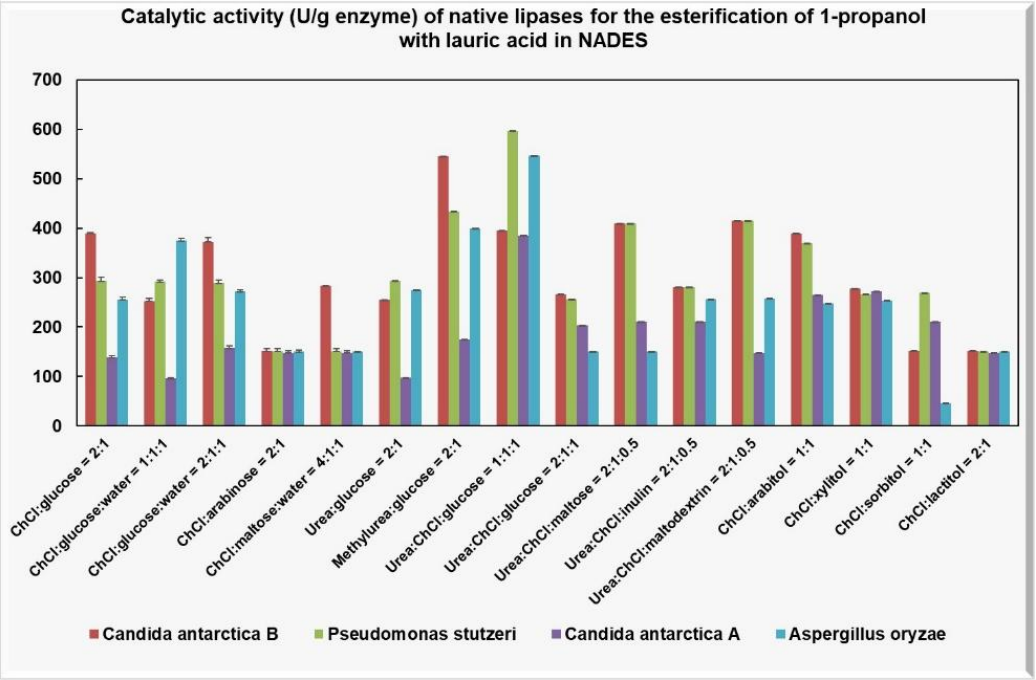

Figure 31 Catalytic activity (U/g enzyme) of selected native lipases for the esterification of n-propanol with lauric acid, at 70 ℃, in reactive NADES mixtures

To enhance thermal stability, CalB and *Pseudomonas stutzeri* lipases were immobilized using sol-gel entrapment, with or without Celite adsorption, and compared to commercial CalB immobilized on acrylic resin (LAR/N435). All immobilized enzymes displayed high esterification activity and thermal stability in NADES media. LAR was the most stable, retaining over 90% activity after 72 h at 70 °C in glucose-ChCl NADES, with minimal activity loss over multiple cycles.

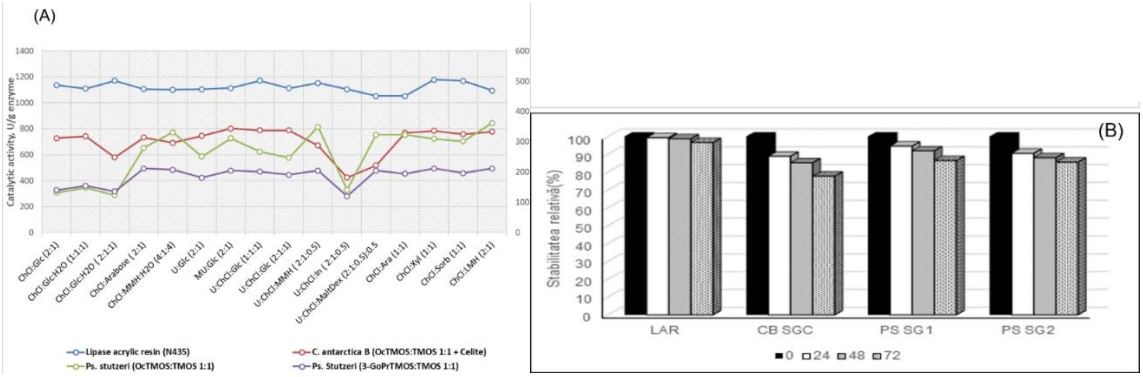

Figure 32 (A) Catalytic activity (U/g enzyme) of immobilized enzymes LAR, CB SGC (CalB immobilized on OcTMOS:TMOS 1:1 + Celite), Ps. SG1 (Ps. stutzeri immobilized în sol gel with OcTMOS:TMOS 1:1), and P.s SG2 (P. stutzeri in sol gel cu 3-GoPrTMOS:TMOS 1:1), for the solventless esterification of n-propanol with lauric acid in R-NADES mixtures, at 70℃, 1:1 molar ratio and 50 U lipase/mL. (B) Thermostability of the immobilized enzymes in R-NADES at 70℃.

The study demonstrated that selected NADES mixtures containing carbohydrates and polyols can serve as both reaction media and substrates for esterification using immobilized CalB (N435). Lauryl esters of monosaccharides and disaccharides were synthesized without the addition of external sugars. The tested NADESs included systems with glucose and a disaccharide (MMH) as well as polyols such as arabitol, xylitol, and sorbitol. This confirms the multifunctionality of these reactive solvents.

Synthesis of mono-lauryl and di-lauryl esters of carbohydrates (e.g. glucose, maltose) and polyols (e.g. arabitol, xylitol, sorbitol) catalyzed by immobilized C. antarctica lipase B (N435) in the corresponding ChCl/sugar or ChCl/polyol reactive NADES was demonstrated by HPLC, MALDI-TOF-MS and 1D and 2D NMR. Highest conversion (23 mol%) was obtained for the arabitol lauryl esters (Figure 33). The type and properties of the NADES has a high influence on the progress of reaction, as shown for glucose esterification, when the highest conversion (16%) was obtained for the low viscosity ChCl/urea/glucose 2:1:1 NADES (Figure 10). The results of the study confirm that the tested NADESs tested did play the double role of reaction medium and substrate source and are real reactive NADES systems.

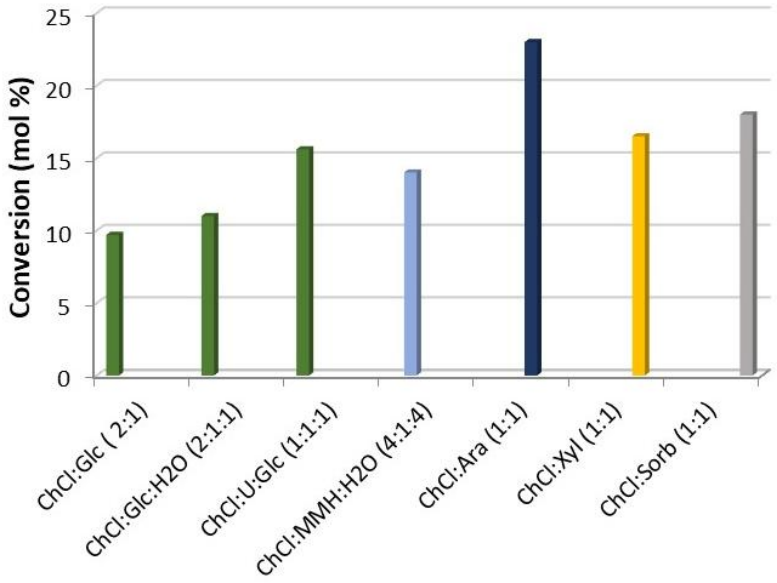

Figure 33 Substrate conversion during esterification of carbohydrates and carbohydrate polyols with immobilized CalB lipase (N435), in reactive NADES, at 70°C.

Preparation and characterization of carbohydrate polyols-based NADES

Three binary hydrophilic R-NADES based on ChCl as HBA and carbohydrate polyols (xylitol, D-arabitol and D-sorbitol) as HBDs, at (1:1) molar ratio, were prepared and characterized to determine the melting temperature (T_m), the thermal stability and the viscosity-temperature profile (

Table 12).

Table 12 Composition and properties of R-NADES.

NADES composition	Molar ratio	Decomposition temperature (°C)	T_m (°C)	Viscosity at 70°C (cP)	Appearance
ChCl:D-arabitol	1:1	276.6	38.6	300	fluid at T > 40°C, colorless
ChCl:xylitol	1:1	277.5	41.0	235	fluid at T > 40°C, colorless
ChCl:D-sorbitol	1:1	277.9	48.4	655	fluid at T > 50°C, colorless

Thermogravimetric analysis revealed high thermal stability up to 278°C for all carbohydrate polyol-based R-NADES. The melting temperatures, ranging between 38°C and 49°C, are significantly lower than that of the constituents of the mixture, namely 302°C for ChCl, 92-96°C for xylitol and D-sorbitol and 102°C for D-arabitol. Surprisingly, the melting temperature of the ChCl:D-arabitol (1:1) R-NADES is lower than that of the NADES based on xylitol, which might be due to the difference in the chirality of the two pentahydroxy-pentols. We could argue that the chiral D-arabitol (2R,4R-pentane-1,2,3,4,5-pentol) can form different interactions with ChCl as compared to the achiral xylitol (2R,4S-pentane-1,2,3,4,5-pentol).

The viscosity of the three R-NADES was measured between 40 and 80°C (Figure 34). For maximum accuracy, the readings were made at a torque range from 10% to 100%, that made viscosity measurements possible at different temperature intervals. Viscosities of R-NADES decreased with increasing temperature following an Arrhenius-like behavior, as at higher temperature the internal resistance of molecules decreases and cause the molecules to flow more easily. The viscosity profiles show that the obtained polyol-based R-NADES are stable fluids with adequate viscosities between 40 and 80ºC, the optimum temperature range for an enzymatic reaction.

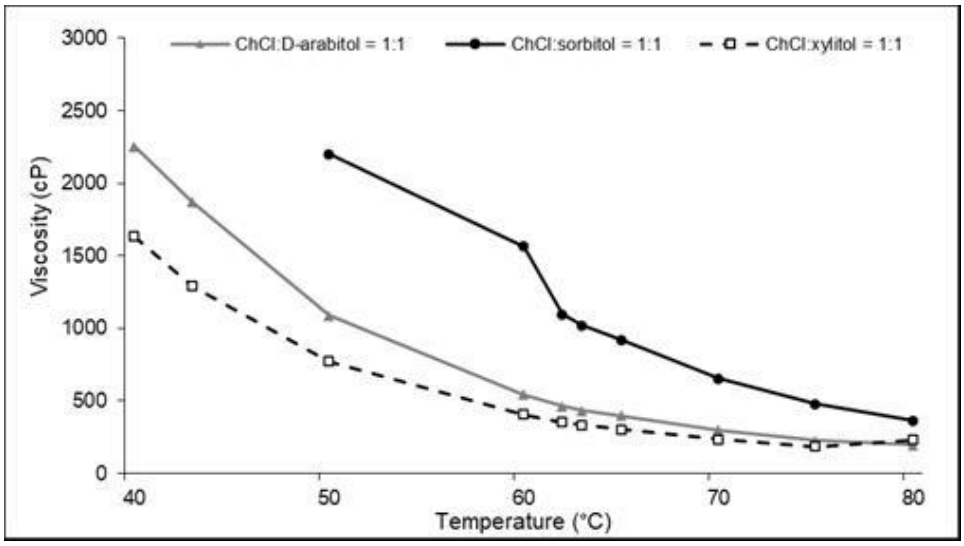

Figure 34 Viscosity curves (cP) of the carbohydrate polyol-based NADES, assessed in the 40-80°C temperature range.

Results show a strong relation between the viscosity and the composition of the deep eutectic solvent, primarily linked to the chain length and the number of hydroxyl groups of the HBD polyol. The viscosity of D-sorbitol-based NADES is considerable higher than that of the pentol-based R-NADESs, over the entire temperature range.

Experimental and theoretical assessment of the effects of NADES composition and properties on the esterification activity and stability of the immobilized lipase [46]

Experimental assessment of the esterification activity of the CalB lipase in polyol-based R-NADES

The esterification activity of industrial lipase B from *Candida antarctica immobilized on acrylic resin* (LAR, formerly Novozym 435) was evaluated in the esterification of 1-propanol with LA, in carbohydrate polyol-based R-NADES, compared to the solvent free system as reference. The lipase showed significant esterification activity in all the tested R-NADES but lower than in solvent free system (Figure 35A). Carbohydrate based R-NADES are quite viscous even at the reaction temperature of 70°C, thus the diffusion and collision of reactant molecules could be slowed down compared to that in solvent free system. Moreover, interactions between

R-NADES and enzyme must be considered, that in some cases can be activating by stabilizing the tertiary structure of the enzyme but in other cases can be inhibiting [59]. For the stability study, the lipase was preincubated at 70°C in each R-NADES for 0, 24, 48 and 72 hours. Then, the esterification activity was measured using the same model reaction of propyl laurate synthesis. Such a study was necessary considering the requirement of conducting the reaction at higher temperatures, to decrease the viscosity of the reaction mixture.

Excellent stability of this lipase in all three tested R-NADES was observed (Figure 35B).

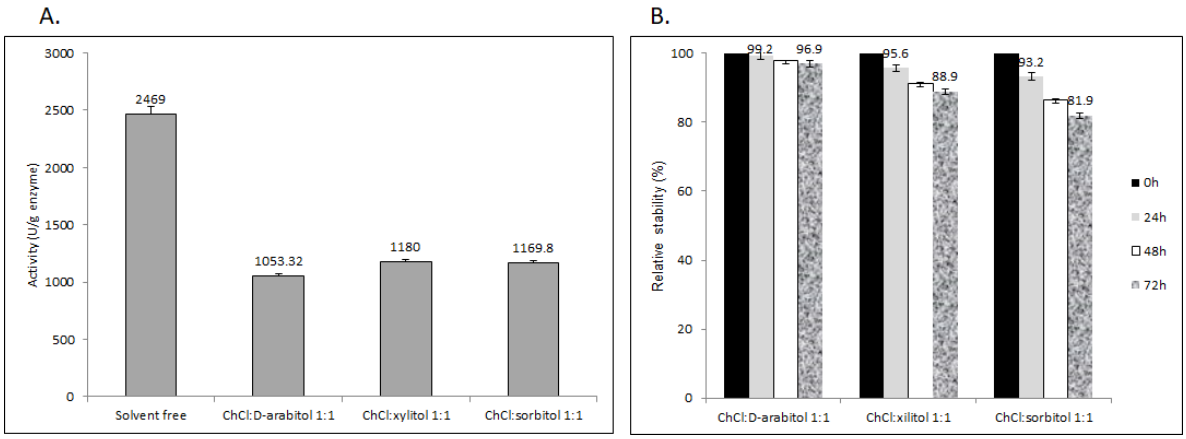

Figure 35 A) Esterification activity (U/g enzyme) of LAR determined in the acylation of 1-propanol with lauric acid, in solvent free system, at 55ºC, and in polyol-based R-NADES at 70ºC. B) Stability of immobilized Candida antarctica B lipase (LAR)in polyol-based R-NADES (ChCl:carbohydrate polyol (1:1)), assayed for the esterification of 1-propanol with LA at 70°C and (1:1) molar ratio of reagents

The highest stability of the immobilized CalB lipase at 72 h incubation time at 70°C was exhibited in ChCl:D-arabitol (1:1) R-NADES (97%), followed by ChCl:xylitol (1:1) (89%) and ChCl:D-sorbitol (1:1) (82%). This strongly suggests that the interaction between the polyol component of the NADES and the amino acid residues at the surface of the enzyme plays an essential role in the stabilization of the biocatalyst. Although measured at a higher temperature than in other reported studies, our results are in good agreement with the conclusions of the thermal stability study of Cao et al. [60] who stated that HBDs containing multiple hydroxyl groups preserve the active structure of the enzyme by substituting the hydration layer of the enzyme surface, thus protecting the enzyme at higher temperature.

Theoretical evaluation of the effect of NADES on the structural stability of CalB lipase

The stability of the CalB in NADES was studied by molecular dynamics (MD) simulations. The residues of the catalytic site were defined as those known to be interacting with the substrates in the acyclic and alcohol/aminic subsites and the stereospecific pocket (see Figure 36A) [61]. MD simulations of CalB in water solvent

were also included for the sake of comparison. Results of the MD trajectories indicate that the conformation of the active site is highly stable in all three NADES over the trajectory. The root mean square deviation (RMSD) values of the active site residues using as template the crystal structure pdbID:1tca remain stable at 1 Å along the trajectory when the protein is solvated in any of the NADES (see Figure 36B). These results contrast with the high RMSD values of 4 Å achieved at the end of the simulations when using water solvent.

Lipases have a funnel-like binding site, which contributes to the selectivity of the catalytic reaction [62]. Thus, the morphology of the entrance of the cavity was studied more in detail by evaluating the minimum distance between residues Ile189 and Leu279 and between Leu144 and Ala282 (see Figure 36A). As a reference, we evaluated both distances in the reference crystal structure (pdbID: 1tca) being 3.2 Å for Ile189-Leu279 distance and 8.1 Å for Leu144-Ala282 distance. The MD simulations show that the evolution of both distances (see Figure 36C) is significantly stable, oscillating around the reference values when CalB is solvated in all three NADES. On the contrary, a water environment leads to the increase of these distances along the trajectories, indicating the modification of the cavity entrance, as already showed in [62]. Moreover, the average volume of the catalytic cavity was calculated considering the most representative conformations of the trajectories. Average volume values of 226, 334 and 268 $Å^3$ were obtained for NADES containing arabitol, xylitol and sorbitol, respectively. Considering that the volume of the cavity in the reference crystal structure (pdbID: 1tca) is 332 $Å^3$, they seem to be slightly smaller for arabitol and sorbitol.

Additional MD simulations of CalB in all three NADES and lauric acid (LA), with LA:polyol molar ratio 1:1, were performed to evaluate the influence of the LA + NADES mixture in the structural stability of the CalB active site. During the annealing phase, the system spontaneously evolved towards a biphasic phase in which the lipase is located at the lipid-NADES interface with the active site oriented toward the hydrophobic phase (see Figure 36C). This behavior agrees with the experimental observation that CalB lipases show an enhanced catalytic rate at hydrophobic interfaces when bulky substrates are involved [63]. Also, higher average volume values of the cavity were observed, as they achieve 307, 334, and 357 ± 3 for arabitol, xylitol and sorbitol, respectively, which are more similar than the one obtained with the reference structure.

To understand the mechanism of catalyzed esterification when the lipase is located at the lipid-NADES interface, the interactions between substrates and the active site residues were analyzed in all trajectories. The most representative scenario is depicted in Figure 36E Two lauric acid molecules enter the catalytic site (80% of probability) occupying the acylic subsite. The location of the carboxylic groups is one of them inside the active site interacting with Ser105 (88%), while the other can be found either outside (65%), or inside (23%). No polyol molecule was found inside the cavity in the simulations, but at least one molecule was located at the entrance of the cavity interacting with the His224 backbone (64%). Two polyols at the cavity entrance region were found with much smaller probability (17%), while three or more polyols

were never found in the simulations. Interestingly, two choline molecules are found in the same entrance interacting with Glu188 and Asp223 (80%). This configuration enables a region of charged groups inside the lipid phase that may stabilize the location of a polyol molecule close to the alcohol/aminic subsite, as well as preserving the active structure of the enzyme.

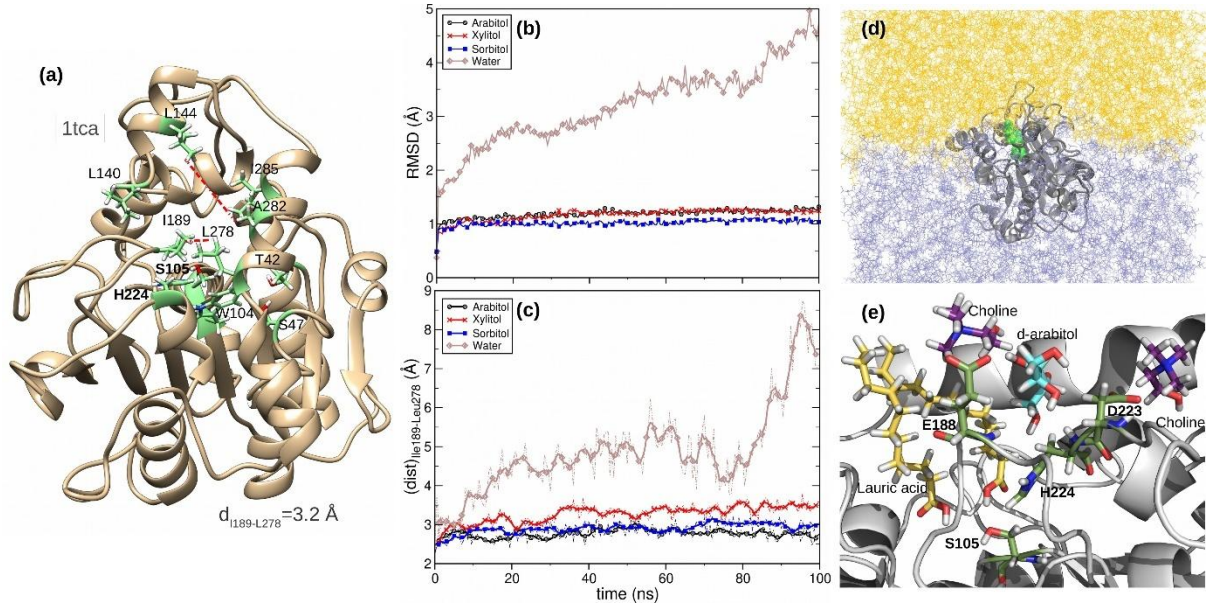

Figure 36 Computational analysis of the structural stability of the CalB active site. (a) Graphical representation of CalB lipase (pdbID: 1tca). Active site residues are colored in light green, while red dashed lines indicate the minimum residue-residue distances. Evolution of (b) root mean squared deviation (RMSD) of the CalB active site and (c) the Ile189-Leu278 minimum distances for CalB in NADES (ChCl:polyol 1:1) and in water solvent along the MD trajectories. Values are averaged over 10 trajectories for each system. (d) Graphical representation of the lipid-NADES interface after the annealing stage. Lauric acid molecules are yellow, NADES is light blue, while the catalytic residues Ser105 and His224 of CalB (dark grey, cartoon) are represented as green surface. (e) Graphical representation of NADES components, lauric acid molecules and the lipase active site residues.

Catalytic efficiency of LAR for synthesizing lauryl esters of carbohydrate polyols in R-NADES

The synthesis of lauryl esters of the selected carbohydrate polyols, catalysed by immobilized LAR lipase, was evaluated in preliminary experiments in ChCl:polyol reactive NADES. Screening small scale reactions were carried out with 300 U enzyme/g polyol, at 70ºC, 67 h reaction time, at a 1:1 molar ratio between LA and the polyol component of the R-NADES of 1. Surprisingly, addition of the lauric acid to the reactive NADES resulted in the formation of a two-phase system, due to the separation of the hydrophobic lauric acid layer from the hydrophilic NADES core containing the solid enzyme. Extensive stirring was required to homogenize the reaction mixture and avoid mass transfer limitations. The product formation was demonstrated by chromatography (HPLC and TLC). The highest lauric acid conversion (23 mol%) was obtained for the ChCl:arabitol (1:1) NADES. The esterification of xylitol and sorbitol attained comparable levels of LA conversion, i.e., 16.5 mol% and 18 mol% respectively, but lower than that obtained for the esterification of D-arabitol. We

suggest that this difference in LA conversion might be induced by the differentiation in the stereo-conformation of the polyols that influence both the enzyme-substrate interactions and the strength of the intermolecular interactions of the constituents of NADES.

Based on these results, the esterification of D-arabitol with lauric acid in R-NADES ChCl:D-arabitol (1:1) was selected as model reaction for optimization of reaction parameters to maximize the conversion and product yield.

Optimization of the esterification reaction in R-NADES by experimental design

The initial stage of the optimization process aimed to identify the key variables that influence the enzymatic reaction. Five critical parameters were selected: (1) temperature, (2) R-NADES viscosity (which affects overall mixture viscosity), (3) reaction time, (4) the molar ratio of lactic acid (LA) to D-arabitol, and (5) enzyme load. Due to the strong correlation between temperature, viscosity, and enzyme performance, a temperature range of 45–80 °C was chosen. The upper limits of enzyme load and molar ratio were doubled based on previous small-scale results (subchapter 3.3) because they were deemed significant. To determine the optimal reaction time, balancing conversion efficiency with enzyme stability, a time-course experiment was conducted. LA conversion increased notably up to 24 hours, reaching ~60 mol%, but gains beyond this point were minimal (an increase of only 6.7% and 12% after 48 and 72 hours, respectively). Thus, 24 hours was selected as the optimal reaction duration for further studies.

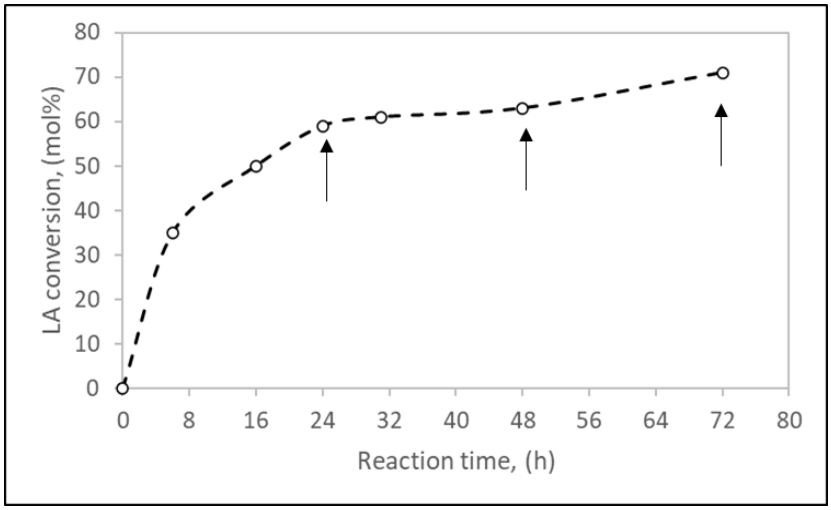

Figure 37 The LA conversion for the esterification of D-arabitol with LA, in ChCl:D-arabitol (1:1), at 70ºC, catalyzed by LAR (400 U/g D-arabitol), at an LA/D-arabitol molar ratio of 1, at different reaction time.

A factorial experimental design employing a Box-Behnken model was used to evaluate the influence of key parameters on product formation. Three variables were tested at three levels: temperature (45, 62.5, and 80 °C), enzyme load (150, 375, and 600 U/g D-arabitol), and LA:D-arabitol molar ratio (1, 1.5, and 2). Two blocks of

experiments, each consisting of 12 runs, along with three center-point repetitions, were conducted with a fixed reaction time of 24 hours. High-performance liquid chromatography (HPLC) analysis confirmed no conversion in control samples, and conversion values for each condition are summarized in Table S1.

The best-fitting model was a quadratic equation with seven regression coefficients. This model was selected based on the highest adjusted R^2 and optimal fit statistics. A very low p-value for the model (<0.0001) and a high F-value (22.15) indicate strong model significance. Significant terms included linear (A, B), interaction (AB, BC), and quadratic (A^2, B^2, C^2) effects. Among these terms, A, B, A^2, and B^2 had the highest F-values and the strongest influence on LA conversion. The model's high adequate precision value (16.703) indicates an excellent signal-to-noise ratio. The adjusted R^2 value (0.8783) is close to the multiple R^2 value (0.9212), reflecting excellent agreement between the observed and predicted results. The resulting quadratic equation can predict LA conversion based on the specific input values of the tested factors.

$$Y = -109.095 + 4.335A + 0.023B - 50.9C + 0.001AB - 0.034BC - 0.064AC - 0.032A^{2} + 0.0008B^{2} + 25.52C^{2}$$

Table 13 Fit statistics and estimated regression coefficients and adjusted R2 obtained for the quadratic BBD model.

Parameter	Estimated regression coefficients	F value	*p*-value	
Model		22.15	< 0.0001	significant
b_0: Intercept	-109.09484			
A: Temperature	4.33565	51.05	< 0.0001	significant
B: Enzyme load	0.02266	89.25	< 0.0001	significant
C: LA/D-arabitol molar ratio	-50.90375	0.0376	0.8482	
AB: Temperature*Enzyme load	0.00107	4.58	0.0456	significant
AC: Temperature*LA/D-arabitol	-0.03400	0.0225	0.8823	
BC: Enzyme load*LA/D-arabitol	-0.06416	13.26	0.0057	significant
A^2: (Temperature)^2	-0.03293	23.90	0.0001	significant
B^2: (Enzyme load)^2	0.00087	4.54	0.0464	significant
C^2: (LA/D-arabitol molar ratio)^2	25.51583	9.56	0.00060	significant
Multiple R^2	0.9212			
Adjusted R^2	0.8783 (>0.8)			
Adequate precision	16.703			

Interactions between variables were visualized by constructing response surface (Figure 38A) and contour plots (Figure 38B and C), which explain the interaction between the response and the experimental data as function of the levels of two variables with the third variable at its central value.

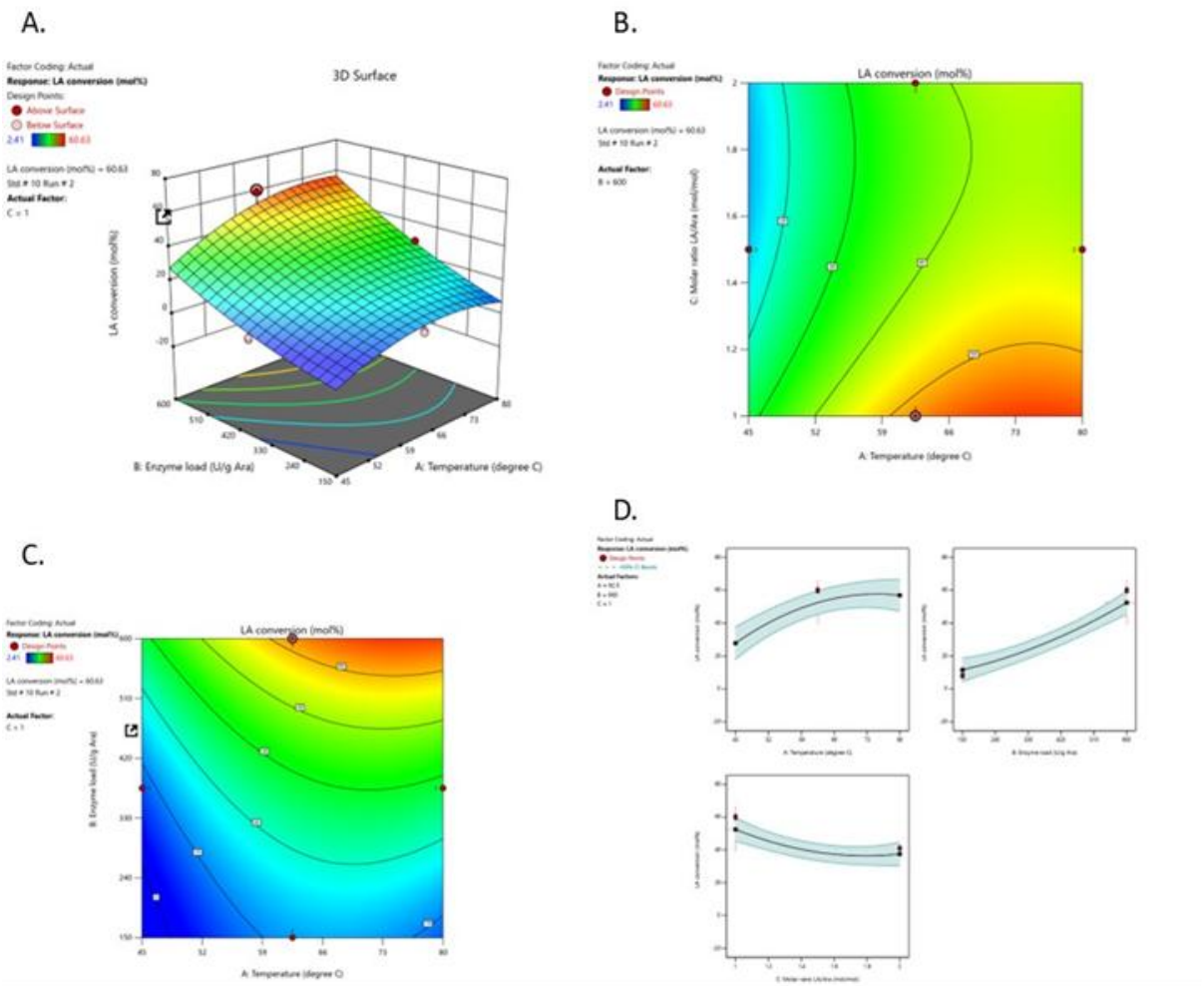

Figure 38 Graphic visualization from Response Surface Methodology (RSM). A) Surface plot for LA conversion, for molar ratio LA/D-arabitol = 1:1. B) Contour plot temperature vs. LA/D-arabitol molar ratio at enzyme load = 600 U/g; C) Contour plot for enzyme load vs temperature, at LA/D-arabitol molar ratio = 1; D) Interaction plot between LA conversion and factors

The highest LA conversion (60.6 mol%) was reached at high enzyme loads (600 U/gram D-arabitol), at high temperatures (above 66 °C) and for a molar ratio LA/D-arabitol of 1. The LA conversion was hardly influenced by increasing the enzyme load. However, the highest possible enzyme load for maximal conversion was not achieved, as illustrated by the increasing trend for enzyme load in Figure 38D. Since the LA conversion is augmented at the borderlines of the design space for variable B, i.e., enzyme load, the experimental design should be extended towards higher enzyme amounts.

The information acquired from the analysis of the surface and contour plots suggest that higher conversions may be possible to be obtained at higher enzyme load. Therefore, to validate the model and this assumption, using the regression equation generated by the model given in equation 2, we have calculated predicted values of the LA conversions for several levels of the enzyme load, two included in the model (i.e., 400 U/g D-arabitol and 600 U/g arabitol), and one higher (i.e., 800 U/g D-arabitol), at two temperatures 60°C and 70°C, at a LA:D-arabitol molar ratio of 1, and

24 h. The additional experiments followed the same procedure used for the design of experiments, with additional conversion measurements at 48h and 72h (Table 14 Experimental validation of the optimization model).

As shown in Table 14 Experimental validation of the optimization model, there is a very good correlation between the predicted values for LA conversion and the experimentally determined values for each experiment. Carrying out the reaction at higher enzyme loading amount (800 U/g D-arabitol) at the specified conditions (70°C, molar ratio LA:D-arabitol of 1), an LA conversion of 80 mol% was obtained already at 24 h reaction time. Increasing the reaction time to 48h and 72h, respectively, increased the LA conversion when reactions were carried out at the lower enzyme loadings. Nevertheless, this effect is minimal at higher enzyme concentration, confirming the assumptions made that the enzyme load and not the reaction time is the critical parameter of the process.

Table 14 Experimental validation of the optimization model

Entry	T (°C)	Enzyme load (U/g D-arabitol)	LA conversion (mol%)			
			Predicted	Experimentally measured		
				24 h	48 h	72.h
1	60	400	52.30	54 ± 0.97	65 ± 0.63	73 ± 0.16
2	70	600	59.31	65 ± 1.28	74 ± 1.56	80 ± 0.82
3	70	800	75.36	78 ± 1.73	82 ± 1.67	85 ± 1.56

Preparative synthesis of the carbohydrate polyol laurate diesters and their characterization

Following the validation of the optimal reaction conditions obtained based on the factorial experimental program, preparative synthesis of lauryl esters of D-arabitol, xylitol and D-sorbitol, mediated by the commercial immobilized CalB lipase (LAR) was at conditions predicted for maximizing LA conversion, given in Table 14 Experimental validation of the optimization model, Entry 3. All reactions (Figure 39).

Results are summarized in Table 15 Yields of enzymatic synthesis of esters of D-arabitol, xylitol and D-sorbitol and their properties.. The structural characterization of the reaction products was performed based on ESI-MS, FTIR, ^{1}H-NMR, ^{13}C-NMR, 2D ^{1}H-^{13}C HSQC NMR and 2D ^{1}H-^{13}C HMBC NMR.

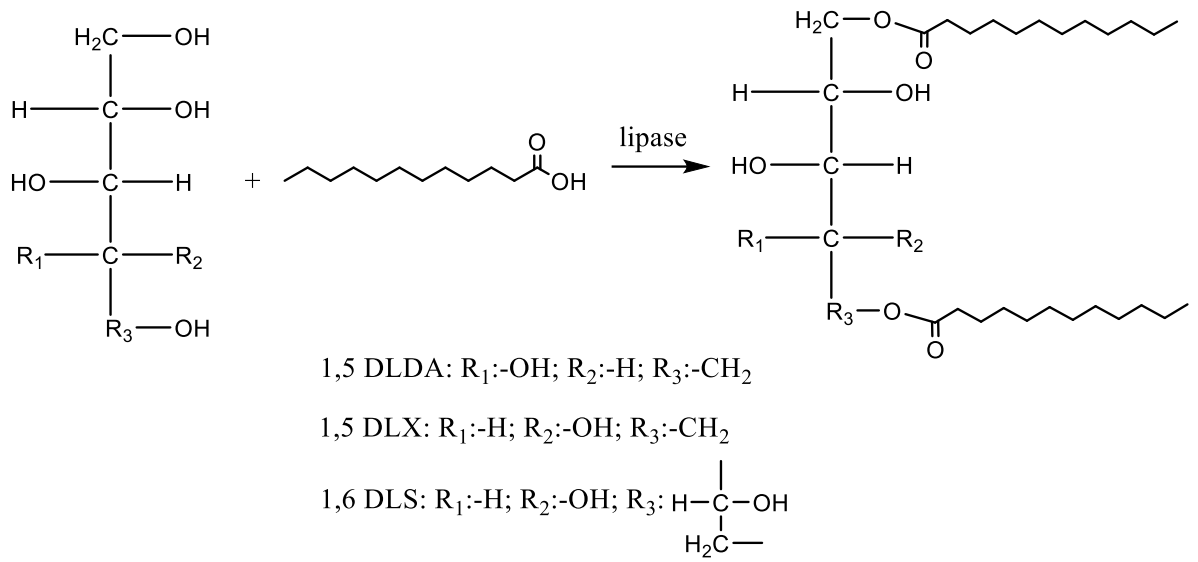

Figure 39 Reaction scheme of the enzymatic synthesis of esters of D-arabitol, xylitol and D-sorbitol

Table 15 Yields of enzymatic synthesis of esters of D-arabitol, xylitol and D-sorbitol and their properties.

Substrate NADES	Product	LA[a)] conversion (mol%)	Product yield (mol%)	Polyol conversion (mol%)	T_m (°C)	HLB
ChCl:D-arabitol, 1:1	1,5-DLDA	80	95	38.7	105.8	5.8
ChCl:xylitol, 1:1	1,5-DLX	56	90	25.0	69.3	5.8
ChCl:D-sorbitol, 1:1	1,6-DLS	62	86	26.5	75.7	6.6

[a)] Reactions were performed at 70°C, with 0.25 g R-NADES, and 800 U/g polyol enzyme catalyst, molar ratio LA/polyol = 1, for 24 hours.

Reactions proceeded with a medium to high conversion of lauric acid of 80 mol%, 56% and 62% for the esterification of D-arabitol, xylitol and D-sorbitol. Surprisingly, LA conversion increased with the same factor for all three substrates (i.e., 3.5) as compared to the results obtained in the preliminary screening experiments, for a 2.7-fold increase of enzyme load and 2.8-fold decrease of reaction time. This confirms the assumption that enzyme-substrate and enzyme-NADES interactions are the main factors controlling the reaction. The isolated products were obtained as white amorphous solids. The structure of the products as well as their purity was elucidated by a combination of spectroscopic, calorimetric, and chromatographic techniques.
1,5-DLDA has a melting temperature of 105.8 °C, which is very close to that of the D-arabitol, (i.e., 102 °C), but a significant drop in the T_m is observed for 1,5-DLX and 1,6-DLDS, from 92-96 °C to 69.3°C and 75.7 °C, respectively (Figure S7). DSC shows only one sharp, symmetric peak for the D-arabitol ester, indicative of a single product, very pure. A discrete tailing of the peak measured for the xylitol product suggests the presence of a minute trace impurity. Nevertheless, DSC shows that the isolated 1,5-DLDS contains traces of lauric acid (T_m: 43.8°C) and of a second compound that can be assigned to sorbitol lauryl monoester with and estimated Tm at 66°C (Figure S7D). However, the concentration of the monoester impurity is very low, and it could not be detected by TLC.

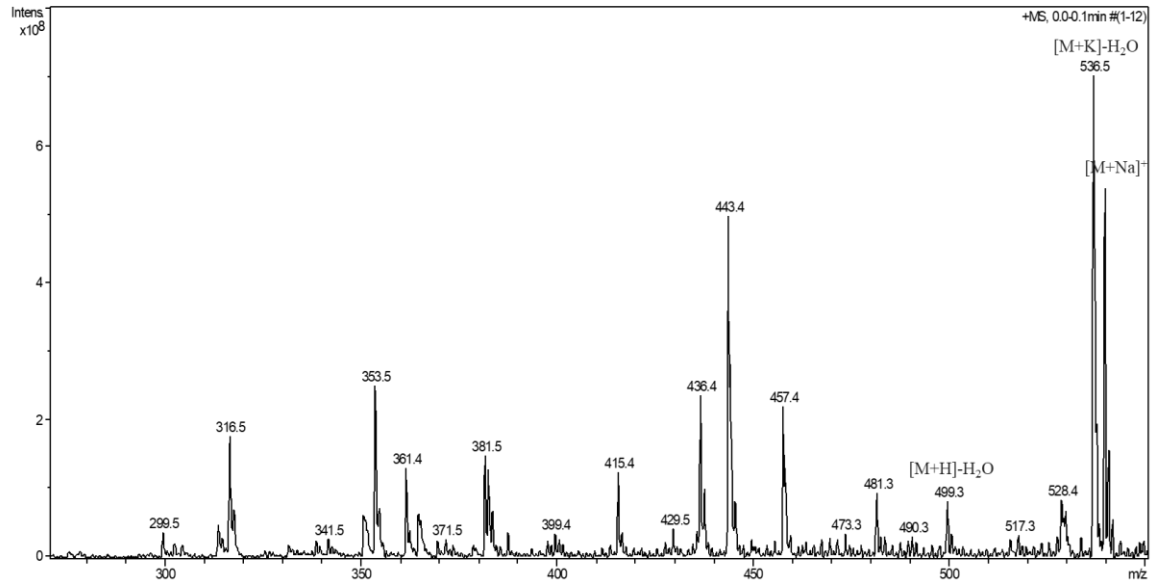

Figure 40 The ESI-MS spectra of 1,5-dilauryl-D-arabitol ester

The ESI-MS spectrum of the purified D-arabitol ester, the presence of m/z: 539 $[M+Na]^+$, 537 ($[M+K]-H_2O$), 517.3 $[M+H]^+$, 499.3 ($[M+H] - H_2O$) demonstrated the formation of the diester Figure 40. This is consistent to the expected molecular mass for 1,5-dilauryl-D-arabitol diester (1,5-DLDA), of 516.8 g/mol.

The NMR spectra demonstrated that the reaction occurred with high regioselectivity, exclusively at the primary hydroxyl groups of the polyols, namely OH-1 and OH-5 groups for D-arabitol and xylitol, and OH-1 and OH-6 for sorbitol. The ratio of the protons of the hydrocarbon chain of LA to the protons of the hydrocarbon chain of polyol in the ^{1}H-NMR spectrum is 46H:7H for D-arabitol ((Figure 7A) and xylitol and 46H:8H for D-sorbitol, which corresponds to diesters of D-arabitol, xylitol and D-sorbitol, respectively. In the ^{13}C-NMR spectrum of the D-arabitol ester, two signals are observed at 173.9 ppm and 173.7 ppm, which correspond to the two carbonyl carbon atoms in the diester. Although we would expect the two carbonyl carbons to be equivalent, they have different chemical shifts due to the presence of the two chiral carbons (2-C and 4-C) that have different configurations (2R, 4R). The presence of the two chirality centers at the 2-C and 4-C carbon atoms makes the protons from the methylene groups 1-CH_2 and 5-CH_2 diastereotopic.

The ^{13}C-NMR spectra of 1,5-DLX and 1,6-DLDS show that the diesters are impurified in a small proportion with the monoester. Three signals are observed for carbonyl carbon and the number of peaks for the carbon atoms in the polyol chains for xylitol and D-sorbitol is double. Indeed, this is in good agreement with the findings from FTIR and DSC analyses discussed above.

The coupling in the 2D ^{1}H-^{13}C HSQCED spectrum (the direct couplings of the methylene and methine carbon atoms respectively have different phases) between the two methylene carbon atoms 1-CH_2 and 5- CH_2 from 68.1 ppm and 67.0 ppm and the protons at 5.51 ppm and 5.01-4.78 ppm, respectively, demonstrate that these protons are the 1-CH_2 and 5-CH_2 diastereotopic protons of the D-arabitol moiety.

In the 2D ^{1}H-^{13}C HMBC spectrum (Figure 41), the long-distance coupling over three bonds between the two carbonyl carbons (173.9 ppm and 173.7 ppm) and the four methylene protons at 5.51 ppm and 5.01-4.78 ppm, respectively, is observed. We also observe the distance coupling over two and respectively three bonds between the two carbonyl carbon atoms and the methylene protons 2'-CH_2, 2''-CH_2 (2.35-2.31 ppm) and respectively 3'-CH_2, 3 ''-CH_2 (1.65-1.59 ppm). These long- distance couplings demonstrate that esterification with LA has occurred at both ends of the D-arabitol. According to the above, it can be concluded that the diester of D-arabitol with LA was obtained at the hydroxy groups in positions 1 and 5.

1,5-dilauryl-D-arabitol (1,5-DLDA), 1,5-dilauryl-xylitol and 1,6-dilauryl-D-sorbitol were identified as the main reaction products, showing an almost quantitative conversion of the monoester into diester and a high conversion of the substrate polyols. The fast and almost complete conversion of the monoester was also confirmed by HPLC that showed that even after a few hours of reaction, at half of the maximum conversion obtained under the optimized conditions, the diester was the main reaction product.

The high selectivity towards the diester can be related to the high preference of CalB for more hydrophobic substrates, thus the monoester could be a better substrate and lead to quantitative formation of the diester. If CalB operates preferentially at lipase-NADES interfaces, as MD simulations predicted, the monoester high solubility in the lipid phase in which the active site is orientated, and the very low concentration of polyols in the same phase, may support the high selectivity towards the diester formation.

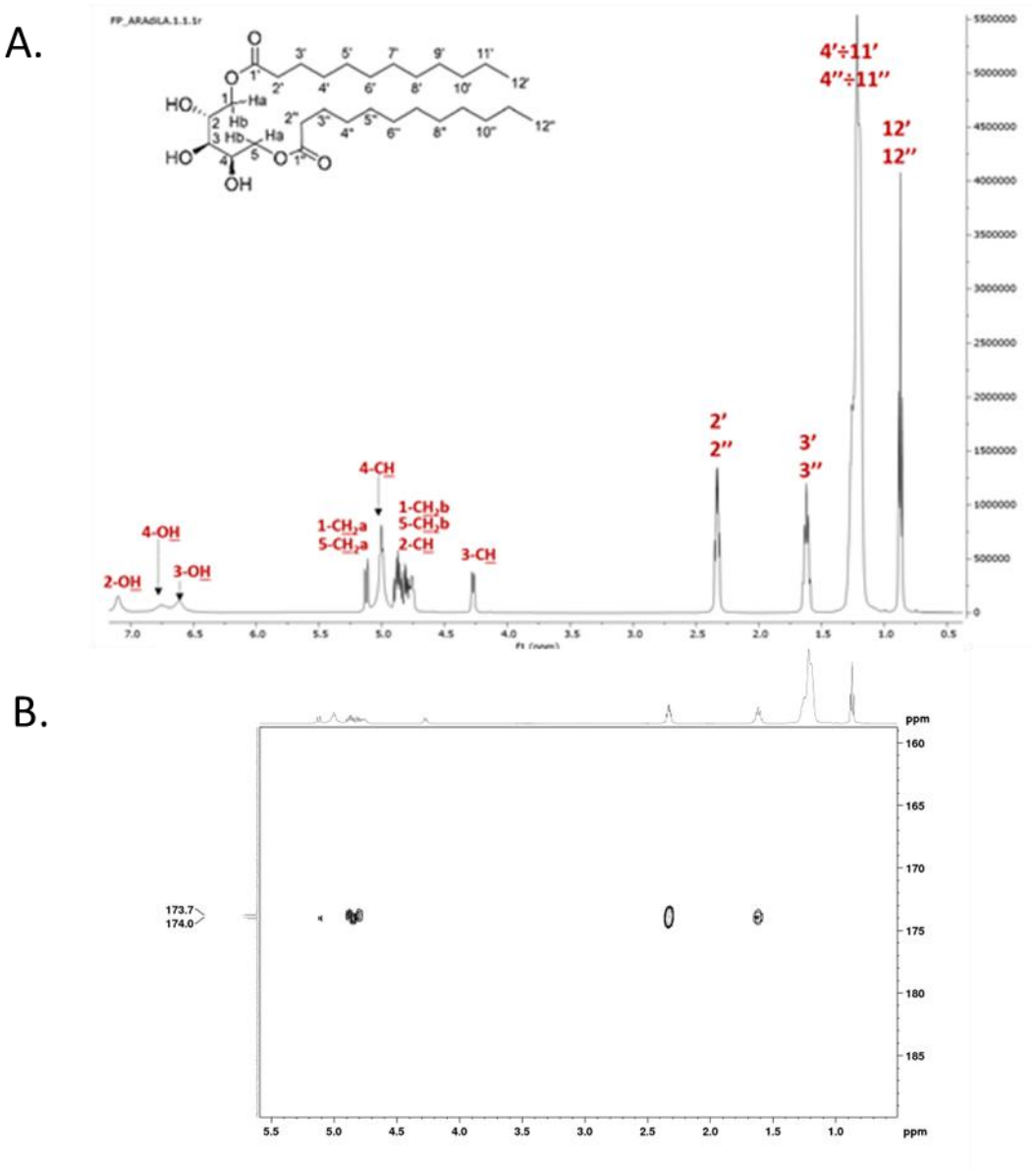

Figure 41 A) ^{1}H-NMR spectrum of 1,5-DLDA. B) Zoom of the 2D ^{1}H-^{13}C HMBC spectrum, the long-distance coupling between the two carbonyl carbons (173.9 ppm and 173.7 ppm) and the four methylene protons at 5.51 ppm and 5.01-4.78 ppm, and with the methylene protons of the aliphatic acid chain.

Molecular docking study of enzymatic synthesis of sugar alcohol diesters in NADES containing carbohydrate polyols as hydrogen bond donors.

A first molecular docking study was performed by using the diesters as substrates and Autodock Vina based on Monte Carlo search and rapid gradient-optimization conformational search coupled with a simple scoring function for free energy estimation [64]. Among the first 10 generated poses ranked by energy the productive poses were selected by identifying those where the substrate assumes a Near Attack Conformation (NAC) compatible with the productive attack of the catalytic serine (Ser105 of CalB) to the carbon atom of the ester groups of the ligands.

In Table 16 the values of the *d* as required and ϑ values compatible with NAC and the correspondent docking energy were included. Even if the values of the docking energies are not very low the protocol led to NAC compatible ϑ and d within 0.2/0.3 Å and the results are in good agreement with the experimental data was obtained.

Table 16 AutoDock Vina data relative to the docking free energies computed only for the poses corresponding to the lowest energy values distances and angles were calculated taking as a reference the C atom of the -COOR ester group.

Substrate	E*abs [kcal/mol]	d [Å]	ϑ [º]
LA2AR	-1.2	3.5	93.5
LA2XL	-1.4	2.2	61.0
LA2SRB	-0.4	3.4	56.5

A plausible reaction pathway for diesterification

Since the sole product of the reaction for arabitol/lauric acid mixtures was 1,5-DLDA we investigated by a combination of docking, energy minimization and short molecular dynamics runs a possible reaction pathway with the following steps:

1) lauric acid esterification with SER 105
2) transesterification with arabitol
3) second lauric acid esterification with SER 105 with the binding cavity occupied by the arabitol-mono-laurate
4) transesterification with arabitol-mono-laurate to produce the final diester product.

With standard choices of parameters all relevant bound configurations could be obtained by autodock vina, without any biasing condition. The only restraining bias was applied afterwards to properly orient the carbonyl oxygen in two of the docking poses, without modifications to the overall position of the molecules. In general, the docking study shows that all intermediate configurations along the reaction pathway do not produce any strain in the cavity of the protein, on the contrary they are obtained among the best configurations produced by the docking algorithm. These considerations are illustrated in Figure 42, together with the hypothesized reaction pathway.

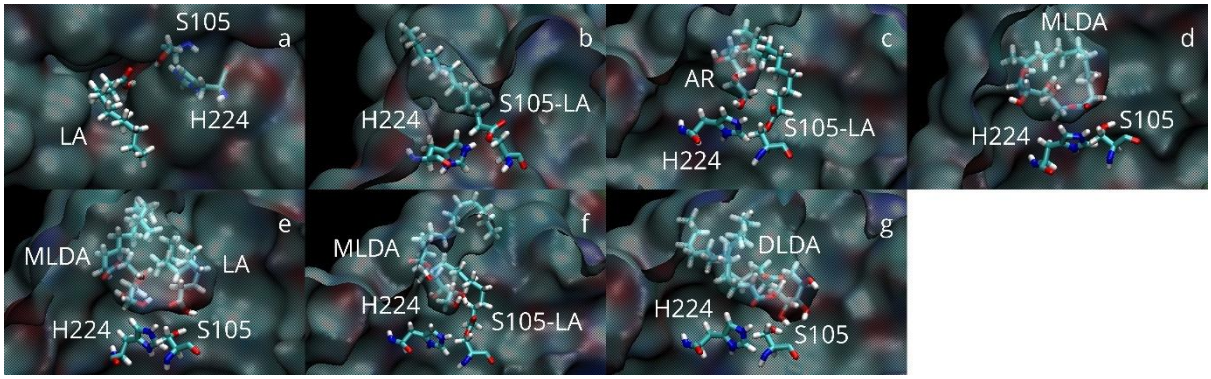

Figure 42 A plausible diesterification reaction pathway illustrated through docking poses. In all figures the protein is shown by its molecular surface, residues SER 105 (esterified or not) and HIS 224 are shown in licorice and are readily identified by the presence of one and three nitrogen atoms, respectively, displayed in blue. Esterification of SER 105 was performed manually defining the corresponding topology in charmm36 forcefield and obtained by energy minimization starting from unreacted compounds. a) lauric acid in the cavity with the protonated carboxylic group in proper arrangement close to SER 105 hydroxyl group; b) the product of esterification of SER 105; c) arabitol in the cavity with one end hydroxyl group close to the ester group of esterified SER 105; d) the monoester product of transesterification of arabitol with SER 105; e) a second lauric acid in the cavity with the carboxyl group close to the hydroxyl group of SER 105; f) the product of esterification of SER 105 in the presence of the monoester in the cavity; g) the diester as the product of transesterification of the monoester with esterified SER 105.

II.5. Development of sustainable bio-based polyesters and polyesteramides

The growing demand for sustainable, eco-friendly materials has driven intensive research into bio-based polymers and more environmentally friendly production methods. Bio-based plastics are increasingly being accepted as a viable alternative to petrochemical polymers, with global production capacity projected to increase threefold from 5.1 million tonnes in 2013 to 17 million tonnes by 2020. This growth is fuelled by public environmental concerns and the desire to reduce dependence on fossil fuels. The development of renewable monomer feedstocks (e.g. microbial fermentation of lactic, succinic or itaconic acid) and integrated biorefineries has expanded the range of building blocks available for polymer synthesis, particularly. However, conventional polymerisation processes often rely on metal catalysts, high temperatures and toxic reagents, which can leave harmful residues and have a significant energy footprint. In this context, enzymatic polymerisation, which uses enzymes as biocatalysts to assemble polymers under mild conditions, has emerged as an attractive green alternative [5].

Enzymatic polymerisation uses hydrolase enzymes, which are nature's catalysts, to form polymer bonds in vitro. This essentially reverses the biological hydrolysis function of these enzymes. Pioneering work by Kobayashi and others in the 1990s demonstrated that lipases, which typically break down esters, could also catalyse polyester synthesis. Over the past two decades, this approach has evolved from an initial proof of concept into a widely adopted strategy for producing polyesters and other polymers with high selectivity and in environmentally benign conditions. Key contributors to this field include researchers such as Shu Kobayashi, Richard Gross, and Alessandro Pellis, who have developed enzymatic methods for polymerising

various bio-based monomers [65]. *Candida antarctica* lipase B (CALB) is a notable catalyst for polyester synthesis thanks to its robustness and its availability in an immobilised form (commercially known as Novozym 435) [5], [66].

Enzyme-catalysed polymerisations offer several sustainability advantages. Operating at moderate temperatures (typically 50–80°C) and under atmospheric pressure avoids the high energy input required for traditional melt polymerisations [67]. They also eliminate the need for toxic metal catalysts, which is particularly important for biomedical polymers as residues from catalysts can cause toxicity. Due to the high selectivity of enzymatic reactions, they can accommodate monomers with sensitive functional groups (e.g. double bonds and heterocycles), which would not survive harsh chemical conditions. The mild conditions also mitigate issues such as the racemisation of chiral monomers, enabling the production of stereochemically pure polymers in some cases. Consequently, enzymatic polymerisation aligns well with the principles of green chemistry and the circular bioeconomy, facilitating the production of bio-derived polymers that are inherently more degradable and easier to recycle.

At the same time, it is important to recognise that enzymatic polymerisation is typically best suited to speciality polymers and oligomers rather than large-scale commodity plastics, at least with the current state of the art. Many enzymatically produced polyesters have relatively low molecular weights and are used in high-value applications, such as biomedical devices, coatings, and nanocomposite precursors, where their biodegradability and tolerance of functional groups are highly valued. However, rapid progress in enzyme engineering, process optimisation and monomer supply continually push the boundaries. In recent years, researchers have synthesised polyesters using various bio-based monomers, including furanics derived from sugars, itaconic acid from fermentation, and glycerol derivatives from biodiesel waste. This chapter provides a comprehensive overview of the enzymatic synthesis of bio-based polymers, with a particular focus on polyester materials.

Enzymatic polymerisation uses enzymes as catalysts to form polymer chains from monomer precursors. In the context of bio-based polymers, lipases are the enzymes that have been studied the most. Lipases are a class of hydrolases that naturally catalyse the hydrolysis of ester bonds (e.g. in triglycerides). Under the right conditions (low water content and the presence of substrates with multiple functional groups), lipases can catalyse the reverse reaction, forming ester bonds and polymerising monomers into polyesters. Two major reaction modes are employed in enzymatic polyester synthesis (Figure 43):

(a) Condensation polymerisation, in which a diacid (or diester) reacts with a diol (or other polyol), releasing a small molecule such as water or alcohol.

(b) Ring-opening polymerisation (ROP) of cyclic esters (lactones) or cyclic carbonates. In both cases, the enzyme catalyses the formation of ester linkages via a mechanism analogous to its hydrolytic action, involving a transient acyl-enzyme intermediate.

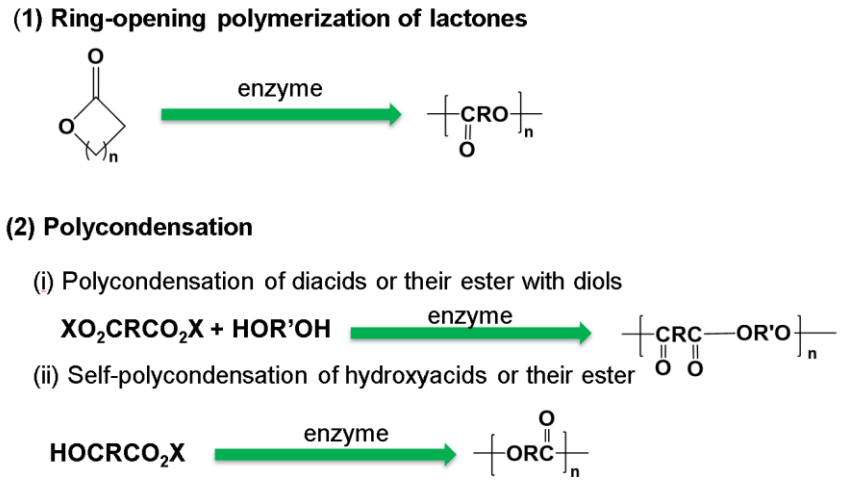

Figure 43 Enzymatic routes for polyester synthesis. (1) Ring-opening polymerization (ROP) of lactones catalyzed by enzymes leads to linear polyesters with repeating ester units. (2) Polycondensation reactions, which include: (i) the condensation of diacids (or their esters) with diols, and (ii) self-condensation of hydroxyacids (or their esters), also catalyzed by enzymes. Enzyme symbols represent the biocatalytic role in each step, promoting ester bond formation under mild and sustainable conditions.

The enzyme essentially binds an acyl donor (e.g. an ester or acid) in its active site to form a covalent acyl-enzyme complex (Figure 44). It then transfers the acyl group to an alcohol nucleophile to extend the polymer chain. This mechanism is sometimes described as the reverse of the in vivo hydrolysis reaction. The same enzymatic cycle that breaks down esters in nature can build them up in vitro when reaction water is removed or limited, thereby driving the equilibrium towards polymer formation.

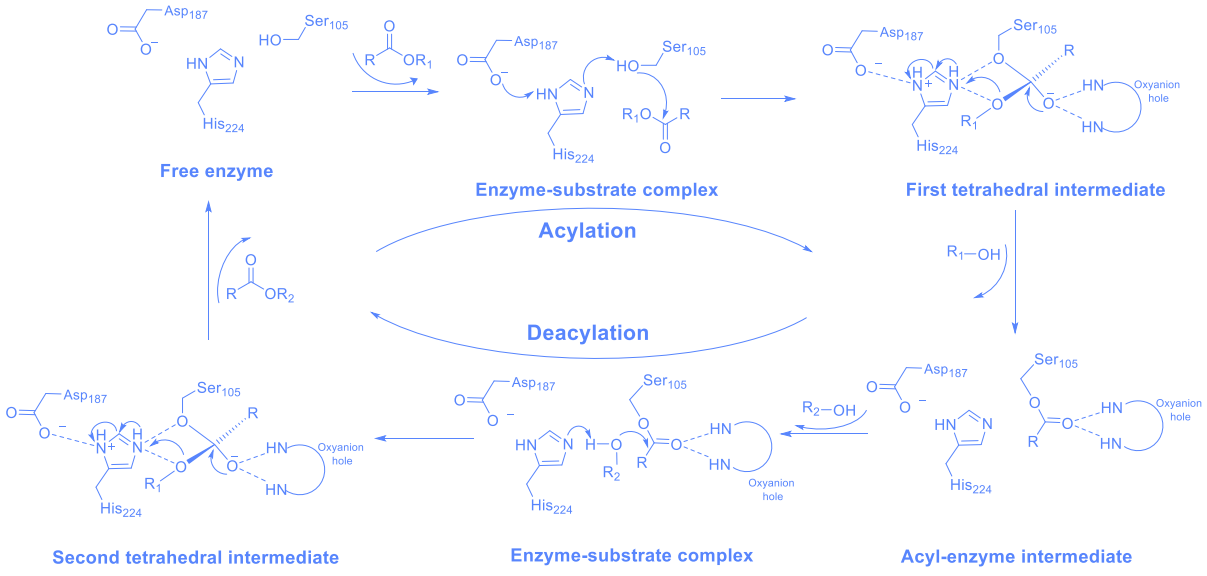

Figure 44 The general catalytic mechanism of serine hydrolases in polyester synthesis is as follows: This process can be divided into two main phases: acylation and deacylation. During the acylation step, the active serine residue attacks the ester bond of the substrate to form a covalent acyl-enzyme intermediate via two tetrahedral intermediates. In the deacylation step, a second alcohol or hydroxyl-containing monomer regenerates the free enzyme and extends the polymer chain. The oxyanion hole stabilises the negatively charged transition states throughout the reaction.

One remarkable aspect of enzymatic polymerisations is their selectivity. Lipase-catalysed reactions exhibit high chemo-selectivity, preferring esters to other groups, as well as regio-selectivity, controlling which hydroxyl or acid in an asymmetric monomer reacts [68]. They also often exhibit enantio-selectivity, distinguishing chiral centres. This means that enzymes can polymerise specific functional groups in the presence of others. For example, an unsaturated diacid such as itaconic acid contains both a carboxylic acid and a carbon–carbon double bond. A lipase will link the acids with diols to form an unsaturated polyester, leaving the C=C bonds intact. In contrast, a harsh chemical process might inadvertently polymerise or hydrogenate the double bond. This enables reactive or delicate functionalities to be incorporated into polymers, providing a means of producing materials that would otherwise be difficult to obtain using conventional catalysis. Additionally, enzymatic processes typically avoid side reactions such as uncontrolled cross-linking or cyclisation, although some cyclic by-products can form, as will be discussed later. The ability to carry out polymerisations under mild conditions (often below 90 °C in an organic solvent or in the bulk phase, and without the use of strong acids or bases) helps preserve the integrity of volatile or thermally sensitive bio-based monomers.

The range of enzymes used in synthetic polymer chemistry is expanding, but lipases have proven to be the most versatile and are used most widely in polyester synthesis. *Candida antarctica* lipase B (CaLB) is by far the most reported biocatalyst and is typically immobilised on a solid support to improve stability and enable reuse. Immobilised CALB (commercially available as Novozym® 435) is active in organic solvents and even in solvent-free molten monomer mixtures. It remains effective at temperatures of up to ~70–80 °C, and some preparations can endure 90 °C for short periods. Other explored lipases include those from *Thermomyces lanuginosus* (Lipase TL), *Burkholderia cepacia* (formerly *Pseudomonas cepacia*, Lipase PS), *Candida rugosa* and *Rhizomucor miehei* (Lipase RM), as well as cutinases (a related class of polyester hydrolases). Each enzyme has its own substrate preferences and temperature stability. For instance, in a study of enzymatic estolide synthesis, lipases from various sources were compared and showed different product distributions. A *Pseudomonas stutzeri* lipase prepared as cross-linked enzyme aggregates (CLEAs) produced the longest oligomer chains (estolides with a degree of polymerisation of up to 10) at 70-75 °C, outperforming other native and immobilised lipases. This demonstrates that the selection of a biocatalyst can significantly impact the outcomes of polymerisation (e.g. chain length and branching), and the choice of enzyme can be adapted to the specific monomers. In general, CALB is highly effective for a broad range of aliphatic monomers, whereas other lipases or engineered variants might be employed for more challenging substrates (e.g. bulky aromatics or secondary hydroxyl monomers).

A typical enzymatic polymerization is conducted either in an organic solvent that dissolves the monomers (e.g. toluene, methyl tert-butyl ether) or under bulk (solvent-free) conditions where one monomer acts as a solvent for the other. Because condensation reactions produce small molecules (water or methanol) that can drive the equilibrium backward, reaction setups often include strategies for continuous

removal of these by-products: for example, applying vacuum, using molecular sieves, or carrying out the reaction in a thin-film or sparged reactor to facilitate evaporation. In ring-opening polymerizations of lactones, the ring strain release helps drive the reaction, and enzymes have been used to polymerize lactones like ε-caprolactone [69], δ-valerolactone, or functional lactones at equilibrium conversions nearing 100%.

Enzymatic ROP generally yields linear polymers (avoiding the transesterification side-reactions that metal catalysts might cause) but can be slower than chemical ROP. On the other hand, enzymatic polycondensation can yield either linear polymers or cyclic oligomers (macrocycles), since the enzyme might cyclize a growing chain – this can limit the molecular weight. Still, by optimizing conditions (temperature, monomer ratio, enzyme amount, reaction time), researchers have achieved number-average molecular weights on the order of 5-10 kDa in many systems which is sufficient for certain applications (oligomers for coatings, prepolymers for thermosets, etc.).

Figure 45 shows the main ways in which renewable materials can be converted into platform compounds and bio-based polymers. It also highlights the potential applications of these compounds in areas such as cosmetics, controlled drug delivery systems, packaging, consumer goods and dental products. All of the colour-coded pathways, except those marked in green which are included for general context, have been investigated experimentally within the Biocatalysis and Green Chemistry Group. These routes were tested and validated by synthesising and structurally and functionally characterising the resulting products. The subsequent chapters of this habilitation thesis will provide detailed insights into these contributions.

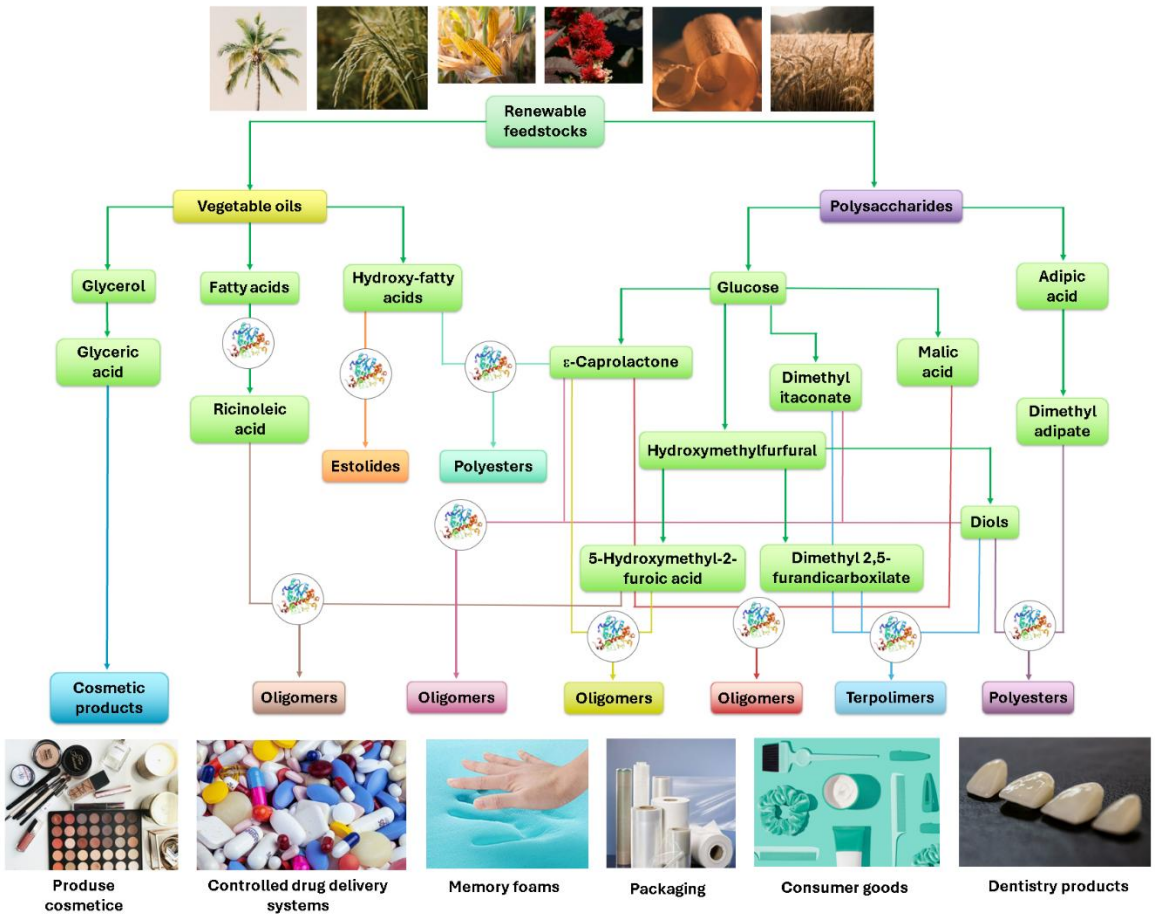

Figure 45 Conversion routes from renewable feedstocks to bio-based oligomers, estolides, polyesters, and terpolymers, and their applications.

It should be noted that enzymatic routes are not limited to polyesters. In principle, enzymes can catalyse the formation of other linkages, such as polyamides (using proteases or esterases for peptide-like bonds), polycarbonates (from carbonate esters), or even polyphenols (using oxidative enzymes). For example, hydrolases have been tested for polycondensation of diesters with diamines to form nylon-type polyamides, and some success has been reported in low-molecular-weight products [70]. The routes tested by authors group are presented in Figure 46.

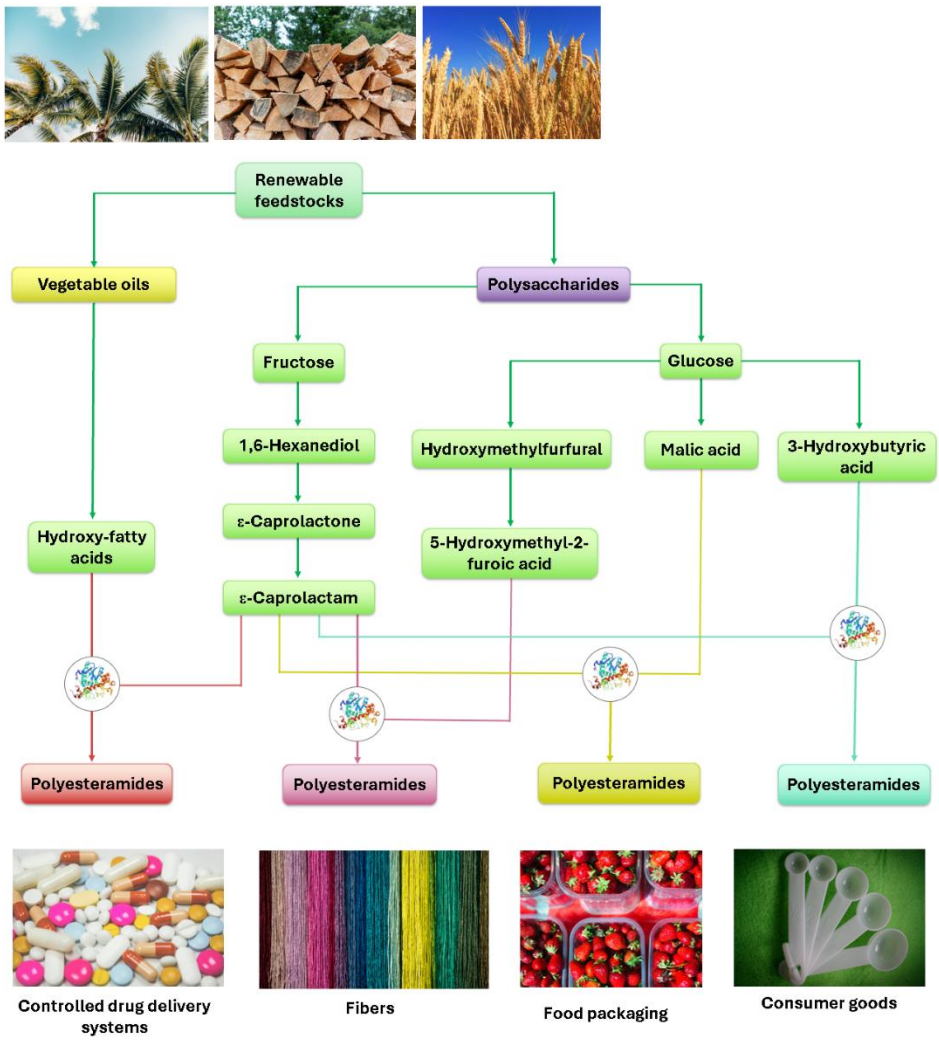

Figure 46 Pathways from renewable feedstocks to functional poly(ester amide)s (PEAs) and their applications. Renewable raw materials such as vegetable oils and polysaccharides (fructose, glucose) are converted into platform chemicals (e.g., hydroxy-fatty acids, ε-caprolactone, 1,6-hexanediol, hydroxymethylfurfural, malic acid) that serve as building blocks for the enzymatic synthesis of poly(ester amide)s.

Sources of monomers and screening of biocatalysts

One of the major advantages of enzymatic polymerisation is the ability to utilise monomers derived from biomass directly. Many of these monomers originate from renewable sources, such as plant oils, sugars, and fermentation products. A wide array of bio-based monomers has been explored, expanding far beyond classic examples such as lactic and sebacic acids.

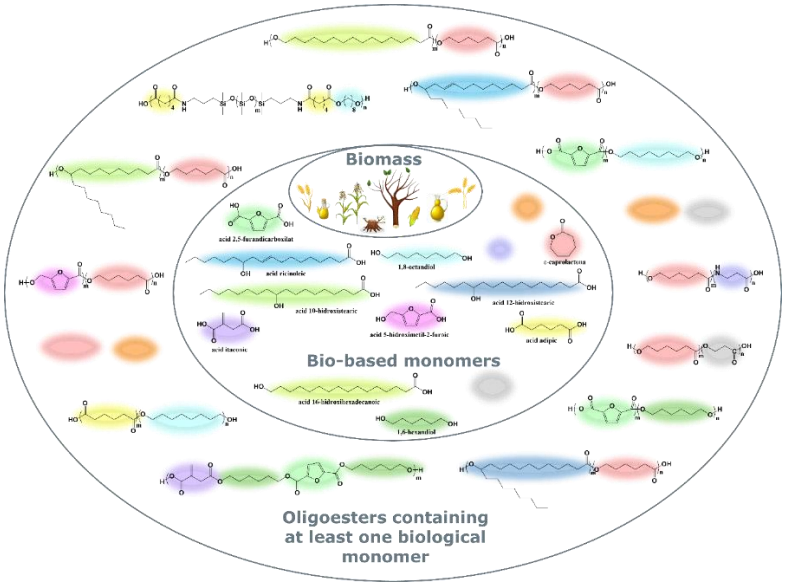

Figure 47 Pathway from biomass to bio-based oligomers containing at least one biological monomer, highlighting the transformation of biomass into monomers and their subsequent oligomerization.

Carbohydrate-derived monomers: Carbohydrates and their derivatives are abundant, renewable resources that can be converted into monomers with ester-forming functionality. An example is δ-gluconolactone, a cyclic lactone derived from sugars, which is obtained by the oxidation of glucose. δ-Gluconolactone [71], which has a seven-membered ring, can be copolymerised with smaller lactones, such as β-butyrolactone, using lipase catalysts. In one study, immobilised CALB was used to incorporate this carbohydrate-derived unit into a hydrophobic polyester backbone, yielding novel biodegradable copolymers [72], [73]. Systematic optimisation via design of experiments was employed to maximise the incorporation of the sugar-based unit and achieve a reasonable degree of polymerisation. The resulting products were cyclic and linear polyesters that clearly exhibited gluconolactone signals in NMR and MALDI-TOF spectra. This demonstrates that even bulky, hydrophilic sugar derivatives can be polymerised using an appropriate strategy (in this case, a solventless system at 80 °C with sufficient reaction time)[74].

II.5.1. Enzymatic synthesis of oligoesters from ε-caprolactone and 5-hydroxymethyl-2-furoic acid

Another important platform derived from sugars is 5-hydroxymethylfurfural (HMF), which can be oxidised to produce 2,5-furandicarboxylic acid (FDCA), a bio-based analogue of terephthalic acid. The U.S. Department of Energy has identified FDCA as a key building block and a top-value bio-based chemical. Enzymatic processes have been employed to polymerise FDCA by reacting its diester forms with diols. For example, dimethyl 2,5-furandicarboxylate (DMFDC) has been condensed with aliphatic diols using CALB to produce furan-based polyesters. Due to its two rigid furan rings, FDCA can impart thermal stability and strength to polyesters comparable to that of petrochemical aromatic monomers.

A derivative of HMF is 5-hydroxymethyl-2-furancarboxylic acid (HMFA), which has one carboxyl and one hydroxyl group, making it essentially a renewable hydroxy acid. HMFA can serve as a monomer capable of forming polyesters through self-condensation or copolymerisation. Todea et al. reported the enzymatic copolymerisation of HMFA with ε-caprolactone (a lactone derived from fossil fuels that can also be obtained from bio-based sources) to produce furan-containing polyesters. In a solvent-free, one-pot reaction at 80°C using immobilised CALB, ε-caprolactone (ECL) acted as a comonomer and a solvent for HMFA, yielding oligoesters that incorporated both the furan ring and the caprolactone units. Interestingly, no measurable homopolymerisation of HMFA alone was observed – the enzyme selectively formed copolymers (linear chains of ECL and HMFA), along with some cyclic and linear PCL homopolymer side products. These findings highlight that carbohydrate-derived monomers (in the form of sugar acids, lactones or furans) can undergo enzymatic polymerisation, albeit often requiring careful adjustment of the conditions (e.g. the use of a comonomer to enhance solubility) [75].

The possible reaction products are cyclic and linear copolyesters, as well as the cyclic and linear correspondent homopolymers, poly-(ε-caprolactone) and poly(5-methoxy-2-furancarboxylate) (Figure 48). In practice, the homopolymers of HMFA were not identified in quantifiable amount among the reaction products and this experimental detail favored the downstream process. The reactions went to completion in 24 h, since unreacted monomers were not detected in the reaction mixture.

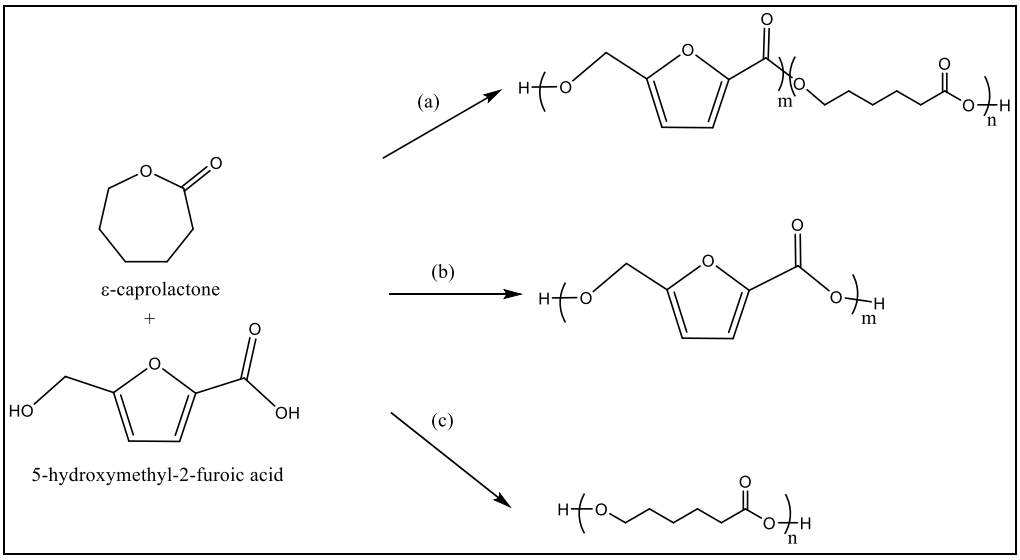

Figure 48 Reaction scheme for the synthesis of copolyesters from 5-hydroxymethyl-2-furoic acid and ε-caprolactone, with formation of copolymer (route a) and homopolymer (route b and c) products

The formation of the copolyesters was demonstrated by MALDI TOF-MS spectrometry. Figure 49 shows the MALDI TOF-MS spectrum of the reaction product obtained in the presence of Novozyme 435 at 80°C, in solventless system. The peak values correspond to the potassium adducts of the potassium salt (formed under MALDI conditions) of the synthesized oligomers, e.g. the peak with m/z 1962.06 corresponds to the K^+ adduct of the copolymer containing 12 ECL units and 4 HMFA

units, while the peak with m/z 3102.70 corresponds to the K^+ adduct of the copolymer containing 22 ECL units and 4 HMFA units.

The reactions were carried out using a 2:1 molar ratio ECL:HMFA, in order to use ECL also as solvent for the HMFA co-monomer. Based on this molar excess, the reaction product contained a certain amount of PCL homopolymer and the copolymers with higher polymerization degree contained a relatively higher number of ECL than HMCA units. The aim of this study was to determine the average molecular mass of the copolymer and the relative composition of the reaction products, but it was not the goal to explore the specificity of the enzyme for the monomers in depth.

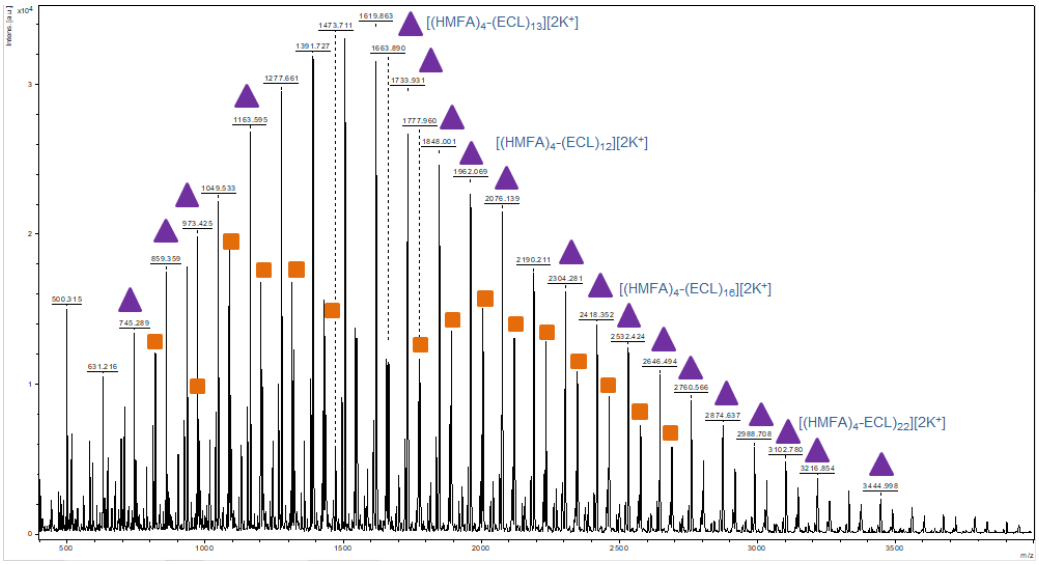

Figure 49 The MALDI TOF-MS spectrum of the copolymer synthesized from HMFA and ECL at 80° C and 24 hours reaction time, without solvent; Linear copolymers (triangles); Cyclic copolymers (squares)

Influence of the biocatalyst and reaction temperature

Three commercially available immobilized lipases from *Candida antarctica* B were tested to select the most suitable biocatalyst, based on the polymerization degree and the copolyester content in the reaction product. Novozyme 435 is the most successfully used as biocatalyst for the synthesis of a variety of polyesters and copolymers, while *Cal*B GF IM was not previously reported for the synthesis of polyesters. The reactions were carried out in the 40-80°C temperature range, to determine the effect of the temperature on the copolymer formation and on the polymerization degree, for each biocatalyst. Because the real lipase content of these commercial products is not disclosed, the same biocatalyst/substrate ratio (100 mg/ 6 mmoles of total monomers) was used in all studies, based on preliminary experiments (data not shown). The relative composition of the reaction products was calculated from the MALDI TOF-MS spectra (Table 17).

Among the tested lipases, the highest linear copolymer content at 40°C was obtained with the *Cal*B GF-IM biocatalyst. Lipozyme *Cal*B was the less performant, as the maximal polymerization degree of the synthesized copolymers did not exceed 10 units. However, this biocatalyst showed an important effect of temperature, since at

60°C the maximal polymerization degree increased to 18. When Novozyme 435 was used, the increase of the temperature within the investigated range of 20°C (from 40 to 60) did not result in higher average molecular weight values, but the relative content of the copolymer exceeded 55%.

As a general tendency, the average molecular mass and the dispersity increased with the increase of the temperature, the highest values being obtained at 80°C. However, at this temperature the relative cyclic copolymer amount exceeded 40% when Novozyme 435 and Lipozyme *Cal*B were used. The most efficient biocatalyst among the tested immobilized lipases was GF-CalB-IM at 80° C, with 60% linear copolymer content in the final product and maximal polymerization degree of 24. Even though the average molecular weight values were comparable, this biocatalyst was selected for the following studies.

Table 17 The influence of the biocatalyst and temperature on the relative copolymer and homopolymer content of the reaction products

Catalyst	T [°C]	M_n [Da]	M_w [Da]	$Đ_M$	Relative composition of the reaction product [%]				DP max[e]
					LC[a]	CC[b]	LH[c]	CH[d]	
Novozyme 435	40	931	1058	1,14	40,6	26,2	26,5	6,7	16
	60	1002	1085	1,08	57,5	10,6	14,5	17,3	15
	80	1280	1481	1,15	49,4	45,4	0,6	4,7	19
Lipozyme *Cal*B	40	695	745	1,07	41,7	22,9	30,2	5,2	10
	60	1113	1220	1,09	53,5	17,3	13,8	15,4	18
	80	1180	1347	1,14	52,7	40,4	0,0	6,9	19
GF-*Cal*B-IM	40	960	1085	1,13	46,9	21,1	21,9	10,2	17
	60	1128	1239	1,09	56,4	12,5	11,4	19,7	18
	80	1091	1404	1,27	60,2	24,0	11,8	3,9	24

[a] Linear copolymer; [b] cyclic polymer; [c] linear homopolymer; [d] cyclic homopolymer; [e] maximal polymerization degree of the copolymer

Influence of the water content on the product formation

The water activity of the reaction mixture was controlled and, in this regard, the substrates and the biocatalyst were pre-equilibrated separately in a desiccator containing saturated solutions of salts whose water activity is known. Subsequently, the reactions were carried out at 40°C for 24 hours. The composition of the reaction products and the dispersity values were calculated based on the MALDI TOF-MS spectra.

Table 18 shows the results calculated from the MALDI TOF-MS spectra. Pre-balancing in the absence of the saturated salt solution (probably the lowest water content) led to the obtaining of copolymers with the highest values of the average molecular weights, but the composition of the copolymerization products was not significantly influenced by the water activity in the reaction system. Although the differences were not high, the average molecular weights decreased at higher water activities, therefore a higher water content hinders the polymerization reaction.

Table 18 Influence of the initial water activity on the molecular weight and composition of the copolymerization products of ECL and HMFA. Reaction conditions: GF-CalB-IM lipase, 40° C, 24 h reaction time, mixing frequency 1000 min^{-1}

Salt	Water activity a_w^e	M_n [Da]	M_w [Da]	$Đ_M$	Relative composition of the reaction product [%]				DP max[e]
					CL[a]	CC[b]	HL[c]	HC[d]	
-	-	891	1011	1,13	35,8	32,5	26,8	4,9	17
$MgCl_2$	0,225	866	972	1,12	36,2	33,1	25,5	5,2	15
K_2CO_3	0,432	865	967	1,11	32,6	35,9	25,7	4,8	15
NaCl	0,750	847	941	1,11	31,2	35,9	27,7	5,2	14
Na_2SO_4	0,950	804	899	1,11	32,2	36,5	25,4	5,7	14
K_2SO_4	0,973	791	874	1,10	37,9	25,4	30,8	5,9	11

[a] Linear copolymer; [b] cyclic polymer; [c] linear homopolymer; [d] cyclic homopolymer; [e] maximal polymerization degree of the copolymer

Characterization of the reaction products by spectroscopy and thermal analysis

The formation of the copolyester by inclusion of 5-oxymethylene-2-furanyl units in the polymeric chain was demonstrated by NMR spectroscopy. The 2D HMBC spectrum, shown in Figure 50, shows the remote coupling between the signals corresponding to the C21 carbon atom with the signals of the C6 carbon protons (1.5 and 4.05 ppm), as well as the signals corresponding to the carbon atom C9 with the proton signals from the C16 carbon atom.

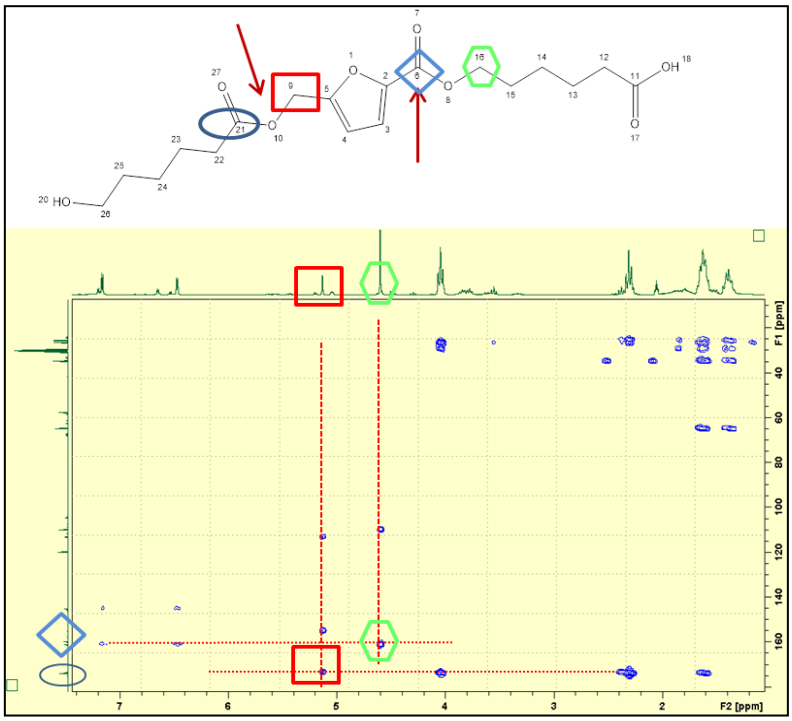

Figure 50 The 2D HMBC NMR spectra of the ECL_ HMFA reaction product obtained at 80°C, 24 h, 1000 rpm. The oligomer shown above to illustrate the spectrum is formed by two structural units derived from ε-caprolactone and one from 5-hydroxymethyl-2-furoic acid

The thermal properties of the copolymers compared to the PCL homopolymer and to the HMFA were evaluated by TG and DSC in nitrogen atmosphere. The

thermograms of the copolymer, PCL homopolymer, and HMFA monomer are shown in Figure 51 and the most representative decomposition parameters, such as the degradation temperatures at 5% and 10% weight loss ($T_{d,5\%}$, $T_{d,10\%}$), maximum decomposition temperature ($T_{d,max}$) are presented in Table 5. The mass loss of the copolymer starts at about 170°C.

Compared to the PCL homopolymer, for the copolymers a decrease of $T_{d,5\%}$ and $T_{d,10\%}$ values were observed, indicating that the thermal stability of the copolymers decreased. The copolymers present a 5% weight loss above 175.8°C. Compared to the previously reported furan-based polyesters, synthesized using tetrabutyl titanate as catalyst [31, 33, 34], the decomposition temperatures of the copolymers are comparable, about 400°C.

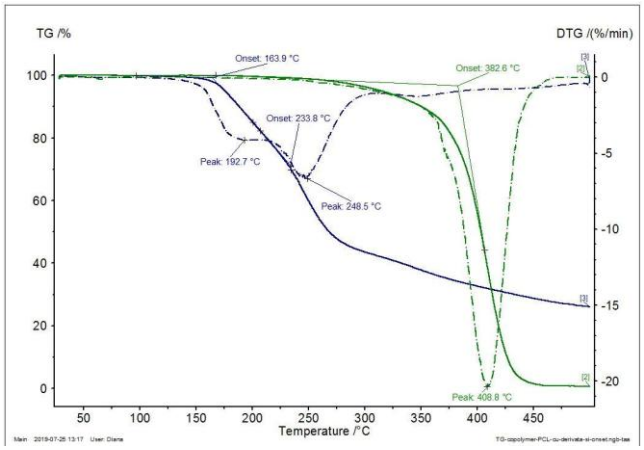

Figure 51 The thermograms of HMFA_ECL copolymers (blue), compared to the PCL homopolymer (green)

The DSC curves (Figure 52) show that the melting temperature of the copolymer is between that of HMFA and the PCL homopolymer. The copolymer exhibits an endothermic peak at 258°C, probably due to internal transitions that may occur at degradation. The melting temperature of the copolymer is about 100° C higher than of the PCL homopolymer. The main TGA and DSC parameters of the copolymer are presented in Table 19, compared to PCL homopolymer and HMFA.

Table 19 Thermal properties of the ECL-HMFA copolymer, compared to the PCL homopolymer

Sample	TGA			DSC				
	$T_{d,5\%}$[°C]	$T_{d,10\%}$[°C]	$T_{d,max}$[°C]	T_i [°C]	T_f [°C]	ΔT [°C]	T_{pk} [°C]	ΔH [J/g]
PCL	314.8	350.4	439.4	41.1	80,5	39,4	66.5	-145.5
				338.1	462.7	124.6	41.,2	-517.2
ECL-HMFA	178.5	188.3	432.8	130,4	171.4	41.0	164.9	-181.9
				214.2	294.1	79.9	258.4	123.4

T_d- the decomposition temperature, T_i - initial peak temperature; T_f - final peak temperature; $\Delta T = T_f - T_i$; T_{pk} - temperature at peak; ΔH - enthalpy

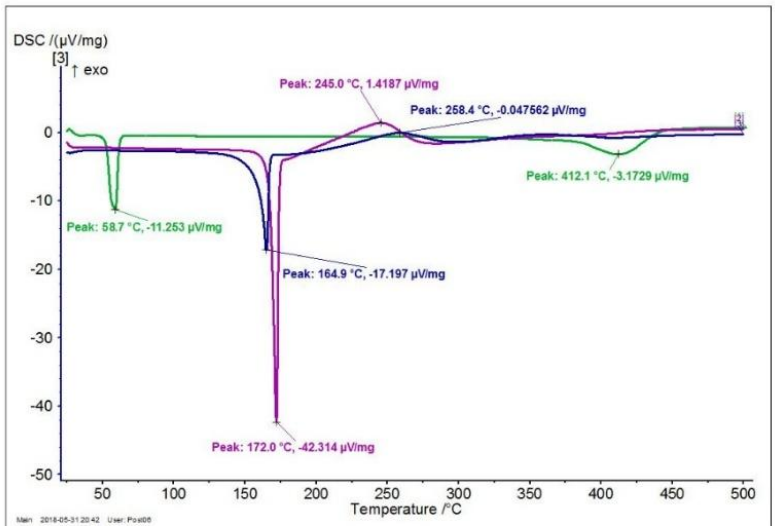

Figure 52 DSC curves of the HMFA_ECL (blue) copolymers, compared to PCL homopolymer (green) and HMFA monomer (purple)

Operational stability of the biocatalyst in repeated reaction cycles

The GF-CalB-IM enzyme was reused in several reaction cycles at 80°C and the same molar ratio 2:1 of the monomers (ECL: HMFA). After 24 h reaction the enzyme was separated, washed three times with THF, and reused in another reaction cycle in the same reaction conditions.

The average molecular weights and relative composition of the products were calculated based on MALDI TOF-MS spectra. After four batch reaction cycles, the composition of the reaction product and the relative copolymer content did not change significantly, although the average molecular weights were lower (Table 20). The maximum degree of polymerization also decreased with recirculation, indicating a gradual diminution in the catalytic efficiency of the enzyme after several cycles of use.

Table 20 Reuse efficiency of the GF-CalB-IM enzyme in multiple reaction cycles

Reaction cycle	M_n [Da]	M_w [Da]	$Đ_M$	Relative content of the reaction products [%]				DP max[e]
				CL[a]	CC[b]	HL[c]	HC[d]	
1	1091	1404	1,24	60,2	24,0	11,8	3,8	20
2	927	1034	1,12	63,3	14,9	20,7	1,0	18
3	805	896	1,13	60,9	18,6	18,0	2,5	13
4	761	823	1,08	55,4	30,6	12,2	1,8	14

[a] Linear copolymer; [b] cyclic polymer; [c] linear homopolymer; [d] cyclic homopolymer; [e] maximal polymerization degree for the copolymer

Stability study of HMFA_ECL copolymers by quantum chemical methods

To find out more details about the monomers binding order a detailed investigation of several possible structures using the molecular mechanics MM+ method, and the PM3 semi-empirical molecular orbital theory was performed. Determination of the most stable structure, at its lowest energy, provides vital information about the polyester type, shape, and spatial orientation.

Based on the MALDI TOF-MS spectra, it was found that the copolymer with 8 polymeric units (4 ECL units and 4 HMFA units) was present in the largest amount in most synthesized products. To determine the monomer sequence that gives the greatest stability to this copolymer, all 70 possible structures which contain 4 units of each monomer were built.

The energetically most stable structure corresponds to an ordered structure, the BBAABBAA chain, where A is ECL and B is the HMFA (Figure 53). Based on the HOMO-LUMO energy difference, the most stable structure in terms of chemical reactivity contains a rather alternately disposed sequence of ECL and HMFA units.

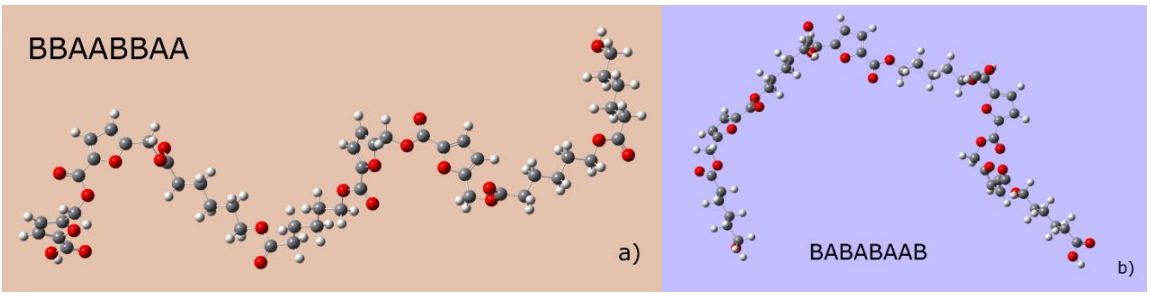

Figure 53 The optimized most stable structures of the linear copolymers containing four HMFA (A) and four ECL (B) monomeric units, based on the energy-stability (a) and chemical reactivity (b).

II.5.2. Enzymatic synthesis of polyesters containing itaconic acid and other fermentation-derived diacids

Itaconic acid, also known as methylene succinic acid, is a diacid produced by the fermentation of sugars by certain fungi. It is considered an important renewable building block and a potential alternative to petrochemical acrylic and acrylate monomers. The challenge with itaconic acid lies in its internal double bond and secondary carboxyl group, which render it less reactive in typical polycondensation processes. However, enzymatic catalysis has enabled the formation of itaconate-containing polyesters under mild conditions that preserve the unsaturated functionality.

A noteworthy example is the enzymatic synthesis of unsaturated poly(itaconate) reported by Pellis et al. They polymerised dimethyl itaconate with 1,4-cyclohexanedimethanol (CHDM) using CALB in bulk at 50 °C under reduced pressure. These mild reaction conditions prevented the polymerisation or degradation of the itaconate's vinyl group, which commonly occurs in high-temperature chemical processes. The resulting poly(CHDM itaconate) had pendant double bonds that were available for post-polymerisation modification. Indeed, the authors demonstrated aza-Michael additions of diamines to these double bonds to modify the polyester and introduce amino functionalities. Although some chain degradation occurred during amine functionalisation, particularly for flexible chains that could cyclise into pyrrolidone rings, the study showed that enzymatically synthesised unsaturated polyesters can undergo further transformation, thereby expanding their utility. Itaconic acid has also been copolymerised with other monomers in an enzymatic reaction to form a terpolymer of itaconic acid, FDCA and hexanediol. In that study, dimethyl

itaconate (DMI) and dimethyl FDCA were used alongside 1,6-hexanediol in toluene with CALB catalysis at 80 °C [76].

The enzyme was able to incorporate both monomers, yielding a predominantly terpolymer product (making up approximately 85% of the total product and having a molecular weight of ~1200), as well as a small amount of FDCA-hexanediol copolymer. Controlling the FDCA to itaconate ratio in the feed allowed the composition to be adjusted, since FDCA was more reactive (possibly due to its rigid structure).

In a 2019 study [76], we reported this novel terpolymer synthesis. We chose FDCA and itaconic acid as the two top renewable monomers and HDO as the flexible aliphatic diol spacer (Figure 54). The reaction was conducted in toluene at 80 °C with CALB, and under the best conditions, the researchers isolated a polymer with a yield of over 80%. MALDI-TOF mass spectra revealed the formation of predominantly terpolyester chains comprising all three monomer units, with an average molecular weight of approximately 1200 Da (DP of around 4–5 for each monomer in a chain). A small fraction (approximately 15%) of a copolymer of FDCA and HDO was also present, likely due to the fact that FDCA reacts slightly faster, resulting in the preferential consumption of some hexanediol by FDCA. By adjusting the feed ratios or extending the reaction time, the product composition could be controlled – a higher concentration of itaconate in the feed resulted in a higher concentration of itaconate in the polymer. However, FDCA tended to incorporate readily even at lower concentrations due to its higher reactivity. NMR analysis revealed interesting regioselectivity: the enzyme showed a preference for one of the two symmetric carboxyl groups of dimethyl itaconate. Specifically, ester linkages were preferentially formed at the itaconate carboxyl group adjacent to the methylene group in the itaconate structure.

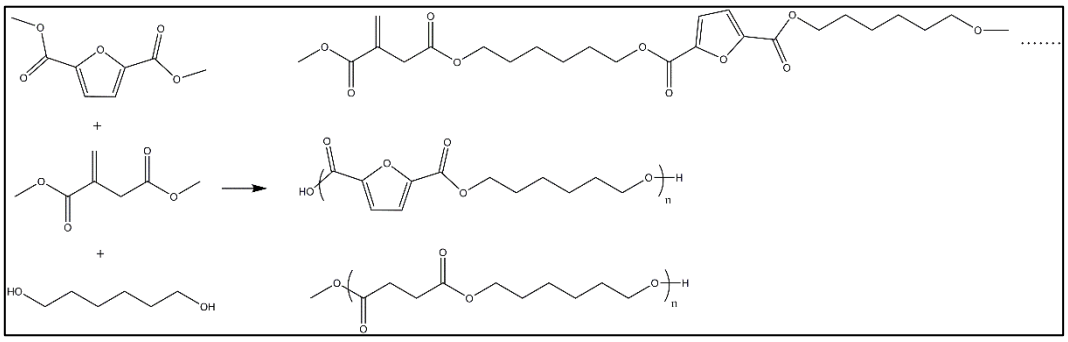

Figure 54 Reaction scheme of the enzymatic synthesis of terpolymers and copolymers from dimethyl furan 2,5-dicarboxylate, dimethyl itaconate and 1,6-hexanediol

The formation of terpolymers was demonstrated based on MALDI-TOF MS spectra. In Figure 55, a typical MALDI-TOF MS spectrum of the reaction products, obtained at 2:1 DMFDC:DMI molar ratio and GF-CalB-IM (5%, wt.%) as biocatalyst, is presented. For example, the peaks at 1560.7, 1799.0 and 2037.3 *m/z* correspond to the K^+ adducts of the polymeric chains consisting of $(DMFDC)_{5-7}$-$(DMI)_1$-$(HDO)_{8-9}$. Polymeric chains containing two DMI moieties were also identified. The peak series 1362.4, 1601.7 and 1839.9 *m/z* correspond to adducts of $(DMFDC)_{4-6}$-($DMI)_2$-$(HDO)_{5-}$

8. As main secondary products, copolymers with DMFDC and HDO moieties were also detected, e.g. the peaks at 1500.6, 1738.9, and 1977.3 *m/z* correspond to (DMFDC)$_{6-8}$-(HDO)$_{6-8}$.

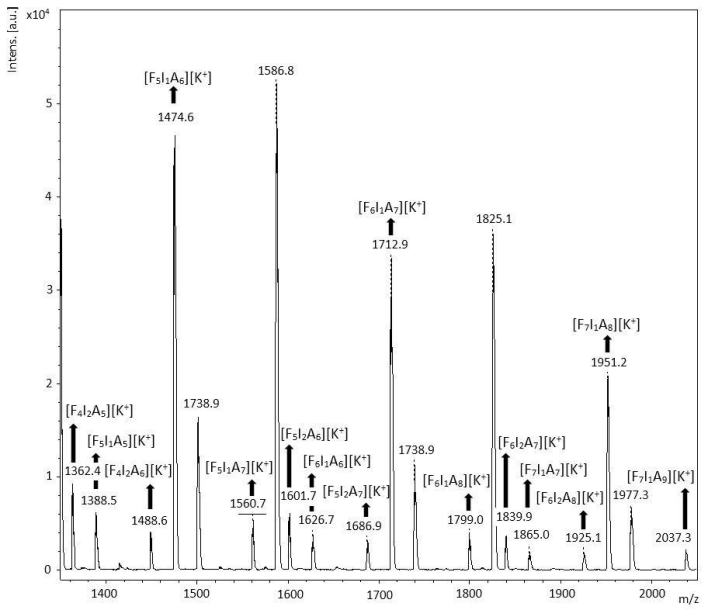

Figure 55 MALDI-TOF MS spectrum (1350-2050 m/z range) of the synthesized polyesterification product, catalyzed by GF-CalB-IM (5%, wt.%), at 2:1 DMFDC:DMI molar ratio. The molecular masses of selected polymeric chains, with different number of 2,5-furandicarboxylate (F), itaconate (I), and 1,6-hexanedioxy (A) units, are indicated by arrows.

The lipase from *Candida antarctica* B immobilized on acrylic resin (Novozyme 435) was selected based on previous reports on successful utilization of this catalyst for polyester synthesis from itaconic acid derivatives and various diols [76]. The effect of the biocatalyst concentration (wt.%, related to the total amount of monomers) and the DMFDC:DMI molar ratio were investigated, targeting an increased terpolymer amount in the polymerization product. Three DMFDC:DMI molar ratios were considered: 1:1, 1:2 and 2:1, at three enzyme concentrations, 3%, 5% and 10% (wt.), respectively. The results are presented in Table 21.

Table 21 Influence of the molar ratio of co-monomers on the composition of the polymerization products, at different Novozyme 435/monomer ratios (wt %, related to the total monomer amount). The reactions were carried out at 80°C, 24 h.

Entry	Enzyme [%]	Molar ratio[a]	M_n [Da]	M_w [Da]	$Đ_M$	Composition of the product [%]				DP_{max} [b]
						Terpolymers		Copolymers (linear and cyclic)		
						Linear	Cyclic	DMFDC_HDO	DMI_HDO	
1	3	1:1:2.5	843	878	1.04	67.9	0.1	32.0	0	14
2	3	1:2:3.5	823	852	1.04	72.0	0	26.8	1.3	12
3	3	2:1:3.5	1093	1223	1.12	32.1	0.1	67.8	0	23
4	5	1:1:2.5	938	997	1.06	53.2	1.1	42.7	3.0	14
5	5	1:2:3.5	843	877	1.04	61.7	0.8	35.5	2	12
6	5	2:1:3.5	935	969	1.04	71.5	0.5	26.1	1.9	16
7	10	1:1:2.5	1041	1121	1.08	74.8	0.7	23.5	1.0	17
8	10	1:2:3.5	836	868	1.04	72.1	0.1	27.3	0.5	12

9	10	2:1:3.5	1205	1343	1.11	71.0	0.5	28.4	0.1	22

[a] Molar ratio of the co-monomers DMFDC, DMI and HDO, respectively; [b] maximal degree of polymerization (of the terpolymer)

Using Novozyme 435 as biocatalyst, at equimolar DMFDC:DMI amounts a slight increase of the average molecular weight with increasing enzyme concentration was observed and the highest terpolymer content of the reaction product (more than 74%) was obtained at 10% Novozyme 435. At DMI molar excess (1:2 DMFDC:DMI molar ratio), the average molecular weight, the maximal polymerization degree and the terpolymer content of the product were lower but not harshly affected, indicating that the enzyme is less selective towards itaconic acid, compared to 2,5-furandicarboxylic acid. This observation is confirmed by the highest molecular weights and terpolymer contents obtained at DMFDC molar excess (2:1 molar ratio), regardless to the enzyme concentration employed. Our data are in concordance with the decrease of the average molecular weights at higher itaconic anhydride molar ratios reported by Yamaguchi et al. for the synthesis of terpolymers from itaconic anhydride, 1,6-hexanediol and succinic/glutaric anhydride, with Novozyme 435 as catalyst [40]. Using Novozyme 435 as biocatalyst, the optimal reaction conditions were 2:1 DMFDC:DMI molar ratio and 10% biocatalyst concentration, leading to average molecular weights higher than 1300 Da, maximal polymerization degree above 20, and more than 70% terpolymer content of the product. The low amounts of DMI_HDO copolymer detected in the polymerization product demonstrate the much higher reactivity of DMFDC compared to DMI in this polycondensation reaction.

Reuse of the biocatalyst in multiple reaction cycles

The operational stability of GF-CalB-IM was tested in five consecutive synthesis cycles. The selected molar ratio was DMFDC:DMI:HDO=2:1:3.5, while the amount of the biocatalyst was 5% (wt.) related to the total monomer mixture. The results, calculated based on the MALDI-TOF MS spectra (Figure 56), indicate that after 3 cycles the reaction mixture still contained about 50% of terpolymer with average molecular weights around 1300 Da and maximal polymerization degrees beyond 20 (not shown in Figure 57). After the third reaction cycle a decrease of the medium molecular weights and of the terpolymer content was observed, due to a possible inhibitory effect of the itaconate derivative.

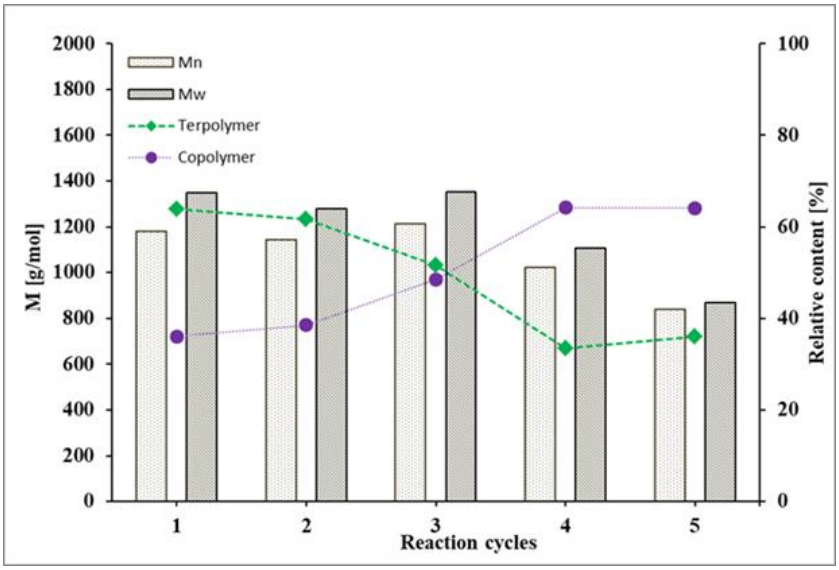

Figure 56 The efficiency of GF-CalB-IM biocatalyst (5%, wt.%) in multiple polymerization reaction cycles (DMFDC:DMI:HDO molar ratio of 2:1:3.5)

Structural characterization of the terpolymers

The chemical structure of the terpolymers was elucidated using ^{1}H NMR, 13C NMR and 2D NMR techniques, including HMBC, COSY, DEPT-135 and HSQC. The HMBC spectrum (Figure 57) confirmed the presence of key ester linkages between the furan and itaconic units via long-range correlations between the carbonylic carbons (at 170.8 and 158.2 ppm) and the methylene protons of the 1,6-hexanediol unit. The furan:itaconic acid ratio was found to be 2:1, and the integration of the ^{1}H NMR peaks indicated that 10 furan units had been incorporated into the chain, along with one terminal unit. Itaconic protons (6.33 and 5.71 ppm) were consistently observed at the chain ends in a 1:1.1 ratio with the terminal methylene signal (3.77 ppm), which confirmed the proposed chain architecture. Coupling between the ester methylene protons and the itaconic carbons revealed regioselective transesterification: 85% of the itaconic moieties reacted at the more reactive carbonyl group adjacent to the methylene group (1-C) and 15% at the 3-C position.

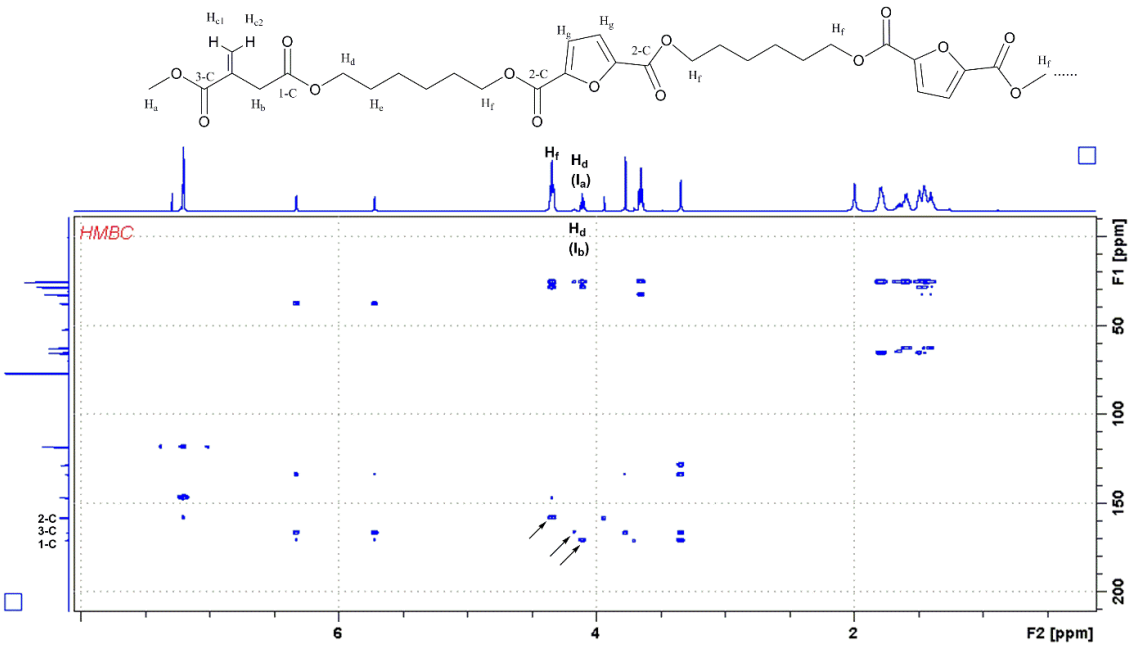

Figure 57 The HMBC NMR spectrum of the synthesized terpolymer by using GF-CalB-IM (5%, wt.%), at DMFDC:DMI:HDO molar ratio of 2:1:3.5 [76]

This kind of selectivity is difficult to achieve through chemical means, but it is a defining feature of enzymatic catalysis. The resulting terpolyester is essentially a random copolymer of three different repeating units. It contains approximately 85% terpolymer sequences (containing both furan and itaconate) and around 15% sequences consisting solely of FDCA-HDO (without itaconate). The presence of the itaconate C=C bonds means that this polyester can be cross-linked or derivatised after synthesis. Indeed, one could envisage thermoset coatings or UV-curable materials being made by cross-linking such unsaturated polyesters, providing a renewable alternative to petrochemical-based unsaturated polyesters used in fibreglass resins, for example. Furthermore, as FDCA is structurally similar to terephthalate, the polymer is likely to have good thermal stability. The study noted the superior thermal stability of the enzymatically produced terpolymer compared to analogous estolides (fatty acid oligomers). This is a significant case as it demonstrates that an enzymatic process can accommodate three monomers and produce a polymer that would not be accessible by traditional means (due to the combination of two different diacids, one of which is unsaturated). This highlights the tolerance of enzymes and opens the door to creating 'designer' polyesters with multiple bio-based functionalities.

II.5.3. Bio-based polyesters from plant oil- and fatty acid-derived monomers

Vegetable oils and fatty acids are another rich source of bio-based monomers. Natural oils, such as castor oil and soybean oil, contain fatty acids that can be functionalised or used directly for polymer synthesis. One category of interest is hydroxy fatty acids [77]. Castor oil, for instance, contains a high proportion of ricinoleic acid (12-hydroxy-9-cis-octadecenoic acid). Other hydroxy fatty acids include 10- and 12-hydroxy stearic acids, which are obtained by the chemical or microbial

hydroxylation of fatty acids, and 16-hydroxy hexadecanoic acid, which is found in some plant cutins. These monomers have both a carboxylic acid group and an internal hydroxyl group, enabling them to self-condense or copolymerise into polyesters, which are often termed 'estolides'[68], [78].

The lipase-catalysed synthesis of estolides from various hydroxy fatty acids has been demonstrated. For example, one study examined the enzymatic oligomerisation of the saturated hydroxy acids C16 and C18, as well as the unsaturated ricinoleic acid. The results showed that different lipases produce different products, with some favouring the formation of lactones (through an intramolecular reaction) over linear estolide chains (through an intermolecular reaction). By selecting a suitable biocatalyst - in this case, a CLEA of *P. stutzeri* lipase and optimising the temperature, estolides with an average polymerisation degree of up to 10 were achieved at a conversion rate of >80%. These estolides, which are produced using enzymes, are of interest as biodegradable lubricants and cosmetic ingredients since hydroxy fatty acids are often derived from the processing of non-edible oils and their oligomers can serve as biolubricants (e.g. as a replacement for petroleum-based lubricants) [68].

Another example related to plant oils involves dicarboxylic acids resulting from the oxidation of fatty acids. Azelaic acid (nonanedioic acid) and sebacic acid (decanedioic acid) can be produced from oleic acid via oxidative cleavage (azelaic acid is found in some plant oils and is also produced industrially from oleic acid). These long-chain diacids impart flexibility and hydrophobicity to polyesters. A recent enzymatic approach tackled the polymerization of glycerol (a trivalent polyol from biodiesel glycerine) with azelaic acid to produce poly(glycerol azelate) – an interesting biodegradable polyester polyol. Glycerol presents a challenge because it has three hydroxyls (two primary, one secondary) and tends to form a hyperbranched or cross-linked polymer if fully reacted. The enzyme (CALB) shows regioselectivity, preferring primary hydroxyls, but uncontrolled glycerol polycondensation can lead to gelation. To address this, we employed a two-step process: an initial enzymatic polycondensation of glycerol and diethyl azelate under carefully controlled conditions (short reaction time to form prepolymers), followed by a second step that allowed non-enzymatic polymerization to proceed to higher molecular weight. A critical innovation was ensuring the immobilized enzyme's stability (preventing enzyme leaching or support abrasion in the viscous reaction) so that the enzyme could be reused and only function in the early stage. This approach yielded poly(glycerol azelate) of reproducible quality on a preparative scale (tens of grams), while preventing excessive branching by stopping enzymatic action once a certain conversion was reached. This work illustrates how enzymatic processes can be adapted to polyols like glycerol, which are cheap and bio-based (glycerol is a byproduct of biodiesel production), to create polyesters that could be useful in biomedical fields (glycerol-based polyesters like poly(glycerol sebacate) are known for tissue engineering applications). It also highlights the interplay between enzyme selectivity and monomer functionality: CALB's regioselectivity helped in controlling the structure (favoring linear or lightly branched structures over a fully cross-linked network)[79].

The reaction scheme of the reaction is presented in Figure 58.

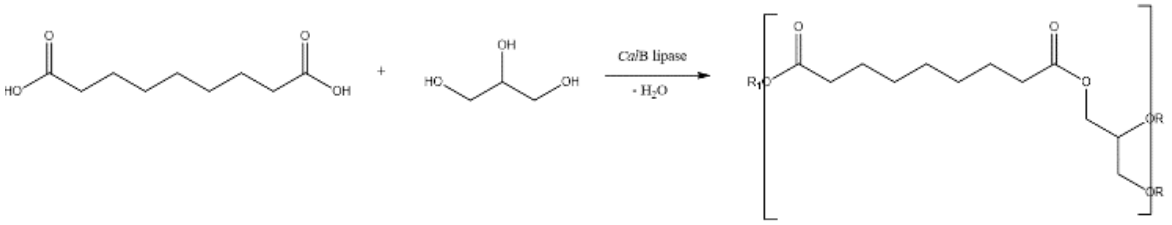

Figure 58 Reaction scheme of the enzymatically catalyzed polycondensation of glycerol with azelaic acid, catalyzed by covalently immobilized lipases.

Table 22 Polycondensation of glycerol with azelaic acid, catalyzed by covalently immobilized lipases.

Cat.	T* [°C]	Time [h]	Pressure [mbar]	M_n** [g/mol]	M_n [g/mol] ESI-MS	M_w** [g/mol]	M_w [g/mol] ESI-MS	ĐM ESI
CalB	70	24	70	524	687	550	754	1.09
no	80	24 (48)	70	631	908	725	919	1.01
no	80	48 (72)	70	744	983	774	1072	1.09

The conversion was determined using ^{1}H-NMR spectra, by monitoring the increase of the integral values of the signals in the interval 2.40 - 2.30 ppm, which correspond to the esterified azelaic acid, and the concomitant decrease of the integral values in the range 2.30 - 2.2, assigned to the free azelaic acid. The conversion values determined based on the sample collected and measured after 24, 48 and 72h are presented in

Table 22. The 1H-NMR spectra of the reaction mixture leading to the highest conversion of AZA are depicted in Figure 59 along with the signal assignments.

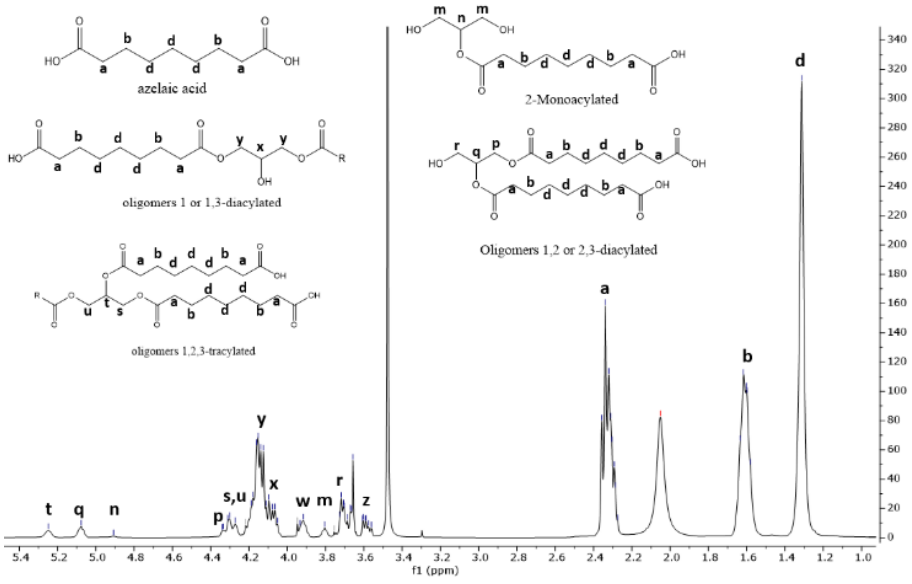

Figure 59 The ^{1}H-NMR spectra of the product obtained after 72h of reaction

Effects of experimental variables on M_n of poly(glycerolazelate)

The analysis of the distribution of medium molecular weights was performed based on the assignments of the masses from the ESI-MS spectra collected for the samples at 24, 48h and after the work-up of the reaction mixture at the end of the reaction.

The spectra were collected in the negative mode as described in the experimental section. Figure 60 reports the ESI mass spectra collected for the sample EXP4 after work-up and they indicate the formation of 3 types of reaction products: [AB], [AB]A and B[AB] where A represents the azelaic acid and B the glycerol molecule. The range of the molecular weights reached after 72h of reaction is comprised between 756 and 1969 Da.

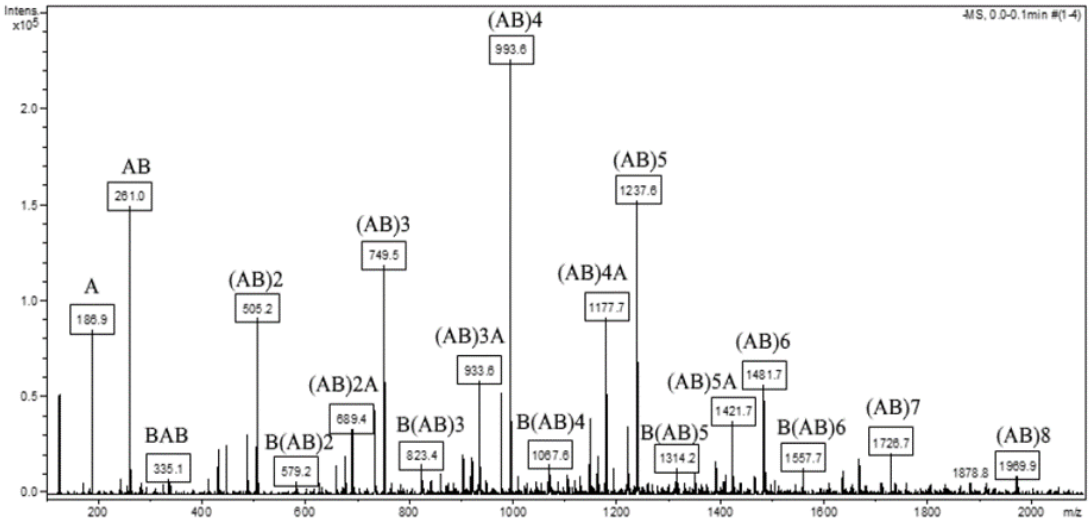

Figure 60 The ESI-MS spectrum of the EXP4 reaction products obtained after 72 hours and work-up of the reaction mixture obtained from the enzymatic polycondensation between azelaic acid (A, molecular weight 188.22 g mol-1) and glycerol (B, molecular weight 92.09 g mol-1), catalysed by covalently immobilized CaLB. Target 1200 m/z, range between 100 and 2200 m/z, negative ions.

Analysis of the regioselectivity of the acylation

The study focused the attention also on the effect of the reaction conditions on the regioselectivity of the acylation of GLO, since hydrophilicity is a desired property of the final product that increases when the secondary alcohol of GLO is not acylated. That result is not achievable using conventional chemical polycondensations that lead to extensive acylation and branching.

The analysis of the product obtained after 24 and after the work-up of the reaction mixture at 72h was carried out by 2D DQCOSY and TOCSY NMR spectra that allowed for the identification of the specific signals of the glycerol acylated at a different extent and in different positions. The percentage of isomers distribution (Figure 61) was calculated based on 1H-NMR spectra and the results clearly indicate that in each experiment the highest content of the products is represented by the 1,3 diacylated followed by the monoacylated forms.

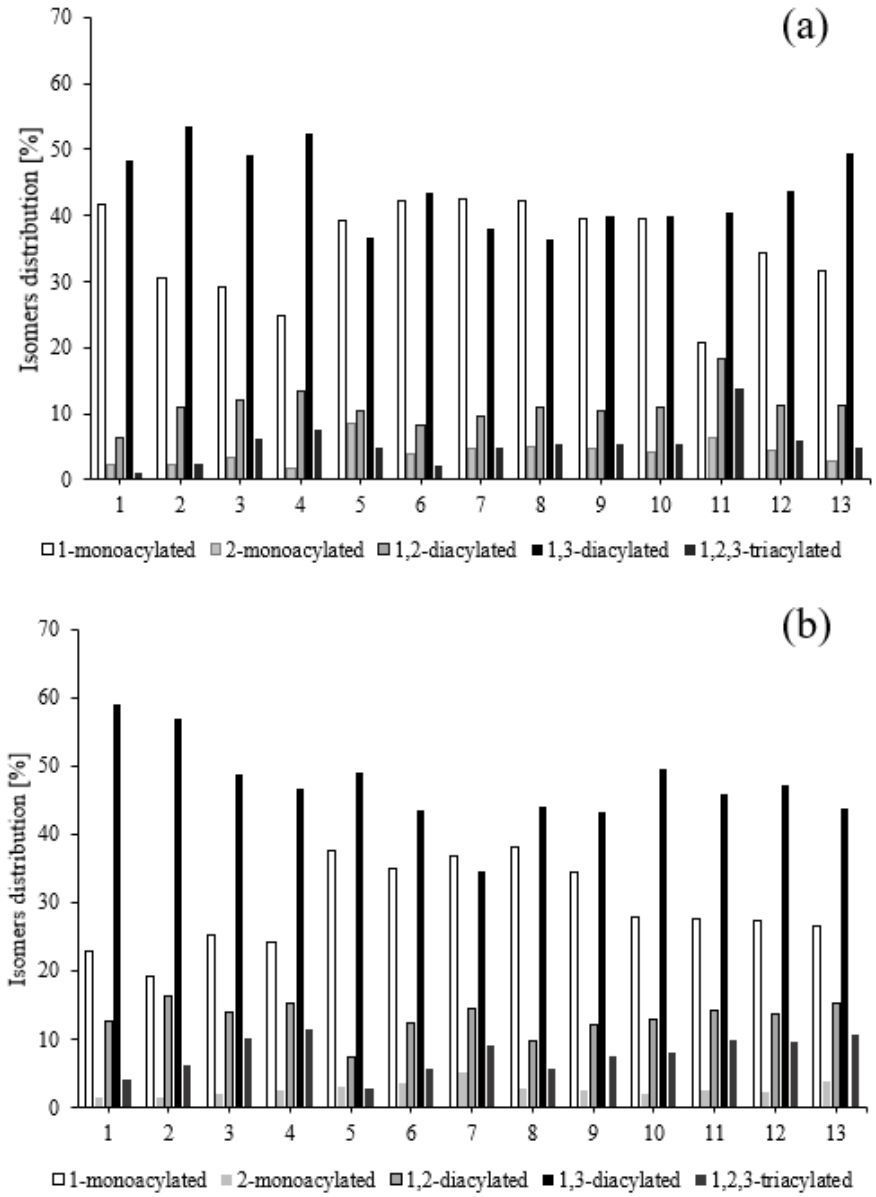

Figure 61 The product percentual distribution after 24h (a) and 72h (b) in the samples considered in the experimental design.

The analysis of the effects of the variables on the acylation of GLO indicates that at higher pressure the formation of the monoacylated glycerol is favoured, probably because of the competing action of water that promotes the hydrolytic reactions. Moreover, to obtain the selective acylation of the primary -OH groups it is preferable the use of a lower amount of biocatalyst.

This approach was novel in that it carefully preserved the integrity of the enzyme, preventing the release of proteins into the reaction mixture and avoiding abrasion of the immobilization carrier during the mechanical mixing of the viscous system. This enabled a two-step process to be developed, in which the enzyme was used only in the initial stage to generate short pre-polymers. The study showed that, when enzymatic polycondensation lasted longer than 24 hours, non-enzymatic reactions became dominant, thereby altering conversion, molecular weight and

regioselectivity. Computational analysis provided valuable insights into the regioselectivity of glycerol acylation, which is essential for the efficient use of this abundant, bio-based polyol. The method was successfully optimised and scaled up to 73.5 g for the synthesis of poly(glycerol azelate), a polymer of interest for dermatological applications, thereby demonstrating the reproducibility of the process. Overall, this investigation clarified and addressed the key challenges that had previously limited the industrial-scale application of enzymatic polycondensation.

One-pot green synthesis of furan-ricinoleic acid copolymers

In the first part of this study [80], the polymerization of ricinoleic acid (RCA) and HFA was investigated as a new green biocatalytic pathway to synthesize unsaturated oligoesters containing furan units. The reaction products were mixtures of linear or cyclic copolymers, along with linear or cyclic homopolymers of RCA, formed as secondary reaction products (Figure 62). The other possible secondary products, the homopolymers of HFA were not identified.

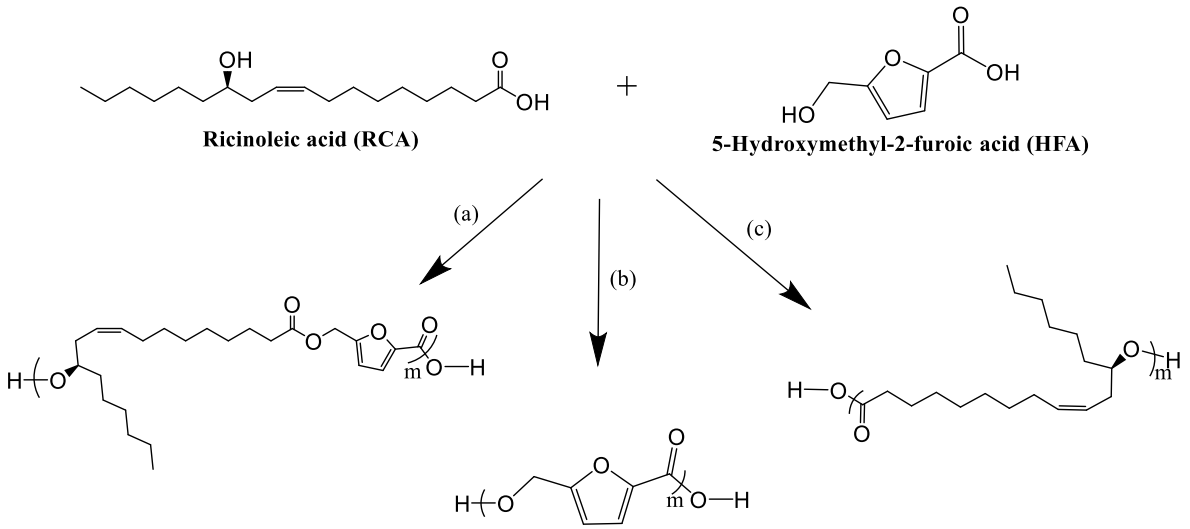

Figure 62 Formation of linear and cyclic copolymers (route a) and homopolymers (routes b and c) as possible reaction products. The alternance of the monomeric units in the copolymer chain is random.

The formation of reaction products was monitored by MALDI-TOF MS spectrometry. An example of MALDI-TOF MS spectrum of poly(5-hydroxymethyl-2-furancarboxylate-*co*-ricinoleate) (RCA-*co*-HFA) is represented in Fig. 62, for a product obtained in solvent-less reaction system, using *Pseudomonas stutzeri* lipase. In all spectra, the identified products were either copolymers (Figure 62, route *a*) or RCA estolides (Figure 62, route *c*). Thus, the series of peaks attributed to the sodium adducts of the oligomer series ($[M+Na]^+$) indicate the formation of linear or cyclic copolymers containing HFA and RCA units, as shown in Figure 63.

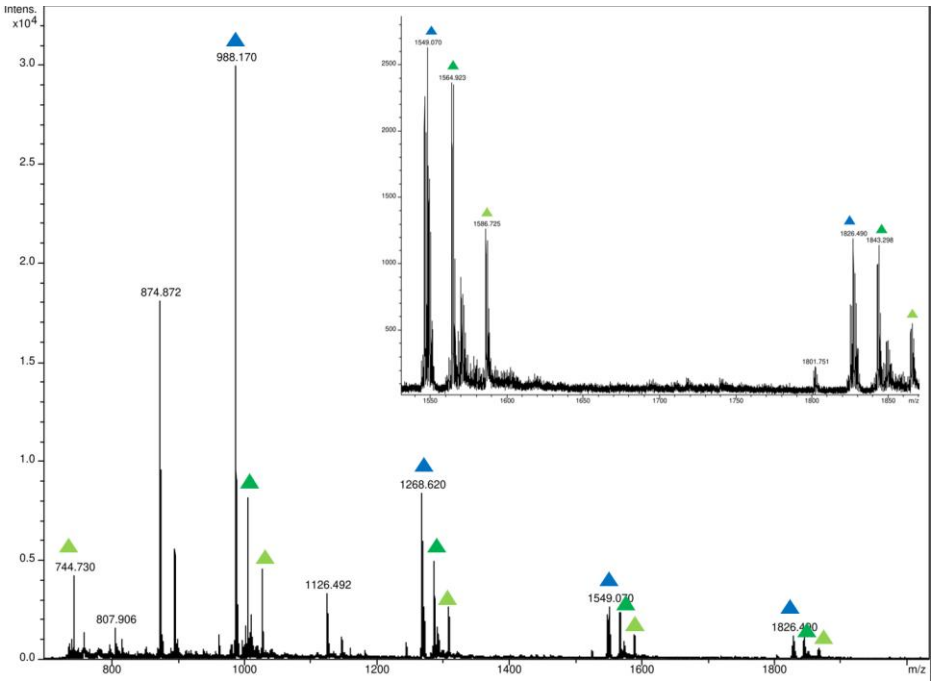

Figure 63 MALDI-TOF MS spectrum of the copolymers obtained from HFA and RCA (1:1 molar ratio) synthesized at 50°C and, 48 h, using the lipase from Ps. stutzeri as biocatalyst, in t-BuOH system. The formation of cyclic copolymers (blue triangles) and linear copolymers (green triangles). Inset the 1550-1850 m/z region.

As an example, the peak with m/z 1549.07 corresponds to the Na^+ adduct of cyclic copolymer with five RCA units and one HFA units while the 1564.92 and 1586.72 corresponds to linear copolymers sodium adducts. The identification of the poly(5-hydroxymethyl-2-furancarboxylate-*co*-ricinoleate) oligoester reaction products by MALDI-TOF MS demonstrates, for the first time, the lipase-catalyzed insertion of HFA into a poly(ricinoleate) chain. The insertion of the furanic units into the hydrophobic chain of ricinoleic acid estolide was also demonstrated by NMR spectroscopy analysis.

Screening of the biocatalyst

The objective of this study was identifying a biocatalyst suitable to mediate the formation of linear oligoesters having a high degree of polymerization. Three native hydrolases were tested: a lipase from *Pseudomonas stutzeri*, subtilisin (a protease) from *Bacillus licheniformis* (Alcalase), and the AR "Amano" esterase from *E. coli.* Besides, three commercially available immobilized lipases, from *Candida antarctica* B (Novozyme 435 and CALB-IM) and *Thermomyces lanuginosus* (Lipozyme TL IM), were also evaluated. The reactions were carried out in *t*-butanol, at 50°C, according to the methodology presented in section 2.3. The *t*-BuOH was selected as solvent because both monomers were soluble, and it is one of the solvents with higher logP compatible for lipases [81]. The relative compositions of the reaction products, calculated based on the corresponding m/z intensities from the MALDI-TOF MS spectra, are shown in Table 1. Among the three native hydrolases, the formation of copolymers was favored by the lipase from *Pseudomonas stutzeri*. Although the

average molecular weights were higher when the protease (Alcalase) and esterase were used as catalysts, the relative content of copolymers in the reaction product did not exceed 6% and it was mostly cyclic copolymer. Immobilized lipases, although those from CalB were efficient biocatalysis for the synthesis of oligoesters with HFA units, were not suitable for these substrates, as CalB favoured the formation of cyclic copolymers and Lipozyme TL IM was more specific for the cyclic RCA homopolymer. Based on these results, the lipase from *Pseudomonas stutzeri* was used in forthcoming studies.

Table 23 The influence of the nature of the biocatalyst on the copolymer synthesis.

Biocatalyst	M_n [g/mol]	M_w [g/mol]	$Đ_M$	LC [%]	CC [%]	CH [%]	LH [%]
Alcalase	1140	1250	1.09	1.28	4.63	34.09	59.99
Esterase AR	840	920	1.10	-	5.66	74.02	20.33
Ps. stutzeri lipase	1040	1150	1.04	13.80	53.45	12.64	20.01
Novozyme 435	870	925	1.07	32.82	38.19	25.27	3.71
Lipozyme TL IM	740	750	1.08	2.42	11.76	64.61	21.21
CALB-IM	750	750	1.03	-	68.18	16.96	14.86

LC – linear copolymer; CC – cyclic copolymer; CH – cyclic homopolymer of RCA;
LH – linear homopolymer of RCA; $Đ_M$ – molar-mass dispersity

The influence of monomers molar ratio of monomers

The molar ratio of the monomers can influence the polymerization degree and the relative content of the monomeric units in the oligomer structure. A study of the polymerization efficiency was conducted varying molar ratio between RCA and HFA from 1:1 to 5:1. A molar excess of HFA was not suitable, as it would lead to solubility problems in case of performing the reaction in organic medium, or impossibility of achieving a homogeneous reaction mixture in the solventless process. The reactions were carried out in *t*-butanol at 50°C, under stirring at 1200 rpm and using the lipase from *Ps. stutzeri,* which previously proved selectivity for the formation of the linear copolymer. The results obtained after 24 h of reaction are presented in Figure 64. A slight increase in average molecular weights was observed with increasing RCA molar excess, while the relative composition of the reaction products has been markedly affected. The highest relative amount of copolymer was obtained at equimolar RCA:HFA ratio and increasing this ratio to 3:1 or higher resulted in the synthesis of the RCA homopolymer as major product, the relative content linear and cyclic RCA estolides exceeding 70%. Increasing the reaction time to 48 h, the average molecular weights did not change significantly (were about 5% higher) and the relative content of the copolymer has shown the same tendency. The selectivity for the linear copolymer was not altered at higher RCA molar excess. Consequently, increasing the molar excess of RCA or the reaction time leads only to higher relative amount of the RCA homopolymer (estolide), without a positive effect on the copolymer content or molecular weight. Therefore, an equimolar ratio of monomers and 24 h reaction time

are the most suitable reaction parameters for the synthesis of oligomers with higher linear copolymer content.

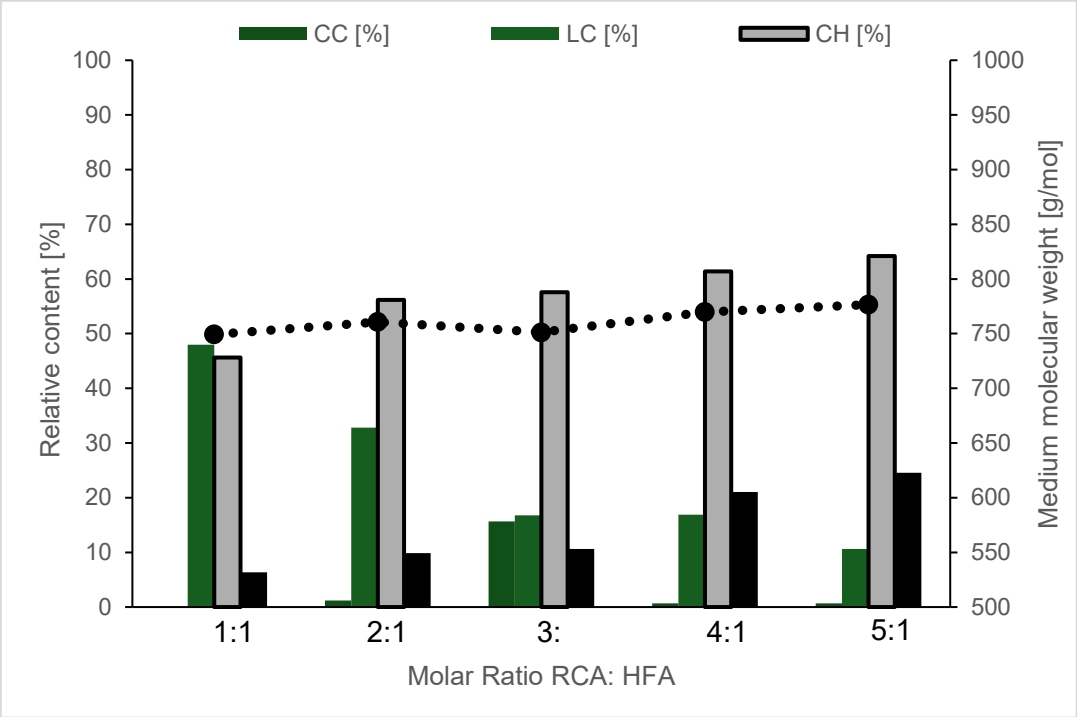

Figure 64 Effect of the molar ratio of the monomers on the average molecular weight and composition of the oligomeric product, at 24 h reaction time. The reactions were carried out at 50°C in t-butanol, using Pseudomonas stutzeri lipase as biocatalyst. LC – linear copolymer; CC – cyclic copolymer; CH – cyclic homopolymer of RCA; LH – linear homopolymer of RCA

Influence of the reaction medium

Based on the results of previous studies showing that lipase activity was not affected in these media [68], the solubility of the raw materials was considered the main selection criterium. Thus, four commercially available ILs and *t*-butanol were investigated as reaction media for the oligoester synthesis catalysed by *Ps. stutzeri* lipase.

As results from Table 24, [Bmim]Tf_2N proved to be the most effective among the ILs investigated, the average molecular weights being slightly higher compared to the product synthesized in *t*-butanol. Although higher average molecular weights were obtained in [Bmim]PF_6 and [Emim]BF_4, in these ILs the relative total copolymer content did not exceed 25%. The solventless reaction system provided higher average molecular weights and total copolymer content similar to *t*-butanol. Consequently, it was selected for the following "one-pot" study, also because t-butanol could not be used in the reduced pressure conditions that were needed to accomplish such a combined hydrolysis/polycondensation process.

Table 24 The influence of the reaction medium on the average molecular weight and relative composition of the oligoester product obtained from HFA and RCA, using Ps. stutzeri lipase.

Reaction medium	M_n [g/mol]	M_w [g/mol]	$Đ_M$	LC [%]	CC [%]	CH [%]	LH [%]
Solventless	1250	1420	1.13	3.80	63.45	20.10	12.64
t-BuOH	1040	1150	1.04	13.80	53.45	12.64	20.01
[Bmim]Tf_2N	960	980	1.03	56.79	-	43.21	-
[Bmim]PF_6	1060	1080	1.02	24.52	-	75.48	-
[Emim]BF_4	1180	1280	1.09	10.90	-	38.26	50.84
[Hmim]BF_4	860	860	1.00	15.44	-	72.15	12.41

LC - linear copolymer; CC – cyclic copolymer;CH – cyclic homopolymer of RCA; LH – linear homopolymer of RCA; $Đ_M$ – molar-mass dispersity

One-pot synthesis of the RCA-co-HFA biobased oligomer from castor oil as ricinoleic acid source

The aim of this study was to evaluate the ability of the lipase from *Pseudomonas stutzeri,* found as the most efficient in the previous polycondensation experiments, to convert triricinolein into RCA that further reacts with HFA present in the reaction mixture, yielding the oligoester. This reaction system can be considered "one-pot" type, involving two successive reactions catalysed by the same enzyme. Recently, a “one-pot” system has been reported in a patent application, which provides a method for the synthesis of oligoesters of hydroxy fatty acids in three steps, by the action of oleate hydratase on an unsaturated fatty acid substrate with a *cis* C9-C10 double bond, and of a lipase for the hydrolysis of triolein and polyesterification. It was demonstrated that in a single aqueous buffered solution it is possible to integrate three consecutive reactions by action of two enzymes, with high or total conversion of triglyceride and of hydroxy fatty acid to oligoester [82].

Since the selectivity of the lipase from *Ps. stutzeri* was not previously reported for the hydrolysis of triglycerides, its selectivity for the hydrolysis of triricinolein was first evaluated. The hydrolysis reaction was performed in 0.1 M phosphate buffer pH 7, substrate concentration 50 mM, at 50°C for 24 h. The reaction product was extracted with $CHCl_3$, the ^{1}H-NMR spectrum indicating the disappearance of the glycerol signal.

In a preliminary experiment, the “one-pot” reaction was carried out starting from castor oil and HFA under controlled reduced pressure conditions to remove the water initially added for the hydrolysis step, using a rotary evaporator system at 100 mbar pressure, 50°C, and 150 rpm. The MALDI-TOF MS analysis of the product after 48 h reaction time indicated an average molecular weight M_n of 1200 g/mol and 63.4% relative linear copolymer content. In the next step, the optimization of selected process variables was performed, to find the best conditions for the oligoester product formation.

Optimization of the reaction parameters of the "one-pot" process by experimental design

To optimize the oligoester synthesis starting from 5-hydroxymethyl-2-furoic acid (HFA) and castor oil, the Box-Behnken statistical Design of Experiments (DoE) technique was used (Unscrambler® multivariate data analysis software package, AspenTech, USA). Three variables were selected (temperature, biocatalyst percentage reported to the amount of monomers, and molar ratio of monomers) and their influence on the average molecular weights. The temperature was set in the 60-80°C range, the amount of the biocatalyst between 15-45 U $mmole^{-1}$ substrate in relation to the raw materials, and the castor oil: HFA molar ratio ranged from 1:1 to 5:1. The average molecular weights (M_n, M_w), were calculated based on GPC analysis and used as response variables. The optimal reaction conditions were determined based on DOE results and statistical analysis. In the first three columns of Table 25 the values of the selected independent variables, temperature, amount of the enzyme, and molar ratio of the co-monomers are presented, while the last two columns contain the M_n and M_w values, determined experimentally by GPC analysis. Statistical analysis of the experimental data was accomplished using ANOVA technique and regression analysis. For the overall analysis of the results, the two-order polynomial model was chosen, because in most cases the p-value was <0.05, which shows that the model is adequate in relation to the experimental data from a statistical point of view. When choosing the model, the multiple correlation coefficient was considered, whose value as close to 1 confirms that the regression model satisfactorily correlates the sample data. R^2 values were in the range [0.747 -0.940].

Table 25 The average numeric and gravimetric molecular weight values of the copolymers, calculated from the GPC analysis of the products synthesized in the specified reaction conditions.

Exp. No	Temperature [°C]	Enzyme amount [a] [U $mmole^{-1}$]	Molar ratio Oil:5	M_n [g/mol]	M_w [g/mol]
1	70	45	5	4520	7240
2	70	15	5	1170	1660
3	70	45	1	2790	4520
4	70	15	1	1850	3490
5	70	30	3	5440	6500
6	60	15	3	2230	3470
7	60	30	1	3570	5950
8	60	30	5	5530	8460
9	60	45	3	6050	9490
10	80	15	3	964	1310
11	80	30	1	1110	1460
12	80	30	5	1660	2980
13	80	45	3	3390	6090
14	70	30	3	2890	5410
15	70	30	3	3920	6180

[a] weight %, related to the mass of monomers

The results of the ANOVA analysis suggest that the chosen model is appropriate. The pure error value determined for the M_n parameter of the copolymer, measured at the central points, was 419 from three repetitions, corresponding to √419 = 20.46% of the standard deviation, which can be considered satisfactory. The *p*-parameter values for the quadratic terms included in the reduced model were less than 0.05, except for the corresponding value for the molar ratio.

Residue analysis is of particular importance for assessing the suitability of the model. For this analysis two graphs were considered (Figure 65A and Figure 65B) the most relevant for the analysis of residues and the model prediction analysis chart, which provides information on how the experimental values are in line with the predictions and the residue analysis graph.

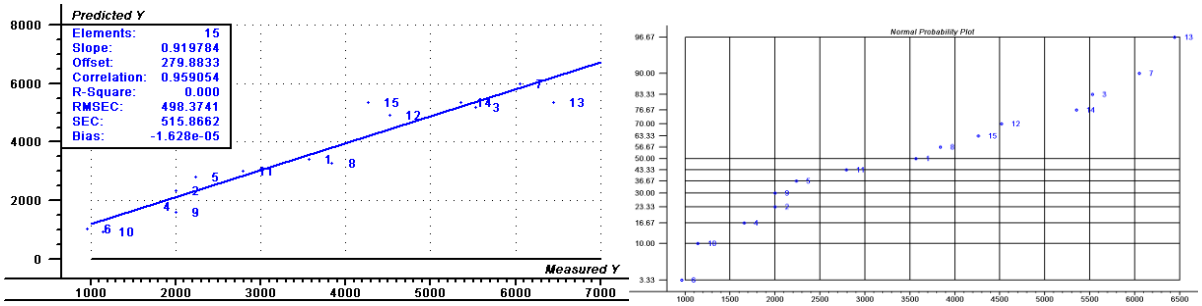

Figure 65 Comparison of the measured and predicted weight average molecular weight of the copolymer (a), and probability plot of residuals (b)

Response surface analysis and contour plots analysis

Although the effect of molar ratio was not significant for the overall process, when M_n was plotted as function of both temperature and enzyme amount, an optimum value was obtained (Fig. 5). The response surface analysis indicates that working at 3.3:1 molar ratio castor oil:HFA, the highest M_n value of 6000 will be achieved at the central point corresponding to 63°C and 33 U mmole^{-1} substrate of enzyme. This limitation of molecular weight increase is probably due to the high content of cyclic copolymer, which cannot be lowered in the given conditions.

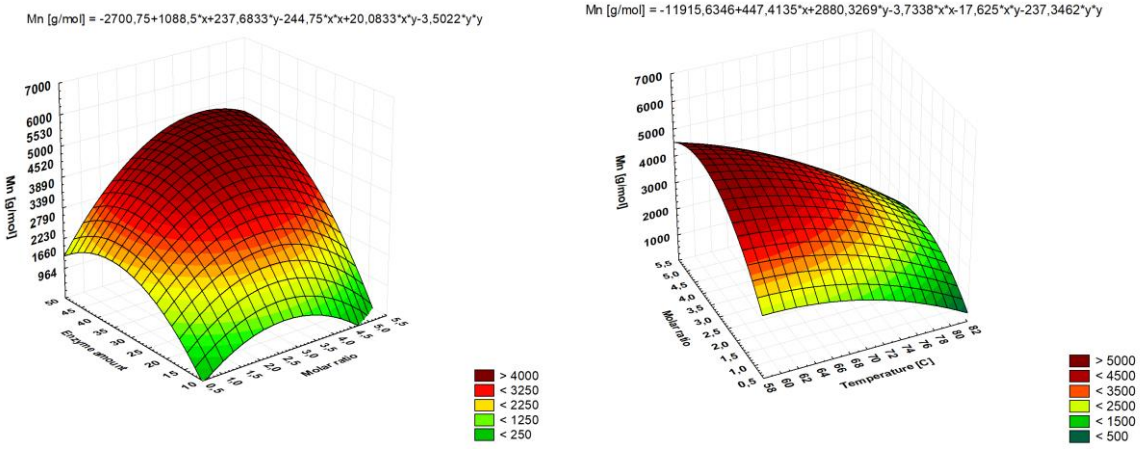

(a) (b)

Figure 66(a) Response surfaces describing the effect of the independent variables on the average molecular weight of the oligoester after 24 h of reaction; (b) effect of enzyme amount and molar ratio.

Structural characterization of the RCA-co-HFA copolymers

The structural characterization of the raw materials and reaction products was carried out by several spectroscopic methods, to highlight the functional groups characteristic of the compounds formed.

The insertion of the furan unit into the estolide chain was demonstrated by 1D and 2D NMR spectroscopy. Figure 67 presents the 2D HMBC spectrum of the reaction product between RCA and HFA obtained after 48 h of reaction at 50°C and 1200 rpm, in *t*-butanol.

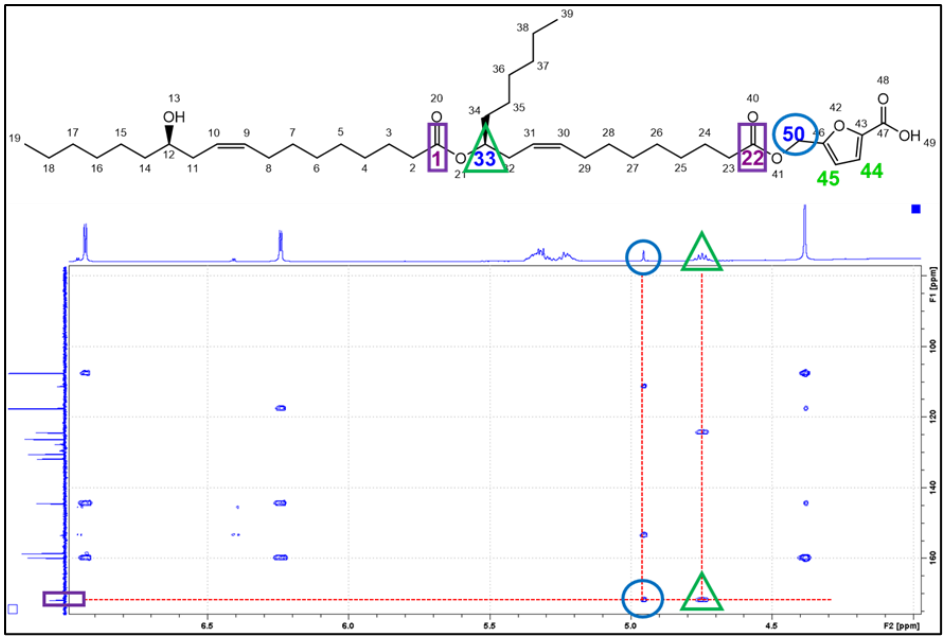

Figure 67 2D HMBC NMR spectrum of the RCA AND HFA reaction product; range (4-7 ppm/80-175 ppm)

The 2D HMBC spectrum shows the distance couplings between the signals corresponding to carbon atoms 1 (171.6 ppm) and 22 (171.6 ppm) with the proton signals from carbon 33 (4.74 ppm) and 50 (4.95 ppm). These 2 distant couplings over 3 bonds demonstrate the formation of the ester bond between the carboxylic group of RCA (C22) and the hydroxyl group (O41) originating from HFA, respectively the esterification between the hydroxyl group (O21) of RCA on the side chain with another RCA molecule (C1). The numbering of atoms relates to the hypothetical oligoester with two RCA units and one HFA unit, having the chemical structure depicted in Figure 67.

From the ^{1}H NMR spectrum (Figure 68) of the RCA and HFA reaction product, the singlet at 4.95 ppm corresponds to the methylene protons from the HFA residue, the quintet at 4.74 ppm corresponds to the methine proton (H33) from the RCA chain. The signals at 6.95 ppm and 6.40 ppm correspond to vinyl protons in HFA each having a coupling constant equal to 3.54 Hz. The ratio in which the protons at 6.94 ppm and

6.40 ppm are found respectively with the quintet at 4.74 ppm is approximately 1:8, which proves that the HFA units were included in the estolide backbone, also confirmed by the MALDI-TOF MS analyses.

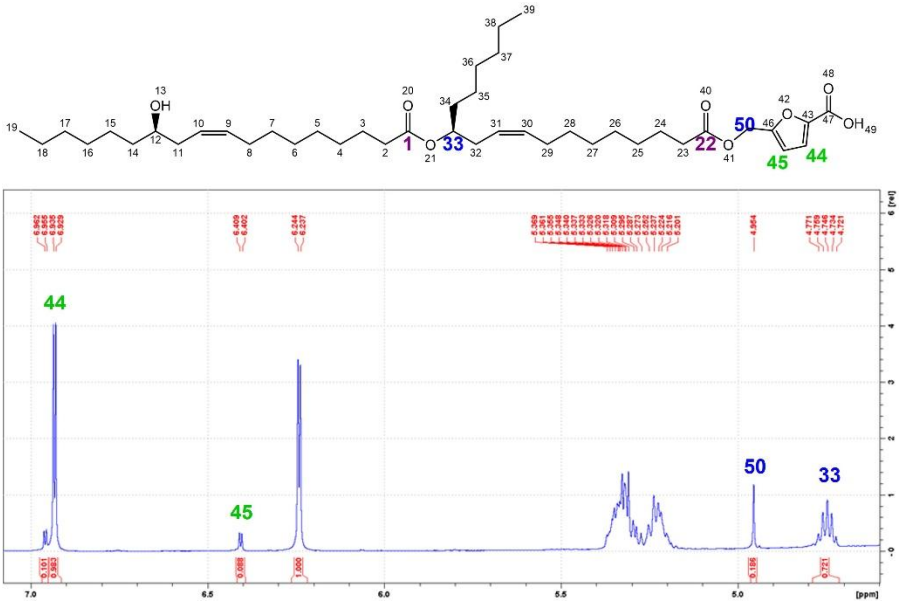

Figure 68 The ^{1}H NMR spectrum of the reaction product obtained from RCA and HFA obtained at 50°C, 48 h, in t-butanol, in the presence of lipase from Pseudomonas stutzeri; range (4-7.1 ppm).

Thermal properties of the RCA-co-HFA copolymers

The thermal properties of the copolymers obtained from RCA and HFA were evaluated by thermogravimetric analysis performing a comparison with the starting materials RCA and HFA.

The thermograms presented in Figure 69 indicate a slight increase in the thermal stability of the copolymer (pink) over the RCA (blue) and HFA (purple) monomers. Mass loss starts around 166ºC. Both the copolymer and the monomers show thermal decomposition in two steps, as confirmed by the two inflections at 177ºC and 324ºC, respectively, in the case of the copolymer.

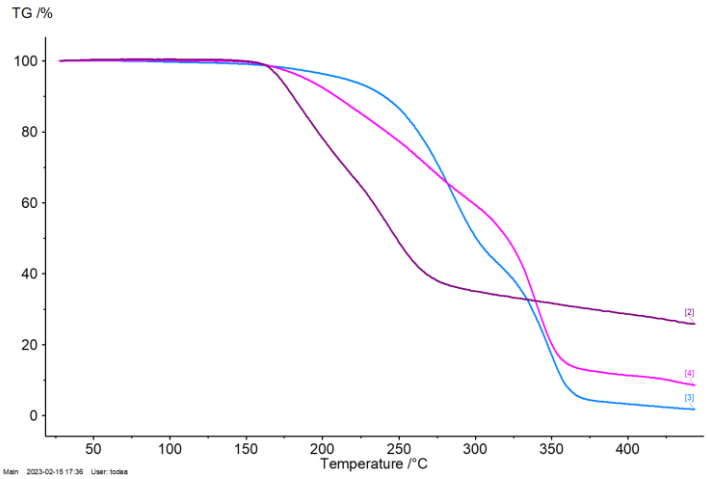

Figure 69 Thermograms of RCA-co-HFA oligoester (pink), RCA (blue) and HFA (purple)

From the TGA thermograms the temperatures at 5%, 10% and 50% mass loss (TD5, TD10 and TD50) were determined and are reported in Table 4. The results show that at 50% mass loss the temperature of the poly(5-hydroxymethyl-2-furancarboxylate-*co*-ricinoleate) is 20°C higher compared to the RCA and with 72°C higher compared to the HFA which indicates a higher stability of the oligoester compared to the raw materials.

Table 26 TGA determination of TD5, TD10 and TD50 for poly(5-hydroxymethyl-2-furancarboxylate-co-ricinoleate) and RCA, HFA monomers.

Sample	TD_5 [°C]	TD_{10} [°C]	TD_{50} [°C]
RCA	214	241	301
HFA	172	181	249
Copolymer	189	209	321

II.5.4. Enzymatic synthesis of model aromatic and aliphatic oligoesters for studies of biodegradation and ecotoxicity

The objective of the study [83] was the synthesis of eleven model substrates used for biodegradation studies, namely the aliphatic and aromatic oligoesters. The use of enzymes as catalysts in polycondensation reactions allows to control their structure and length, maintaining the molecular weights below 2000 Da. In this way it was possible to study the biodegradation of the oligomers at molecular level, minimizing solubility problems or thickness variability.

A pool of a total of 6 monomers, 3 diacids (adipic acid (AA), 2,5 furandicarboxylic acid (FDCA) and terephthalic acid (TA)) and 3 diols/polyols (1,4-butandiol (BDO), glycerol (GLY) and erythritol (ERY)) was used in different combinations for co-polymers or terpolymers synthesis. The enzymatic polycondensations were performed either in solvent-less systems or in the presence of organic solvents. The general reaction scheme is presented in Figure 70. Six copolymers and five terpolymers were enzymatically synthesized and fully characterized in terms of structural and thermal properties. In the case of copolymers, we exhaustively combined the three diacids with two polyols (BDO and GLY), whereas in the case of terpolymers we added the more hydrophilic monomer ERY, with the aim to increase the product solubility, as described below.

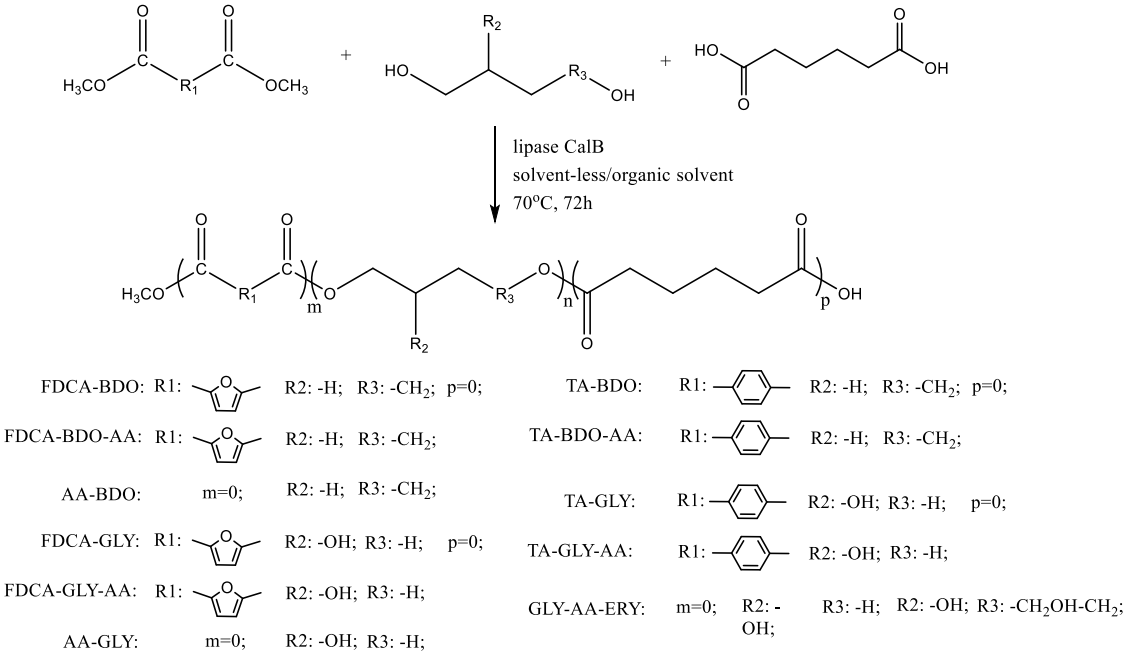

Figure 70 General reaction scheme for the enzymatic synthesis of the considered oligoesters.

All the reactions were performed at 70°C by using either covalently immobilized lipase from *Candida antarctica* B $CalB_{cov}$ (specific activity = 234.33 U/g_{dry}), prepared in our group, or the commercial highly active N435 (Novozyme 435, specific enzymatic activity = 2201.53 TBU/g_{dry}). The latter was employed when the monomers conversion with $CalB_{cov}$ was unsatisfactory (4 out of 11). The advantage of using the covalent immobilized formulation resides in the higher stability of the covalent bonds that prevents the detachment of the lipase from the support. We already studied the experimental conditions of enzymatic polycondensations [79], [84], and the optimization of the reaction conditions was here limited to monomers' viscosity and melting temperature adjustment, in order to reduce the final viscosity (of the mixture). For this reason, some aliphatic oligoesters were synthetized in solvent less systems as previously described [79], obtaining > 90% conversions, whereas only the use of organic solvents guaranteed acceptable monomer conversions for aromatic oligoesters. Preliminary reaction media screening included the greener solvents 2,5-dimethyltetrahydrofuran (DMTHF), 2,2,5,5-tetrahydrofuran and *t*-butanol, but in a few cases (3 out of 11) the use of toluene was mandatory.

In Table 27 the medium molecular weight values, the substrate conversions and the reaction media used for the oligoesters selected for further studies: the covalently immobilized lipase was successfully used for the synthesis of all biobased oligoesters, whereas for the synthesis of the TA-containing oligoesters only the highly active N435 led to good conversions.

Table 27 The reaction media, monomers conversions, medium molecular weights (numerical and gravimetric) and dispersity values determined for the enzymatically synthesized oligoesters.

Sample	Solvent	Enzyme	Monomer conversion (%)*			M_n**	M_w**	Đ
			M1	M2	M3	[g/mol]	[g/mol]	
Co-oligomers								
BDO-FDCA	toluene	$Calb_{cov}$	97	84	-	635	742	1.16
BDO-TA	*t*-BuOH	N435	90	65	-	694	838	1.20
BDO-AA*	-	$Calb_{cov}$	95	94	-	683	729	1.06
GLY-FDCA	*t*-BuOH	$Calb_{cov}$	96	87	-	551	936	1.69
GLY-TA	*t*-BuOH	N435	98	88	-	960	1169	1.21
GLY-AA	-	$Calb_{cov}$	92	96	-	912	940	1.03
Ter-oligomers								
BDO FDCA AA	toluene	$Calb_{cov}$	81	63	91	844	901	1.06
BDO TA AA	toluene	N435	72	94	99	615	747	1.21
GLY FDCA AA	*t*-BuOH	$Calb_{cov}$	86	67	49	481	551	1.25
GLY TA AA	*t*-BuOH	N435	94	97	96	582	675	1.15
GLY ERY AA	-	$Calb_{cov}$	88	81	94	845	1140	1.35

*determined based on NMR spectra; ** determined based on ESI-MS spectra.

Oligoesters structural characterization by ESI-MS and NMR

The composition of the product mixtures was evaluated by ESI-MS spectrometry. Two typical ESI-MS spectra of the reaction products are reported in Figure 71. The m/z values of several peaks can be assigned to the Na^+ adducts of the oligoesters formed in the polymerization reaction. For example, for the co-oligoesters containing BDO and FDCA (Figure 71A) the peaks with m/z 475, 685 and 899 were assigned to the Na+ adducts of linear co-oligoesters formed by 2 - 8 monomers.

For the ter-oligoesters containing BDO, AA and FDCA (Figure 71B) the peaks with m/z 455, 661 and 875 were assigned to the Na^+ adducts of linear ter-oligoesters (highlighted by green in Figure 71B) constituted by 4 - 8 monomers. No traces of unreacted monomers were observed in the product mixtures. It must be underlined that the synthesis of the terpolymers led to a product mixture that includes also co-oligoesters (BDO-AA in yellow and BDO-FDCA in blue) although as a minor component.

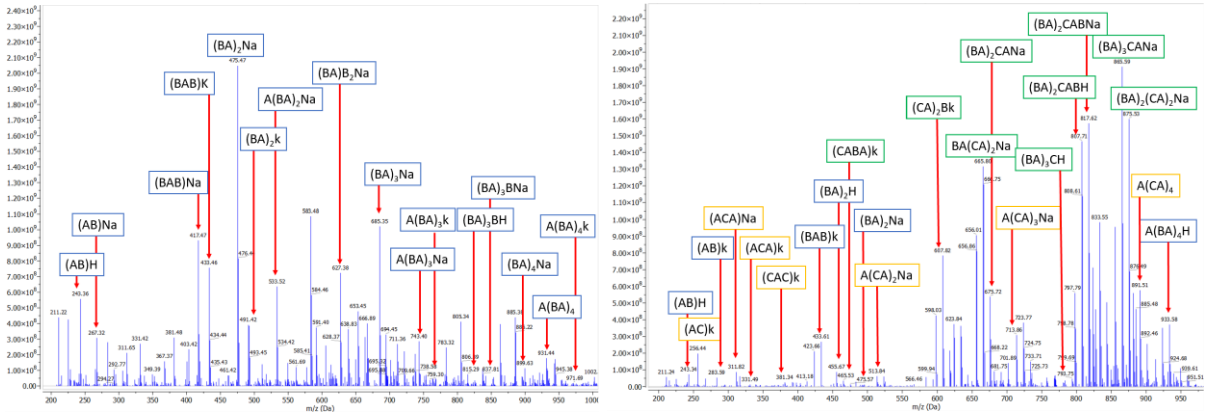

Figure 71 (A) The ESI-MS spectrum of the enzymatically synthesized poly(butylene furanoate) obtained in toluene at 70℃ in the presence of covalently immobilized CalB lipase. Legend: A=BDO; B=FDCA. (B) The ESI-MS spectrum of the enzymatically synthesized poly(butylene adipate furanoate) obtained

in toluene at 70°C in the presence of covalently immobilized CalB lipase. Legend: A=BDO; B=FDCA; C=AA

Chemo-enzymatic synthesis and characterization of epoxy fatty acids

To better understand the effect of the introduction of the epoxy rings on the biodegradation of the cardoon seed oil derivatives, oleic, linoleic, and linolenic acids were epoxidized using CaLB as a biocatalyst. In the enzymatic route, the formation of stable peroxy acids took place in situ by means of the enzymatically catalyzed reaction of H_2O_2 with the carboxylic group of free fatty acids, allowing for a significant suppression of side reactions.

Although CaLB is classified as a carboxylic ester hydrolase (3.1.1), it is endowed with perhydrolysis activity, since it replaces water with hydrogen peroxide as a nucleophile to attack the first tetrahedral transition state complex, forming an acyl–enzyme intermediate, and then releasing peracids [85]. Then, the peroxy acids formed in situ spontaneously react with the C=C, yielding the epoxide [86] through the Prilezhaev epoxidation mechanism for alkenes [87].

The different fatty acids were epoxidized (the chemical structures of the products are presented Figure 72.

Table 28, and in all cases the epoxidation of the alkene bonds was >95%, as demonstrated by the disappearance of protons corresponding to the double bond in the ^{1}H-NMR spectra. Notably, the reactions were fast (2–3 h), and no other solvent was employed aside from 30% H_2O_2 solution. The recovery of the products was almost quantitative in all cases for an easy work-up.

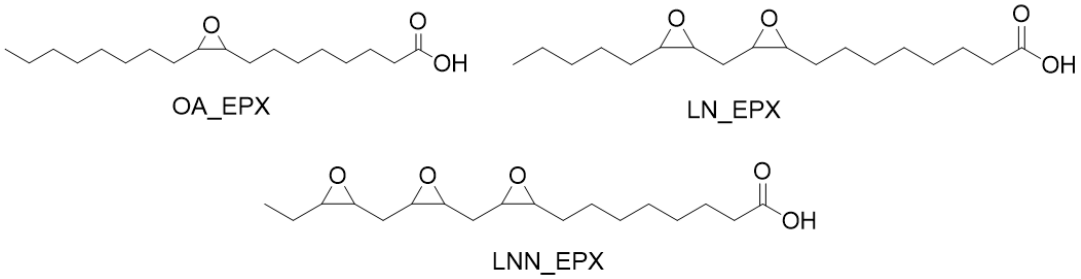

Figure 72 Structures of the products obtained from the enzymatically catalyzed epoxidation of oleic, linoleic, and linolenic acids. Codes refer to marine biodegradation tests.

Table 28 Experimental conditions for the epoxidation of pure oleic, linoleic, and linolenic fatty acids. Reactions were performed in the presence of immobilized CaLB (Novozyme 435) on a 2 g scale at 50 °C. The molar ratio between C=C bonds and H_2O_2 = 1:2.

Substrate	Amount of Enzyme ($U/g_{substrate}$)	Reaction Time (h)	Conversion * C=C bond (%)
Oleic acid	225	2	>99
Linoleic acid	450	2	95
Linolenic acid	450	3	98

* Determined by ^{1}H NMR.

Thermal analysis of the selected compounds

The thermal properties of the oligoesters were evaluated by TG. Details about the mass loss at different temperature intervals are presented in Table 29. Among the tested molecules, the ECO-SRB showed a slightly lower thermal stability at temperatures of up to 300 °C. For all of the samples, more than 70% of the mass was lost at temperatures below 400 °C, which confirms the organic origin of the samples.

Table 29 Mass losses over different temperature ranges of the oligoester and plasticizer.

Compound	Mass Loss (%)			
	20–200 °C	**20–300 °C**	**20–400 °C**	**20–500 °C**
(BDO-AA)n	1.17	4.15	59.22	98.74
ECO-BDO	4.22	19.80	67.87	99.98
ECO-SRB	6.93	25.96	69.31	99.10

DSC Analysis

The use of differential scanning calorimetry (DSC) is relevant to deeply understand and correlate the effects of any type of degradation [88].

The DSC results obtained by cooling the samples from 20 to −50 °C and then heating them from −50 to 180 °C at the same scanning rate are reported in Figure 73

The values of the glass transition temperatures (T_g), melting temperatures (T_m), and melting enthalpies (ΔH_m) determined from the areas of the melting peaks for the oligoesters are presented in Table 30.

For all of the samples- especially for the plasticizers and the azelaic acid oligoesters, which are viscous liquids at room temperature-the melting temperature was the last value of the peak obtained from the second heating cycle. The presence of different endothermic peaks on the DSC thermograms for the oil derivatives was previously studied by several groups and attributed to their different crystalline forms [89].

The melting behavior of BDO-AA-a semicrystalline polyester-indicates the presence of two closed endothermal peaks due to its polymorphic structure. This behavior was previously observed and studied in detail by Woo and Wu [90].

Among the plasticizers, the lowest melting point value was obtained for the product modified using sorbitol (ECO-SORB), followed by the samples modified with 1,4-butandiol (ECO-BDO) and with the epoxy oil.

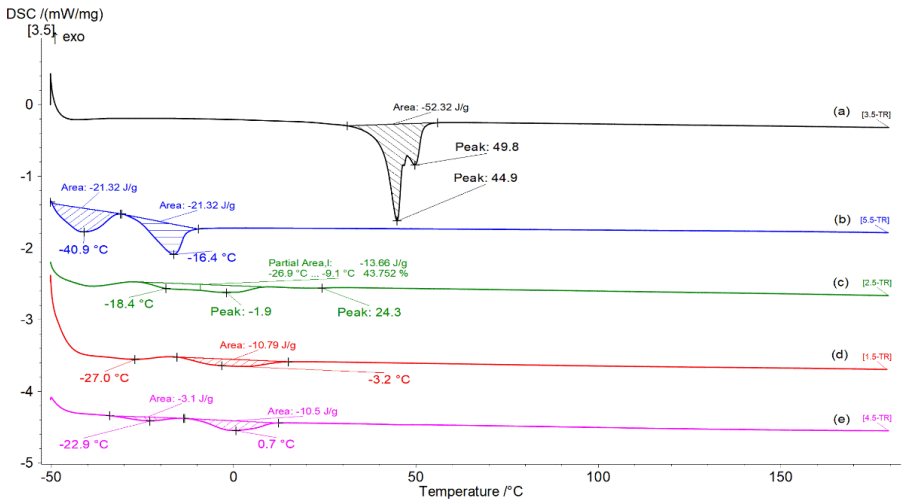

*Figure 73 DSC thermograms of the samples (**a**) (BDO-AA)n, (**b**) (Gly-AZA)n, (**c**) ESO-BDO, (**d**) ECO-SORB, and (**e**) EPX-OIL.*

Table 30 DSC parameters of the oligoesters and plasticizers

Compound	T_i (°C)	T_f (°C)	ΔT (°C)	T_m (°C)	ΔH_m (J/g)	T_g (°C)
(BDO-AA)n	27.6	48.1	20.5	44.9	51.39	n.d.
(GLY-AZA)n	−29.2	9.4	19.8	−16.4	21.52	n.d.
ECO-BDO	−8.8	9.1	17.9	−1.9	13.66	−12.7
ECO-SORB	−1.3	13.5	14.8	−3.2	10.79	−16.0
EPX-OIL	−12.8	13.6	26.4	0.7	10.50	−11.2

II.6 Assessment of the ecological impact of enzyme-derived oligoesters: biodegradation studies in freshwater and saltwater liquid environments

The presence of polymers and plastics in marine environments is a well-recognised environmental concern. It is estimated that around 80% of marine debris consists of plastic waste originating from sources such as uncontrolled littering, industrial discharges, inland waterway transport, wastewater effluents and atmospheric deposition via wind or tidal movement [91]. Furthermore, microplastics originating from tyre abrasion and textile laundering contribute significantly to this pollution. The negative impacts of such contaminants on marine organisms, ecosystem functioning and human health, particularly through the consumption of contaminated seafood, have been extensively documented in the literature [92], [93].

Polyesters, a subclass of polymers, degrade in seawater at rates strongly influenced by their chemical structure and environmental factors such as temperature, salinity and nutrient availability [94], [95]. The development of biodegradable plastics is not intended to condone the improper disposal of waste, even if such materials pose a lower environmental risk than conventional, fossil-derived plastics. Instead, they are intended to reduce ecological harm in applications where environmental release is difficult to avoid. Relevant examples include polymers used in cosmetic formulations, lubricants, and materials used in agriculture and fisheries.

The global plastic production landscape remains heavily dependent on fossil resources, with data from 2021 indicating that over 390 million tonnes of plastics were

manufactured, the vast majority derived from petrochemical feedstocks. In contrast, plastics from recycled or renewable sources represented less than 10% of total output. The environmental burden associated with fossil-based plastics arises not only from waste generation and disposal challenges but also from upstream processes, including greenhouse gas (GHG) emissions and pollution linked to fossil fuel extraction and refining [96].

Bio-based polymers offer a sustainable alternative to fossil-derived plastics, but their adoption requires verified environmental benefits beyond mere functionality. While the biodegradability of materials such as PLA, PCL and PHBV has been studied in soil and compost, their behaviour in marine environments, where much of the plastic waste ends up, remains poorly understood [97].

For a polyester to be used in cosmetic applications, it must be biocompatible, biodegradable and non-toxic. The biodegradability of plastics in a liquid environment refers to their degradation in fresh water (e.g. lakes and rivers), salt water (e.g. seas and oceans), and in aerobic and anaerobic sludge (e.g. wastewater treatment).

Various reports exist on laboratory degradability studies of plastics in defined synthetic or nutrient-rich mixtures, which can be considered preliminary degradation studies in liquid media. Todea et al. previously reported on the biodegradation of 2-hydroxymethyl-2-furanecarboxylic acid oligoesters with ε-caprolaconone in river water, obtaining promising results, although only mass loss was evaluated [75].

The aim of this study was to perform a preliminary assessment of the biodegradability of the oligosters enzymatically synthesized, in liquid media using oxygen consumption monitoring systems, i.e., microorganism inoculum in salt water (seawater) and fresh water (river water).

In contrast to other degradation studies reported in the literature, which are generally restricted to the degradation of polymers formulated in film form and the analyses are limited to the observation of surface erosion or plastic debris, two different phenomena were considered in this study:

(i) the initial biodegradation phase, involving the breaking of the most labile bonds, generally corresponding to the hydrolysis of ester bonds;

ii) biodegradation of individual monomers and model triglycerides.

The combination of the two distinct biodegradation information provides useful insight into how the specific structural components, but also the nature of the chemical bonding of the building blocks, affect the biodegradability of each product.

It is important to emphasize that biodegradation results are considered valid when they relate to the specific inoculum used, geographical and seasonal variability and incubation temperature. However, they allow a comparative evaluation of the effects attributable to the reactivity of the chemical bonds and physico-chemical properties of the molecules. It is known that abiotic and biotic processes proceed slowly and depend on a number of factors, such as molecular weight and surface-to-volume ratio, or water solubility [98].

The reaction products synthesized and characterized in the previous chapters were selected for this study, and to give a clearer picture of their biodegradability in freshwater and saltwater liquid environments they were grouped into 3 categories.

- aliphatic oligoesters
- aliphatic or aromatic monomers
- monomers

The biodegradability studies were performed according to the OECD 306 protocols, as previously reported by Zappaterra et al [98].

During the degradation processes, promoted by enzymes from sea water inoculum microorganisms, new degradation molecules can be released, as the monomers deriving from the hydrolysis of the ester bonds, or the final products CO_2 and H_2O. The outcome depends on the metabolic pathways of the microorganisms present in the inoculum, but seasonality can also influence their presence and concentration. Therefore, for completeness, the biodegradation study was also carried out on the starting monomers to define the biodegradability of the monomers themselves.

II.6.1. Biodegradation of co-oligomers

In the case of co-oligomers, comparing Dt_{21} values we observed a clear negative effect of the FDCA (likely due to the furanic group) when combined with both GLY and BDO. Along the series of BDO- and GLY-containing copolymers, both products with fully aliphatic (AA) and fully aromatic (TA) moieties are more degradable than FDCA; however, for BDO we observed a prevalence (in terms of biodegradability) of the aliphatic AA over the aromatic TA, whereas when combined with GLY, we observed a different pattern, with a slight prevalence for the TA over the AA copolymers.

We might speculate that a significant aliphatic portion guarantees a high degree of degradation, and that the different structures of GLY and BDO do not significantly affect the (high) biodegradability of oligoesters containing the aliphatic and more flexible adipic acid (AA).

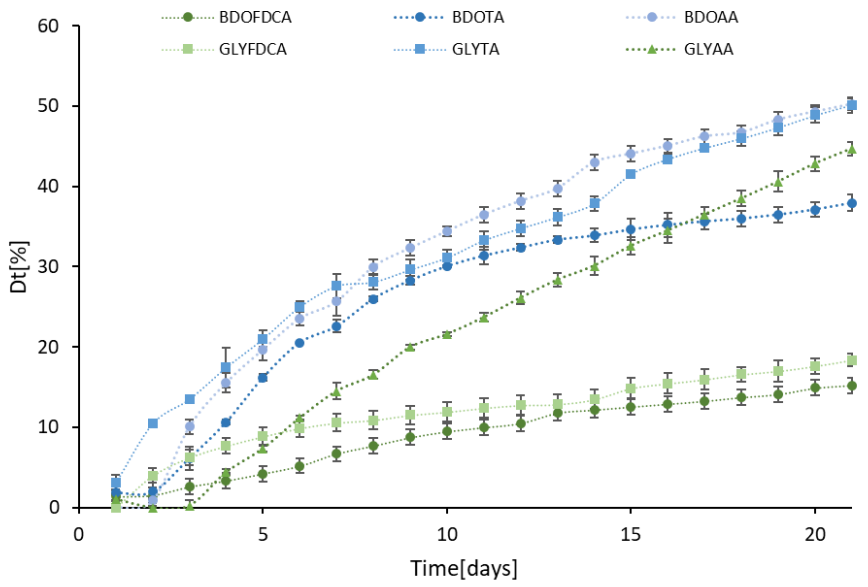

Figure 74 Degree of marine biodegradation after 21 days of incubation obtained for the different co-oligomers. Data were normalized by subtracting the values of the control samples.

The co-oligoesters were also thermally characterized as described in the methods section. It is known that the main characteristics that affect erosion processes of plastic debris are the degree of crystallinity, thickness, shape, molecular weight, water solubility, hydrophilic/hydrophobic properties, T_g and T_m [99].

Table 31 presents the relevant parameters measured by differential scanning calorimetry of the oligoesters, listed in decreasing order according to the D_t value, previously calculated from the biodegradability tests. The corresponding DSC graphs are reported in the Supplementary section. Limitedly to solid copolymers, by looking to biodegradability data from the molecular perspective we could confirm the inverse relationships between T_g and the degradation rate expressed as D_t: BDO-TA (T_g = -55.9 °C) displays a D_{t21} value 2.5 higher compared to BDO-FDCA (-6.6 °C). The analysis of T_m needs further distinction: GLY-based copolymers have comparable values, whereas for BDO-based copolymers the D_{t21} value increases as the T_m values decreases, with a maximum of D_{t21} = 49.95% for the aliphatic BDO-AA (T_m = 45.3°C).

Table 31 The thermal parameters of co-oligomers determined by differential scanning calorimetry in comparison with Mn, dispersity, and biodegradability.

Product	T_g [°C]	T_m [°C]	ΔH_μ [ϑ/γ]	T_c [°C]	Physical state	M_n [g/mol]	Đ	D_{t21} [%]
Co-oligomers								
GLY-TA	-54.6	109.6	14.66	90	S	960	1.21	50.23
BDO-AA	n.o.	45.3	74.27	26.9	S	683	1.06	49.95
GLY-AA	-41.3	n.d.	n.d.	amorph	L	887	1.41	46.90
BDO-TA	-55.9	89.4	10.63	79.7	S	694	1.20	37.92
GLY-FDCA	n.o.	105.2	93.49	86.7	S	551	1.69	18.36
BDO-FDCA	-6.6	92.9	7.66	amorph	S	635	1.16	15.22

Although the lower biodegradability of furan-based oligomers is affected by thermal properties, there might be also a contribution deriving from the lack of specific enzymatic activity in the water sea inoculum able to catalyze the hydrolysis of the BDO-FDCA ester bond. In fact, in the case of the GLY-based co-oligomers, the structural effect of FDCA is even more visible.

Notably, the aromatic GLY-TA displays the highest D_{t21} value (50.23%) among the six co-oligomers investigated, in agreement with the very low T_g value (-54.6°C) as already discussed. However, GLY-TA has also the highest T_m value (109.6 °C), comparable with the less biodegradable GLY-FDCA (T_m of 105.2 °C and D_{t21} value 18.36%, 3.6 folds lower).

Of course, more data would be necessary to confirm that, although thermal properties of co-oligomers affect their biodegradability, they are not fully responsible of the variability in the behavior observed in the marine biodegradation studies.

Biodegradation of bio-based oligoesters and epoxidized bioproducts

Enzymatic Synthesis and Characterization of Oligoesters

The bio-based oligoesters poly(butyleneadipate) and poly(glycerolazelate) were investigated to understand some of the drivers of marine biodegradation in bio-based polyesters, which are not natural polymers but are obtainable through the enzyme-catalyzed synthesis of ester bonds connecting the bio-based monomers. The use of a lipase as a catalyst allowed for the control of the molecular weight and the structure of the products-for instance, avoiding branching [79].

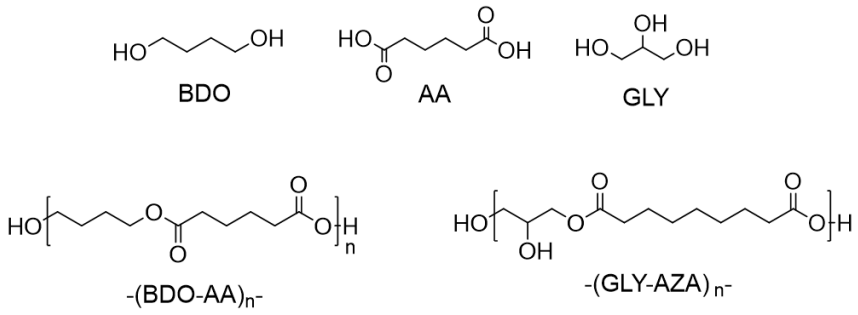

Figure 75 Structure of the bio-based monomers and the corresponding bio-based oligoesters obtained by enzymatic polycondensation. Codes refer to marine biodegradation tests.

Lipase B from *Candida antarctica* (CaLB) was employed for catalyzing the polycondensation of adipic acid and 1,4-BDO to obtain poly(butyleneadipate) (BDO-AA), as well as that of azelaic acid and glycerol to yield poly(glycerolazelate) (Gly-AZA), exploiting the specificity of CalB for the primary hydroxyl groups [100]. The process was carried out at 70 °C under solventless conditions and using a thin-film system, as previously described by Todea et al. [79].

These oligoesters were selected not only for their potential industrial relevance, but also because they have already been the object of extensive investigations concerning their synthesis, structural properties, and degradation. Previously, we have

reported the synthesis of oligoesters of poly(glycerolazelate) [79] for potential use in dermatological and cosmetic formulations, due to the pharmacological properties of azelaic acid [101]. Therefore, these oligoesters are subjected to be washed off and collected in the wastewater, ultimately reaching the sea.

The fate of poly(butileneadipate) is similar, since it cannot be recovered or recycled, due to its final use as an ingredient of adhesive and coating formulations. Indeed, the synthesis of poly(butileneadipate) was the first enzymatic polycondensation carried out on the industrial scale, achieved in the 1990s by Baxenden Chemicals (UK) for the production-later dismissed-of highly regular structures of polymers used for these applications [102]. More recently, we investigated the same enzymatic polycondensation but using recyclable covalently immobilized enzymes in thin-film systems [103]-also on a pilot scale [104]-to overcome the technical limitations observed by Binns and co-workers [102]. Our previous studies on the enzymatic synthesis of both poly(butileneadipate) and poly(glycerolazelate) indicated that the processes are potentially scalable, since the biocatalyst can be efficiently removed after the synthesis of short prepolymers. As a matter of fact, even in the absence of the enzyme, the elongation of the polyesters can be effectively pushed thermodynamically, via the removal of the water produced in the esterification.

Notably, previous computational simulations shed light on the ability of different hydrolases to recognize poly(glycerolazelate) as a substrate in both synthetic and hydrolytic reactions [79]. As the synthesis of the ester bond is a reversible reaction, these oligoesters can in principle undergo hydrolytic degradation catalyzed by the same enzymes used for their synthesis-namely, triacylglycerol hydrolases, which are quite ubiquitous in nature. Furthermore, these oligoesters (Table 32) can be also considered as simplified models of polymers that are usable for formulating bio-based plastics. with low molecular weights Their low molecular weight (between 683 and 926 g mol^{-1}) allows us to neglect factors such as the shape and thickness of samples, while focusing the attention solely on specific chemical and structural factors at the molecular level.

Table 32 Conversions and medium molecular weight values of the enzymatically synthesized polyesters.

Sample	**BDO-AA**	**Gly-AZA** [79]
Conversion AA/AZA * (%)	94	96
M_n ** (g mol^{-1})	683	926
M_w ** (g mol^{-1})	729	945
Đ **	1.06	1.02

* Calculated based on NMR spectra; ** calculated based on micro-TOF spectra.

However, the translation of the potential biodegradability of a chemical product-whether natural or obtained by synthesis-into actual biodegradation depends strictly on the environmental conditions. The data presented herein provide information on the marine biodegradation of a set of bio-based products (chemical structures presented in Figures 1, 2 and 3), which are potentially biodegradable according to the OECD 306 protocols and under controlled conditions.

Biodegradation studies of bioplasticizers and biolubricants derived from cardoon seed oil

Plant oils are prone to different chemical modifications, such as transesterification, estolide formation, double-bond hydrogenation and epoxidation, subsequent ring opening and, finally, acylation of the resulting -OH groups. Cardoons (*Cynara cardunculus* var. *Altilis*) are typical of the biomass of marginal and sub-arid. This oil has a fatty acid profile similar to that of sunflower oil, with 11% palmitic, 4% stearic, 25% oleic, and 60% linoleic fatty acids [105].Therefore, cardoon seed oil can be considered to be a sustainable, non-edible alternative for the purposes of biorefineries, since the plant can withstand severe drought and high soil salinity, with beneficial effects regarding soil properties, erodibility, and biological and landscape diversity [105]. In the present study the triglycerides were first modified at the level of the C=C bonds of the unsaturated fatty acids to create structural complexities that confer them with properties as either plasticizers or lubricants. The oil was epoxidized with performic acid produced in situ by a reaction between hydrogen peroxide and formic acid in presence of the orthophosphoric acid. The final product was analyzed to evaluate the iodine number (I.N.) according to the Wijs method [106] and the oxirane number (O.N.) according to standard method ASTM D1652–11 [98].

The epoxidized cardoon oil was then modified by reaction with 1,4-butandiol and sorbitol, through an acid-catalyzed ring-opening mechanism to obtain polyols, as shown in Figure 76.

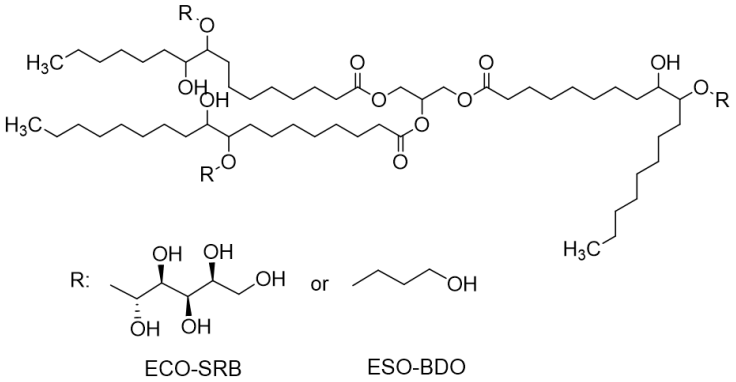

Figure 76 Schematic representation of products obtainable from the ring opening of the epoxidized triolein.The structure does not represent the actual chemical complexity of the composition of cardoon seed oil; rather, it aims at simplifying the illustration of the concept. Codes refer to marine biodegradation tests.

All derivatives of cardoon seed oil were investigated to understand the extent to which the structural modification of a natural molecule (i.e., the triglyceride) modifies the marine biodegradability of its derivatives. Notably, the marine biodegradation tests also involved natural cardoon seed oil. Generally, the biodegradability of natural molecules cannot be taken for granted, since they are the results of biosynthetic processes. Therefore, it is generally assumed that nature provides degradation pathways to ensure the closure of the biogeochemical cycle of carbon. Nevertheless, there are various abundant natural materials, including lignin and rubber, which are quite resistant to biodegradation in most natural environments because of their

function in nature, which requires high chemical stability and scarce reactivity of the bonds connecting their monomers [107]. As a consequence, they undergo biodegradation only under certain conditions and when attacked by specific enzymes, such as laccases in the case of lignin [108]. Conversely, we wanted to verify how the highly hydrophobic triglycerides are biodegraded in a diluted marine environment.

The results obtained within the biodegradation studies expressed as BOD (mg/L) and D_t (%) after 10 and 21 days, are summarized in Table 33. The complete values are presented in

Figure 77 and Figure 78.

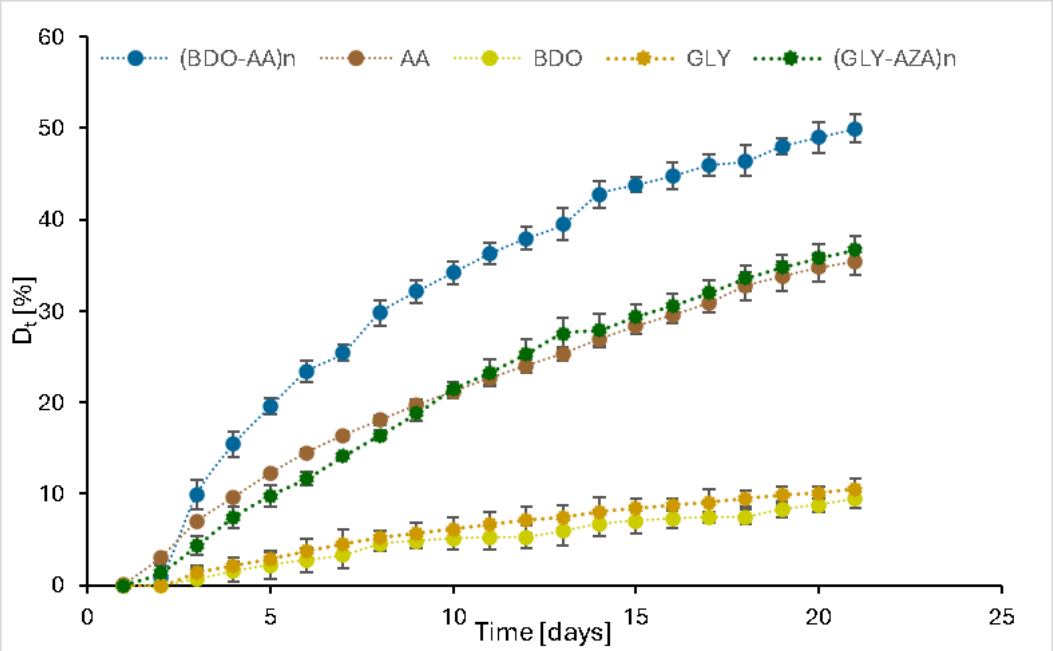

Figure 77 Degree of degradation of the oligoesters after 21 days of incubation in a marine environment; the data were normalized by subtracting the values of the control samples.

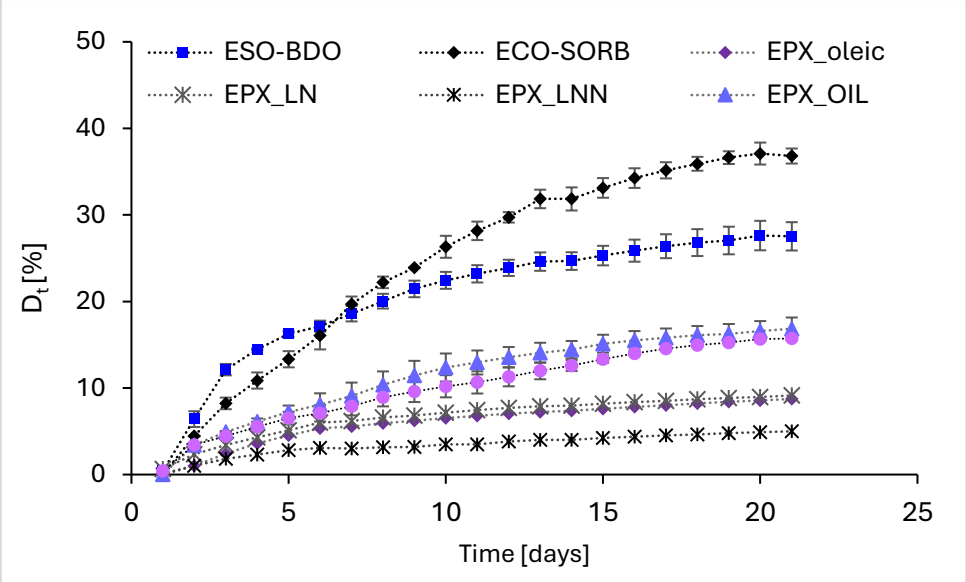

Figure 78 Degree of degradation of the epoxy cardoon oils and their derivatives after 21 days of incubation in a marine environment; the data were normalized by subtracting the values of the control samples.

The results obtained for the tested monomers (Table 33, entries 1–3 and 10–12) indicate that after 21 days the compound with the lowest biodegradability was the epoxylinolenic acid (D_{t21} = 5%). On the other hand, the highest D_t value was obtained for adipic acid (D_{t21} = 35.44%). Even though glycerol is a non-toxic molecule-as previously reported by Wolfson et al. [109]- and the addition of glycerol in the structures of different polymers increased the biodegradability of the final products [110], in the marine environment the BOD_21 and D_{t21} values reached values of 55.95 mg/L and 10.55%, respectively.

Table 33 The BOD and Dt values obtained after 5, 10, and 21 days of degradation in a marine environment, along with the ThOD values of the monomers and oligoesters considered for biodegradation [98].

No	Sample	ThOD (mg/mg)	BOD_5 (mg/L)	D_{t5} (%)	BOD_{10} (mg/L)	D_{t10} (%)	BOD_{21} (mg/L)	D_{t21} (%)
1	BDO	13.62	30.10	2.21	69.50	5.10	128.90	9.43
2	AA	6.38	28.11	12.23	48.70	21.19	81.90	35.44
3	GLY	5.30	15.50	2.92	32.80	6.18	55.95	10.55
4	(BDO-AA)n	1.32	25.95	19.55	45.40	34.20	66.30	49.95
5	(GLY-AZA)n	1.31	12.90	9.80	28.25	21.45	48.35	36.71
6	ESO-BDO	1.66	27.10	16.25	37.90	22.44	48.65	27.53
7	ECO-SORB	1.05	14.40	13.33	28.45	27.53	41.85	36.81
8	EPX_OIL	2.39	14.60	6.13	29.65	12.37	40.40	16.85
9	Cardoon_oil	2.69	14.90	5.52	27.55	10.20	42.25	15.72
10	EPX_oleic	7.21	34.55	4.51	50.60	6.53	67.25	8.74
11	EPX_LN	6.30	34.30	5.12	48.60	7.15	61.80	9.14
12	EPX_LNN	5.51	17.50	2.81	22.80	3.49	31.80	5.00

The biodegradation trends recorded during the exposure time were not similar when comparing the tested chemicals. In some cases, over 50% of the total biodegradation occurred early and within 10 days of exposure. In fact, D_{t21} was less

than 50% higher than D_{t10}. The increase in biodegradation during the period D_{t21}–D_{t10} ranged from 21.8% (EPX_LN) to 45.9 (BDO). A group of chemicals (BDO-AA, EPX_oleic, EPX_LNN) showed more than 68% of the total biodegradation occurring within $D_{t10.}$ Two chemicals (BDO and AA), although principally biodegraded within the first experimental time periods, showed that about 40–45% of biodegradation occurring in the second period of exposure.

The biodegradability data obtained with the oligoesters (entries 4 and 5) indicate that after 5 days the biodegradability of the oligoesters based on adipic acid and BDO was about twice as high as the D_t values of the oligoesters containing azelaic acid and glycerol. After 21 days, the ratio between the D_t values decreased to 1.36, and the adipic-acid-based oligoesters reached the value D_{t21} = 49.95%. This value is about 15% higher compared to the previous value reported by Kasuya et al. [111] for poly(butyleneadipate).

For the cardoon seed oil and its derivatives (entries 6–9), the highest D_t values were obtained for ECO-SORB and ECO-BDO-derivatives without double bonds or oxirane rings in the molecules, and probably with greater hydrophilicity compared to the starting oil or the epoxidized one. Interestingly, the biodegradation rate within the first 5 days was about 1.2-fold higher for the ECO-BDO sample compared to ECO-SORB, but later the order changed, and after 21 days the ECO-SORB sample reached a value of D_{t21} = 36.81%—about 1.33-fold higher compared to the ECO-BDO. The observed biodegradation behavior could be correlated with the T_m and T_g values determined by DSC and was consistent with the previously summarized data, where lower values of T_g and T_m were correlated with a higher degradation rate [88].

The degradation of the cardoon oil and the epoxidized oil (entries 8 and 9) was comparable; the values for the epoxidized sample were slightly higher after 21 days, but in the first 5 days the values were similar. These results indicate that the biodegradability is not affected by the presence of the oxirane rings.

The molecules with the lowest biodegradability were the epoxy fatty acids. The results indicated comparable values for epoxy oleic and epoxy linoleic acids, while the lowest values were for linoleic acid. The BOD values increased exponentially in the first 5 days, but later the biodegradation rate was much slower. These results could be attributed to the rigidity and low solubility of the molecules.

According to the US-EN ISO 14851:2019 guidelines, a substance can be considered biodegradable if the BOD is higher than 60% ThOD. Although longer degradation times than those reported in this study were proposed in the literature (i.e., 60–180 days, ISO 19679; ISO 23977-2; ASTM D7991-15), longer exposure times are also associated with an increased frequency of experimental failures due to the increasing difficulty in the execution of the test.

In some of the test cases, longer exposure times should be considered and tested, as the stability of the biodegradation curve was not completely reached during the exposure times tested (21 days) [112].

With respect to the degradation trend during the experimental time, the temporal delay reported for AA in the degradation process could be due to the need for a preliminary reduction in the molecular weight to allow the microbial attack [113].

Recent research analyzed the biodegradation of PVA in marine environments, showing a role of the glycerol component in blended materials during the biodegradation process [110].

Biodegradation evaluation of poly(5-hydroxymethyl-2-furancarboxylate-co-ricinoleate)

Polyesters with furan units selected for this study were poly(5-hydroxymethyl-2-furancarboxylate-co-ricinoleate)-the synthesized in subchapter 2.3, poly(2,5-bis-hydroxymethylfuran adipate)-the synthesized in subchapter 2. 4, and the model molecule poly(butylene-2,5-butylen-2,5-furanoate)-poly(butylene-2,5-furanoate), also synthesized enzymatically using 1,4-butanediol and 2,5-dimethylfuranoate as starting materials.

The highest BOD values [mg/L], shown in Figure 79, were obtained for all the three oligoesters considered in salt-water medium, and the increase was realized in the following order:

- poly(5-hydroxymethyl-2-furanecarboxylate-co-ricinoleate)>poly(2,5-bis-hydroxymethylfuran adipate)>poly(butylene-2,5-furanoate).

The same trend was observed in the experimental study conducted in water collected from the Bega river. The difference between the values obtained in brackish and fresh water are 10-15 mg/L.

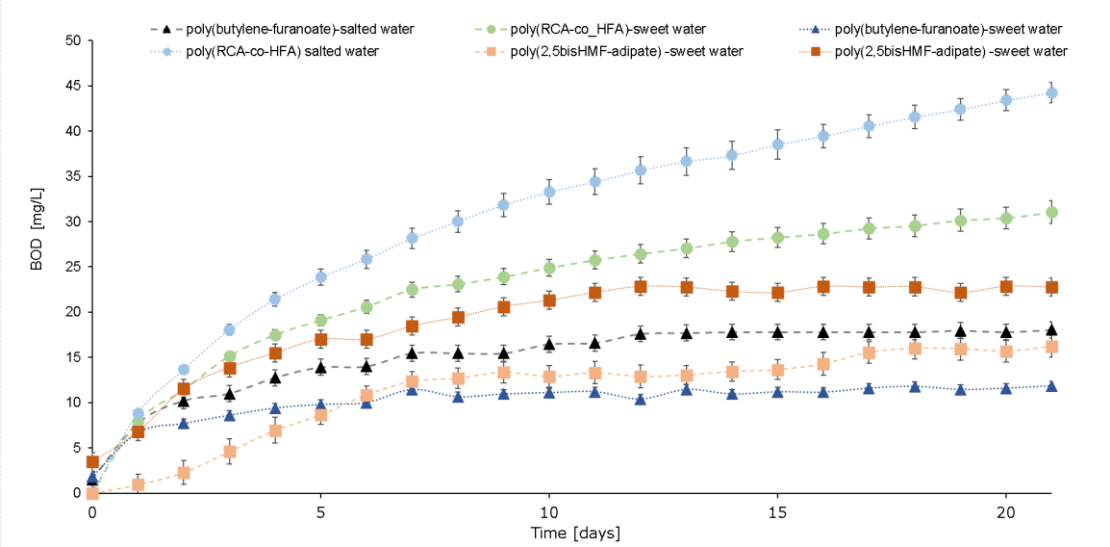

Figure 79 BOD values as a function of time determined in freshwater and saltwater medium for three types of furan oligoesters of adipic acid furan oligoesters with diols

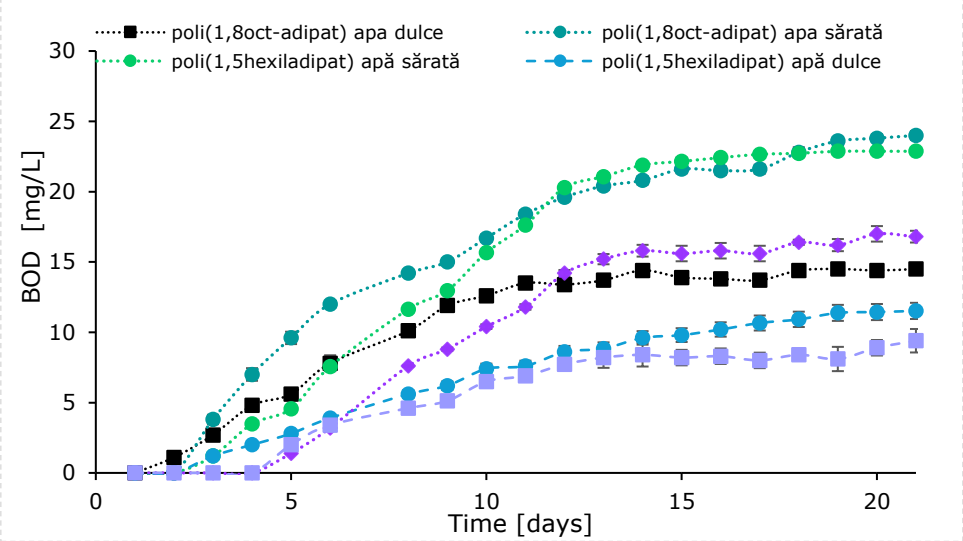

Figure 80 BOD values as a function of time determined in freshwater and saltwater environments for aliphatic oligoesters of adipic acid with diols

The selection of these oligoesters partially formed from renewable units (adipic acid being a bio-organic diacid) was made on the basis of the molecular weights obtained but also taking into account the structure of the co-monomer chain: linear, branched or cyclic. As with the furan derivatives, the highest BOD values [mg/L], shown in Figure 79, were obtained for all three oligoesters after incubation in salt water medium, and the increase was realized in the following order: poly(1,8-octanediol adipate) > poly(1,5-hexanediol adipate) > poly(1,4-cyclohexyldihydimethanol adipate). In comparison with the furan derivatives the values are slightly lower, but the difference between the values obtained in salt water and fresh water remain in the range 10-15 mg/L.

The biodegradation of some of the raw materials used to obtain the oligoesters was also studied and the following three were selected: castor oil, 2,5-furandicarboxylic acid and 5-hydroxymethyl-2-furoic acid. The degradation of adipic acid and 1,4-butanediol in salt water was previously reported by the group from the University of Trieste, Italy, using a similar method [98].

For castor oil the values were comparable to those previously reported and these lower values are probably due to the insolubility of the ricinoleic acid resulting after hydrolysis of triricinolein in aqueous medium. The reduced solubility but also the rigidity of the molecules may also be responsible for the degradation differences obtained for furan 2,5-dicarboxylic acid and 5-hydroxymethyl-2-furoic acid. The BOD values for 2,5-furandicarboxylic acid were 0 in the first days, followed by an increase but thereafter the biodegradation rate was slow (Figure 88).

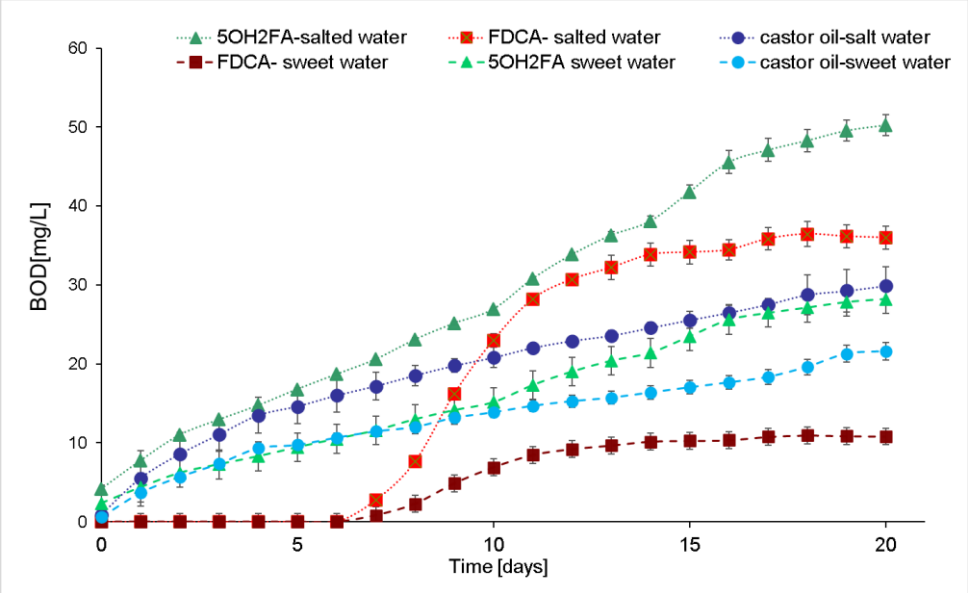

Figure 81 BOD values as a function of time determined in freshwater and saltwater environments for furan monomers and castor oil.

Table 34 shows the results expressed in percent biodegradability for the polyesters considered in this study. The percentage compositions of elements C, H and O were calculated for each polyester considering a tetramer. Using the percentage composition, the theoretical biochemical oxygen consumption (TOD) and the degree of biodegradability (Dt) were calculated.

The biodegradation trends of the tested compounds, as in other cases, are different. In some cases more than 50% of the total biodegradation occurred within the first 10 days after exposure. In fact values determined for Dt_{21} in all cases were higher compared to Dt_{10} values by less than 50%. The Dt_{21} values obtained for the oligoesters were in the range 6.12-74.23%.

The biodegradability data obtained for the oligoesters with furan units (positions 1-6 in the table) indicate that after 5 days the biodegradability of the oligoesters based on adipic acid and 2,5-HMF was about 2 times higher compared to the D_t value of the oligoesters containing PBF and 1.5 times higher than for the oligoesters with ricinoleic acid.

The differences between the adipic acid oligoesters are also due to the molecular masses, which in this case were different and for the calculation of the percentage biodegradation the molecular mass plays a major role.

After 21 days the ratio of D_t values was lower for samples 3 and 5 in brackish water, but the same trend was maintained for samples 4 and 6, evaluated in fresh water.

For aliphatic oligoesters (positions 7-12) the highest D_t values were obtained for the oligoester with 1,8-octanediol units, followed by the cyclic oligoesters with cyclohexane units. In comparison with the oligoesters with branched or cyclic units it can be observed that for the linear oligoester (position no. 7) the degradation percentage in the first 5 days reaches the value of about 30%, 10% higher than the value previously reported for poly(1,4-butylene adipate). However, after the first 10 days of incubation the degradation rate decreases. The observed biodegradation

behavior can be correlated with the values of degradation temperatures determined by TG and DSC and is in agreement with previously reported data, where lower values of T_g and T_m are correlated with a higher degradation rate [88].

The results obtained for the monomers tested (Table 34 No 13-18) indicate that after 21 days the compound with the lowest biodegradability was 2,5-furandicarboxylic acid (D_{t21} = 4.34% in salt water and 2.86% in fresh water). The highest Dt values were obtained for castor oil (D_{t21}=12.60% in salt water).

Table 34 Dt values obtained after 5, 10 and 21 days of degradation in salt water and fresh water of the monomers and oligolesters considered for biodegradation.

Nr	Proba	D_{t5} [%]	D_{t10} [%]	D_{t21} [%]
1	PBFs	12.86	15.22	16.70
2	PBFd	9.06	10.28	10.97
3	P2,5HMFs	36.35	45.55	48.65
4	P2,5HMFd	18.49	27.58	34.64
5	PRCA-HFAs	22.5	31.36	41.74
6	PRCA-HFAd	18.01	23.49	29.29
7	P1,8As	29.97	52.13	74.93
8	P1,8Ad	17.48	39.33	45.27
9	P1,5As	2.42	8.32	12.15
10	P1,5Ad	1.48	3.93	6.12
11	P1,4As	1.70	12.64	20.70
12	P1,4Ad	2.16	7.02	9.62
13	Ulei ricin s	6.16	8.76	12.60
14	Ulei ricin d	4.10	5.84	9.10
15	FDCAs	0.00	0.84	4.34
16	FDCAd	0.00	1.58	2.48
17	2,5HMFs	2.54	4.08	7.62
18	2,5HMFd	1.43	2.29	4.28

PBF- poly(1,4-butylene-2,5-furanoate); P2,5HMF- poly(2,5-bis-hydroxymethylfuran adipat); PRCA-HFA- poly(5-hydroxymethyl-2-furancarboxylate-co-ricinoleate); P1,8A- poly(1,8-octanediol adipate); P1,5A- poly(1,5-hexanediol adipate); P1,4A- poly(1,4-cyclohexyl dimethanol adipate); s- salt water and d-sweet water

II.6.2. Biodegradation of ter-oligomers

Concerning the marine biodegradation of the ter-oligomers mixtures, the interpretation of the results is more complicated because of their inhomogeneous composition.

The aliphatic ERY monomer was introduced in the study because of its high polarity and hydrophilicity, which is expected to increase the solubility of the corresponding oligomers. Indeed, data indicate that oligomers are more biodegradable when ERY is introduced in place of the aromatic FDCA or TA. Overall, pairwise analysis of Dt_{21} data suggests a less pronounced stability of FDCA-containing

products, compared to data observed for co-oligomers. In support of these findings, it must be noted that all the five ter-oligomers mixtures considered in the study contain other aliphatic moieties (see Figure 82), which might mask or counterbalance the effect of FDCA. Altogether, the difficulty establishing the effect of the structural moieties on stability/biodegradability prompted us to further investigate the data with additional tools, as described in the next section.

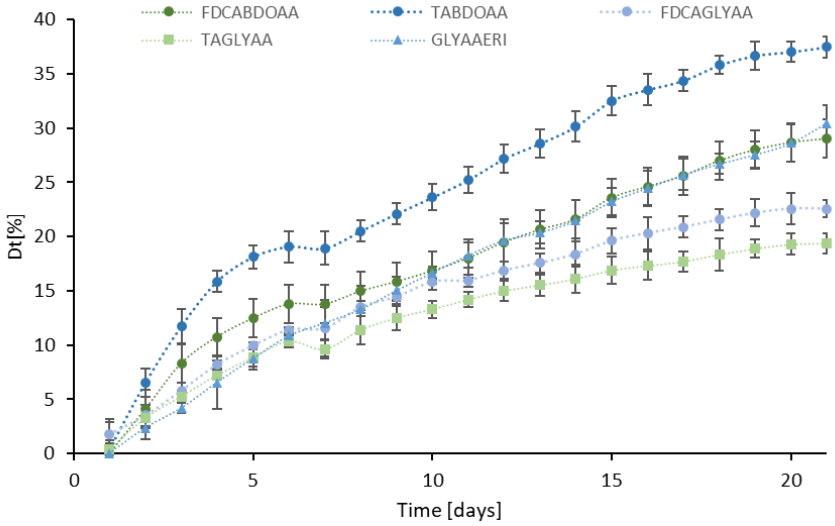

Figure 82 Degree of marine biodegradation (Dt_{21}) obtained for the mixtures of ter-oligomers after 21 days of incubation. Data were normalized by subtracting the values of control samples.

Biodegradability of enzymatically synthesized bio-based terpolymers derived from ε-caprolactone

In the case of terpolymers based on *ε*-caprolactone, it was observed for 21 days that the highest biochemical oxygen consumption, reaching up to 59-66 mg/L, was recorded for the block copolymers of *ε*-caprolactone with dimethyl adipate and 1,8-octanediol and for the block copolymers of *ε*-caprolactone with dimethyl adipate and 1,8-octanediamine, respectively (Figure 83). Compared to the BOD for the *ε*-caprolactone homo-oligomer, the evolution of the oxygen consumption curve is highly similar, particularly with the *ε*-CL:DMA:ODO system. This can be co-related with block polymers that integrate a large fraction of polycaprolactone segments into their chemical composition, which is confirmed by the species identified in the MALDI-TOF MS spectra, hence the similarity to the evolution of the BOD curve for the *ε*-CL homo-oligomer. This accelerated metabolization of *ε*-caprolactone during this biodegradation can be connected with a metabolic process in which microbial enzymes attack the ester bonds in the polymer chain, breaking large molecules into smaller fragments, which are then metabolized by microorganisms. However, the presence of amide bonds inside the polymeric architecture increases the amount of oxygen required to completely metabolize the compounds, therefore inducing a delay in the biodegradation rate. In practice, this should result in higher values of BOD recorded for polyesteramides, but in the case of the two block polyesters and polyesteramides counterparts, the BOD for the *ε*-CL:DMA:ODA system registered lower values and

therefore lower degradation rates. This can be attributed to the presence of amide bonds, which are less prone to hydrolysis by the microbes present in the aquatic medium and reduce the susceptibility of the polyesteramides to degradation by the enzymes produced by microorganisms [114].

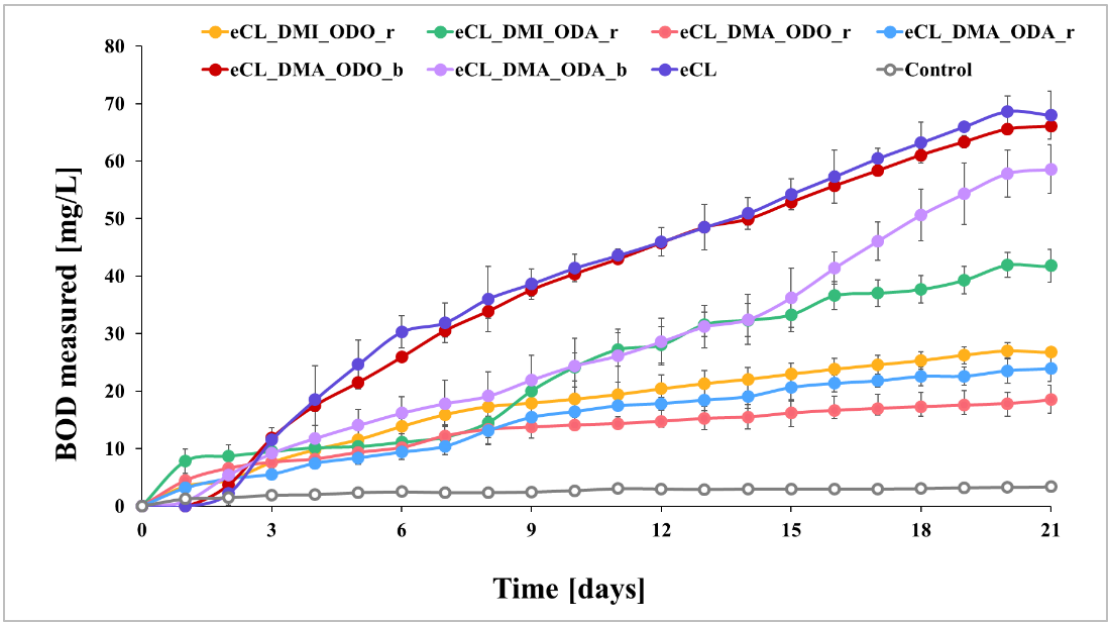

Figure 83 Biochemical oxygen consumption (BOD) monitored using the OxiTop systems over a period of 30 days to monitor the microbiological degradation of the random products of ε-caprolactone copolymerized with dimethyl itaconate and either 1,8-octanediol (orange) or 1,8-octanediamne (green), the random products of ε-caprolactone copolymerized with dimethyl adipate and either 1,8-octanediol (pink) or 1,8-octanediamne (light blue), the block products of ε-caprolactone copolymerized with dimethyl adipate and either 1,8-octanediol (red) or 1,8-octanediamne (dark blue), and the ε-caprolactone homo-oligomer in comparison to the control sample (grey).

In the case of the random copolymers, the BOD measured registered lower values. The ε-caprolactone with dimethyl itaconate and 1,8-octanediamine polymer registered the highest concentration of biochemical oxygen, encompassing 42 mg/L, being consumed for the metabolization of the ε-CL:DMI:ODA polymer. The other systems presented comparable values of BOD in the range of 19-27 mg/L. The BOD for the random copolymers was higher in the case of the systems containing the ODA functionalities, as the ThOD is also elevated along with the presence of the nitrogen atoms in the polymeric chain. For the short period of time of 21 days, these overall values of biochemical oxygen consumption continue to indicate an intense biodegradation of the terpolymers under the experimental conditions applied, highlighting their high susceptibility to degradation in the presence of microorganisms from the natural river water environment.

In terms of the D_t biodegradability degree, the results expressed as percentage of degradability after 5, 10, and 21 days are presented in Table 35. After 21 days of monitoring, the block copolymer of ε-caprolactone with dimethyl adipate and 1,8-octanediol, the block copolymer of ε-caprolactone with dimethyl adipate and 1,8-octanediamine as well as the ε-caprolactone homo-oligomer, were completely degraded. This result indicates a highly efficient biodegradation process for these

polymers, with microorganisms in the tested medium able to completely decompose these materials in a relatively short period [114].

Table 35 The biodegradability degree Dt calculated for the random terpolymers of ε-caprolactone with dimethyl itaconate or dimethyl adipate, and 1,8-octanediol or 1,8-octanediamine, respectively, after 21 days of incubation.

Terpolymer	ThOD[a] [mg/mg]	BOD_5 [mg/mg]	D_{t5} [%]	BOD_{10} [mg/mg]	D_{t10} [%]	BOD_{21} [mg/mg]	D_{t21} [%]
ε-CL:DMI:ODO random	0.430	0.092	21	0.159	37	0.2345	55
ε-CL:DMI:ODA random	0.534	0.08	15	0.215	40	0.3845	72
ε-CL:DMA:ODO random	0.437	0.070	16	0.114	26	0.152	35
ε-CL:DMA:ODA random	0.659	0.061	10	0.138	22	0.206	33
ε-CL:DMA:ODO block	0.417	0.215	52	0.400	96	0.427	100
ε-CL:DMA:ODA block	0.448	0.141	31	0.240	54	0.456	100
ε-CL	0.704	0.247	35	0.410	58	0.674	96

[a]ThOD-The percentage composition of C, H, N, and O elements was calculated considering (i) 21 ε-CL molecules, 6 DMI molecules, 6 ODO molecules for random ε-CL:DMI:ODO; (ii) 10 ε-CL molecules, 9 DMI molecules, 9 ODA molecules for random ε-CL:DMI:ODA, (iii) 27 ε-CL molecules, 3 DMA molecules, 2 ODO molecules for random ε-CL:DMA:ODO, (iv) 10 ε-CL molecules, 6 DMA molecules, 6 ODA molecules for random ε-CL:DMA:ODA, (v) 32 ε-CL molecules, 1 DMA molecule, 1 ODO molecule for block ε-CL:DMA:ODO, (vi) 46 ε-CL molecules, 3 DMA molecules, 2 ODA molecules for block ε-CL:DMA:ODA, respectively.

The ε-CL:DMA:ODO block terpolymer showed nearly a degradation of nearly 52% after just 5 days, while the ε-caprolactone homo-oligomer degraded more slowly, reaching a D_t of 23% after 5 days of incubation, while the ε-CL:DMA:ODA block terpolymer also demonstrates a relatively high degree of biodegradability, with a D_t of 31% after 5 days of incubation in the presence of the inoculum. The degradation mechanism seems to be more suited to hydrolysis of the ester bond of polycaprolactone, since all these compounds incorporate large amounts of polycaprolactone. The ε-CL-based polymers demonstrated a high susceptibility to enzymatic hydrolysis due to the presence of ester bonds in the chemical structure with microbial enzymes, such as esterases and lipases, catalyzing the cleavage of these bonds in rapid and complete degradation process. This is supported by the fact that solely the copolymer of adipic acid and 1,4-butadiol was observed to reach a degradation degree of 50% after 21 days of incubation in the presence of Adriatic see water inoculum, as reported by Zappaterra *et al.* [98]. Therefore, the synthetic strategy to obtain terpolymers with ε-caprolactone seems to improve the biodegradation properties of the DMA-based materials.

It can be observed that the DMI-based random products showed a higher degree of biodegradability compared to DMA-based random products. For example, the ε-CL:DMI random terpolymer reaches a remarkable 96% D_t after 30 days, the highest among the samples tested, suggesting that DMI confers superior degradation properties. This trend is consistently observed, as ε-CL:DMI random also shows significant biodegradability, reaching a Dt of 77% over the same period. On the contrary, DMA-based terpolymers, ε-CL:DMA exhibit a lower degree of biodegradability, which can also be co-related with their high molecular weights determined from GPC analysis. Furthermore, the influence of the diol or diamine component is evident in the case of the random structure, in contrast with the block terpolymers, and the biodegradation results indicate that the random structure has a higher complexity and becomes more difficult to disassemble by the microbial enzymatic mechanism than the block structures, which integrate mainly polycaprolactone chains. Only in the case of the ε-CL:DMI:ODA system, the ODA-containing terpolymers show better biodegradability than those with ODO, which can be correlated with the presence of pyrrolidone conformations in the terpolymer structure. From the biodegradability behaviour of these terpolymers, the pyrrolidone containing products appears to be more prone to biodegradation in comparison to the classical amide bond. These differences highlight the critical role of polymer composition in biodegradability and indicate that the use of DMI and ODA in terpolymer formulations can significantly improve the environmental performance of these materials.

In conclusion, considering that both the block terpolymer of ε-caprolactone with dimethyl adipate and 1,8-octanediol, and the ε-caprolactone homo-oligomer are fully biodegradable in the selected conditions, their ability to fully degrade under natural conditions suggests potential for use in low-environmental impact products, such as biodegradable packaging, matrixes for the encapsulating of bioactive compounds, and other applications where biodegradability is essential. Complete biodegradability becomes crucial for green applications, ensuring that materials do not persist in the environment as harmful residues. Moreover, this susceptibility to enzymatic hydrolysis can be harnessed to design new materials with controllable degradation rates, tailored to different usage and disposal needs, and exclusively contain ester bonds in their chemical structure. As a result, they are more susceptible to enzymatic hydrolysis and are more readily degraded by microorganisms in the natural environment. This can also be applied to other systems with high biodegradation rates such as ε-CL:DMA:ODA block terpolymers and in particular DMI based terpolymers containing the ODA component.

II.6.3. Study of the marine biodegradation of monomers composing the oligoesters model.

To evaluate the biodegradability of the monomers that are obtainable from the hydrolysis of the oligoesters, the same protocols were applied performing all tests in duplicate for each monomer.

The Dt_{21} values (Table 36) indicate that under the current conditions and using an inoculum of sea water as marine biodegradation test, FDCA has a very low biodegradability (Dt21 = 6.83%) while the biodegradability of TA is negligible (0.08%). Notably, the ECHA database reports that TA is “readily biodegradable” in water [115] but the conditions used for the assay involved a much more active inoculum with the addition of activated sludge (e.g from the sewage) or mixtures of sewage, soil, and natural water.

That is in line with the OECD 301 guidelines, which report six methods to screen chemicals for ready biodegradability in aerobic aqueous medium [116].

To further investigate how the inoculum may affect the marine biodegrability data, we decided to sample inside the industrial harbor of Trieste (Zaule, 45.613298 N, 13.810115 E). The selected area is close to a sewer pipe, a water treatment plant, an oil tanker terminal with connected pipeline and underwater oil storage. The Zaule channel area is affected by numerous additional sources of pollution compared to the Molo Audace area. Indeed, the navigable channel concentrates major productive industrial activities that negatively impact the sediments and consequently the quality of the sea water. Firstly, there is the presence of two rivers (Rio Ospo and Torrente Rosandra) that discharge directly into the Zaule channel, bringing organic load and fertilizers. From 1896 to 2020, the Servola ironworks was active, discharging metalworking residues into the sea [117]. Lastly, the bay area of Muggia, along with the Zaule channel, suffers from significant pollution by hydrocarbon compounds due to the construction in 1967 of the Trieste–Munich (SIOT) oil-pipeline [118].

The collected data, shown in Table 36, clearly demonstrate how the inoculum colected from the more polluted area causes an increase of the biodegradability of the monomers, confirming that the cleaner is the sea the higher is the risk of accumulation of microplastics or other products formed during the biodegradation process.

Table 36 ThOD values are considered for the calculation of biodegradation and Dt values obtained after 5, 10, and 21 days of incubation of the monomers composing the oligoesters, using two different samples of sea water as inoculum from the sea water from Trieste (A) and Zaule (B).

Sample	Inoculum	ThOD [mg/mg]	BOD_5 [mg·L^{-1}]	BOD_{10} [mg·L^{-1}]	BOD_{21} [mg·L^{-1}]	Dt_5 [%]	Dt_{10} [%]	Dt_{21} [%]
FDCA	Trieste	4.34	5.05	12.90	23.50	1.16	2.82	6.83
FDCA	Zaule	4.34	16.35	46.15	53.65	3.77	10.63	12.59
TA	Trieste	7.60	0.00	1.25	2.15	0.00	0.08	0.08
TA	Zaule	7.60	54.25	98.15	102.6	7.14	12.91	13.50
AA	Trieste	6.38	65.77	128.36	200.65	10.31	20.12	31.8
AA	Zaule	6.38	89.00	101.85	110.15	13.95	15.96	17.26
BDO	Trieste	13.62	30.10	69.50	128.90	2.21	5.10	9.43
BDO	Zaule	13.62	45.65	82.05	96.10	3.35	6.02	7.06
GLY	Trieste	5.30	15.50	32.80	55.95	2.92	6.18	10.51
GLY	Zaule	5.30	55.80	76.95	102.45	10.53	14.52	19.33

ERY	Trieste	3.98	11.95	24.65	44.85	2.99	6.55	14.22
DMT	Trieste	7.69	1.10	18.60	48.30	0.14	2.28	6.15
DMF	Trieste	5.48	11.9	18.35	24.25	2.17	3.23	5.28

The differences observed in the biodegradation studies underscore the significant influence of the inoculum on the biodegradation process, especially for the aromatic monomers. Microbial communities play a pivotal role in determining the rate and extent of biodegradability, and their potential can be exploited for optimizing degradation in various environmental contexts.

Moreover, these findings raises intriguing questions about the remarkable adaptability to diverse environmental conditions of microbial communities present in the same gulf at a 9.2 km distance.

The dynamic nature of microbial interactions with different environments and their pollutants suggest that a broader exploration of microbial diversity could unveil novel solutions for improving the biodegradability of synthetic polymers.

II.6.4. Biodegradation studies of a oligoester-amides

The method for the study of marine biodegradation of oligoesters described above was also validated on an oligoamide. In particular, we intended to have a kind of “recalcitrant” bio-based substrate as a reference.

Polyamides are generally resistant to microbial degradation due to their synthetic nature and the stability of the amide bonds in their molecular structure [119]. While the ester bond is quite reactive and can be hydrolyzed in slightly acidic environments, the amide bond is very stable also at extreme pH and high temperatures, which makes protein and synthetic polyamides difficult to hydrolyze. As a consequence, fragments from the laundry of nylon-based textiles constitute one of the main sources of marine microplastics [120].

In fact, aliphatic esters and polyesters can be readly hydrolyzed by numerous hydrolases, such as cutinases and lipases that are ubiquitous in different eco-systems, whereas polyamides and nylon are not recognized by natural peptidases and amidases, which accept very specific amide substrates [121]. Previous bioinformatic studies have also demonstrated that polyamides are more polar than polyesters and the hydrophobic active site of cutinases and lipases prevent the approach of polar molecules [120].

Dimethyl adipate (DMA) and 2,5-bis(aminomethyl)furan (DAF) were used to synthetize the bio-based aromatic oligoamide DAF-AA in the presence of immobilized lipase N435. The product contained oligomers constituted by 2-6 units.

Table 37 The Dt values obtained after 5, 10, and 21 days of degradation in a marine environment for the oligomer and the constituting monomers, along with the ThOD values considered for biodegradation.

No	Sample	BOD_5 [$mg \cdot L^{-1}$]	D_{t5} [%]	BOD_{10} [$mg \cdot L^{-1}$]	D_{t10} [%]	BOD_{21} [$mg \cdot L^{-1}$]	D_{t21} [%]
1	DAF	0.01	0.10	0.05	0.36	0.05	0.37
2	DAF-AA	0.01	0.41	0.05	1.44	0.05	1.59

The marine biodegradability assay of DAF-AA led to a D_{t21} value of 1.59%, which indicates a negligible biodegradability (Table 37). For the bio-based DAF Dt_{21} value of 0.37% was recorded. The pattern for the aromatic DAF appears quite flat, and confirm the high stability of aromatic monomers, as observed for TA and FDCA. Data confirm that the oligoamide is recalcitrant to marine biodegradation, although the profile reported in Figure S8 shows some minor variation occurring after 5 days of incubation, which might suggest some positive perspective for the identification of enzymatic activity towards aromatic amides hydrolysis.

Biodegradability of enzymatically synthesized bio-based oligoesteramides derived from ε-caprolactam

The biodegradation behavior of the enzymatically synthesized oligoesteramides derived from *ε*-caprolactam and 5 different hydroxy acids, namely L-malic acid (MA), 3-hydroxybutyric acid (3HBA), 12-hydroxystearic acid (12HSA), 16-hydroxyhexadecanoic acid (16HHDA) and 5-hydroxymethyl-2-furancarboxylic acid, respectively, was analyzed in comparison to the *ε*-caprolactam homo-oligomer obtained as well as a product of enzymatic polymerization. The BOD in the presence of the Bega River water inoculum was measured over a period of 21-day and reported compared to the control sample.

As can be observed in Figure 84 at the end of 21 days of incubation, oligoesteramides based on *ε*-caprolactam and hydroxy fatty acids displayed a high degree of metabolic activity from the interaction with the river water microorganisms compared to the control sample.

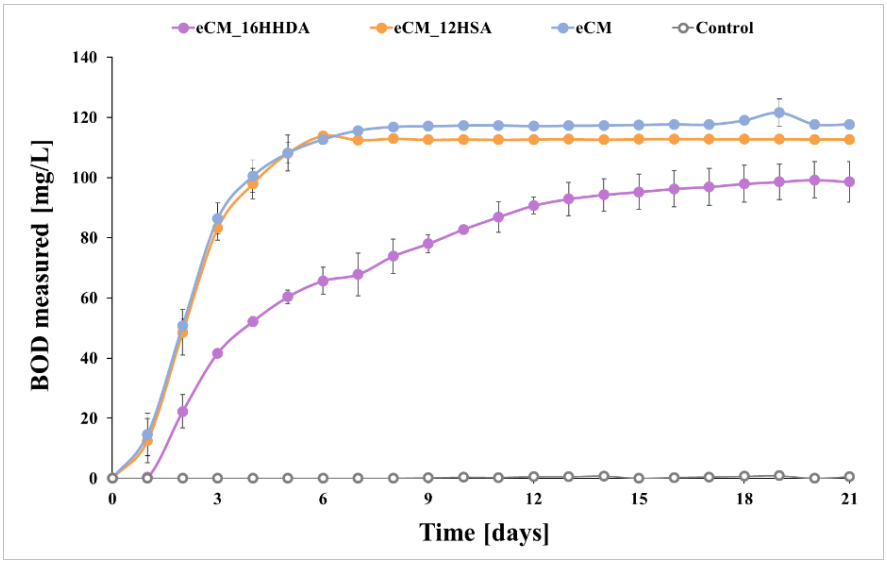

Figure 84 Biochemical oxygen consumption (BOD) monitored using the OxiTop systems over a period of 21 days to monitor the microbiological degradation of the oligoesteramides based on ε-caprolactam with 16-hydroxyhexadecanoic acid (purple) and with 12-hydroxystearic acid (orange), and the ε-caprolactam homo-oligomer (blue) in comparison to the control sample (grey).

The highest biochemical oxygen demand was measured for the polyesteramide derived from *ε*-caprolactam and 12-hydroxystearic acid, reaching a value of 113 mg/L, in contrast to the polyesteramide based on *ε*-caprolactam and 16-hydroxyhexadecanoic acid, which achieved a slightly lower biochemical oxygen demand, 99 mg/L. These small differences can be correlated with the *ε*-CM:12HSA system is characterized by a higher theoretical oxygen demand, so more oxygen is required to completely oxidize this sample, while also having a lower average molecular weight compared to the *ε*-CM:16HHDA system.

Average molecular weight is an essential factor in the biodegradation process, with lower molecular weight oligomers usually being more accessible to microbial enzymes and hydrolysis processes. This aspect contributes to an increased susceptibility to microbial decomposition, which ultimately leads to more rapid degradation and metabolism. Thus, on the account of having a moderately lower molecular weight, the co-oligomers of *ε*-caprolactam with 12-hydroxystearic acid are prone to a more accessible interaction between the oligomers and the microorganisms in the environment, leading to accelerated biodegradation compared to co-oligomers with higher molecular weight, such as the co-oligomer between *ε*-caprolactam and 16-hydroxyhexadecanoic acid. On the other hand, the ability of the microbial species to biodegrade the *ε*-CM derivatives depends on the susceptibility of the amide bond to being hydrolyzed by the enzymatic equipment of the specific microorganisms present in the river water. For the *ε*-CM homo-oligomer, the theoretical oxygen demand for complete metabolization of these oligomers is increased due to the high share of nitrogen. The measured BOD of the *ε*-CM homo-oligomer was slightly higher, but comparable with the *ε*-CM:12HSA system. This can be attributed to the similarity in the composition of the reaction products, the main products of the *ε*-CM:12HSA system having one additional 12HSA unit compared to with the *ε*-CM homo-oligomer.

The highest values of biochemical oxygen consumption, in the case of *ε*-caprolactam-based oligoesteramides, were determined for the system containing the co-oligomer of *ε*-caprolactam with 5-hydroxymethyl-2-furancarboxylic acid (Figure 2.58). The values recorded reached 117 mg/L for the *ε*-CM:5HMFCA, while the other oligomers of *ε*-caprolactam and 3-hydroxybutyric acid or L-malic malic reached slightly lower BOD values in the range 96-105 mg/L. As the average molecular weights of these oligomers are all in the 300-500 Da range, the differences in BOD values are most likely due to the theoretical oxygen consumption required to metabolize the samples.

The lowest ThOD values were calculated for the *ε*-CM:MA system, limited at 2.088 mg/mg, and the lowest evolution in biochemical oxygen consumption was also registered for this system, while the increase in ThOD for the *ε*-CM:5HMFCA and *ε*-CM:3HBA can be correlated with an increase in the registered values of BOD. In the same time, the aspect that the highest ThOD values were determined for the *ε*-CM homo-oligomer can be correlated with the highest values of the BOD registered for this system. This highlights the importance of the ester bonds in the chemical architecture of the oligoesteramides, which contribute significantly to the

biodegradability of the bio-based oligomers, reducing the oxygen demand necessary for the metabolism of the oligomeric compound.

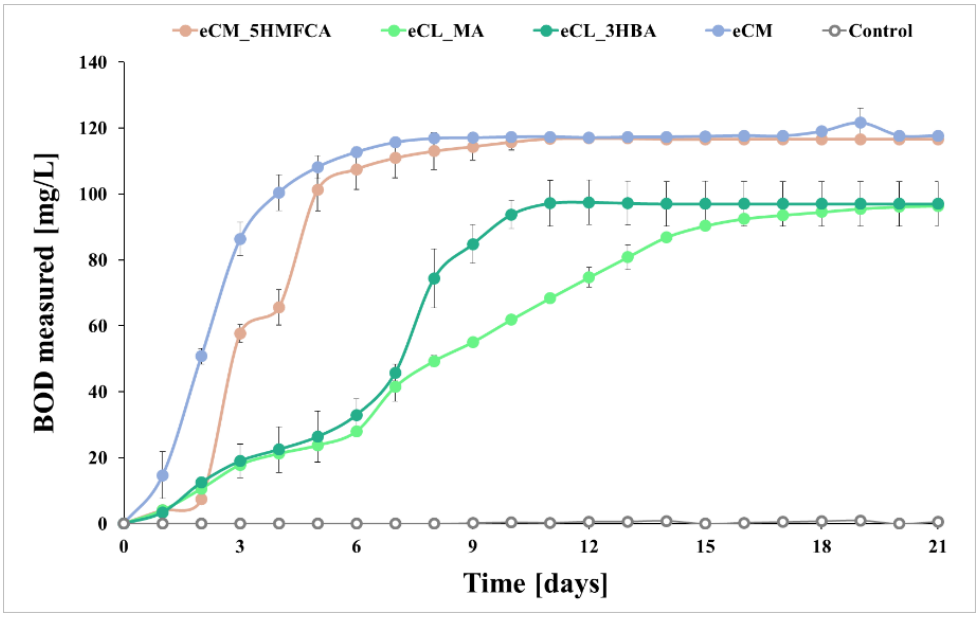

Figure 85 Biochemical oxygen consumption (BOD) monitored using the OxiTop systems over a period of 21 days to monitor the microbiological degradation of the oligoesteramides based on ε-caprolactam the oligoesteramides based on ε-caprolactam with 5-hydroxymethyl-2-furancarboxylic (brown), with 3-hydroxybutyric acid (dark green), with L-malic acid (light green), and the ε-caprolactam homo-oligomer (blue) in comparison to the control sample (grey).

A more in-depth influence of the ester linkage can be analyzed from the biodegradability degree (D_t). The degree of biodegradability after 21 days exhibited by the oligoesteramides derived from *ε*-caprolactam was lower compared to the oligoesters based on *ε*-caprolactone, with a D_t of 37% for *ε*-CM:12HSA, 39% for *ε*-CM:16HHDA, and 40% for *ε*-CM:5HMFCA, 35% *ε*-CM:3HBA, and 45% for *ε*-CM:MA (Table 38). This decrease in biodegradability can be attributed to the presence of *ε*-caprolactam units in the chemical structure of oligoesteramides, a monomer commonly used industrially to synthesize materials such as polyamide 6 (also known as Nylon), which is renowned for its high resistance to biodegradation. The limitation identified is also confirmed by the reduced degree of the biodegradability of the *ε*-CM homo-oligomer, which accounted for on only 29% after 21 days of analysis, the lowest value of D_t among all *ε*-CM derivatives. Although the average molecular weight of this oligomeric compounds is reduced, the biodegradation is highly limited by the presence of the amide bound.

These differences highlight the critical role of oligomer composition in biodegradability and suggest that careful selection of monomers to modulate the composition of oligoesters and oligoesteramides can significantly enhance the environmental performance of these materials. Although the biodegradation rate for oligoesteramide is slightly slower compared to oligoesters, the overall capacity to be susceptible to microbial metabolization under the experimental conditions applied still

indicates good biodegradation of these co-oligomers, with 35-45% biodegradability over a 21-day period.

Table 38 The biodegradability degree Dt calculated for the co-oligomers of ε-caprolactam with L-malic acid (MA), 3-hydroxybutyric acid (3HBA), 12-hydroxystearic acid (12HSA), 16-hydroxyhexadecanoic acid (16HHDA), 5-hydroxymethyl-2-furancarboxylic acid and ε-caprolactam homo-oligomer respectively, after 21 days of incubation.

Oligomer	ThOD[a] [mg/mg]	BOD_5 [mg/mg]	D_{t5} [%]	BOD_{10} [mg/mg]	D_{t10} [%]	BOD_{21} [mg/mg]	D_{t21} [%]
ε-CM:16HHDA	2.666	1.081	16	1.123	31	1.121	37
ε-CM:12HSA	2.893	0.604	29	0.824	39	0.980	39
ε-CM:5HMFCA	2.907	1.013	35	1.154	40	1.160	40
ε-CM:3HBA	2.948	0.578	20	1.028	34	1.020	35
ε-CM:MA	2.088	0.214	10	0.592	28	0.580	45
ε-CM	4.045	1.082	27	1.165	29	1.171	29

[a]ThOD-The percentage composition of C, H, N, and O elements was calculated considering (i) 2 ε-CM molecules, 2 16HHDA molecules for ε-CM:16HHDA; (ii) 3 ε-CM molecules, 1 12HSA molecules for ε-CM:12HSA; (iv) 3 ε-CM molecules, 1 5HMFCA molecules for ε-CM:5HMFCA; (v) 2 ε-CM molecules, 2 3HBA molecules for ε-CM:3HBA; (vi) 3 ε-CM molecules, 1 MA molecules for ε-CM:MA; (vii) 3 ε-CM molecules for ε-CM, respectively.

II.6.5. Computational analysis of tetramer structures using VolSurf[3] molecular descriptors

The computational study aimed to numerically describe different copolymers and terpolymers that can be formed in the enzymatic polycondensation, to identify the molecular properties related to biodegradation. Given the intrinsic difference among the two classes (copolymers and terpolymers), we built a set of comparable molecular structures through the use of tetramers, by linking diacids and diols, as reported in Table 6. In some cases, both monomers were repeated twice, whereas in other cases only one monomer was repeated twice, and the other was present with two different forms: for example, FDCA-GLY-AA-GLY contains two different diacids whereas AA-GLY-AA-ERY contains two different diols.

We applied the VolSurf method originally developed for the prediction of properties of drugs [122] related to permeability issues such as membrane permeation and ADME properties in general [123], [124] but suitable for additional tasks. It converts GRID-derived Molecular Interactions Fields (MIF) [125], [126] into simple quantitative molecular descriptors; MIF can be seen as a quantitative computation of the ability of the molecule (in our case, the tetramer) to establish specific interactions with a chemical probe; default probes for VolSurf procedure are DRY (for hydrophobic), OH2 (water), N1 and O (polar probes, to to distinguish donating and accepting hydrogen bonding interactions).

The software has been recently revised, and we used the version 3 [127], [128]. The original matrix of 126 molecular descriptors (obtained with default options) was

subjected to pretreatment, to exclude variables with no variance (9 variables) as well as those variables specifically designed to model drugs ADME properties, such as CACO2 (to predict intestinal absorption), MetStab (CYP-mediated metabolic stability), PB (protein binding), VD (Volume of distribution), LgBB (blood-brain permeability) and SKIN (skin permeability).

The SMILES codes of the tetramers considered for the computational studies are presented in Table 39, together with the biodegradation experimental values used as input for computational-experimental data correlation. An example of molecular representation is reported in Figure 86.

Table 39 Tetramers SMILES codes and biodegradation experimental values of the correspondent oligomers.

Objects	SMILES codes of the tetramers	Biodegradation [%]
AA-BDO-AA-BDO	C(CCCO)OC(=O)CCCCC(=O)OCCCCOC(=O)CCCCC(=O)O	50.23
AA-DAF-AA-DAF	NCc1ccc(o1)CNC(=O)CCCCC(=O)NCc1ccc(o1)CNC(=O)CCCCC(=O)N	1.59
AA-GLY-AA-GLY	C(C(O)CO)OC(=O)CCCCC(=O)OCC(O)COC(=O)CCCCC(=O)O	46.9
AA-GLY-AA-ERY	OCC(O)C(O)COC(=O)CCCCC(=O)OCC(O)COC(=O)CCCCC(=O)O	30.9
BDO-FDCA-BDO-AA	O=C(CCCCC(=O)O)OCCCCOC(=O)c1ccc(o1)C(=O)OCCCCO	26.81
BDO-FDCA-BDO-FDCA	OCCCCOC(=O)c1ccc(o1)C(=O)OCCCCOC(=O)c1ccc(o1)C(=O)O	15.22
BDO-TA-BDO-TA	OCCCCOC(=O)c1ccc(cc1)C(=O)OCCCCOC(=O)c1ccc(cc1)C(=O)O	37.92
FDCA-GLY-AA-GLY	OC(COC(=O)c1ccc(o1)C(=O)O)COC(=O)CCCCC(=O)OCC(O)CO	22.55
FDCA-GLY-FDCA-GLY	OCC(O)COC(=O)c1ccc(o1)C(=O)OCC(O)COC(=O)c1ccc(o1)C(=O)O	18.36
GLY-TA-GLY-TA	OCC(COC(=O)c1ccc(cc1)C(=O)OCC(COC(=O)c1ccc(cc1)C(=O)O)O)O	50.12
TA-BDO-AA-BDO	O=C(CCCCC(=O)O)OCCCCOC(=O)c1ccc(cc1)C(=O)OCCCCO	37.48
TA-GLY-AA-GLY	OC(COC(=O)c1ccc(cc1)C(=O)O)COC(=O)CCCCC(=O)OCC(O)CO	19.38

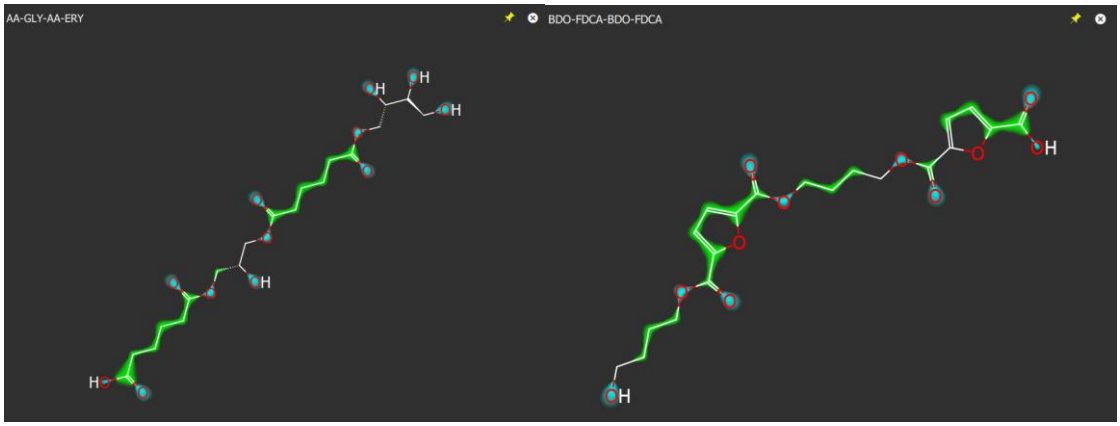

Figure 86 Molecular representation as provided by the new GUI of VolSurf[3]. Two tetramers (AA-GLY-AA-ERY and BDO-FDCA-BDO-FDCA) are reported as example, represented as OH2 and DRY probes (green and cyan).

The resulting matrix of 112 descriptors underwent unsupervised analysis via Principal Component Analysis (PCA), with the aim of pattern recognition, with a clustering approach, used to identify clusters in the dataset.

The graphical analysis of the objects is provided in the score plot (Figure 87) a where the two-components-model PCA distinguishes three groups, as shown by differently coloured clusters.

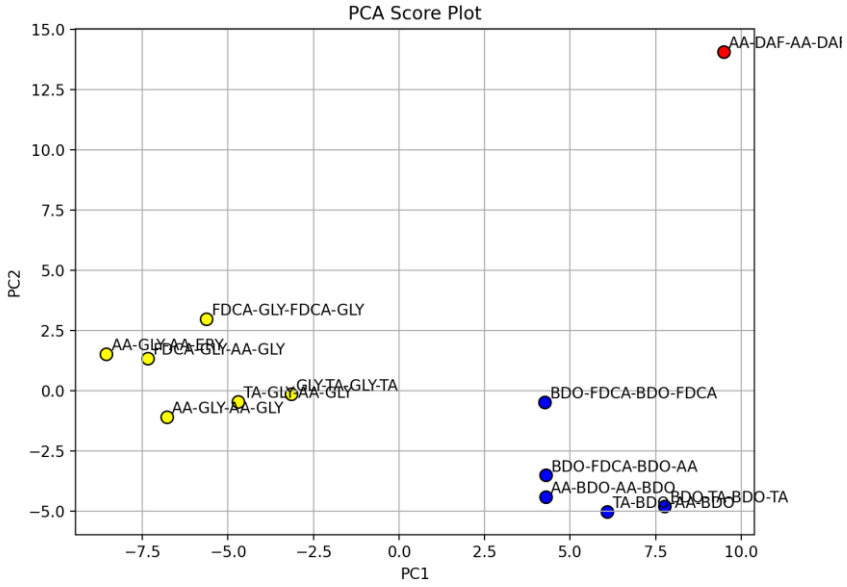

Figure 87 PCA score plots PC1 vs PC2, with objects coloured by the clustering.

The choice of a two-component model was based on the percentage of the X-matrix variance explained by each component: the first two components accounted for about 63% (38.9% for PC1 and 23.8% for PC2, whereas PC3 accounted for about 15.6%).

On the PCA scores, through the use of K-Means [129], a largely used clustering technique , we identified two clusters and one outlier, briefly described below. Red outlier: the only nitrogen-containing molecule; Yellow cluster: tetramers with several OH groups as common feature (most hydrophilic ones), with two molecules of the polyalcol GLY; the only tetramer with ERY is in this cluster, too. Blue cluster: tetramers with two molecules of BDO.

A further analysis involved a regression method, based only on a subset of variables, according to a feature selection analysis to investigate the impact of different groups of descriptors.Overall, only 18 molecular descriptors were selected. Out of these, 12 are variables derived from the GRID OH2 probe: four integy moments (IW1-IW4), which represent the unbalance between the centre of mass of a molecule and the barycenter of its hydrophilic regions (i.e. vectors pointing from the centre of mass to the centre of the hydrophilic regions), and eight capacity factors (CW1-CW8), which represent the ratio of hydrophilic volumes over the total molecular surface. Other selected variables are logP (the logarithm of the partition coefficient between *n*-octanol and water), the Polar Surface Area (PSA), calculated via the sum of polar region

contributions, and its counterpart hydrophobic (Hydrophobic Surface Area, HSA). Finally, three variables which were added in the new release of the software: MpKaA, which represents the most acidic pKa value, the “Attraction Energy Difference” (EMDIF), which reports the difference between the most polar and apolar interaction values, and the “Attraction Energy Distance” (EMDIS), which is the distance between atoms with most polar and apolar interactions.

The PLS (Partial Least Square analysis) [130] was used as regression method, with a dataset of 12 molecules because the outlier identified in the PCA was excluded from the analysis. Although the low number of objects, positive Q^2 values were obtained for dimensionality 4 and 5, and we finally selected a model with 5 latent variables, which yielded R^2=0.98 and Q^2=0.57. Scatterplots reporting the fitting obtained for biodegradation values are reported in Figure 88, with tetramers grouped in three groups by different degradation values.

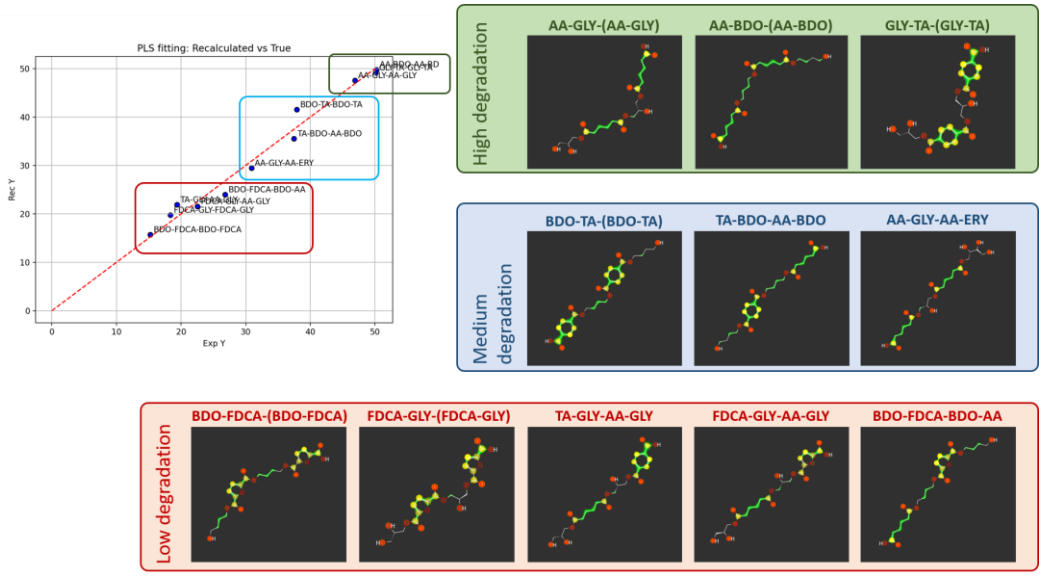

Figure 88 PLS fitting graph and the chemical structures of the oligoesters atoms are colored as follows: yellow = apolar atoms, red = polar atoms, green = hydrophobic atoms.

To identify the relationships between molecular features of the tetramer and polymers’ biodegradation, we report as Figure 89 the PLS coefficients, where positive values indicate a direct relationship with the extent of biodegradation, and negative values indicate a direct relationship with stability.

In brief, stability is related to higher polarity, as suggested by variables IW3 and IW4 which numerically describe hydrophilic volumes when they are very close to each other and CW8, which refers to strong hydrophilic interactions, compared to molecular surface. These hydrophilic regions might be easily associated to GLY (three out of the four more stable tetramers contain GLY: FDCA-GLY(-FDCA-GLY), FDCA-GLY-AA-GLY and TA-GLY-AA-GLY), but this is not enough without the effect of an aromatic diacid, which likely confers peculiar geometric configurations, hence stability.

Vice versa, apolar regions are important for polymers with higher degradation values, and all the most unstable polymers have aliphatic constituents such as BDO or AA; again, the presence of one of these does not guarantee good degradation, being BDO-FDCA the most stable polymer of the series. Interestingly, the descriptor

with higher impact is EMDIS, that is a measure of the distance between atoms with most polar and apolar interactions; its negative coefficient reflects an inverse relationship with degradation: more stable tetramers have larger distances between polar and apolar moieties, compared to tetramers more prone to degradation.

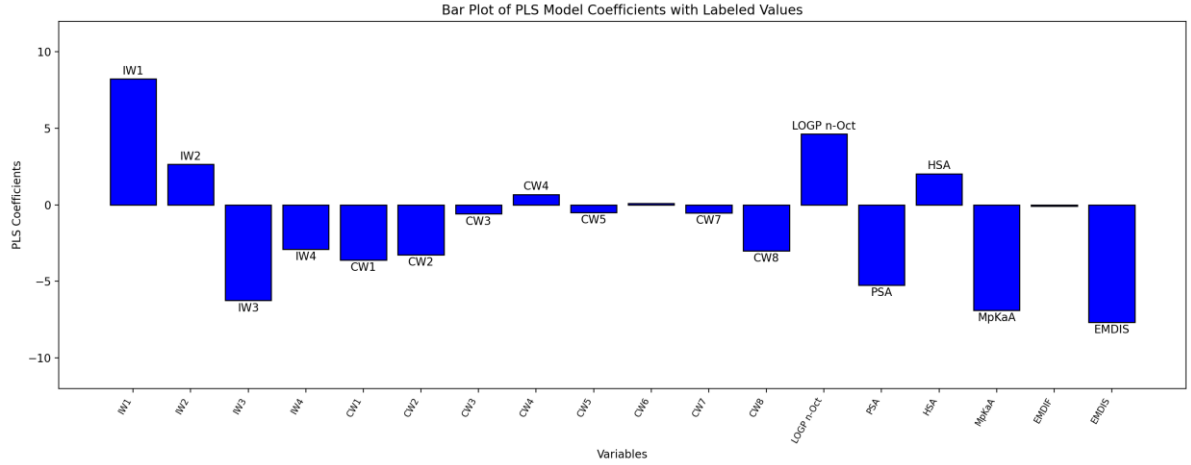

Figure 89 Plot of PLS model coefficients.

II.6.6. Ecotoxicity studies of model systems

This study concentrated on analyzing the ecotoxicity of model oligomers to understand how these molecules, or their biodegradation processes, influence various organisms, given the scant literature on ecotoxicity and biobased oligoesters. These organisms included: *Aliivibrio fischeri*, a bioluminescent marine bacterium utilized in both freshwater and marine water assays; *Phaeodactylum tricornutum*, a unicellular saltwater alga; *Paracentrotus lividus*, a sea urchin for marine ecosystems; *Raphidocelis subcapitata*, a unicellular alga; and *Daphnia magna*, a cladoceran crustacean for freshwater ecosystems. The response of a particular organism to a specific substance was observed by analyzing different endpoints such as the inhibition of natural bioluminescence emission (bacteria), the inhibition of the growth (algae), anomalies in larval development (sea urchin) and motility (crustaceans) as specified in the materials and methods chapter below. In this section, results are presented both as inhibition percentage (I%) or mean effects at the maximum concentration tested, and as EC (Effective Concentration).

The monomers constituting the oligoesters were also investigated. Previously reported studies, highlights how the hydrolysis of ester bonds during polyester degradation leads to the formation and accumulation of monomers, often not biodegraded as rapidly [98]. Therefore, it is crucial to verify the toxicity not only of the macromolecule itself but also of its derivatives after degradation.

Aliivibrio fischeri (Luminescent bacteria test)

The test was performed following the APAT CNR IRSA 8030 Man 29:2003 method with *Aliivibrio fischeri*, a marine bioluminescent bacterium used to test both freshwater and marine aquatic ecosystems. The assay was based on readings of the

natural bioluminescence emission at 490 nm with a luminometer. The test is based on calculating the percentage of the inhibition of bioluminescence (I%) over time (15, 30 minutes). Data are reported in Figure 90, where the comparison of the effect, I% values (SD= standard deviation, n= 2 replicates) are reported for 15 and 30 minutes, for various sample types, at the maximum concentration tested (100 mg/L).

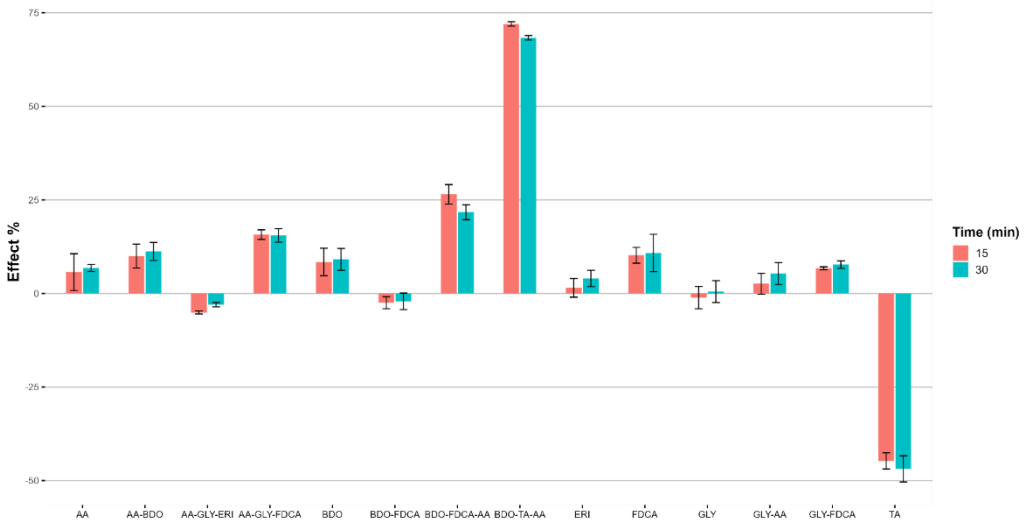

Figure 90 Ecotoxicological assessment of sample monomers and polymers using Aliivibrio fischeri bioluminescence inhibition assay. The graph represents the percentage inhibition (I%) of bacterial bioluminescence after exposure to different polymer samples at two time points (15' and 30'). Error bars denote the standard deviation from the mean of multiple measurements. The negative values indicate a stimulatory effect on the bacterial bioluminescence, whereas positive values suggest inhibitory effects.

Regarding the behavior of monomers, GLY and ERY exhibit no inhibition, whereas the monomer FDCA and BDO have the highest inhibition values of the series, with 10.8% and 9.1% after 30 minutes. Despite these findings, the EC20,50 values for all monomers exceed 100 mg/L demonstrating no toxicity. In the literature, GLY has been demonstrated to be non-toxic [131], whereas FDCA has been found to be toxic to *Aliivibrio fischeri* [132]. Comparing aromatic furan-based copolymers, it is observed that the oligoester (BDO-FDCA) has no effect on bioluminescent reduction while its glycerol-based counterpart (GLY-FDCA) had a low effect, the same is observed for AA-BDO and GLY-AA.

As for linear hydrophilic terpolymers (AA-GLY-ERY and AA-GLY-FDCA), the presence of the hydrophilic monomer ERY is observed to reduce the effect on the bacterium *Aliivibrio fischeri*. It is noted that among the aromatic polymers, BDO-TA-AA is the product with the greatest toxic effect (EC_{20} 40 mg/L after 30 min.) among those tested and is still more toxic than the furan-based terpolymer BDO-FDCA-AA.

Phaeodactylum tricornutum **(Marine algal growth inhibition test)**

The algal growth was monitored through spectrophotometer analysis following the UNI EN ISO 10253:2017 method. The variation in absorbance of light at 690 nm after 72 hours of exposure to the substance of interest was used as proxy of the algal

growth using a function of correlation between the absorbance and the cell density of an algal culture. The difference of absorption recorded at the beginning (T_0) and at the end (T_{72}) of the exposure allowed for the calculation of the inhibition of the algal growth. Data are graphically reported in Figure 91; recorded data are expressed as percentage of inhibition (I%, SD= standard deviation, n=3 replicates) at the maximum concentration tested (100 mg/L).

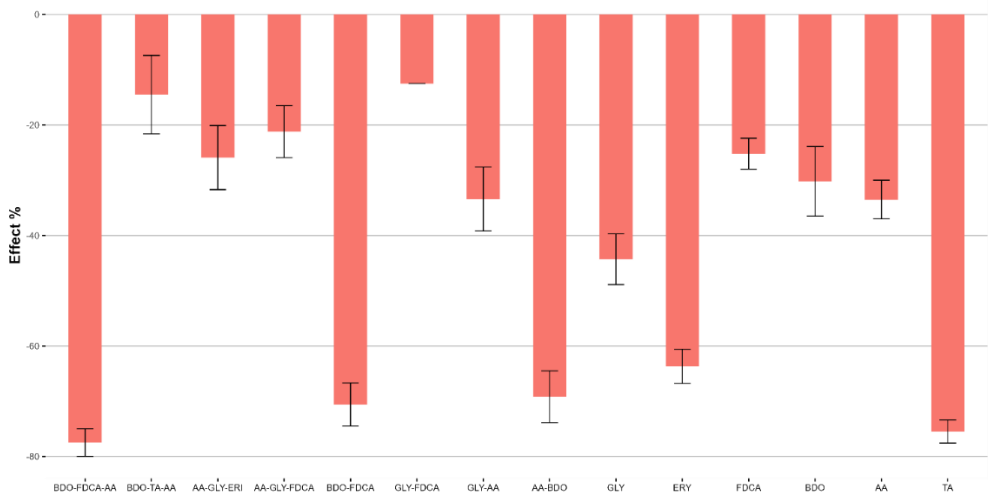

Figure 91 Ecotoxicity assessment of different polymers using Phaeodactylum tricornutum growth inhibition assay. The graph shows the percentage inhibition of light absorbance after 72 hours of exposure to different samples. Values represent the % effect with error bars indicating the standard deviation (SD) based on three replicates. Higher percentage inhibition indicates greater toxicity.

It is observed that all products do not yield inhibition values; instead, biostimulation was recorded. Therefore, algae seem not to be affected by toxic effects.

Paracentrotus lividus **(Embriotoxicity test)**

The test allows defining embryotoxicity, i.e., toxicity on embryos following the EPA/600/R-95-136/Sezione 15 +ISPRA Quaderni Ricerca Marina 11/2017 method. The test is carried out through visual observation over a 72-hour exposure period, measuring the percentage of malformed embryos normalized compared to the negative control. In Figure 92, the respective observed data are reported as measured mean, standard deviation (SD, n=3 replicates), and Abbott's adjusted mean related to the effect measured in negative controls at the maximum concentration tested (100 mg/L).

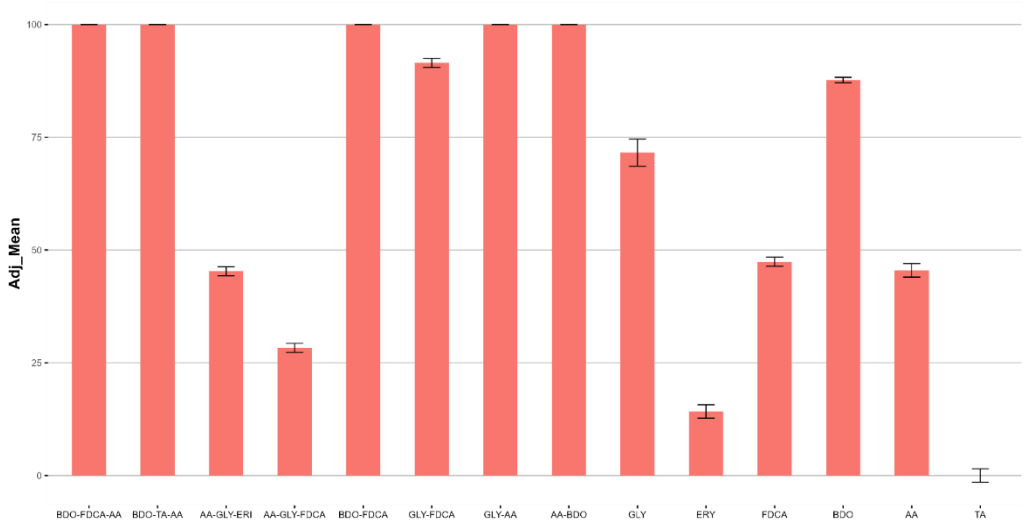

Figure 92 Ecotoxicity assessment of different polymers using Paracentrotus lividus embryo abnormality assay. The graph shows the mean percentage of abnormal Paracentrotus lividus embryos after 72 hours of exposure to different polymer samples, with error bars representing the standard deviation (SD) based on three replicates. The adj_mean values indicate the Abbott's adjusted mean percentage of abnormalities relative to the negative control at the maximum tested concentration (100 mg/L). Higher adj_mean values indicate greater toxicity.

All tested products elicit a moderate to high effect. ERY, AA, FDCA monomer and the terpolymers AA-GLY-FDCA, AA-GLY-ERY values are recorded below or equal to 50%.

The ECx values for *Paracentrotus lividus* (Table 40), reveal a diverse range of toxicities among the tested compounds. Notably, BDO-TA-AA and GLY-FDCA exhibited higher toxicities with EC_{50} values of 64.46 mg/L and 66.6 mg/L, respectively. In contrast, compounds like AA-GLY-ERY, AA-GLY-FDCA, Erythritol, FDCA, GLY and BDO showed significantly lower toxicity, indicated by their EC_{50} values exceeding 100 mg/L. Other samples, including BDO-FDCA-AA, BDO-FDCA, PD13, AA-BDO, and AA, displayed a range of EC_{50} values from 74.02 mg/L to 92.9 mg/L, suggesting moderate toxicity under the assay conditions.

Table 40 EC20 and EC50 values from the ecotoxicity tests by using marine organisms (data are expressed as mg/L).

	Aliivibrio fischeri		***Phaeodactylum tricornutum***		***Paracentrotus lividus***	
Samples	**EC_{50}**	**EC_{20}**	**EC_{50}**	**EC_{20}**	**EC_{50}**	**EC_{20}**
BDO-FDCA-AA	>100	95 (15 min); 98 (30 min)	>100	>100	74.0	46.3
BDO-TA-AA	71 (15 min); 75 (30 min)	32 (15 min); 40 (30 min)	>100	>100	64.5	26.4
AA-GLY-ERY	>100	>100	>100	>100	>100	82.7
AA-GLY-FDCA	>100	>100	>100	>100	>100	>100
BDO-FDCA	>100	>100	>100	>100	66.6	32.3
GLY-FDCA	>100	>100	>100	>100	74.3	35.3

GLY-AA	>100	>100	>100	>100	87.3	73.4
AA-BDO	>100	>100	>100	>100	87.3	73.4
GLY	>100	>100	>100	>100	100.0	83.0
ERY	>100	>100	>100	>100	>100	>100
FDCA	>100	>100	>100	>100	>100	95.9
BDO	>100	>100	>100	>100	92.9	78.2
AA	>100	>100	>100	>100	>100	90.9
TA	>100	>100	>100	>100	>100	>100

Daphnia magna (Mobility test)

The reading was conducted during exposure of the organisms to substances for a period of exposure of 24-48 h following the method UNI EN ISO 6341:2013. Figure 93 and presents the corresponding data obtained as mean immobilization value and standard deviation (SD, n=3 replicates) at the maximum concentration tested (100 mg/L).

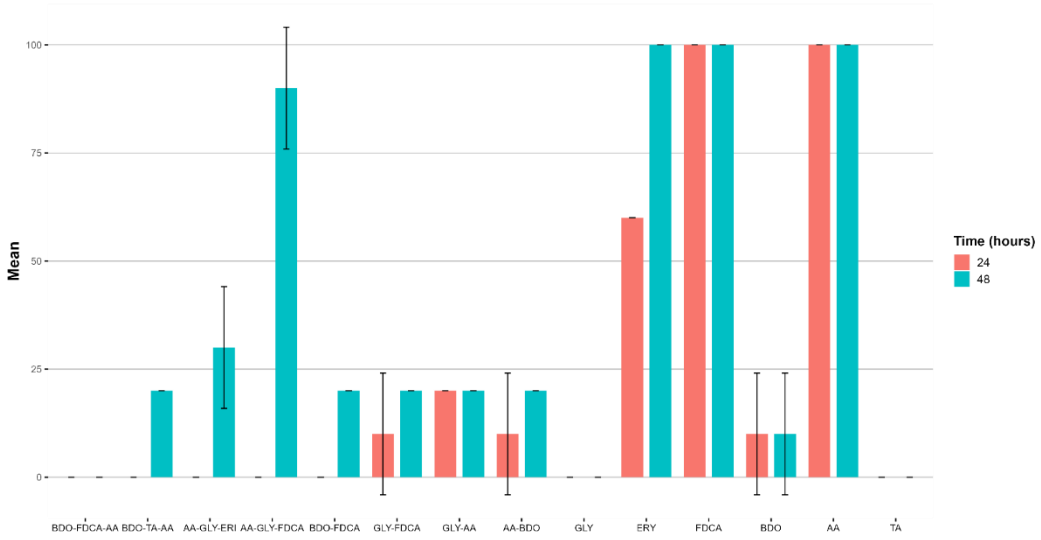

Figure 93 Ecotoxicological assessment of various polymers using the Daphnia magna immobility test. The graph displays the number of immobilized organisms per treatment group after 24 and 48 hours of exposure to different polymer samples. Error bars represent the standard deviation from the mean of multiple measurements. Higher mean values (%) indicate greater toxicity.

The monomers ERY, FDCA, and AA induce a drastic toxic effect on the cladoceran population. The European Chemicals Agency (ECHA) portal [133] reports that the EC_{50} values for *Daphnia magna* for these three monomers do not indicate toxicity. This finding presents a significant bibliographic inconsistency regarding the actual toxicity levels of these monomers (Table 41).

Most of the copolymers and terpolymers do not cause a consistent decrease in motility in *D. magna* after 24 hours. However, after 48 hours, initial effects begin to be observed, all of which are moderate, except for the terpolymer AA-GLY-FDCA, which causes a high mortality on *Daphnia magna*.

***Raphidocelis subcapitata* (Freshwater algal growth inhibition test)**

The algal growth after 72 hours of exposure was monitored using spectrophotometric analysis as previously reported for the marine species following the method UNI EN ISO 8692:2012. Recorded data are shown in Figure 94 as percentage of inhibition after 72 hours of exposure and standard deviation (SD, n=3 replicates) at the maximum concentration tested (100 mg/L).

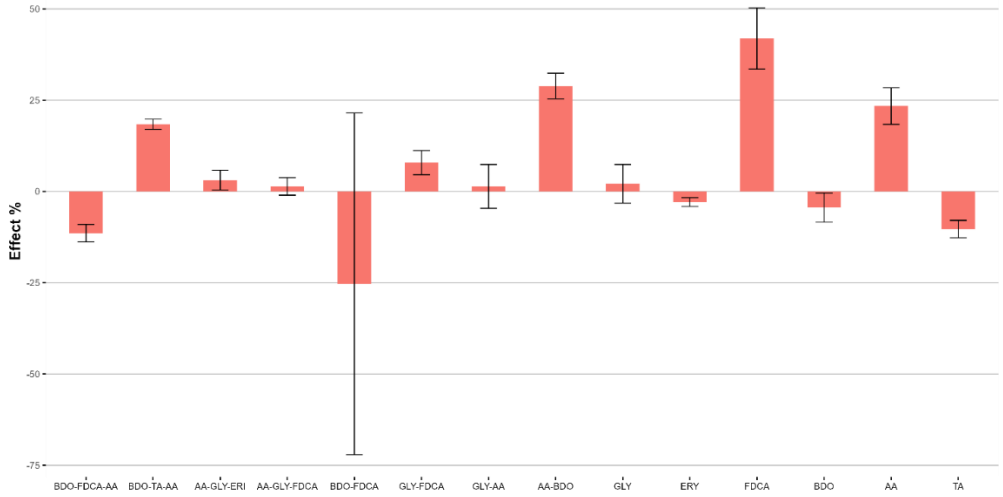

Figure 94 Ecotoxicity assessment of different polymers using Raphidocelis subcapitata growth inhibition assay. The graph shows the percentage inhibition of light absorbance after 72 hours of exposure to different samples. Values represent the % effect with error bars indicating the standard deviation (SD) based on three replicates. Higher percentage inhibition indicates greater toxicity.

Contrary to what observed earlier for the marine algae Table 41, the FDCA monomer exhibits a growth inhibition percentage of almost 42% and an EC_{20} of 53 mg/L, different values compared to what was stated by ECHA (100 mg/L).

For the oligomers BDO-FDCA and BDO-FDCA-AA, enhancing growth values are recorded, indicating that the toxicity of FDCA is expressed only when released in the form of a monomer.

Table 41 Values of EC_{20} and EC_{50} (mg/L) for the two types of freshwater organisms studied.

Sample	*Daphnia magna*		*Raphidocelis subcapitata*	
	EC_{50}	EC_{20}	EC_{50}	EC_{20}
BDO-FDCA-AA	>100	>100	>100	>100
BDO-TA-AA	>100	100 (48 h)	>100	>100
AA-GLY-ERY	>100	40.9 (48 h)	>100	>100
AA-GLY-FDCA	56.5 (48 h)	27.9 (48 h)	>100	>100
BDO-FDCA	>100	100 (48 h)	>100	>100
GLY-FDCA	>100	100 (48 h)	>100	>100
GLY-AA	>100	100 (24 - 48 h)	>100	>100
AA-BDO	>100	100 (48 h)	>100	95.6
GLY	>100	>100	>100	>100
ERY	72.7 (24 h)	<100	>100	>100
FDCA	>100	<100	>100	53.0
BDO	>100	>100	>100	>100

AA	32.5 (48 h)	17.9 (48 h)	>100	97.3
TA	>100	>100	>100	>100

It is essential to consider that the tests allow constructing a scale of relative toxicity. The values obtained must be necessarily considered and discussed in light of what could be a real natural environmental concentration to which the organism is effectively exposed.

II.7. General remarks

The scientific achievements included in the thesis address several interdependent aspects of modern biocatalysis that have direct implications for green chemistry, materials science, and sustainable process development. These aspects include enzyme stabilization through immobilization, using green and reactive solvents (especially deep eutectic solvents, or DESs), enzymatic synthesis of bio-based oligoesters, and the subsequent environmental fate of these compounds. Together, these topics form a coherent research focus on designing cleaner, safer, and more efficient chemical processes that align with the principles of the circular bioeconomy.

A central focus of this chapter is developing and optimizing enzyme immobilization techniques, particularly for lipases, a versatile class of enzymes used in hydrolytic and synthetic reactions. The thesis thoroughly compares several immobilization strategies, including physical adsorption, covalent binding, and entrapment in sol–gel matrices, and experimentally validates their effects on enzyme activity, selectivity, thermal stability, and operational reusability. The author demonstrates how immobilization can be employed to tailor biocatalysts for specific reaction systems, media, and substrates, beyond its well-known role in enabling enzyme recycling.

Importantly, this study does not treat immobilization as an isolated methodological element, but rather as a functional design strategy integrated into complex biocatalytic processes. Immobilized enzymes are used to synthesize bio-based oligoesters from renewable monomers, such as glycerol, xylitol, and fatty acids.

This highlights their potential as a sustainable alternative to petroleum-based polymers. The author’s approach reflects an understanding of enzyme-support interactions and their influence on catalysis in practical settings, such as packed-bed flow reactors. This illustrates an advanced level of process engineering, in which immobilization contributes to not only enzyme stability, but also reactor design, productivity, and scalability.

Another innovative aspect of the chapter is the use of deep eutectic solvents (DESs) as reactive components (R-NADESs) in enzymatic esterification as alternative green solvents. This dual role as both medium and reactant adds a high level of sophistication to solvent system design. The author addresses important aspects regarding the effect of DES composition (e.g., choline chloride/glycerol and choline chloride/arabitol) on enzyme activity and stability while considering factors such as water content, viscosity, and hydrogen-bond network structure. The author's

distinction between NADESs used as co-solvents and R-NADESs used as reaction substrates is especially commendable, as is the critical discussion of the limitations of generalizing enzyme performance across different types of DES.

Regarding application, the enzymatic synthesis of oligoesters is presented with a clear focus on structural control, monomer selection, and process sustainability. The author demonstrates how enzyme-mediated polycondensation in green solvents or under solvent-free conditions can form functionalized polyesters with tunable properties. These materials are positioned as candidates for various green applications, including cosmetics, biodegradable packaging, and controlled-release formulations. The synthetic strategies align with green metrics, such as atom economy, energy efficiency, and the reduction of hazardous reagents, which reinforces the thesis's commitment to sustainability.

The final section of the chapter focuses on the environmental evaluation of the synthesized materials, particularly their biodegradability in water systems. The degradation behaviour is systematically correlated with polymer composition, particularly the degree of branching, the hydrophilic/hydrophobic balance, and crystallinity. The author illustrates how subtle changes in monomer structure (e.g., the use of more hydrophobic diols or polyols) can dramatically affect degradation rates and mechanisms. This insight into the relationship between structure and degradability is essential for guiding the molecular design of future generations of environmentally friendly polymers.

The integration of eco-design principles and safe-and-sustainable-by-design concepts is of particular importance. This research demonstrates biodegradation under realistic conditions and incorporates early-stage ecotoxicity screening and risk-benefit considerations. These efforts align with European regulatory frameworks and funding priorities that emphasize the need for inherently safe, circular materials from the design phase onward.

III. Development plan of scientific, academic and professional career

III.1. Strategic scientific and academic cooperation

One of the candidate's central goals for her future academic pathway is to actively pursue international scientific collaborations, recognising that interdisciplinary and transnational partnerships are essential for solving complex global challenges in chemical and biochemical engineering. Collaborating with prestigious universities and research institutions abroad will facilitate joint research projects, student and staff exchanges, as well as coordinated funding applications. Such partnerships will amplify the influence of the candidate's current research in the fields of enzyme engineering, green chemistry, biocatalytic synthesis, and development of new biodegradable materials.

Over the next few years, the candidate intends to collaborate with research groups in Western and Central Europe on projects focusing on enzyme cascade systems, biobased polymers and sustainable process engineering. Through these collaborations, they seek to expand access to resources such as high-throughput experimentation tools and bioreactors, as well as to co-publish findings in high-impact journals and co-organise international symposia. Participation in long-term academic consortia will facilitate the transfer of knowledge across borders, support early-career researchers, and enhance the research reputation of the home institution.

Formal agreements such as Memorandums of Understanding (MOUs) and Erasmus+ bilateral contracts will facilitate this strategic engagement. Another key objective is the co-supervision of PhD students in joint degree frameworks, which would promote research diversity, cultural exchange and higher impact through interdisciplinary training. Ultimately, the candidate aims to become a key academic connector between institutions and disciplines.

III.2. Leadership in research projects and competitive funding

Securing competitive research funding is crucial for sustaining and expanding the candidate's scientific output. The career development plan involves active participation as a principal investigator or work package leader in national and European research consortia. Building upon her previous experience with grant proposals, the candidate will lead ambitious research initiatives that align with the priorities of Horizon Europe framework program, national science foundations and other international programmes that support green chemistry, the bioeconomy and sustainability.

Beyond writing and coordinating grant proposals, the candidate will support junior colleagues in developing their own skills, thereby fostering a collaborative and resilient research culture within the department. There will be a particular focus on innovative project ideas centred on enzyme design, hybrid biocatalytic systems, and utilisation of waste biomass in circular bioeconomy models. The goal is to establish a

continuous funding stream that supports PhD students, postdoctoral researchers, and international cooperation.

Projects will have a strong translational element, showing how fundamental enzymology and polymer chemistry research can be applied to industries such as food packaging, pharmaceuticals, and bioremediation. The candidate will also liaise with companies to explore co-funding mechanisms and industrial PhD schemes, further bridging the gap between basic science and applied research.

III.3. Networking, scientific visibility, and conference leadership

The candidate recognises that active engagement in scientific networks and visibility at academic events are essential for a sustainable academic career. Therefore, an important aim is to strengthen her participation in scientific conferences, not only as a speaker, but also by joining scientific committees, organising thematic sessions and chairing discussions. Key conferences such as The International Symposium on Biocatalysis and Biotransformations (Biotrans), The International Congress on Biocatalysis (Biocat), The EFB Congress, and The Green & Sustainable Chemistry Conference will provide valuable exposure and a platform for disseminating research.

Furthermore, the candidate intends to co-organise conferences and specialised workshops at national and international levels focusing on enzyme cascades, biocatalysis in unconventional media and biodegradable polymer applications. This will attract renowned researchers to the home institution and strengthen local research initiatives.

The candidate also intends to become part of editorial boards and act as a peer reviewer for top-tier journals, thereby reinforcing her role in the academic quality control process. These activities will help to shape research directions and keep the candidate informed of the latest advancements in the targeted fields.

III.4. Engagement in professional and academic organizations

The candidate’s development strategy involves active participation in international professional associations such as the European Federation of Biotechnology (EFB), European Society of Applied Biocatalysis (ESAB), and American Chemical Society (ACS), as well as relevant working groups within national chemistry and chemical engineering societies (Romanian Chemical Society, Romanian Catalysis Society). Membership of these organisations facilitates collaboration, advocacy and knowledge sharing.

Participation in specialised interest groups will enable the candidate to engage in dialogue around emerging trends in green and sustainable chemistry, educational reform, and industrial transitions to bio-based technologies. Furthermore, she intends to contribute to policy-shaping documents, white papers and position statements related to biocatalysis and sustainable chemistry, thereby influencing the scientific and technological agenda in Europe and beyond.

Engaging with these organisations also involves participating in event organisation, judging student competitions, and mentoring young researchers. These activities will help to build a strong academic network and support the development of the next generation of chemical engineers.

III.5. Research directions within the Biocatalysis and Green Chemistry Group

The core of the candidate's scientific work lies within the Biocatalysis and Green Chemistry Group. Future research will expand upon existing topics, incorporating new methods and broader objectives. The computational modelling of enzyme systems will remain a central focus in order to enhance the predictive power of enzyme-substrate interactions, stability and product specificity. Advanced modelling techniques, including molecular docking and dynamics simulations, will be employed to design novel biocatalysts with improved properties.

Based on a recent patent co-authored by the candidate, special attention will be paid to the enzymatic valorisation of vegetable oils for polyester synthesis. This work will involve optimising the enzymatic toolkit to customise the properties of biopolymers for specific applications, such as medical devices, food packaging and controlled drug delivery systems. The mechanical, thermal and barrier properties of these novel biopolymers will be studied to enable them to be used as sustainable alternatives to petrochemical-based plastics.

Another key area of research involves multi-enzyme cascade reactions, which are highly efficient and environmentally beneficial due to their similarity to metabolic pathways. The candidate will develop free and immobilized cascade systems to enhance substrate channelling, product yields and operational stability. This line of work is well aligned with industrial goals for eco-efficient and cost-effective production systems.

Priority will also be given to the development of bio-based, biodegradable polymers through chemical and enzymatic synthesis. Using renewable feedstocks, such as plant-derived monomers and microbial polysaccharides, will support a low-carbon footprint and the use of circular materials. These materials will be adapted for use in a range of applications, from agriculture to biomedical engineering.

Finally, efforts will be expanded to explore enzyme immobilization techniques that enhance biocatalyst stability under industrial conditions, including high temperatures, organic solvents and extreme pH values. The stabilised enzymes will then be incorporated into continuous-flow reactors and biosensors to contribute to process intensification in green manufacturing.

III. 6. Professional development and research dissemination

To remain at the forefront of research management, communication, and leadership, the candidate will pursue ongoing professional development. To support this goal, attendance at specialised workshops and training sessions focusing on grant writing, academic leadership, and innovation management will be accomplished.

Courses on science communication will also be undertaken to enhance public engagement and the impact of scientific dissemination.

Publication in high-impact journals such as Green Chemistry, Applied Catalysis B: Environmental, and Biotechnology Advances, will be also a main scientific objective. The candidate will prioritise open-access venues to maximise the visibility and accessibility of research outputs. Research findings will be presented at international symposia, workshops and university seminars to foster collaborative ties and establish a consistent academic presence.

Alongside individual dissemination efforts, the candidate will mentor junior researchers in preparing abstracts, papers and presentations, thereby embedding scientific communication within the group's research culture. By encouraging students to publish and present their work, the candidate will foster a productive and self-sustaining academic environment.

III.7. Enhancement of teaching methodology and curriculum innovation

The candidate is committed to improving her teaching methodology, primarily by developing modern, engaging courses that closely align with industry demands. Future activities will focus on integrating student-centred learning strategies, such as flipped classrooms, collaborative projects, and inquiry-based problem-solving approaches.

New course content will support emerging areas of study such as green chemistry, biochemical engineering and sustainable biopolymer science. These courses will feature practical case studies, real-world problems and data-driven decision-making scenarios that mirror the challenges encountered by chemical engineers in their professional lives.

To further engage students, the candidate will make greater use of digital educational platforms to enable blended and hybrid teaching formats. Tools such as virtual laboratories, interactive simulations, and peer-reviewed digital assignments will help students to grasp complex concepts more effectively. Furthermore, online learning modules will enhance accessibility and inclusivity for a more diverse student population.

The candidate will also lead efforts to revise and update laboratory manuals, ensuring that experiments reflect current industrial and research practices. This will better prepare students to transition from academia to professional settings with confidence and owning the relevant skills.

III.8. Student involvement, mentorship, and outreach

The active involvement of students in research and outreach is an essential component of the candidate’s academic vision. Undergraduate and postgraduate students will be integrated into research projects from an early stage in their academic careers, with roles adapted to their level of experience. This hands-on experience of

experimental design, data collection and result interpretation will foster scientific curiosity and build essential skills.

The candidate will establish a structured mentorship programme to guide BSc, MSc and PhD students through their academic pathways. This will include academic planning, career development sessions and enhancement of soft skills, such as scientific writing, public speaking and teamwork. The overarching aim is to cultivate independent researchers who are well prepared for careers in academia or industry.

Additionally, the candidate will organise study visits and excursions to industrial partners such as bioplastics producers, biorefineries and environmental technology companies. These visits will bridge the gap between theory and practice and introduce students to potential future career opportunities.

The candidate will also prioritise outreach to high schools and science fairs to promote STEM disciplines and raise awareness of biocatalysis and the bioeconomy. Through hands-on demonstrations, public talks and science competitions, the candidate will inspire the next generation of engineers and scientists.

III.9. Development of research and teaching Infrastructure

Maintaining and expanding the infrastructure of laboratories and educational facilities is essential for sustaining high-quality research and teaching activities. The candidate intends to play an active role in infrastructure development projects within the department and through institutional initiatives to ensure the research environment meets current and future requirements.

In terms of research, the candidate will work to acquire state-of-the-art equipment for biocatalytic reactions, enzyme immobilization and kinetics studies, polymer characterisation and computational modelling, all of which are vital for current and planned research. Collaborating with technical staff will be essential to optimise the use and maintenance of these instruments. Furthermore, improvements to laboratory safety, sustainability and accessibility will be pursued to align with best practices in research management.

In terms of teaching, the candidate is committed to improving student laboratory experiences by updating protocols, incorporating modern instrumentation into practical courses and integrating data analysis tools into lab-based learning. These efforts aim to provide students with real-world experience that mirrors the challenges and tools they will encounter in industrial or academic careers.

In parallel with scientific projects, grant applications targeting high-value infrastructure investment will be pursued, e.g., through national development programmes or EU structural funds. This dual strategy will ensure that the teaching and research environments develop in harmony, remaining competitive in their ability to attract students, staff and collaborators.

III.10. Active participation in institutional and community activities

The candidate recognises the importance of being an active member of the academic and wider community. In addition to their research and teaching commitments, they will contribute to university life by participating in faculty committees, curriculum boards and interdisciplinary working groups that influence the direction of education and research.

A key focus will be the internationalisation of the university, including attracting foreign students and staff, and contributing to the development of English-language programmes within the Department of Chemical Engineering. They will also contribute to quality assurance and accreditation processes, drawing on their experience of curriculum design and outcome-based education. Developing a multicultural environment within the faculty will help students with different backgrounds and needs to succeed, encouraging acceptance and inclusion in an exponentially diverse world.

Outside of the university, the candidate will engage in public science communication to promote science literacy and demonstrate the importance of biocatalysis and green chemistry in sustainable development. Outreach initiatives will include organising science cafés, contributing to science communication campaigns and publishing articles in popular science outlets. These initiatives aim to foster public trust in science and encourage young people to pursue scientific careers.

Additionally, the candidate intends to undertake research internships or visiting scholar roles at leading institutions in Europe and worldwide. These experiences will facilitate knowledge transfer and allow benchmarking against leading research systems, while also bringing fresh perspectives to local academic practices. They also represent a valuable opportunity to extend the influence and visibility of the home institution internationally.

III.11. Conclusion: vision for future academic leadership

The career development objectives set out in this Habilitation Thesis represent a comprehensive and strategic approach to achieve academic excellence, innovation and leadership in the field of chemical engineering. By combining scientific ambition, pedagogical dedication and institutional engagement, the candidate envisages a future in which research in biocatalysis and sustainable biomaterials can make a significant contribution to solving societal and environmental challenges.

The focus on enzyme systems, biopolymers, and green chemistry processes is timely and forward-looking, and is situated within the broader context of the circular economy, resource efficiency, and clean technologies. Reinforced by international collaborations and interdisciplinary work, these research efforts will elevate the quality and relevance of scientific outputs, supporting innovation across multiple sectors.

At the same time, the candidate will remain deeply engaged in teaching and mentoring, ensuring that educational strategies evolve alongside emerging technologies and student expectations. Through curriculum development,

infrastructure enhancement and student-centred teaching, the candidate will prepare future engineers and scientists to solve problems in a rapidly changing world.

The candidate's commitment to community engagement, international visibility and professional development highlights a personal vision for inclusive, collaborative and impactful academic leadership. By engaging in continuous learning and serving the scientific and academic community, the candidate will contribute to a dynamic and sustainable future of her institution and of the field of chemical engineering as a whole.

IV. References

[1] A. S. Campbell, C. Dong, N. Wu, J. S. Dordick, and C. Z. Dinu, “Enzyme-based technologies: Perspectives and opportunities,” *ACS Symp. Ser.*, vol. 1144, pp. 15–27, 2013, doi: 10.1021/bk-2013-1144.ch002.

[2] A. Fryszkowska and P. N. Devine, “Biocatalysis in drug discovery and development,” *Curr. Opin. Chem. Biol.*, vol. 55, pp. 151–160, 2020, doi: 10.1016/j.cbpa.2020.01.012.

[3] V. Kumar *et al.*, “Recent advances in bio-based production of top platform chemical, succinic acid: an alternative to conventional chemistry,” *Biotechnol. Biofuels Bioprod.*, vol. 17, no. 1, pp. 1–39, 2024, doi: 10.1186/s13068-024-02508-2.

[4] A. V. Vasileiou, S. T. Korfia, M. Sarigiannidou, and D. Maniar, “Macromolecular design for biobased polymers,” *Polymer (Guildf).*, vol. 312, no. September, p. 127652, 2024, doi: 10.1016/j.polymer.2024.127652.

[5] A. Todea, D. M. Dreava, I. C. Benea, I. Bîtcan, F. Peter, and C. G. Boeriu, “Achievements and trends in biocatalytic synthesis of specialty polymers from biomass-derived monomers using lipases,” *Processes*, vol. 9, no. 4, pp. 1–26, 2021, doi: 10.3390/pr9040646.

[6] I. Roy and M. N. Gupta, “White & grey biotechnologies for shaping a sustainable future,” *RSC Sustain.*, vol. 66, pp. 1722–1736, 2023, doi: 10.1039/d3su00174a.

[7] P. Lozano and E. García-verdugo, “From green to circular chemistry paved by biocatalysis,” *Green Chem.*, no. 25, pp. 7041–7057, 2023, doi: 10.1039/d3gc01878d.

[8] R. A. Sheldon and J. M. Woodley, “Role of Biocatalysis in Sustainable Chemistry,” *Chem. Rev.*, vol. 118, no. 2, pp. 801–838, 2018, doi: 10.1021/acs.chemrev.7b00203.

[9] S. Wu, R. Snajdrova, J. C. Moore, K. Baldenius, and U. T. Bornscheuer, “Biocatalysis: Enzymatic Synthesis for Industrial Applications,” *Angew. Chemie - Int. Ed.*, vol. 60, no. 1, pp. 88–119, 2021, doi: 10.1002/anie.202006648.

[10] R. Wohlgemuth, “Biocatalysis-key to sustainable industrial chemistry,” *Curr. Opin. Biotechnol.*, vol. 21, no. 6, pp. 713–724, 2010, doi: 10.1016/j.copbio.2010.09.016.

[11] E. L. Bell *et al.*, “Biocatalysis,” *Nat. Rev.*, vol. 0123456789, pp. 1–21, 2021, doi: 10.1038/s43586-021-00044-z.

[12] M. D. Truppo, “Biocatalysis in the Pharmaceutical Industry : The Need for Speed,” 2017, doi: 10.1021/acsmedchemlett.7b00114.

[13] X. Wang, T. Saba, H. H. P. Yiu, R. F. Howe, and J. A. Anderson, “Cofactor NAD(P)H Regeneration Inspired by Heterogeneous Pathways,” *CHEMPR*, vol. 2, no. 5, pp. 621–654, 2017, doi: 10.1016/j.chempr.2017.04.009.

[14] F. H. Arnold, “Design by Directed Evolution Some Directed Evolution Experiments :,” *Acc. Chem. Res*, vol. 31, no. 3, pp. 125–131, 1998.

[15] K. Chen and F. H. Arnold, “Engineering new catalytic activities in enzymes,” *Nat. Catal.*, vol. 1, no. 46, 2020, doi: 10.1038/s41929-019-0385-5.

[16] R. A. Sheldon, I. Arends, and U. Hanefeld, *Green Chemistry and Catalysis*. Wiley-VCH Verlag GmbH & Co. KGaA, 2007.

[17] R. A. Sheldon and R. A. Sheldon, “The E factor at 30: a passion for pollution prevention,” *Green Chem.*, vol. 25, no. 5, 2023, doi: 10.1039/d2gc04747k.

[18] K. Srirangan, V. Orr, L. Akawi, A. Westbrook, M. Moo-young, and C. P. Chou, “Biotechnological advances on Penicillin G acylase : Pharmaceutical implications , unique expression mechanism and production strategies,”

Biotechnol. Adv., vol. 31, no. 8, 2013, doi: 10.1016/j.biotechadv.2013.05.006.
[19] R. A. Sheldon and D. Brady, “Broadening the Scope of Biocatalysis in Sustainable Organic Synthesis,” *ChemSusChem*, vol. 12, pp. 1–24, 2019, doi: 10.1002/cssc.201900351.
[20] D. J. Pollard and J. M. Woodley, “Biocatalysis for pharmaceutical intermediates : the future is now,” *Trends Biotechnol.*, vol. 25, no. 2, 2010, doi: 10.1016/j.tibtech.2006.12.005.
[21] R. A. Sheldon, D. Brady, and M. L. Bode, “Chemical Science The Hitchhiker ’ s guide to biocatalysis: recent advances in the use of enzymes in organic synthesis,” *Chem. Sci.*, no. 11, pp. 2587–2605, 2020, doi: 10.1039/c9sc05746c.
[22] U. T. Bornscheuer, G. W. Huisman, R. J. Kazlauskas, S. Lutz, J. C. Moore, and K. Robins, “Engineering the third wave of biocatalysis,” *Nature*, vol. 485, no. 7397, pp. 185–194, 2012, doi: 10.1038/nature11117.
[23] B. Hauer, “Embracing Nature ’ s Catalysts: A Viewpoint on the Future of Biocatalysis,” *ACS Catal.*, vol. 10, no. 15, 2020, doi: 10.1021/acscatal.0c01708.
[24] R. A. Sheldon and R. A. Sheldon, “Biocatalysis and biomass conversion: enabling a circular economy,” *Phil.Trans.R.Soc.A*, vol. 378, 2020.
[25] P. Domínguez de María, “Biocatalysis, sustainability, and industrial applications: Show me the metrics,” *Curr. Opin. Green Sustain. Chem.*, vol. 31, p. 100514, 2021, doi: 10.1016/j.cogsc.2021.100514.
[26] E. P. Cipolatti *et al.*, “Current status and trends in enzymatic nanoimmobilization,” *J. Mol. Catal. B Enzym.*, vol. 99, pp. 56–67, 2014, doi: 10.1016/j.molcatb.2013.10.019.
[27] A. S. Bommarius and M. F. Paye, “Stabilizing biocatalysts.,” *Chem. Soc. Rev.*, vol. 42, pp. 6534–65, 2013, doi: 10.1039/c3cs60137d.
[28] S. Cantone *et al.*, “Efficient immobilisation of industrial biocatalysts: criteria and constraints for the selection of organic polymeric carriers and immobilisation methods.,” *Chem. Soc. Rev.*, vol. 42, pp. 6262–76, 2013, doi: 10.1039/c3cs35464d.
[29] A. Todea, A. Hiseni, L. G. Otten, I. W. C. E. Arends, F. Peter, and C. G. Boeriu, “Increase of stability of oleate hydratase by appropriate immobilization technique and conditions,” *"Journal Mol. Catal. B, Enzym.*, vol. 119, pp. 40–47, 2015, doi: 10.1016/j.molcatb.2015.05.012.
[30] E. Biró, D. Budugan, A. Todea, F. Péter, S. Klébert, and T. Feczkó, “Recyclable solid-phase biocatalyst with improved stability by sol-gel entrapment of β-d-galactosidase,” *J. Mol. Catal. B Enzym.*, vol. 123, pp. 81–90, 2016, doi: 10.1016/j.molcatb.2015.11.006.
[31] R. A. Sheldon, “Enzyme Immobilization : The Quest for Optimum Performance,” 2007, doi: 10.1002/adsc.200700082.
[32] D. Brady and J. Jordaan, “Advances in enzyme immobilisation,” *Biotechnol. Lett.*, vol. 31, pp. 1639–1650, 2009, doi: 10.1007/s10529-009-0076-4.
[33] A. Todea, P. Borza, A. Cimporescu, C. Paul, and F. Peter, “Continuous kinetic resolution of aliphatic and aromatic secondary alcohols by sol-gel entrapped lipases in packed bed bioreactors,” *Catal. Today*, vol. 306, pp. 223–232, 2018, doi: 10.1016/j.cattod.2017.02.042.
[34] A. Cimporescu, A. Todea, V. Badea, C. Paul, and F. Peter, “Efficient kinetic resolution of 1,5-dihydroxy-1,2,3,4-tetrahydronaphthalene catalyzed by immobilized Burkholderia cepacia lipase in batch and continuous-flow system,” *Process Biochem.*, vol. 51, no. 12, pp. 2076–2083, 2016, doi: 10.1016/j.procbio.2016.09.023.

[35] C. Vasilescu *et al.*, “Enzymatic synthesis of short-chain flavor esters from natural sources using tailored magnetic biocatalysts,” *Food Chem.*, vol. 296, no. May, pp. 1–8, 2019, doi: 10.1016/j.foodchem.2019.05.179.
[36] A. Todea, I. Cristina, I. Bîtcan, P. Francisc, S. Kl, and E. Bir, “One-pot biocatalytic conversion of lactose to gluconic acid and galacto-oligosaccharides using immobilized β -galactosidase and glucose oxidase,” vol. 366, no. November 2019, pp. 202–211, 2021, doi: 10.1016/j.cattod.2020.06.090.
[37] V. Recarte, L. Cervera, M. D. Ugarte, E. C. Mendonça, and J. G. S. Duque, “Tailoring the structural and magnetic properties of Co-Zn nanosized ferrites for hyperthermia applications,” *J. Magn. Magn. Mater.*, vol. 465, pp. 211–2019, 2018, doi: 10.1016/j.jmmm.2018.05.051.
[38] I. Bîtcan *et al.*, “Enzymatic route for selective glycerol oxidation using covalently immobilized laccases,” *Enzyme Microb. Technol.*, vol. 163, no. November 2022, 2023, doi: 10.1016/j.enzmictec.2022.110168.
[39] R. C. Rodrigues, Á. Berenguer-Murcia, D. Carballares, R. Morellon-Sterling, and R. Fernandez-Lafuente, “Stabilization of enzymes via immobilization: Multipoint covalent attachment and other stabilization strategies,” *Biotechnol. Adv.*, vol. 52, pp. 1–37, 2021, doi: 10.1016/j.biotechadv.2021.107821.
[40] T. Fukuoka, H. Habe, D. Kitamoto, and K. Sakaki, “Bioprocessing of glycerol into glyceric acid for use in bioplastic monomer,” *J. Oleo Sci.*, vol. 60, no. 7, pp. 369–373, 2011, doi: 10.5650/jos.60.369.
[41] B. Wang *et al.*, “Production of D-glyceric acid by a two-step culture strategy based on whole-cell biocatalysis of acetobacter tropicalis,” *Chem. Biochem. Eng. Q.*, vol. 32, no. 1, pp. 135–140, 2018, doi: 10.15255/CABEQ.2017.1181.
[42] I. I. Rădoi *et al.*, “FTIR microscopy for direct observation of conformational changes on immobilized ω-transaminase: effect of water activity and organic solvent on biocatalyst performance,” *Catal. Sci. Technol.*, vol. 13, no. 17, pp. 4955–4967, 2023, doi: 10.1039/d2cy01949c.
[43] A. K. Bakunova *et al.*, “From Structure to Function : Analysis of the First Monomeric Pyridoxal-5 ′ -Phosphate-Dependent Transaminase from the Bacterium Desulfobacula toluolica,” *Biomolecules*, vol. 14, 2024.
[44] Q. Zhang, K. De Oliveira Vigier, S. Royer, and F. Jérôme, “Deep eutectic solvents: Syntheses, properties and applications,” *Chem. Soc. Rev.*, vol. 41, no. 21, pp. 7108–7146, 2012, doi: 10.1039/c2cs35178a.
[45] A. Paiva, R. Craveiro, I. Aroso, M. Martins, R. L. Reis, and A. R. C. Duarte, “Natural deep eutectic solvents - Solvents for the 21st century,” *ACS Sustain. Chem. Eng.*, vol. 2, no. 5, pp. 1063–1071, 2014, doi: 10.1021/sc500096j.
[46] A. R. Buzatu *et al.*, “Reactive natural deep eutectic solvents increase selectivity and efficiency of lipase catalyzed esterification of carbohydrate polyols,” *Catal. Today*, vol. 426, no. September 2023, 2024, doi: 10.1016/j.cattod.2023.114373.
[47] T. El Achkar, H. Greige, and G. Sophie, “Basics and properties of deep eutectic solvents : a review,” *Environ. Chem. Lett.*, vol. 19, no. 4, pp. 3397–3408, 2021, doi: 10.1007/s10311-021-01225-8.
[48] P. D. De María, N. Guajardo, and J. González-sabín, “ScienceDirect Recent granted patents related to Deep Eutectic Solvents,” *Curr. Opin. Green Sustain. Chem.*, vol. 38, p. 100712, 2022, doi: 10.1016/j.cogsc.2022.100712.
[49] A. R. Buzatu, A. Todea, F. Peter, and C. G. Boeriu, “The Role of Reactive Natural Deep Eutectic Solvents in Sustainable Biocatalysis,” *ChemCatChem*, vol. 16, no. 13, 2024, doi: 10.1002/cctc.202301597.
[50] X. Sun, Z. Zhou, D. Tian, J. Zhao, J. Zhang, and P. Deng, “International Journal

of Biological Macromolecules Acidic deep eutectic solvent assisted mechanochemical delignification of lignocellulosic biomass at room temperature," *Int. J. Biol. Macromol.*, vol. 234, no. January, p. 123593, 2023, doi: 10.1016/j.ijbiomac.2023.123593.

[51] H. Wang *et al.*, "Effects of deep eutectic solvents on the biotransformation efficiency of x -transaminase," *J. Mol. Liq.*, vol. 377, p. 121379, 2023, doi: 10.1016/j.molliq.2023.121379.

[52] A. R. Buzatu *et al.*, "Lipase-catalysed esterification in a reactive natural deep eutectic solvent leads to lauroylcholine chloride rather than glucose ester," *React. Chem. Eng.*, pp. 2623–2634, 2024, doi: 10.1039/d4re00209a.

[53] R. Amoroso, F. Hollmann, and C. Maccallini, "Choline chloride-based des as solvents/catalysts/chemical donors in pharmaceutical synthesis," *Molecules*, vol. 26, no. 20, 2021, doi: 10.3390/molecules26206286.

[54] Ö. Erol and F. Hollmann, "Natural deep eutectic solvents as performance additives for biocatalysis," *Adv. Bot. Res.*, vol. 97, pp. 95–132, 2021, doi: 10.1016/bs.abr.2020.09.004.

[55] A. A. Elgharbawy, A. Hayyan, M. Hayyan, and S. N. Rashid, "Shedding Light on Lipase Stability in Natural Deep Eutectic Solvents," *Chem. Biochem. Eng. Q*, vol. 32, no. 3, pp. 359–370, 2018, doi: 10.15255/CABEQ.2018.1335.

[56] L. V. Hoyos, L. Ramírez, C. J. Yarce, C. Alvarez-Vasco, and N. H. C. Ortega, "Sustainable production of glycolipids by biocatalyst on renewable deep eutectic solvents," *Catalysts*, vol. 11, no. 7, pp. 1–13, 2021, doi: 10.3390/catal11070853.

[57] M. Kapoor and M. N. Gupta, "Lipase promiscuity and its biochemical applications," *Process Biochem.*, vol. 47, no. 4, pp. 555–569, 2012, doi: 10.1016/j.procbio.2012.01.011.

[58] A. R. Buzatu *et al.*, "Designed Reactive Natural Deep Eutectic Solvents for Lipase-Catalyzed Esterification," *Molecules*, vol. 30, no. 4, 2025, doi: 10.3390/molecules30040778.

[59] R. Hollenbach, K. Ochsenreither, and C. Syldatk, "Enzymatic synthesis of glucose monodecanoate in a hydrophobic deep eutectic solvent," *Int. J. Mol. Sci.*, vol. 21, no. 12, pp. 1–11, 2020, doi: 10.3390/ijms21124342.

[60] J. Cao, R. Wu, F. Zhu, Q. Dong, and E. Su, "How to improve the efficiency of biocatalysis in non-aqueous pure deep eutectic solvents: A case study on the lipase-catalyzed transesterification reaction," *Biochem. Eng. J.*, vol. 179, no. January, p. 108336, 2022, doi: 10.1016/j.bej.2022.108336.

[61] P. Braiuca, K. Lorena, V. Ferrario, C. Ebert, and L. Gardossi, "A three-dimensional quanititative structure-activity relationship (3D-QSAR) model for predicting the enantioselectivity of candida antarctica lipase B," *Adv. Synth. Catal.*, vol. 351, no. 9, pp. 1293–1302, 2009, doi: 10.1002/adsc.200900009.

[62] V. Ferrario *et al.*, "Conformational changes of lipases in aqueous media: A comparative computational study and experimental implications," *Adv. Synth. Catal.*, vol. 353, no. 13, pp. 2466–2480, Sep. 2011, doi: 10.1002/ADSC.201100397.

[63] C. C. Gruber and J. Pleiss, "Lipase B from Candida antarctica binds to hydrophobic substrate-water interfaces via hydrophobic anchors surrounding the active site entrance," *J. Mol. Catal. B Enzym.*, vol. 84, pp. 48–54, 2012, doi: 10.1016/j.molcatb.2012.05.012.

[64] O. Trott and A. J. Olson, "AutoDock Vina: Improving the speed and accuracy of docking with a new scoring function, efficient optimization, and multithreading," *J. Comput. Chem.*, vol. 31, no. 2, p. NA-NA, 2009, doi: 10.1002/jcc.21334.

[65] G. Lombardo *et al.*, “Sustainable Synthesis of Terpolyesters Based on a Levoglucosenone-Derived Cyclic Acetal Diol,” 2025, doi: 10.1021/acssuschemeng.4c10010.
[66] S. Yamaguchi, M. Tanha, A. Hult, T. Okuda, H. Ohara, and S. Kobayashi, “Green polymer chemistry: Lipase-catalyzed synthesis of bio-based reactive polyesters employing itaconic anhydride as a renewable monomer,” *Polym. J.*, vol. 46, no. 1, pp. 2–13, 2014, doi: 10.1038/pj.2013.62.
[67] N. Schulte, G. Damonte, V. M. Rocca, A. Todea, O. Monticelli, and A. Pellis, “Bis-pyrrolidone structures as versatile building blocks for the synthesis of bio-based polyesters and for the preparation of additives,” vol. 27, 2025, doi: 10.1039/d4gc04951a.
[68] A. Todea, L. G. Otten, A. E. Frissen, I. W. C. E. Arends, F. Peter, and C. G. Boeriu, “Selectivity of lipases for estolides synthesis,” *Pure Appl. Chem.*, vol. 87, no. 1, pp. 51–58, 2015, doi: 10.1515/pac-2014-0716.
[69] D. M. Dreava *et al.*, “Biocatalytic Approach for Novel Functional Oligoesters of ε-Caprolactone and Malic Acid,” *Processes*, 2021.
[70] I. C. Benea *et al.*, “Efficient biotransformation of biobased raw materials into novel polyesters / polyesteramides; comparative investigation of enzymatic synthesis of block and random copolymers and terpolymers,” *Int. J. Biol. Macromol.*, vol. 282, 2024, doi: 10.1016/j.ijbiomac.2024.137046.
[71] A. Todea, D. Aparaschivei, I. Bîtcan, I. Valentin, G. Bandur, and F. Péter, “Thermal behavior of oligo [(ε - caprolactone)- co - δ - gluconolactone] enzymatically synthesized in reaction conditions optimized by experimental design,” *J. Therm. Anal. Calorim.*, vol. 141, no. 3, pp. 1017–1026, 2020, doi: 10.1007/s10973-020-09557-3.
[72] S. Kakasi-Zsurka *et al.*, “Biocatalytic synthesis of new copolymers from 3-hydroxybutyric acid and a carbohydrate lactone,” *J. Mol. Catal. B Enzym.*, vol. 71, pp. 22–28, 2011, doi: 10.1016/j.molcatb.2011.03.004.
[73] A. Todea *et al.*, “Optimization of enzymatic ring-opening copolymerizations involving δ-gluconolactone as monomer by experimental design,” *Pure Appl. Chem.*, vol. 86, no. 11, pp. 1781–1792, 2014, doi: 10.1515/pac-2014-0717.
[74] A. Todea, V. Badea, L. Nagy, S. Kéki, C. G. Boeriu, and F. Péter, “Biocatalytic synthesis of δ-gluconolactone and ε-caprolactone copolymers *,” *Acta Biochim. Pol.*, vol. 61, no. 2, pp. 205–210, 2014.
[75] A. Todea *et al.*, “Biodegradable oligoesters of ε-caprolactone and 5-hydroxymethyl-2-furancarboxylic acid synthesized by immobilized lipases,” *Polymers (Basel).*, vol. 11, no. 9, pp. 1–17, 2019, doi: 10.3390/polym11091402.
[76] D. Aparaschivei *et al.*, “Enzymatic synthesis and characterization of novel terpolymers from renewable sources,” *Pure Appl. Chem.*, vol. 91, no. 3, pp. 397–408, 2019, doi: 10.1515/pac-2018-1015.
[77] A. Todea, D. Aparaschivei, V. Badea, C. G. Boeriu, and F. Peter, “Biocatalytic Route for the Synthesis of Oligoesters of Hydroxy-Fatty acids and ε-Caprolactone,” *Biotechnol. J.*, vol. 13, no. 6, pp. 1–9, 2018, doi: 10.1002/biot.201700629.
[78] D. Aparaschivei *et al.*, “Synthesis, characterization and enzymatic degradation of copolymers of ε-caprolactone and hydroxy-fatty acids,” *Pure Appl. Chem.*, vol. 88, no. 12, pp. 1191–1201, 2016, doi: 10.1515/pac-2016-0920.
[79] A. Todea *et al.*, “Rational Guidelines for the Two-Step Scalability of Enzymatic Polycondensation: Experimental and Computational Optimization of the Enzymatic Synthesis of Poly(glycerolazelate),” *ChemSusChem*, vol. 15, no. 9,

2022, doi: 10.1002/cssc.202102657.
[80] I. Bîtcan *et al.*, “One-pot green synthesis and characterization of novel furan-based oligoesters,” *Sustain. Chem. Pharm.*, vol. 35, p. 101229, 2023, doi: 10.1016/j.scp.2023.101229.
[81] A. Bazin, L. Avérous, and E. Pollet, “Lipase-catalyzed synthesis of furan-based aliphatic-aromatic biobased copolyesters: Impact of the solvent,” *Eur. Polym. J.*, vol. 159, no. July, 2021, doi: 10.1016/j.eurpolymj.2021.110717.
[82] C. G. Boeriu, A. Todea, I. W. C. E. Arends, and L. G. Otten, “Production of fatty acid estolides,” US010920252B2, 2016
[83] A. Todea *et al.*, “Enzymatic Synthesis and Structural Modeling of Bio-Based Oligoesters as an Approach for the Fast Screening of Marine Biodegradation and Ecotoxicity,” *Int. J. Mol. Sci.*, vol. 25, no. 10, 2024, doi: 10.3390/ijms25105433.
[84] A. Pellis *et al.*, “Fully renewable polyesters: Via polycondensation catalyzed by Thermobifida cellulosilytica cutinase 1: An integrated approach,” *Green Chem.*, vol. 19, no. 2, pp. 490–502, Jan. 2017, doi: 10.1039/c6gc02142e.
[85] P. Bernhardt, K. Hult, and R. J. Kazlauskas, “Molecular Basis of Perhydrolase Activity in Serine Hydrolases,” *Angew. Chemie*, vol. 117, no. 18, pp. 2802–2806, 2005, doi: 10.1002/ange.200463006.
[86] C. Aouf *et al.*, “The use of lipases as biocatalysts for the epoxidation of fatty acids and phenolic compounds,” *Green Chem.*, vol. 16, no. 4, pp. 1740–1754, 2014, doi: 10.1039/c3gc42143k.
[87] N. A. Zainal, N. W. M. Zulkifli, M. Gulzar, and H. H. Masjuki, “A review on the chemistry, production, and technological potential of bio-based lubricants,” *Renew. Sustain. Energy Rev.*, vol. 82, no. September 2017, pp. 80–102, 2018, doi: 10.1016/j.rser.2017.09.004.
[88] K. Min, J. D. Cuiffi, and R. T. Mathers, “Ranking environmental degradation trends of plastic marine debris based on physical properties and molecular structure,” *Nat. Commun.*, vol. 11, no. 1, 2020, doi: 10.1038/s41467-020-14538-z.
[89] M. F. Colella, N. Marino, C. Oliviero Rossi, L. Seta, P. Caputo, and G. De Luca, “Triacylglycerol Composition and Chemical-Physical Properties of Cocoa Butter and Its Derivatives: NMR, DSC, X-ray, Rheological Investigation,” *Int. J. Mol. Sci.*, vol. 24, no. 3, p. 2090, 2023, doi: 10.3390/ijms24032090.
[90] E. M. WOO and M. C. WU, “Thermal and X-Ray Analysis of Polymorphic Crystals, Melting, and Crystalline Transformation in Poly(butylene adipate),” *J. Polym. Sci. Part B Polym. Phys.*, vol. 43, pp. 1662–1672, 2005.
[91] Bhattacharya Piyal, “A Review on the Impacts of Microplastic Beads Used in Cosmetics,” *Acta Biomed. Sci.*, vol. 3, no. 1, pp. 47–52, 2016.
[92] M. Bilal, S. Mehmood, and H. M. N. Iqbal, “The Beast of Beauty : Environmental and Health Concerns of Toxic Components in Cosmetics,” *Cosmetics*, vol. 7, no. 13, pp. 1–18, 2020, doi: 10.3390/cosmetics7010013.
[93] G. Chen, Y. Li, and J. Wang, “Chemosphere Occurrence and ecological impact of microplastics in aquaculture ecosystems,” *Chemosphere*, vol. 274, p. 129989, 2021, doi: 10.1016/j.chemosphere.2021.129989.
[94] Y. Tokiwa, B. P. Calabia, C. U. Ugwu, and S. Aiba, “Biodegradability of plastics,” *Int. J. Mol. Sci.*, vol. 10, no. 9, pp. 3722–3742, 2009, doi: 10.3390/ijms10093722.
[95] S. Thakur, S. Mathur, S. Patel, and B. Paital, “Microplastic Accumulation and Degradation in Environment via Biotechnological Approaches,” *Water (Switzerland)*, vol. 14, no. 24, 2022, doi: 10.3390/w14244053.

[96] E. A. R. Zuiderveen *et al.*, “The potential of emerging bio-based products to reduce environmental impacts,” *Nat. Commun.*, vol. 14, no. 1, 2023, doi: 10.1038/s41467-023-43797-9.
[97] S. M. Emadian, T. T. Onay, and B. Demirel, “Biodegradation of bioplastics in natural environments,” *Waste Manag.*, vol. 59, pp. 526–536, 2017, doi: 10.1016/j.wasman.2016.10.006.
[98] F. Zappaterra *et al.*, “Understanding Marine Biodegradation of Bio-Based Oligoesters and Plasticizers,” *Polymers (Basel).*, vol. 15, no. 1536, 2023.
[99] S. Teixeira, K. M. Eblagon, F. Miranda, M. F. R. Pereira, and J. L. Figueiredo, “Towards Controlled Degradation of Poly(lactic) Acid in Technical Applications,” *J. Carbon Res.*, vol. 7, no. 2, p. 42, 2021, doi: 10.3390/c7020042.
[100] F. Zappaterra *et al.*, “Xylitol as a Hydrophilization Moiety for a Biocatalytically Synthesized Ibuprofen Prodrug,” *Int. J. Mol. Sci.*, vol. 23, no. 4, p. 2026, 2022, doi: https://doi.org/10.3390/ijms23042026.
[101] A. Todea *et al.*, “Azelaic Acid: A Bio-Based Building Block for Biodegradable Polymers,” *Polymers (Basel).*, vol. 13, no. 23, p. 4091, 2021, doi: 10.3390/polym13234091.
[102] F. Binns, P. Harffey, S. M. Roberts, and A. Taylor, “Studies leading to the large scale synthesis of polyesters using enzymes,” *J. Chem. Soc. - Perkin Trans. 1*, no. 19, pp. 2671–2676, 1999, doi: 10.1039/a904889h.
[103] A. Pellis *et al.*, “Towards feasible and scalable solvent-free enzymatic polycondensations: Integrating robust biocatalysts with thin film reactions,” *Green Chem.*, vol. 17, no. 3, pp. 1756–1766, Mar. 2015, doi: 10.1039/c4gc02289k.
[104] G. Cerea, L. Gardossi, L. Sinigoi, and D. Fattor, “Process for the production of polyesters through synthesis catalyzed by enzyme,” 2013
[105] A. L. Fernando, J. Costa, B. Barbosa, A. Monti, and N. Rettenmaier, “Environmental impact assessment of perennial crops cultivation on marginal soils in the Mediterranean Region,” *Biomass and Bioenergy*, vol. 111, pp. 174–186, 2018, doi: 10.1016/j.biombioe.2017.04.005.
[106] T. Cogliano, R. Turco, V. Russo, M. Di Serio, and R. Tesser, “1H NMR-based analytical method: A valid and rapid tool for the epoxidation processes,” *Ind. Crops Prod.*, vol. 186, no. July, p. 115258, 2022, doi: 10.1016/j.indcrop.2022.115258.
[107] F. Bosco and C. Mollea, “Biodegradation of Natural Rubber: Microcosm Study,” *Water. Air. Soil Pollut.*, vol. 232, no. 6, 2021, doi: 10.1007/s11270-021-05171-7.
[108] V. Ferrario *et al.*, “Investigating the Role of Conformational Effects on Laccase Stability and Hyperactivation under Stress Conditions,” *ChemBioChem*, vol. 16, no. 16, pp. 2365–2372, 2015, doi: 10.1002/cbic.201500339.
[109] A. Wolfson, C. Dlugy, and Y. Shotland, “Glycerol as a green solvent for high product yields and selectivities,” *Environ. Chem. Lett.*, vol. 5, no. 2, pp. 67–71, 2007, doi: 10.1007/s10311-006-0080-z.
[110] A. L. Olalla, L. I. Sara, and B. Ricardo, “Assessment of toxicity and biodegradability of poly(Vinyl alcohol)-based materials in marine water,” *Polymers (Basel).*, vol. 13, no. 21, pp. 1–9, 2021, doi: 10.3390/polym13213742.
[111] K. I. Kasuya, K. I. Takagi, S. I. Ishiwatari, Y. Yoshida, and Y. Doi, “Biodegradabilities of various aliphatic polyesters in natural waters,” *Polym. Degrad. Stab.*, vol. 59, no. 1–3, pp. 327–332, 1998, doi: 10.1016/s0141-3910(97)00155-9.

[112] P. Reuschenbach, U. Pagga, and U. Strotmann, “A critical comparison of respirometric biodegradation tests based on OECD 301 and related test methods,” *Water Res.*, vol. 37, no. 7, pp. 1571–1582, 2003, doi: 10.1016/S0043-1354(02)00528-6.
[113] A. Folino, A. Karageorgiou, P. S. Calabrò, and D. Komilis, “Biodegradation of Wasted Bioplastics in Natural and Industrial Environments: A Review,” *Sustain.*, vol. 12, no. 15, pp. 1–37, 2020.
[114] I. C. Benea *et al.*, “Biocatalytic synthesis of new polyesteramides from ε -caprolactam and hydroxy acids : Structural characterization , biodegradability , and suitability as drug nanocarriers,” *React. Funct. Polym.*, vol. 191, 2023, doi: 10.1016/j.reactfunctpolym.2023.105702.
[115] “Biodegradation in water : screening tests,” 2012. https://echa.europa.eu/it/registration-dossier/-/registered-dossier/15563/5/3/2
[116] OECD, “OECD Guidelines for the Testing of Chemicals, Section 3: Degradation and Accumulation,” 2006. http://www.oecd-ilibrary.org/
[117] G. Modaffari, “Blueing the Coastline . From Heavy Industry to Sport Tourism in the Years Following World War II : The Case of Trieste,” 2023. https://rosa.uniroma1.it/rosa03/semestrale_di_geografia/article/view/18302
[118] V. Solis-Weiss, F. Aleffi, N. Bettoso, P. Rossin, G. Orel, and S. Fonda-Umani, “Effects of industrial and urban pollution on the benthic macrofauna in the Bay of Muggia (industrial port of Trieste, Italy),” *Sci. Total Environ.*, vol. 328, no. 1–3, pp. 247–263, 2004, doi: 10.1016/j.scitotenv.2004.01.027.
[119] S. Negoro, “Biodegradation of nylon oligomers,” *Appl Microbiol Biotechnol*, no. 54, pp. 461–466, 2000.
[120] S. Fortuna, M. Cespugli, A. Todea, A. Pellis, and L. Gardossi, “Criteria for engineering cutinases: Bioinformatics analysis of catalophores,” *Catalysts*, vol. 11, no. 7, pp. 1–16, 2021, doi: 10.3390/catal11070784.
[121] V. Ferrario *et al.*, “BioGPS Descriptors for Rational Engineering of Enzyme Promiscuity and Structure Based Bioinformatic Analysis,” *PLoS One*, vol. 9, no. 10, pp. 1–13, Oct. 2014, doi: 10.1371/journal.pone.0109354.
[122] P. Crivori, G. Cruciani, P. A. Carrupt, and B. Testa, “Predicting blood-brain barrier permeation from three-dimensional molecular structure,” *J. Med. Chem.*, vol. 43, no. 11, pp. 2204–2216, 2000, doi: 10.1021/jm990968+.
[123] C. Koukoulitsa, G. D. Geromichalos, and H. Skaltsa, “VolSurf analysis of pharmacokinetic properties for several antifungal sesquiterpene lactones isolated from Greek Centaurea sp.,” *J. Comput. Aided. Mol. Des.*, vol. 19, no. 8, pp. 617–623, 2005, doi: 10.1007/s10822-005-9018-y.
[124] E. Carosati *et al.*, “Ligand-based virtual screening and ADME-tox guided approach to identify triazolo-quinoxalines as folate cycle inhibitors,” *Bioorganic Med. Chem.*, vol. 18, no. 22, pp. 7773–7785, 2010, doi: 10.1016/j.bmc.2010.09.065.
[125] P. J. Goodford, “A Computational Procedure for Determining Energetically Favorable Binding Sites on Biologically Important Macromolecules,” *J. Med. Chem.*, vol. 28, no. 7, pp. 849–857, 1985, doi: 10.1021/jm00145a002.
[126] G. Cruciani, P. Crivori, P. A. Carrupt, and B. Testa, “Molecular fields in quantitative structure-permeation relationships: The VolSurf approach,” *J. Mol. Struct. THEOCHEM*, vol. 503, no. 1–2, pp. 17–30, 2000, doi: 10.1016/S0166-1280(99)00360-7.
[127] S. Tortorella *et al.*, “Combining machine learning and quantum mechanics yields more chemically aware molecular descriptors for medicinal chemistry

applications," *J. Comput. Chem.*, vol. 42, no. 29, pp. 2068–2078, 2021, doi: 10.1002/jcc.26737.
[128] "VolSurf^3," 2021. https://www.molhorizon.it/software/volsurf3/
[129] F. Pedregosa *et al.*, "Scikit-learn: Machine Learning in Python Fabian," *J. Mach. Learn. Res.*, vol. 12, no. 9, pp. 2825–2830, 2011, doi: 10.1289/EHP4713.
[130] S. Wold, M. Sjöström, and L. Eriksson, "PLS-regression: A basic tool of chemometrics," *Chemom. Intell. Lab. Syst.*, vol. 58, no. 2, pp. 109–130, 2001, doi: 10.1016/S0169-7439(01)00155-1.
[131] J. I. García, E. Pires, L. Aldea, L. Lomba, E. Perales, and B. Giner, "Ecotoxicity studies of glycerol ethers in Vibrio fischeri: checking the environmental impact of glycerol-derived solvents," *Green Chem.*, vol. 17, no. 8, pp. 4326–4333, 2015, doi: 10.1039/c5gc00857c.
[132] S. P. M. Ventura, P. De Morais, J. A. S. Coelho, T. Sintra, J. A. P. Coutinho, and C. A. M. Afonso, "Evaluating the toxicity of biomass derived platform chemicals," *Green Chem.*, vol. 18, no. 17, pp. 4733–4742, 2016, doi: 10.1039/c6gc01211f.
[133] "European Chemicals Agency." https://echa.europa.eu/it/home